



# Pilkington Library

Author/Filing Title ..... LOCKER, G.J. .....

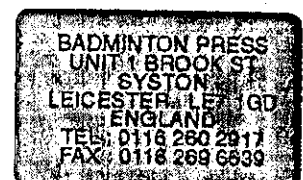
Accession/Copy No. ....

Vol. No. ....

Class Mark ..... T .....

LOAN COPY

040199144X



# **Fretting Corrosion of Tin Plated Separable Connectors Used in Automotive Applications.**

**By**

**Graham J. Locker B.A.**

**A DOCTORAL THESIS**


**Supervisors: Drs. G. W. Critchlow & D. M. Brewis**

**Director of Research: Prof. K. R. A. Ziebeck**

**Submitted in partial fulfilment of the requirements for the award of Degree of Doctor of Philosophy of the Loughborough University.**

**April 1998.**

**© G.J.Locker, 1998**

	<b>Loughborough University</b> P.L. Library
Date	Mar 99
Class	
Acc No	040199144

K0642951

*To Sheila, Katie, Stephanie and Stella.*



## Abstract

Greater demands are being placed on the separable connector to perform with higher reliability in harsher automotive environments. Corrosion in its various forms is a major mechanism which affects contact reliability and this current work focuses on surface oxidation and the related phenomenon of fretting corrosion, from which hot dipped tin (HDT), a common automotive connector coating, is known to suffer. For an in-depth study of high contact resistance, in both static conditions and when subjected to relative micro-movement, an interdisciplinary approach was necessary, drawing on the results of published work carried out in the fields of Contact and Surface Science, Corrosion and Tribology. In addition, it was deemed important to select the materials characterisation techniques which would provide the greatest benefits for this current study. This necessitated a comprehensive review of the literature.

Tests were performed on HDT plated bronze coupons, both in controlled laboratory conditions and on vehicles operating in the field. Their surface composition and properties were studied using contact resistance measurements and a variety of analytical techniques. It has been concluded that the major influence on contact resistance was from thermal effects resulting in the promotion of oxide growth, rather than from other corrosive species found in the field environments.

The composite nature of HDT plated bronze was extensively evaluated and coupons were wear tested under low frequency, dry fretting conditions in a laboratory atmosphere, using a purpose built rig. The results suggested that tin coatings operating in relatively high temperature environments, probably perform worse than no coating at all. However, it was found that copper/tin intermetallics had superior wear and corrosion resistance properties over tin in a fretting wear regime.

By using a range of lubricants, low cycle fretting tests were carried out to identify the composition giving the best performance in terms of time-to-failure. It was found that mineral oils containing lithium 12 - hydroxystearate showed superior performance. The

adsorption properties of a thickening agent were studied using Infrared Reflection Absorption Spectrometry and it was found that a related soap molecule, 12 - hydroxystearic acid, bonded chemically to tin at room temperature but showed a greater degree of chemisorption at elevated temperatures.

The reactivity, as measured by the leakage current between two HDT plates, of each of a range of lubricant formulations was also determined, to ascertain if this property was related to fretting performance, in order to provide a rapid ranking technique. Those containing highly polar molecules were found to exhibit both high reactivity and the longest time-to-failure.

The copper/tin intermetallic phases,  $\text{Cu}_6\text{Sn}_5$  and  $\text{Cu}_3\text{Sn}$ , were studied in HDT samples by Auger Electron Spectroscopy, Scanning Electron Microscopy, X-Ray Diffraction Spectrometry, Image Analysis and non contact Surface Profilometry. A diffusion rate for copper in tin, to form the copper rich phase, was measured over a distance of approximately  $1\mu\text{m}$ . Intermetallic growth rates have been determined by other workers using traditional cross-sectioning methods. However, for the limited (2 -  $3\mu\text{m}$ ), tin plating thickness used in this study, a novel alternative technique was developed using Energy Dispersive Spectrometry.

### **Keywords**

Fretting, Corrosion, Hot Dipped Tin, Connector, Contact, Lubrication, Wear, Contact Resistance, Diffusion, Intermetallics.

# Acknowledgements

Some parts of this work were carried out whilst I was a member of a European Commission Brite/Euram funded project investigating improvements into the surface preparation of electrical contacts. The remainder and bulk of the research has been performed under my own funding together with grants from Lucas Varity plc for university fees. I am indebted to several of my colleagues at Lucas Electrical and Electronic Systems (LE&ES), Technical Centre and Loughborough University, Institute of Surface Science and Technology. I am particularly indebted to Mr. David Bowie, manager of the Technical Operations Group of LE&ES for use of sophisticated analytical equipment, to David Chambers, project controller of the above project, for use of the contact resistance rig and field test samples and Brian Norway for performing thermogravimetric analyses of the lubricants and the thioacetamide environmental testing of coupon samples. My thanks are also extended to James Dixon formerly of Rocol Ltd., for the supply of many of the lubricants and Dr. Gary Critchlow of ISST for carrying out AES analyses and for proof reading this work. Finally, I would like to thank Professor Tom Wood of GKN plc, for his encouragement and my wife Sheila, for putting up with countless journals and papers around the house and missed weekends on country walks.

# CONTENTS

<b>1. INTRODUCTION</b>	<b>1</b>
<b>2. LITERATURE REVIEW</b>	<b>4</b>
2.1 Introduction	4
2.2 Connector Materials	8
2.3 Connector Coatings	10
2.4 Contact Geometry	14
2.5 The Contacting Surfaces	18
2.6 Contact Resistance	22
2.7 Corrosion	26
2.7.1 'Wet' Corrosion	27
2.7.2 'Dry' Corrosion	31
2.7.3 Surface Oxidation of Tin Contacts	35
2.7.4 Stress Corrosion	37
2.8 Intermetallic Formation	38
2.8.1 Kinetics of Cu/Sn Intermetallic Formation	39
2.9 Tribology	43
2.9.1 Adhesive Wear	44
2.9.2 Abrasive Wear	46
2.9.3 Fretting Wear and Fretting Corrosion	47
2.10 Lubricants for Automotive Connectors	59
2.10.1 Lubricant Reactivity	61
2.11 Materials Analysis Techniques	64
2.11.1 Scanning Electron Microscopy (SEM)	64
2.11.2 Energy Dispersive Spectrometry (EDS)	67
2.11.3 X-ray Diffraction (XRD)	68
2.11.4 Fourier Transform Infrared Spectrometry (FTIRS)	69
2.11.5 X-ray Photoelectron Spectroscopy (XPS)	70
2.11.6 Auger Electron Spectroscopy (AES)	72
2.11.7 Applications of Surface Analytical Techniques	73
2.12 Conclusions from the Literature Survey.	76
<b>3. EXPERIMENTAL</b>	<b>85</b>
3.1 Design and Construction of Test Equipment	86
3.1.1 Field Test Enclosures	86
3.1.2 Reactivity Cell	86
3.1.3 Contact Resistance Apparatus	88
3.1.4 Low Frequency Fretting Test Rig	89

<b>3.2</b>	<b>Characterisation and Testing</b>	<b>92</b>
3.2.1	Test Coupons	92
3.2.2	Lubricant Analysis	96
3.2.3	Controlled Corrosion and Thermal Testing	97
3.2.4	Field Testing	104
3.2.5	Fretting Tests	104
3.2.6	IRAS Study of 12-Hydroxystearate	105
<b>4.</b>	<b>RESULTS AND DISCUSSION</b>	<b>109</b>
<b>4.1</b>	<b>Evaluation of Test Materials</b>	<b>109</b>
4.1.1	Coupon Analysis	109
4.1.2	Lubricant Analysis	117
<b>4.2</b>	<b>Corrosion Testing</b>	<b>127</b>
4.2.1	Field Testing	131
<b>4.3</b>	<b>Analysis of Thermally Aged Coupons</b>	<b>137</b>
4.3.1	SEM Examination of Microsections	142
4.3.2	AES Depth Profile Analysis	143
4.3.3	XRD Analysis	148
4.3.4	Copper Diffusion Rate Measurements	150
4.3.5	Intermetallic Morphology	155
<b>4.4</b>	<b>Fretting Tests</b>	<b>161</b>
4.4.1	Dry Fretting Tests	161
4.4.2	Lubricated Fretting Tests	162
<b>4.5</b>	<b>IRAS Analysis of 12-Hydroxystearic Acid Films on Tin</b>	<b>168</b>
<b>4.6</b>	<b>Discussion</b>	<b>175</b>
4.6.1	Degradation of the Contact	175
4.6.2	Intermetallic Formation	179
4.6.3	Fretting Corrosion	183
4.6.4	Lubricants for Fretting Regimes	187
4.6.5	Intermetallics as Contacts	194
<b>5.</b>	<b>CONCLUSIONS</b>	<b>197</b>
<b>6.</b>	<b>RECOMMENDATIONS</b>	<b>200</b>
<b>APPENDICES A and B</b>		

# Abbreviations

ABS <sup>A</sup>	Anti-lock Braking Systems
ABS <sup>B</sup>	Acronitrile Butadiene Styrene
AES	Auger Electron Spectroscopy
ASTM	American Society for Testing and Materials
ATR	Attenuated Total Reflection
BET	Brunauer, Emmet and Teller
BSE	Back-scattered Electron
CR	Contact Resistance
CRT	Cathode Ray Tube
CTE	Coefficient of Thermal Expansion
EDS	Energy Dispersive Spectrometry
EDXRF	Energy Dispersive X-ray Fluorescence Spectrometry
ESCA	Electron Spectroscopy for Chemical Analysis
EP	Extreme Pressure
FET	Field Effect Transistor
FTIRS	Fourier Transform Infrared Spectrometry
G	Gibbs Free Energy
HALT	Hot Air Levelled Tin
HDT	Hot Dipped Tin
IRAS	Infrared Reflection Absorption Spectroscopy
IDC	Insulation Displacement Cable
IEEE	Institute of Electrical and Electronic Engineers
IMFP	Inelastic Mean Free Path
JCPDS	Joint Committee on Powder Diffraction Standards
MIL STD	Military Standard
NFF	No Fault Found
NOX	Nitrogen Oxides
PA	Polyamide
PAG	Polyalkelyne Glycol
PBS	Polyphenyl Sulphide
PBT	Polybutylene Terephthalate
PCTF	Polychlorotrifluoroethane
PP	Polypropylene
PPE	Polyphenyl Ether
PPO	Polyphenyloxid
PHFP	Polyhexafluoropropylene Epoxide
PFPE	Perfluoropolyether
PTFE	Polytetrafluoroethylene
SE	Secondary Electron
SEM	Scanning Electron Microscope
SIMS	Secondary Ion Mass Spectroscopy
TTF	Time-To-Failure
UHV	Ultra High Vacuum
WDS	Wavelength Dispersive Spectrometry
XPS	X-ray Photoelectron Spectroscopy

XRD	X-ray Diffraction
XRFS	X-ray Fluorescence Spectrometry
Z	Atomic number
ZAF	Atomic Number, Absorption, Fluorescence

(Note: References in the text to the term ‘plated’ or ‘plating’, when referring to HDT and HALT and to the deposition process of such coatings, imply from the molten state and not electrolytically).

## Symbols Used in this Thesis

$A$	Total Contact Area
$A_r$	Real Area of Contact
$D$	Density
$D_0$	Frequency Factor
$d$	Grain Size
$E$	Modulus of Elasticity
$e^-$	Electron
$G$	Gibbs Free Energy
$H$	Hardness
$H_a$	Abrasive Hardness
$H_s$	Surface Hardness
$H_v$	Vickers Hardness
$k$	Wear Coefficient
$k_{el}$	Electrical Conductivity
$k_t$	Thermal Conductivity
$L$	Lorentz Constant
$M$	Molar Mass
$m$	Atomic mass
$P$	Load
$P_m$	Yield Pressure
$Q$	Activation Energy
$Q_s$	Sliding Distance
$R_b$	Bulk Resistance
$R_c$	Constriction Resistance
$R_f$	Film Resistance
$R_t$	Total Resistance
$R_a$	Centre Line Average
$RH$	Relative Humidity
$T$	Absolute Temperature
$T_m$	Maximum Contact Spot Temperature
$T_0$	Bulk Temperature
$U$	Sliding Velocity
$\nu$	Poisson's Ratio
$Z_{av}$	Average Atomic Number
$\sigma_c$	Hertzian Stress
$\sigma_y$	Yield Stress
$\sigma_i$	Frictional Stress
$\lambda$	Wavelength
$\eta$	Viscosity
$\rho$	Resistivity
$\mu$	Coefficient of Friction

(Note: other symbols, where used, are identified in the text)



# **1. Introduction**

The use of the electrical connector is being increasingly extended as a result of the complexity of modern automotive circuitry. With the introduction of, for example, 'brake-by-wire', engine management and integrated suspension systems, the requirement for sensors and control modules has dramatically increased, with greater demands being placed on the connector to perform with higher reliability in harsher environments.

Corrosion in its various forms is the major mechanism affecting contact reliability due to the formation of highly resistive corrosion products and, as a consequence, this study focuses on surface oxidation and the related phenomenon of fretting corrosion, from which tin, a common automotive connector coating, is known to suffer. An understanding of this wear process is complicated by intermetallic phases, which form in the tin coating from the melt and during thermal ageing. As wear progresses their presence results in a sudden change from a wear regime associated with a relatively soft, high friction, metal, prone to surface oxidation, to that of a hard material whose properties are little known. A considerable part of the thesis is therefore devoted to characterising their properties.

Fretting corrosion can be minimised by using a suitable lubricant, to reduce friction at the contacts and act as a barrier to reactive species. This current work investigates a number of commercial lubricants, having different formulations, to determine their performance under fretting conditions, enabling the generation of a ranking order. The lubricant showing the longest time-to-failure, under the test conditions used, is further

investigated in order to gain an understanding of the mechanism responsible for reducing fretting wear.

Similar studies have been carried out by other researchers working mainly in the disciplines of electrical or mechanical engineering. However, it is intended, in this work, to approach the subject from the viewpoint of the materials analyst, supported by the use of a wide range of analytical techniques.

The objectives of this study are as follows:

- (i) to review the literature relating to the design, materials selection and failure mechanisms of automotive connectors and the analytical techniques available to study the material changes occurring as a result of exposure to hostile environments;
- (ii) to determine the physical, chemical and mechanical properties of the hot dipped tin plated electrical contact, including a study involving the use of a novel technique used to determine the diffusion rate of copper in tin;
- (iii) to determine the chemical and metallurgical effects on hot dipped tin plated bronze coupons which have been exposed to both simulated and real automotive environments;
- (iv) to measure the low cycle fretting corrosion performance of the tin plated connector, in both dry conditions and when lubricated with a range of grease formulations and to investigate the mechanism responsible for superior performance.
- (v) to evaluate a novel technique used as an aid in the selection of greases for separable connectors, exposed to low cycle fretting conditions.

- (vi) to evaluate the copper/tin intermetallic as an alternative coating for contacts prone to low frequency micro-motion.

This study is divided into the following chapters:

- (i) A review of the literature which has been published on the mechanisms involved in contact degradation, together with a description of the analytical techniques employed in their study.
- (ii) An experimental chapter describing the test equipment used and the materials evaluation and performance tests.
- (iii) The test programme results and discussion.
- (iv) The conclusions drawn from the study.
- (v) Recommendations for future work.

## **2. Literature Review**

### **2.1 Introduction**

This review is the result of a survey of the many and varied disciplines drawn upon to investigate the physical and chemical phenomena influencing electron flow across the contacting surfaces of a separable electrical connection. The affect of placing two surfaces in intimate contact and introducing relative movement, together with the passage of an electric current, creates an extremely complex system and as a consequence, numerous papers on the subject have been published. The importance of connector reliability and performance has been recognised by the industry world-wide, to the extent that the topic forms a major part of the annual conference organised by the Institute of Electrical and Electronic Engineers (IEEE), Holm Conference. Studies of connector failure are almost invariably interdisciplinary and as a result this literature survey reports on published work in the fields of Contact Science, Corrosion and Tribology and the analytical techniques used in their study.

The designers of electrical and electronic systems have found it necessary to be able to dissociate circuit components into functional modules or packages, yet still maintain the ability to electrically connect and disconnect them in order to:

- (i) simplify assembly and testing;
- (ii) provide circuit options and expansion;
- (iii) allow rapid replacement of defective units.

To meet this need, the separable connector was developed and from it a whole industry has grown, producing a vast range of connector designs with applications throughout virtually all technologies where there is a requirement to carry an electric current. The harness on a modern family saloon for example has of the order of several hundred separable connections, whilst an aircraft may utilise many thousands.

The separable connector industry has developed world-wide into a multimillion dollar industry for power and signal distribution circuitry, manufacturing connectors varying in complexity from the simple 'Lucar', used on most white goods and general electrical appliances to sophisticated 1000 pin aerospace connectors designed to withstand, for example, the harsh environment of the outer casing of a gas turbine engine.

The connector, or more accurately the connector assembly, consists of male and female components, the ends of which having permanent connections to conducting pathways such as insulated wire, flexible flat cable or the leadframe of an electronic module. Figure 2.1 shows typical multi-pin separable connector assemblies used in a sensing and control circuit of a modern vehicle. Unlike the permanent contact such as the soldered, welded or crimped (cold welded) joint, electron transfer across separable, sliding and switching contacts is achieved through the intimate contact of the conducting materials, held together purely by mechanical means. It would be the ultimate aim of the connector designer to be able to achieve contact between the two surfaces in much the same way as that which exists between those of individual crystals in a pure metal. However, surfaces possess properties which differ from those of the bulk material, and, particularly if operating under low voltage and current conditions, degradation of these surfaces will be the major factor determining the ultimate reliability of the connector.

There is today a large range of connectors available but few designed specifically for the conditions experienced in the various automotive environments; see Appendix A. Such connectors are required to carry both power and signal currents with high reliability and yet at the same time be manufactured at low cost. In addition, demands are now being placed on the designer for:

- (i) miniaturisation and higher pin counts;
- (ii) more safety critical applications, e.g. ABS<sup>A</sup> and airbag circuits;
- (iii) higher environmental demands (e.g. higher under-bonnet temperatures, exhaust gas sensing circuits);
- (iv) lower currents or dry circuits;
- (v) new technologies (insulation displacement connectors (IDC), surface mounting);
- (vi) system changes (permanent energisation, higher voltages, multiplexing).

The ability to make and break circuits is not without inherent drawbacks in terms not only of added cost but also of reliability, as any discontinuity in any conducting track or lead is a possible site of electrical resistance. Reliance on electrical contact by simple mechanical pressure alone is predisposed to failure due for example to: stress relaxation, ingress of foreign debris, and build-up of corrosion products, yet this principle is the basis of all separable connector joints.

A survey of Connection/Connector failures; Fig.2.2, carried out by the Automobile Association<sup>1</sup>, showed that the majority of vehicle roadside failures occurred with high current battery and starter motor connections. However 'other connections' on the remaining circuits, representing some 37% of the total failures, were corrected by no more than simply disturbing the connector. These would be expected to contribute to many of the 'No Fault Found' (NFF), service returns received and investigated by electrical and electronic component manufacturers.

Contact reliability may be defined in various ways by different engineers but all agree that the Contact Resistance (CR) value is of most concern. There is a limiting value which is purely application dependant and cannot be generalised. For example, it is possible that an increase in CR of only a few milliohms might lead to the failure to operate of a low signal sensing circuit, whereas in conventional automotive electrical power circuits, there is normally sufficient energy for electrons to tunnel through very thin films at contact interfaces. The connector therefore is defined as 'failed' when its CR exceeds a certain specified limit.

To minimise as far as possible potential environmental influences on connector reliability, it is important that the physics and chemistry of the contact surfaces and

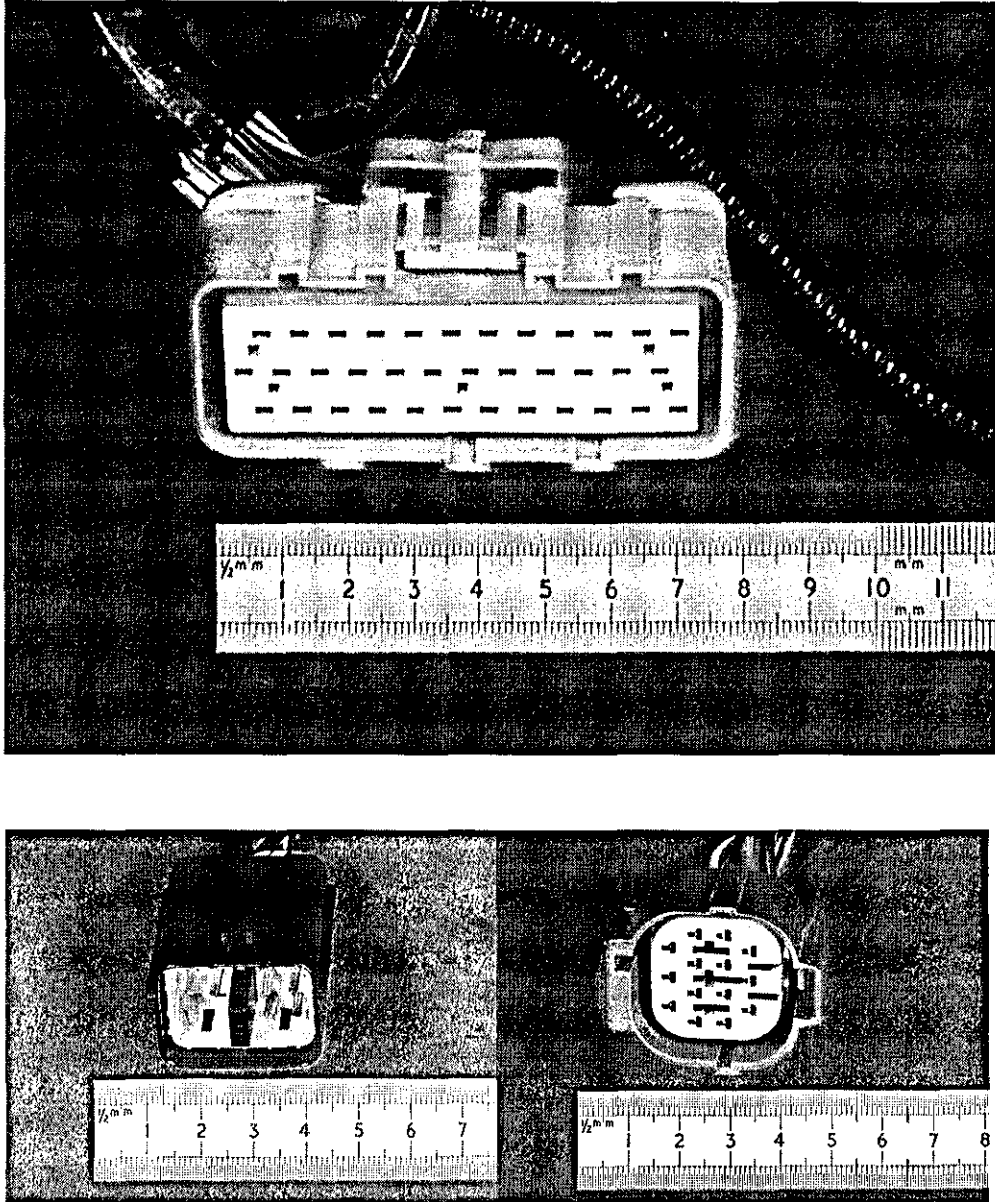


*Fig. 2.1 Examples of Typical Modern Automotive Separable Connectors*

their interactions with each other and their surroundings is well researched. For almost all components and devices, ultimate reliability can, in most cases, be approached if not actually achieved by using the best designs and materials, regardless of the expense involved. However, in the competitive markets of today, the designer is being

continually forced to reduce material and processing costs. For connectors on automobiles, apart from the rigorous requirements of safety critical circuits such as those found in ABS<sup>A</sup> braking and air-bag systems, gold platings, which are now the industrial standard in aerospace applications, would usually be prohibitive and cheaper alternatives must be sought.

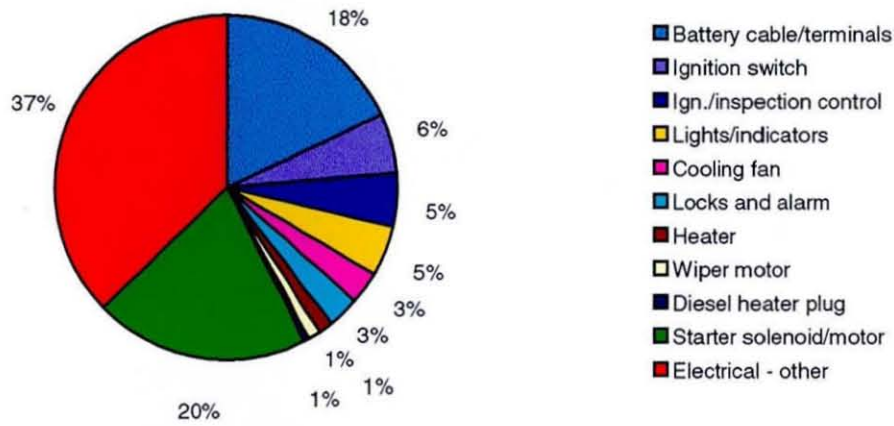


**Fig. 2.2 Results of a Survey of Automotive Electrical Connector/Connection Failures<sup>1</sup>**

## 2.2 Connector Materials

### *Metallic Components*

Correct materials selection is paramount for any design but conflicting material requirements may result in the optimisation of fundamental properties. For example in the demand for miniaturisation, high strength, good electrical conductivity and resistance to stress relaxation must still be maintained. A higher strength is required to obtain the required contact force, better conductivity is needed to minimise ohmic heating and low stress relaxation is necessary to ensure stable contact at high ambient



temperatures over long periods of time. This may not be achievable using a single material and may therefore necessitate the use of composite materials and platings.

Historically, contact materials for automotive applications were limited to low cost and low performance alpha brass and higher cost, higher performance phosphor bronze. Today, however, the interaction of operating parameters and their relative importance, cannot be satisfied by these alloys alone and therefore a whole range of copper-based alloys have been introduced. These include alloying additions of for example: nickel, aluminium, zirconium, magnesium, silicon, cobalt, iron, titanium and chromium, to tailor mechanical properties to specific applications<sup>2</sup>.

The condition of the contacting surfaces is of major importance in any electrical contact. Although this will be dominated by the properties of a surface coating, the substrate can, if manufactured using inferior processing methods, result in the formation of accentuated topographical features which will reduce the true contact area. Almost all connectors are manufactured from strip material and the ductility of the alloy must be considered when complex forming processes are required without the introduction of microcracks. Connector insertion forces must be relatively high to ensure good electrical contact and alloys possessing low hardness values, which are prone to surface scoring, are particularly vulnerable if, during the lifetime of the connector, there are numerous separations.

The female half of the connector assembly is a spring which is deflected during insertions and, under high vibration conditions, may be subjected to repeated and fluctuating stresses. Low fatigue resistant alloys are therefore to be avoided together with any high stress raisers in the form of small radii which may initiate fatigue fracture. Although not normally considered to be a potential cause of failure, the siting of a connector assembly where it may, for example, experience high rotational speeds at relatively high temperatures, could facilitate the onset of creep resulting in the continuing deformation with time of the female connector, if subjected to a constant stress.

In miniature high dissipation contacts, thermal conductivity may become an important factor in material selection. Copper alloys, as with most metals, have both high thermal and electrical conductivity, the two parameters being related, as they both depend on lattice and electron contributions. But although the thermal conductivity of pure copper is high ( $389 \text{ Wm}^{-1} \text{ K}$ ), this can reduce with cold working and the presence of only low concentrations of impurities such as zinc, silicon, aluminium and phosphorus.<sup>3</sup>

### *Housings*

The connector is generally insulated and the insulation acts not only to electrically isolate individual male or female contacts but also to act as a housing for multi-pin devices. Contacts, either male or female, are simply inserted into plastic mouldings or are moulded into the polymer. A large variety of polymers are used for automotive connectors, which are excellent insulators (typically  $10^{16} \Omega \text{ cm}$ ). These include: nylon-polyamide 66 (PA), polybutylene terephthalate (PBT), polyphenylene sulphide (PPS), polypropylene (PP), polyphenylene oxide (PPO) and acronitrile butadiene styrene (ABS<sup>B</sup>).

## **2.3 Connector Coatings**

The contacting surfaces of connectors can be that of the bulk materials themselves or applied finishes such as electroplated, hot dip coatings or clad metals. Chemical or physical vapour deposited and electroless metal coatings are alternatives but are not generally used for automotive applications. The connector is coated in order to provide a satisfactory combination of: good wear and mechanical properties; low and reproducible CR and; corrosion resistance, all at an acceptable cost level.

Each finish will have particular properties which will depend on the material used and in some cases on the method of application. Furthermore, the properties of the base alloy must be considered in order to avoid the possibility of material interactions under specific service conditions. For example, an incorrect combination may result in

the production of a bimetallic couple with accompanying corrosion attack or diffusion of substrate metal atoms into the coating with temperature, resulting in the formation of possibly undesirable intermetallics. Most electroplated connectors should incorporate an underplate of either copper, nickel or palladium nickel alloy to act as a barrier and thus reduce the risk of this solid state diffusion. Coatings are unlikely to be pure metals and will either contain contaminants such as carbon from organics in the electroplating process or deliberate additions such as lead in electroplated tin. As a result the applied surface coating will not possess the same physical and chemical properties as the pure metal.

Due to the increase in the requirements for low power and safety critical electronics on vehicles and the developments in selective plating techniques, bright acid hard gold contacts are seeing increasing usage on vehicles<sup>4</sup>. One major advantage of gold as a contact material is its ability to withstand large numbers of insertions and withdrawals without a significant increase in CR. Although gold is inert to most corrosive media, electroplated gold, depending on thickness, suffers from the consequences of porosity<sup>5</sup>, that is the formation of galvanic cells with the less noble underplate. In aggressive environments, porosity leads to pore corrosion where an electrolytic cell is set up between the gold and the nickel underlayer and eventually the copper alloy substrate. This can result in the corrosion film progressing across the gold surface, which may eventually cause high CR. It has been shown<sup>6</sup> that a porous gold finish may be less reliable than a good tin coating in a salt-laden environment. This is particularly true on brass substrates where the gold acts as an accelerator for dezincification.

Palladium and platinum contact metals have been used in corrosive environments but both have a very high catalytic activity and in a fretting regime can promote the polymerisation of organic contaminants or lubricants to produce insulating films known as frictional polymers<sup>7</sup>.

In contrast, silver is not a widely-used coating for automotive connectors due to tarnishing in atmospheres containing sulphur and to its tendency to migrate in the presence of moisture, forming dendritic growths which are liable to cause current leakages.<sup>8</sup> The relatively low popularity of silver is reflected by the small number of papers published relating to its use compared to the large amount of information available on the behaviour of gold and tin finishes.

There are a few high temperature automotive applications, e.g. the exhaust gas sensor, where nickel finishes are applied. In general nickel is avoided as it forms a hard insulating oxide which is difficult to fracture under normal contact loading.

Tin is a successful coating due to a combination of low hardness, and good corrosion resistance and can be applied to connector alloys either from the molten state as pure tin or electrolytically as matte tin using alkaline sodium or potassium stannate or acid stannous sulphate or fluoborate baths. Bright tin is produced either using proprietary chemical additions or by reflowing. Although tin forms a natural oxide layer, this is both thin and stable and the softness of tin allows break up and displacement of oxide during the wiping actions of insertion.

Electroplating is a common method of depositing a metal coating onto the contact base alloy. Stamped out contacts are either vat or barrel plated with a variety of metals and alloys which may be with or without underplates. The process employs an aqueous solution of a salt containing the metal ion which is deposited on the connector which forms the cathode. An anode of the same metal as the metal ion in solution is usually used. By applying a potential across the electrodes, the positive ions migrate to the cathode where they gain electrons and are chemically reduced. For selective deposition, particularly of gold, a process known as jet plating may be adopted. Brighteners in the form of organic compounds can be added to electroplating baths to improve the appearance and in some cases to increase the hardness of the deposit.

Electroless plating as the name suggests precludes the need for an external electrical source but makes use of galvanic cell reactions or catalysts with self-reducing plating baths. The technique is the basis of printed circuit and additive technology and as such may be used at some stage in the formation of the male connector with final finishes being normally applied electrolytically. Another method of applying a metal coating is to join the dissimilar metal strips to one another by co-rolling or diffusion bonding. This technique, known as 'cladding' is often used in the manufacture of lead-frames for electronic packaging where aluminium is bonded to copper.

An investigation into the properties of HDT is the focus of this study. Hot dipping requires the immersion of the substrate material, usually pure copper or a copper base alloy strip, into a molten metal, usually tin. There are two methods of ensuring a controlled thickness of the tin: hot dipping followed by mechanical wiping for coating thicknesses between 0.8 and 2.0  $\mu\text{m}$ , and; hot dipping with air knife finishing known as 'Hot Air Levelled Tin' (HALT), for tin coatings thicker than 1.5  $\mu\text{m}$ . Both methods require only a brief contact with the melt (approximately 1 second) and as a result high production output can be achieved with travelling speeds of about 100 m/min. HDT and HALT plated strip have characteristic stripes of intermetallics which form at the tin/copper interface, the significance of which has not always been appreciated and will be examined in some depth in this study.

Connector components can either be stamped out of pre-plated HDT or HALT stock or they can be post-plated, with the former constituting a major economic advantage over post-plating. Thus for economical reasons, most automotive contacts are made from pre-tinned strip. The process, however, is not without its drawbacks. For example, on stamping the cut edges are exposed, introducing a potential site for galvanic corrosive attack.

In Asia and especially Japan, electroplated tin followed by re-flowing is the preferred method of coating connector substrates. Electroplated tin is prone to whisker formation due to residual stresses and the addition of a few weight percent of lead

followed by reflow techniques has been found to overcome the problem.<sup>9</sup> To minimise costs, the tin thickness is generally limited to 2-5 microns and it has been found beneficial to use an intermediate barrier layer of nickel to reduce the diffusion of substrate elements. This applies particularly to zinc migration from brass substrates. Electroplated tin has been found to contain high levels of carbon<sup>10</sup> and if re-flowed can form an intermetallic layer at the copper/tin interface. Tin plated by this process does, however, allow complete coverage of the connector or lead-frame.

Tin plating, from the melt or by electrodeposition, has been shown to offer good corrosion protection at significantly lower cost than gold.<sup>11,12</sup> Unfortunately, due to high frequency micro-motion such as that induced by vibration and low frequency relative movement caused by differential thermal expansion, tin is prone to fretting wear, with the resultant generation of electrically resistive oxides.<sup>13,14</sup> The effects of this wear regime, more accurately described as *fretting corrosion*, have however, been shown to be reduced by the application of a suitable lubricant chosen to allow sufficient metal-to-metal contact for electrical conduction and at the same time act as a barrier to reactive gases, including oxygen, present in the environment.<sup>15,16</sup>

## 2.4 Contact Geometry

The connector is essentially a spring utilising the high elastic strain of the material, usually a metal or alloy, to apply a load normal to the contacting surface. A variety of spring systems have been developed to give the necessary contact force with either the spring itself providing electrical contact or it in turn applying a load to a separate contact. The loading is critical for it must be high enough to deform contact asperities, yet at the same time allow minimal insertion forces during 'make and break' operations. There are three principal contact geometries for connectors; Fig. 2.3, for which the Hertzian elastic stress equations due to pressures on elastic bodies are given below<sup>17</sup>:

(i) Sphere on flat:

$$\sigma_c = 0.918 \left[ \frac{P}{D^2 C_E^2} \right]^{1/3} \quad (2.1)$$

where:

$$C_E = \frac{(1-\nu_1^2)}{E_1} + \frac{(1-\nu_2^2)}{E_2} \quad (2.2)$$

(ii) Cylinder on flat:

$$\sigma_c = 0.798 \left[ \frac{P}{D^2 C_E} \right]^{1/2} \quad (2.3)$$

(iii) Cylinder on cylinder:

$$\sigma_c = \frac{1.5P^{1/3}}{\pi\alpha\beta} \left[ \frac{D_1 + D_2}{C_E D_1 D_2} \right]^{2/3} \quad (2.4)$$

Notation:  $P$  = total load (N),  $\sigma$  = stress ( $\text{Nm}^{-2}$ ),  $\nu$  = Poisson's ratio,  $E$  = modulus of elasticity ( $\text{Nm}^{-2}$ ) and  $\alpha$  and  $\beta$  depend on  $\frac{D_1}{D_2}$  according to the following; Table 2.1:

$D_1/D_2$	1	1.5	2	3	4	6	10
$\alpha$	0.908	1.045	1.158	1.350	1.505	1.767	2.175
$\beta$	0.908	0.799	0.732	0.651	0.602	0.544	0.481

NB: as  $D_1/D_2$  tends to 1, then the solution tends towards the sphere on a flat.

**Table 2.1 Factors for  $\alpha$  and  $\beta$  for Various Values of  $D_1/D_2$**

By plotting Hertzian stress against normal force for the different contact geometries and by using the mechanical properties typical of a connector alloy, the superior design is found to be that of 'sphere on flat' followed by 'cylinder on cylinder' and 'cylinder on flat'; see Fig. 2.4.

Although the actual behaviour of the materials at the contact interface is extremely complex, involving elastic/plastic deformation of contact asperities, the Hertzian stress calculations based on elastic theory of the area of contact and stress distribution

therein, can be a useful design tool. The models, however, soon break down as the values used rapidly change during a fretting wear process. Katner and Hobgood<sup>18</sup> have shown that the amount of Hertzian stress necessary to ensure stable dry circuit CR in miniature contacts is in excess of  $2000 \text{ MNm}^{-2}$ , but when thin metal coatings are used calculations are further complicated by plating thickness, hardness and microstructure.

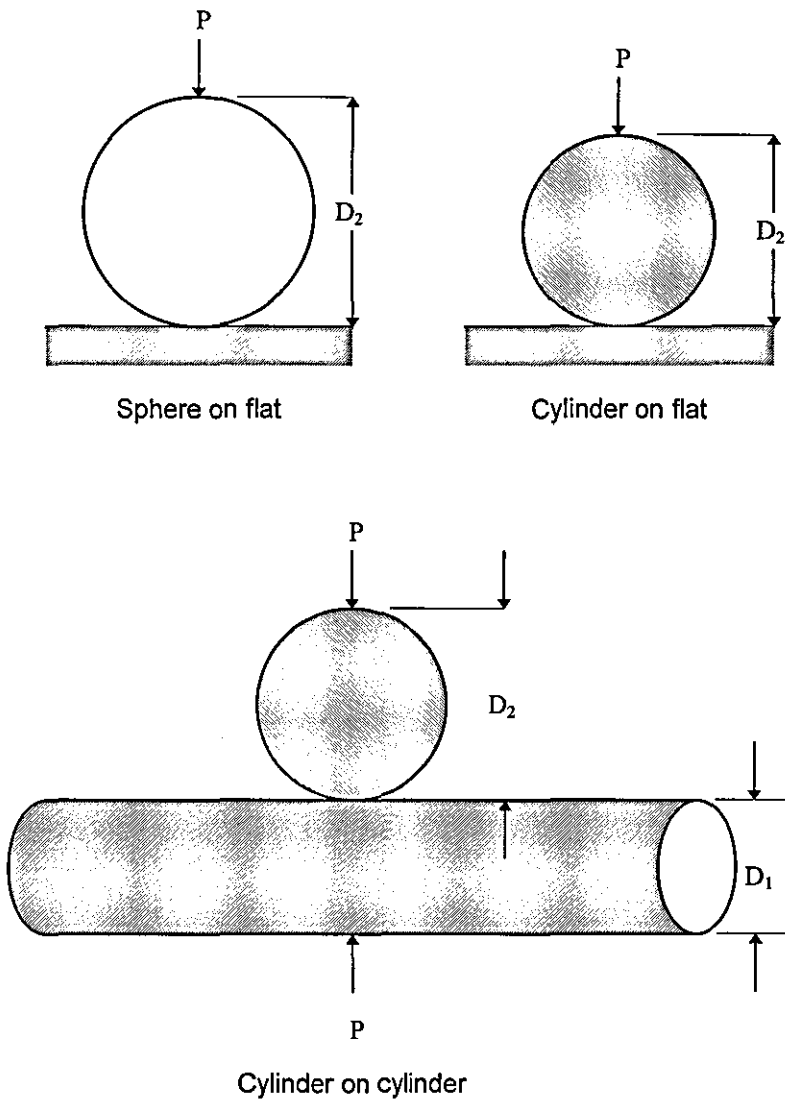


**Fig. 2.3 Principal Connector Contact Geometries**



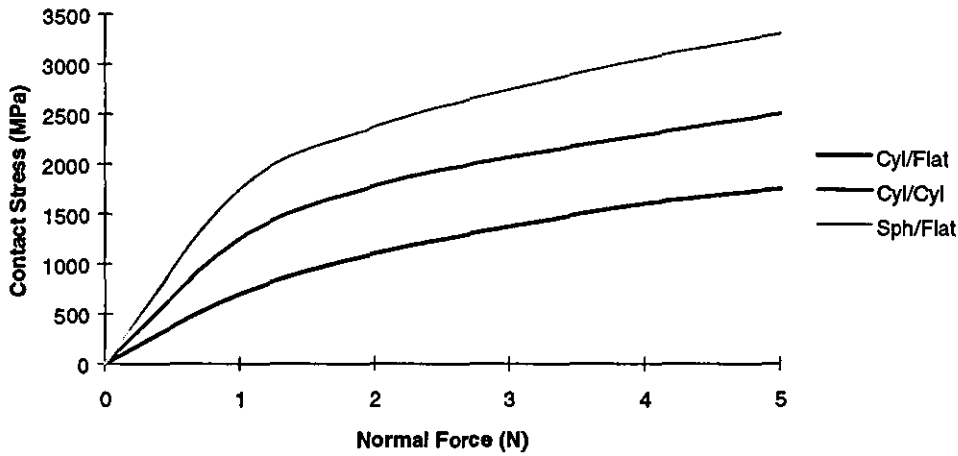


**Fig. 2.4 Schematic Plot of Resultant Hertzian Stress for Three Contact Geometries.**

It is generally assumed that the contact force provided by the spring members of the connector remain constant after insertion. Unfortunately this is not always the case, since the residual stresses remaining in the spring after forming relax due to a variety of factors, which are primarily temperature dependant<sup>19</sup>. As the contact area is a function of contact pressure, Hertzian stress relaxation is clearly an important reliability issue, highlighting the need for stress relaxation resistant materials.

The causes of stress relaxation are similar to those of creep, that is, over a period of time under load, at a rate dependant on temperature and other factors, the high energy dislocation structure induced by cold rolling and forming is re-arranged. This occurs due to dislocation movement resulting in a lower energy structure. In a material which has undergone creep, the result is a change in geometry, whereas stress relaxation causes a lowering of the internal stresses. This means that the normal forces acting on connector spring elements will reduce in service, as elastic displacement is converted into permanent deformation. There are several factors which affect the stress relaxation rate, which include rolling direction, grain size and temper but the major effects are stress level, time and temperature. Generally, the higher the stress level the

faster the rate of relaxation. As for thermally activated processes such as diffusion, tempering and creep in metals, the rate of relaxation follows the Arrhenius equation:

$$D = D_0 \exp^{(-Q/RT)} \quad (2.5)$$

where  $D$  is the rate in  $\text{cm}^2\text{s}^{-1}$ ,  $D_0$  is a constant ( $\text{cm}^2\text{s}^{-1}$ ),  $Q$  is the activation energy of the process ( $\text{kJmol}^{-1}$ ),  $R$  is the gas constant ( $\text{Jmol}^{-1}\text{K}^{-1}$ ) and  $T$  is the temperature (K).

## 2.5 The Contacting Surfaces

In an effort to understand the mechanisms which operate to cause connector failure, it is necessary to examine the nature of a surface in terms of its topography, mechanical and physical properties and chemical composition. Highly polished surfaces are known to contain peak to valley heights of submicron dimensions and when two such metal surfaces are brought gently together, contact occurs only at the higher isolated points where the asperities on the two mating surfaces touch. At the asperities, contact pressures can be extremely high even for very light loads of  $<10^{-2}\text{N}$ , resulting in their elastic and plastic deformation<sup>20</sup>. The summation of the resultant areas of contact under normal loading for a given surface profile, hardness and applied load, will determine the 'real' contact area.

Pioneering experiments by Bowden and Tabor<sup>21,22</sup> showed that the real area of contact for extended surfaces is a minute fraction of the nominal area but to ascertain this true contact area by direct measurement is extremely difficult. However, a number of models have been proposed which predict the real contact area for various parameters.<sup>23</sup> As an example of just how different real to apparent contact areas are, in some early work by Antler and Gilbert<sup>24</sup> it was calculated that for finely lapped steel plates having an apparent area of  $21\text{cm}^2$  when in contact at  $19.6\text{N}$  load, the true contact area was only  $2 \times 10^{-4} \text{cm}^2$ .

Surface features may be classified at the macro, micro and atomic levels. Relatively large surface topographic features of the order of microns and above may be introduced during processing, e.g. rolling, machining, grinding and the application of a coating. On the microscopic scale, such features are dominated by changes in orientation of individual crystallites, inclusions, open porosity, corrosive attack causing pitting and the formation of corrosion products. Finally, on the atomic scale, vacant lattice sites, minute asperities of extra atoms protruding above the surface, lattice distortion by interstitial and substitutional atoms and adsorbed atomic and molecular species all combine to modify the surface profile. When a free surface is produced, newly exposed atoms in the lattice relax into an equilibrium configuration which differs from that of the bulk due to the lack of balancing forces but an atom residing in the centre of the lattice will be influenced by the neighbouring atoms which surround it and will thus possess a different specific energy. The surface plane may relax outwards, with the atomic arrangement parallel to the surface remaining unchanged, which can result in the occurrence of a surface electrical dipole moment. In addition, electrons of atoms in the surface may occupy energy levels which do not exist in the bulk, which may affect chemical reactivity.

Macro surface characteristics can be relatively easy to control but micro and particularly atomic scale features are almost impossible without extensive surface treatments. As a consequence, over any selected area of the contact surface of a mass produced electrical connector, there are generally, at this scale, wide variations in topography.

In an attempt to quantify surface irregularities, a number of techniques have been developed, from those with spatial resolutions on the scale of atoms and molecules e.g. scanning tunnelling and atomic force microscopy, to less sensitive methods adequate for the study of most engineering surfaces, such as the stylus profilometer and optical interferometer. Scanning electron and confocal microscope imaging using stereo pairs and sophisticated software are now being increasingly used.

To calculate the real contact area it is obviously necessary to determine the number of peaks in contact. Each surface will have its own surface profile or 'roughness' which can be described in a variety of ways. The most common measurement is the centre-line-average or  $R_a$  which is defined as the average (absolute) deviation from a datum line having equal areas above and below. Unfortunately, however, this value alone is insufficient, as not all asperity radii are the same for any given surface. As a result when two surfaces are placed in contact with each other, many of the peaks will not be touching, thus decreasing the calculated contact area. To improve results it is therefore necessary to measure: the statistical height distribution, sampling distances, the number of asperities and their mean radius of curvature. In a paper by Greenwood<sup>25</sup> it was shown that by producing a histogram of curvatures of 749 peaks on a specimen of bead-blasted gold, the distribution was Gaussian. This is, however, in terms of topography, an isotropic surface with generally uni-axed indentations. For a connector contact using a rolled metal alloy, the surface features would tend to show some directionality on the micro and macro scale, making the distribution almost certainly skewed.

A first approximation to determining the total contact area ( $A$ ) between two solids is from the equation:

$$A = \frac{P}{H} \quad (m^2) \quad (2.6)$$

where  $P$  is the load and  $H$  is the hardness of the material. This assumes ideal (i.e. perfectly smooth) surfaces and a hardness value derived from bulk material measurements. For 'real' surfaces the degree of elastic and plastic deformation of asperities will be a function of the material's bulk hardness but this value may be modified by mechanical work hardening, chemical surface modification and heat treatments, as well as by local heating. Residual stresses, for example, induced by mechanical processing may alter the bulk shear strength of the asperity dramatically. It has also been reported<sup>26</sup> that as a result of these stresses volume changes can occur in electroplated tin coatings due to the growth of whiskers.

Elastic and plastic strain of the asperities will by definition be dynamic, that is on loading there will be deformation with time and as a result, new contacts will be continually forming, continuously changing the contact area. In a study by Pashley and Pethica<sup>27</sup>, to determine how asperities deform elastically, a fine point of nickel was brought into contact with a single crystal of the same metal in an ultra high vacuum. It was found that if a single region of contact is assumed, the electrical conductance could be measured and the area of contact determined. On applying a load of the order of micro-Newtons, the area of contact increased with applied load due to elastic deformation. On releasing the load, the area of contact remained constant, until a negative load was applied, implying that strong metal-metal interactions had occurred. It was concluded that elastic contact caused tensile plastic deformation at the asperity interface, when the original surfaces were pulled apart.

Such measurements assume the existence of ultra-clean surfaces in contact and *in vacua* but this is rarely the case in practice, as contaminants and oxide films are invariably present. It is generally considered that a surface consists of the 'actual' surface, that is the topmost atomic layers of the bulk material or any applied coating, together with anything that it may be supporting, such as an oxide film or contamination by, for example, particulates and/or hydrocarbon films. Any 'clean' surface, when exposed to the atmosphere will, because of its surface energy, possess a potential field and will attract gaseous molecules with or without chemical bonding. In a comprehensive review on the subject by Adamson<sup>28</sup>, the adoption of adsorption time, i.e. the time of stay of molecules in the vicinity of the surface as a function of pressure and temperature, is a useful approach in the study of gas/solid surface interactions.

Where there is a transfer of electrons between the adsorbed molecule and the single layer of atoms or molecules at the surface of the solid, adsorption is known as 'chemisorption', which is reported<sup>29</sup> to involve energies of the order of  $200\text{kJmol}^{-1}$ . Where no chemical reaction takes place, i.e. 'physisorption', bonding to the substrate relies on electrostatic, Van de Waals and polarisation forces, with typical energies of  $20\text{ kJmol}^{-1}$ . Ultraclean surfaces are, however, difficult to produce without

sophisticated techniques such as plasma etching but within the local gas, contaminant and oxide free region, formed as a result of the shearing of two mating asperities, it may be clean enough for metal-metal interactions and instant microwelding to occur.

In Adamson's critical discussion a number of models are evaluated, which attempt to describe the physisorption processes. Among the most widely applied are those of Langmuir, 'BET's' (Brunauer, Emmet and Teller), Temkin and Freundlich. Langmuir's adsorption isotherm assumes that molecules are adsorbed as a single layer with no interactions between them and the amount of a substance adsorbed (at constant temperature), is proportional to pressure and the BET equation determines the adsorption rate of a film more than one molecule thick by computing the surface area of the top layer. The Temkin isotherm describes the extent of adsorption of a species on a surface as a function of concentration, whilst that of Freundlich relates the volume of a gas that is adsorbed onto a surface at a given temperature to the pressure of the gas. To determine compositional changes experimentally, there are various surface analytical techniques such as depth profiling to identify and quantify the species attached to or lying on the surface of the substrate and those that occur within the outermost atomic layers of the substrate itself.

## 2.6 Contact Resistance

Any energy distribution system resistance to flow, in this case electrons, must be kept to a minimum. Therefore, materials with low electrical resistivity must be employed. Resistivity ( $\rho$ ) is the reciprocal of conductivity and is measured in  $\Omega\cdot\text{m}$  and for most metals increases with temperature. For example brass doubles its resistance over  $\Delta T$  of 50 °C and tin shows a  $\Delta\rho$  from 0.11 to 0.20  $\mu\Omega\cdot\text{m}$  between 0 and 200°C<sup>30</sup>. In addition, intrinsically low resistivity materials must be selected to reduce the effects of ohmic heating.

Resistivity can be increased by the presence of structural imperfections brought about by quenching, cold working and impurities. The addition of alloying or impurity elements to copper for example, increases the electrical resistivity at a rate dependant

on the element, where the greater the solubility, the greater the effect. Variations in even trace levels of phosphorus, arsenic, iron or silicon will drastically decrease the conductivity of the metal<sup>31</sup>. There is a strong relationship between a metal's electrical and thermal conductivities, as both parameters depend on lattice and electron contributions. This is described by the Wiedeman-Franz-Lorentz law<sup>32</sup>:

$$\frac{k_t}{k_{el}T} = \text{constant} \quad (W\Omega K^{-1}) \quad (2.7)$$

where  $k_t$  and  $k_{el}$  are thermal ( $Wm^{-1}K^{-1}$ ) and electrical ( $\Omega^{-1}m^{-1}K^{-1}$ ) conductivities respectively and  $T$  is the temperature (K).

For the electrical connector, contact is achieved by sliding the contacting surfaces over each other causing the female connector contact springs to deflect and supply the required contact force. After manufacture, the surfaces will have an initial topography and composition but during insertion, high spots will be deformed as a result of this wiping action to produce multiple metallic contact points. Electrical continuity is established through metal to metal junctions called 'a-spots' which form under local loading when asperities yield, oxide films fracture and metal from both sides flow together as in Fig. 2.5. (Examination of the literature indicates that there is some confusion with regard to the use of the term 'a-spot', which has been erroneously used by some researchers to describe the asperity<sup>33</sup>).

Where oxide and contaminant films are thin enough, electrons are able to tunnel through certain very thin films by a process known as quantum barrier penetration, whereby a charged particle can penetrate and cross a small region where the potential is greater than the particle's available energy. Mathematical expressions have been derived by Holm to describe this tunnelling effect.<sup>34</sup> Electron transfer is, however, generally via the a-spots but as these contact points are extremely small, electron movement may be limited causing current flow lines to be constricted.

In summary, current flow is influenced by:

- (i) metal contact where current passes through without perceptible transition resistance at the interface, apart from the resistivity of the materials themselves;
- (ii) a-spots and quasi-metallic spots which, due to their dimensions, can constrict the passage of electrons;
- (iii) areas covered by relatively thick films which are practically insulating.

As a consequence, the total CR ( $R_t$ ) is the sum of three terms:

$$R_t = R_b + R_c + R_f \quad (\Omega) \quad (2.8)$$

Where  $R_b$  is the region of constant current density, that is the resistance of the bulk material(s), which will be dependent on bulk resistivity,  $R_c$  the constriction resistance across a-spots and quasi-metallic spots and  $R_f$  the resistance due to films and other contaminants.

A number of models have been proposed by various workers to link constriction resistance, resistivity ( $\rho$ ) and real contact area<sup>35,36,37,38</sup> with a refinement to this early work being published by Boyer et al.<sup>39</sup> Constriction resistance can be expressed as a function of hardness  $H$ , if the contact normal force  $P$  and resistivity  $\rho$  are constant<sup>40</sup>.

Work by Runde *et al*<sup>41</sup> suggested that for aluminium contact interfaces carrying direct current, the electric current itself was responsible for degradation of the a-spots by a process known as electromigration. From SEM examinations of microsections through mating contacts, they observed voids and cavities in the cathode which severely affected the electrical properties, resulting in the inability of the a-spots to pass the high current densities. They proposed that as a result of this, new a-spots



were being continually formed and the process continued until the asperity and ultimately the entire contacting surface would be degraded. The general view, however, is that for non-noble metals degradation is as a result of a gradual oxidation or corrosion around the periphery of the a-spots causing the metallic junctions to shrink.

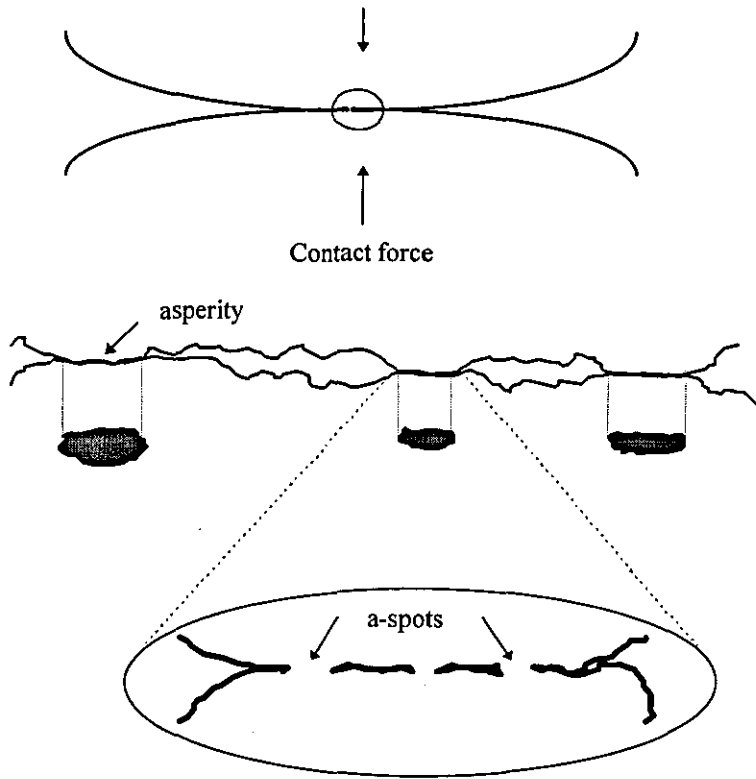


**Fig. 2.5 a - Spot Formation at the Contact Interface.**

In the author's opinion, it is likely that, for certain metals and alloys, electromigration may be the dominant mechanism. This form of mass transport was once prevalent in aluminium metallised microcircuits until the addition of a few percent of copper<sup>42</sup>, however, due to localised temperature increases, oxidation will almost certainly contribute to failure. A definitive test would of course be to carry out the experiment in an inert gas atmosphere to minimise the occurrence of oxidation.

## 2.7 Corrosion

Corrosion is the process which returns a metal to a lower energy form (i.e. oxide, sulphide, chloride, etc.), by reacting with its environment, and in doing so, accounts for costs to industry and society of billions of pounds per annum.<sup>43</sup> In general, the costs attributable to corrosion can be separated into two terms:<sup>44</sup>

- (i) Costs associated with the provision of systems to resist corrosive attack - plating, surface treatments, lubricants, conformal coatings, housings, over-design, etc.
- (ii) Costs associated with failures resulting from corrosion.

Corrosive attack can operate through a variety of mechanisms but, whilst still obeying the laws of electrochemistry and thermodynamics, it can nevertheless often be unpredictable.

Corrosion of electrical and electronic components has traditionally been described as being either 'wet' or 'dry', with the latter being by direct gas or vapour/metal reactions, where oxidation of the metal and reduction of the non-metal occurs at the metal/gas interface. In such cases, the continuous film of reaction product is rate determining, i.e. as the film thickens the growth rate decreases. 'Wet' corrosion on the other hand requires the electron acceptor or oxidising agent to be in solution (usually aqueous) and the resultant corrosion products formed at the metal/solution interface being transported away by a variety of mechanisms (e.g. diffusion, migration and convection), thus resulting in a more linear growth rate. Shreir<sup>45</sup> in his classic textbook on corrosion, realising the ambiguities associated with this simple definition suggested the following 'Classification of Spontaneous Corrosion Reactions':

- (i) Film Free Chemical Interaction - where there is a direct chemical reaction with a metal and its environment and no transport of charge, and;

- (ii) Electrochemical - involving an electronic exchange mechanism resulting in a flow of current.

From Shreir's definition, corrosion of electrical contacts in automotive environments will almost always be electrochemical, resulting in general corrosion and degradation of the connector and in the formation of electrically insulating oxides and other films at the contact interface. Electrochemical corrosion can further be subdivided into specific forms depending on the materials involved and the presence of applied stresses and electrical currents.

### **2.7.1 'Wet' Corrosion**

For the electrical connector, 'wet' corrosion, as galvanic and aqueous and 'dry' corrosion, in the form of surface oxidation, are the major forms encountered. Galvanic corrosion is dependent on the presence of at least two dissimilar metals (or phases) and a conductive solution between them to set up an electric circuit. The dissimilar metals provide an inherent electromotive potential which, when connected by the conductive solution, forms an ionising circuit, see Fig 2.6. It is possible to predict to some extent the degree of galvanic corrosion, depending on how far apart the metals are in the galvanic series, however, it must be realised that these values refer to ideal conditions and whether or not the metal forms a passivating film on its surface. In practice the potential of a metal in a solution depends on the composition of the particular solution as well as the metal. In addition, the ratio of the exposed area of cathodic metal to that of the anodic metal in a galvanic couple will influence the extent to which galvanic corrosion will take place. If the cathode area is large compared to that of the anode, the anodic current density is high, with the resulting polarization leading to an increase in galvanic corrosion.

In automotive harnesses, dissimilar metals are often found at connectors, crimps and soldered joints but the galvanic circuit remains passive until the two metals are bridged by an electrolyte or other conductive pathway. An electrolyte may be formed from contaminants which are activated by moisture, or may originate from lubricants

intentionally applied to the connector which have additives which themselves contain ionic species.

Tin is a widely used protective coating for steel and from an examination of the electrode potentials for iron and tin ( $-0.440\text{V}$  and  $-0.136\text{V}$  respectively<sup>46</sup> expressed on the hydrogen scale), it can be seen that tin is cathodic to iron whereas for tin plated copper, the substrate element has an electrode potential of  $+0.521$  and is therefore cathodic to tin. Britton<sup>47</sup> reports that intermetallic tin-copper compounds ( $\text{Cu}_6\text{Sn}_5$  and  $\text{Cu}_3\text{Sn}$ ) are cathodic to tin, copper and copper compounds. It is therefore likely that local corrosion of the tin plating and the underlying copper may be accelerated if the intermetallics which have formed, are exposed during fretting wear in the presence of an electrolyte, as in Fig. 2.7.

Aqueous corrosion occurs when a conductive solution comes into contact with a metal of a different potential from that of the solution. In an attempt to balance the potentials and reach an electrochemical equilibrium there is direct ion transfer. Fig 2.8 illustrates the case where a metal is in contact with an aqueous solution of for example, sodium chloride, where metal ions leave the metal to form the metal chloride.

The rate at which corrosion occurs can be increased by the effect of higher temperatures and applied voltage potentials. For example, if a conductive material is allowed to bridge between the voltage potential of the connector and either ground or another connector at a lower voltage, a continuous ionising cell may be set up as in Fig. 2.9. Corrosion products may change the electrical path through connectors when they react with moisture to form thin electrolytic films. These may spread and cause current leakage and undesirable conductive paths between electrodes, resulting in erratic signals. On the other hand, where moisture is absent the corrosion products may act as insulators providing a barrier to normal conductivity. As a consequence, changes in ambient conditions can cause a shift from a leakage pathway to an insulating barrier thus changing the mode of failure from electronic noise to high CR.

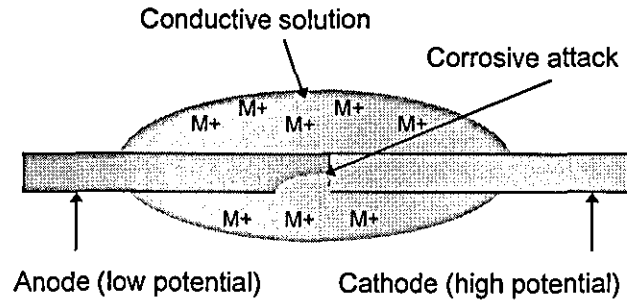


**Fig. 2.6 The Galvanic Cell**

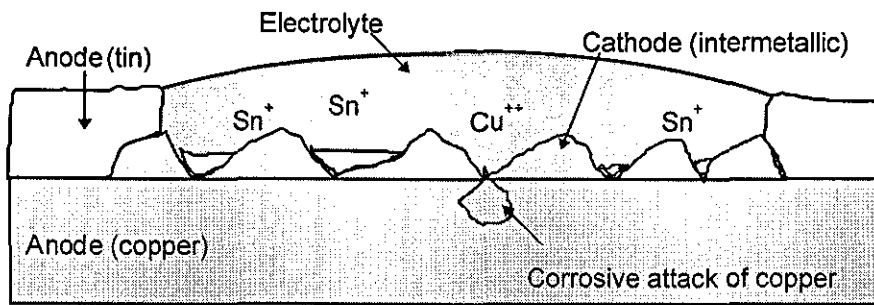


**Fig. 2.7 Galvanic Corrosion of Tin Plated Copper and Effect of Intermetallics**

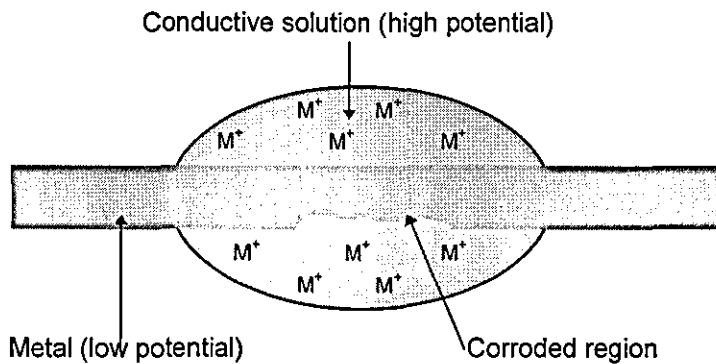


**Fig. 2.8 Aqueous Corrosion Cell**

Apart from contact with bulk liquid during, for example, rainfall or washing, corrosion can proceed as a result of the presence of a thin condensed or adsorbed film on the metal surface, the composition and thickness of which being influenced by the

species present and the physical and chemical atmospheric conditions. The concentration of the various ions present in the film and the ambient temperature will determine the degree of corrosion of the surface, whilst the presence of a thin layer of for example electrically insulating hydrocarbons will reduce attack. Reactions with the metal can also be slowed down by the development of patinas on the surface.

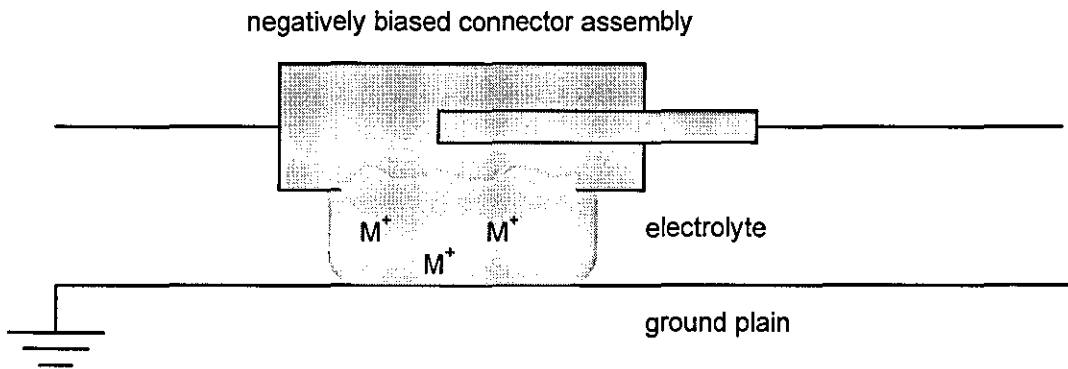


**Fig. 2.9 Corrosion Caused by a Leakage Current Pathway**

The critical relative humidity (RH) required to promote corrosion of clean metals is typically between 60% and 80%, where,

$$\text{RH} = \frac{\text{Water vapour pressure (at temperature (T))}}{\text{Saturated water vapour pressure (at temperature (T))}} \quad (2.9)$$

The periods of time for which the RH exceeds the critical level is known as the 'time-of-wetness'.<sup>48</sup>

Atmospheric corrosion is a discontinuous process. Initially, the liquid film containing the dissolved species condenses onto the metal surface. Corrosion then proceeds at a relatively constant rate until, due to evaporation, the salts are concentrated and

corrosive attack increases. Complete evaporation results in the halting of the corrosion process and may cause the solid salts to change state. Finally re-wetting of the surface may either remove the salts and reduce attack or cause the formation of a concentrated electrolyte and thus increase attack. Tin is regarded to be generally resistant to attack in most aqueous environments but localised corrosion around discontinuities have been reported,<sup>49</sup> which although usually associated with total immersion, could occur during cyclic condensation conditions.

### 2.7.2 'Dry' Corrosion

The transformation of a metal surface to its oxide on heating in the presence of air is generally termed oxidation. The same process may take place in the absence of oxygen by other oxidising agents present in the atmosphere such as ozone, hydrogen sulphide, halides and oxides of nitrogen and sulphur. When a metal oxidises there is a change in the Gibbs free energy (G), of the system which is equal to the work done or absorbed during the process. That is:

$$\Delta G = G(\text{products}) - G(\text{reactants}) \quad (2.10)$$

For a reaction to take place,  $\Delta G$  must be negative, i.e. there must be a decrease in free energy of the system.  $\Delta G$  for almost all metal oxide formation is negative, implying that metals are not thermodynamically stable in oxygen atmospheres and therefore oxidation will always tend to take place. For example SnO and SnO<sub>2</sub> have a Gibbs free energy of formation of -286.6 and -581.6 kJ/mole respectively, indicating that thermodynamically at least, oxidation will readily occur.

Oxidation is, as described by Shreir, electrochemical in nature, i.e. electron transfer is fundamental to the corrosion process. In the anodic reaction, the metal is oxidised forming a metal ion:



In the corresponding cathodic reaction, a simultaneous consumption of electrons occurs, which for atmospheric corrosion involves the reduction of oxygen. Here the gas is adsorbed onto the metal surface where it decomposes into atoms and ionises:



or in the presence of water vapour,



These reactions initiate the first oxide layer, which once formed, may provide a protective barrier to further metal/oxygen contact but as oxides are generally capable of continued growth, other mechanisms are therefore responsible. Some metallic oxide films, particularly if grown under controlled conditions may be continuous and non-porous as well as being adherent, non-volatile and non-reactive with many environments. Some metals on the other hand can form discontinuous (porous) oxide films, which contain microcracks due to thermal mismatch or differences in volume between the growing film and the substrate and in these cases the rate controlling process is other than solid state diffusion and cannot easily be predicted.

The mechanisms controlling the growth of both types of film have been extensively researched by Wagner and co-workers.<sup>50</sup> In their classic study it was proposed that the following four mechanisms are responsible for oxide growth and are dependant on the ionic diffusivity and electrical conductivity of the oxide film:

- (i) Oxygen molecules may pass relatively easily through porous films to reach the underlying metal where reaction takes place; see Fig. 2.10.



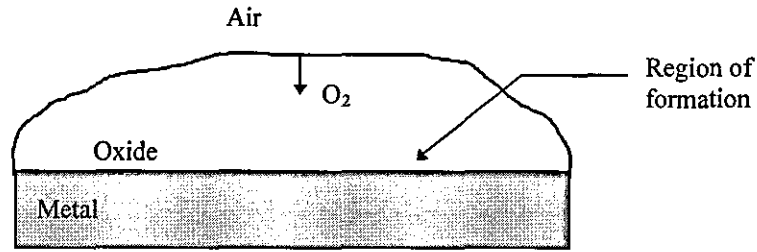


**Fig. 2.10 Oxide Formation at the Oxide/Metal Interface**

- (ii) In non-porous films, metal ions diffuse via lattice defects and electrons migrate to the oxide/air interface as in Fig. 2.11.

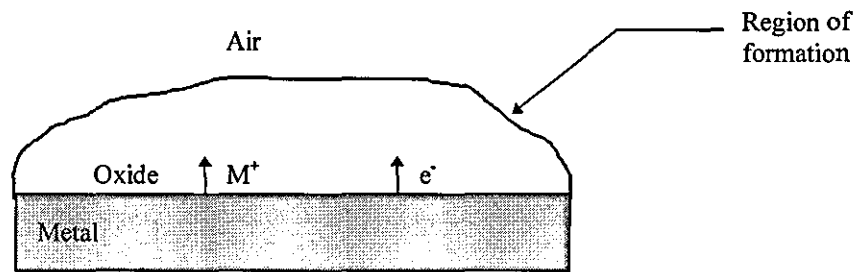


**Fig. 2.11 Oxide Formation at the Air/Oxide Interface**

- (iii) For continuous films, oxygen ions diffuse through the film to the metal/oxide interface and electrons migrate to the air/oxide interface; see Fig. 2.12.

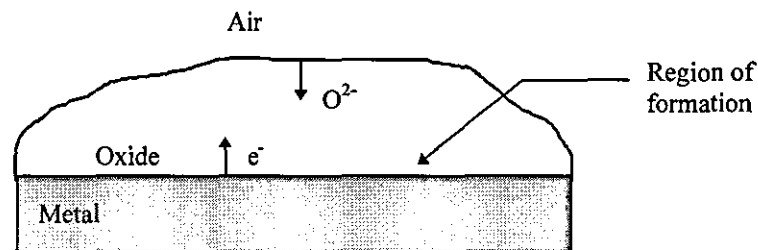


**Fig. 2.12 Oxide Formation at the Oxide/Metal Interface**

- (iv) If a combination of (i) and (ii) occur, oxide can form anywhere within the film as illustrated in Fig. 2.13.

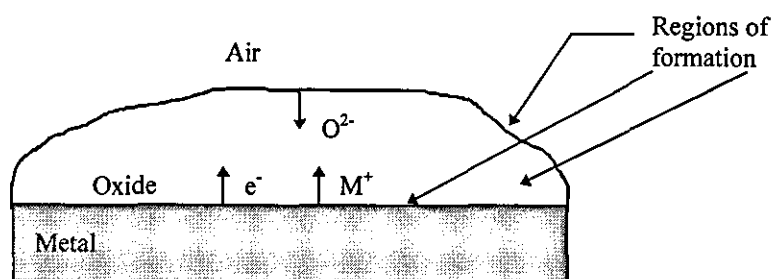


**Fig. 2.13 Oxide Formation at Each Interface and Within The Oxide Layer**

For non-protective films there is a linear growth rate, i.e. for an oxide thickness ( $x$ ) and time ( $t$ ):

$$x = x_0 + k_0 t \quad (2.14)$$

where  $x_0$  and  $k_0$  are constants depending on temperature and porosity.

For continuous films, the thickening of the layer requires the diffusion of metal ions, oxygen ions, or electrons across the film and follows Fick's first law of diffusion<sup>51</sup> giving a parabolic oxidation growth:

$$\text{Rate} = \frac{dx}{dt} = \frac{\text{constant}}{x}$$

i.e.

$$x^2 = k_1 t + x_0^2 \quad (2.15)$$

For protective films such as tin oxide formed below 160°C and having low electrical conductivity, logarithmic oxidation kinetics apply, due to the build up of an immobile layer of positive or negative charge. Here:

$$x = k_1 \ln t \quad (2.16)$$

Although not applicable in all cases, particularly if oxide growth relies on movement of oxygen inwards towards the metal, the nature of the oxide formed can be determined by an expression known as the Pilling-Bedworth ratio.<sup>52</sup>

$$\frac{\text{Vol. of oxide}}{\text{Vol. of metal}} = \frac{Md}{amD} \quad (2.17)$$

where M is molar mass of oxide ( $A_aO_b$ ) with density (D), (m) is atomic mass of metal with density (d) and (a) is the number of metal atoms per molecule of oxide.

For ratios less than 1, the oxide tends to be porous and non-protective, for ratios approximately equal to one, the oxide is non-porous, and if greater than one, a highly compressively stressed oxide may form. It has been argued however, that the rule may only be applied to predict whether or not the oxide layer will be in lateral compression or lateral tension<sup>43</sup>.

### 2.7.3 Surface Oxidation of Tin Contacts

The oxidation of tin has been extensively researched. In one early study it was found that at ambient temperatures in dry air and free from contaminants, the metal exhibited after 100 days, only slight evidence of oxidation and after 150 days a faint yellow-grey tarnishing observed.<sup>53</sup> Above 190°C, a film thickness sufficient to produce interference colours was reportedly produced in a few hours.<sup>54</sup> In studies using oxygen alone<sup>55,56</sup> it was shown that the microstructure of the oxide influenced further oxidation behaviour. Oxygen pressures under 133 Nm<sup>-2</sup> produced dendritic  $\alpha$ -SnO crystallites which grew at an increasing rate, determined by the dissociation of oxygen. Above 133 Nm<sup>-2</sup> the oxidation rate was initially dominated by the lateral spread of oxide from numerous nuclei to form  $\alpha$ -SnO platelets. Subsequent growth followed logarithmic oxidation kinetics, being controlled by metal ion diffusion through the oxide film.<sup>57,58,59</sup> At ambient temperatures, tin was reported to be passivated with a layer of SnO 2-6 nm thick<sup>45</sup>, which became disbonded, through stress relief, when the thickness increased.

The effects of impurities on the oxidation rate of tin have been investigated by Warwick,<sup>60</sup> who found that alloying elements forming an oxide more readily than SnO such as zinc, undergo preferential oxidation at the surface, thus inhibiting the oxidation of tin. This was confirmed by Gruhl<sup>61</sup> who also found that zinc decreased the oxidation rate and also that levels of lead > 1 wt% increased the temperature at which significant oxidation occurred. For tin platings, as well as the presence of metallic impurities, substrate atoms may diffuse through a tin layer and influence oxidation kinetics or form oxides themselves and create their own electrically resistive films. This has been found to be a significant problem with brass connectors but is minimised by the deposition of a nickel barrier layer.<sup>62</sup>

Oxidation of molten tin, has also been investigated, the results of which may be useful in determining the thickness of the oxide formed during coating of the substrate from the liquid phase and for localised heating of contacts which are subject to melting voltages. The study found variable oxidation rates and it was concluded that this was due to crystal orientation in the oxide film,<sup>63,64</sup> or the continuous conversion of SnO to a less protective SnO<sub>2</sub>.<sup>65</sup> According to Jenkins,<sup>66</sup> SnO was found to form on tin immediately at temperatures above its melting point with SnO<sub>2</sub> forming at higher temperatures.

For the gases normally encountered in the automotive environments, molten tin is relatively unreactive, although it has been reported that molten tin will react with water vapour to form SnO<sub>2</sub> and hydrogen and with carbon dioxide to form SnO<sub>2</sub> plus carbon monoxide<sup>44</sup>. Hydrogen sulphide, a common emission gas from exhaust gas catalytic converters, has little apparent effect on tin, however, at temperatures above 100° C, SnS is formed. The metal has also been found to be readily attacked by chlorine becoming significant at temperatures above 100°C.<sup>44</sup> Yasuhiro<sup>67</sup> *et al* and Yasuda *et al*<sup>68</sup> have compared the effects of a mixture of SO<sub>2</sub>, NO<sub>2</sub> and Cl<sub>2</sub> on gold and tin connector coatings where it was concluded that tin performs better due to the porous nature of electroplated gold with the consequent formation of galvanic cells between the noble metal and the underplate or substrate.

As we have seen above in Fig. 2.5, electrical contact is made between the touching metallic a-spots which are within the load-bearing areas at the interface between asperities. Seepage of air into these regions will gradually oxidise these metallic contacts and reduce their volume, causing a constriction of current and an accompanying increase in apparent CR. The total resultant constriction resistance is the summation of numerous elementary contact areas and the measured CR changes little until the smaller elementary contact areas diminish due to complete oxidation. With time the number and size of the electrically conducting contact points decrease and local ohmic heating may occur, accelerating the oxidation process. This runaway situation then leads to rapid failure.

#### **2.7.4 Stress Corrosion**

When there exists a combined and synergistic interaction of corrosion reactions and mechanical tensile stress, as may for example occur in the elastically deformed region of the spring on an electrical connector, stress corrosion can take place with grain boundary attack which may result in intergranular fracture. Crack initiation is greatly enhanced if a surface defect is present or the design includes a small radius to act as a stress concentrator. As the loading of the spring in a connector is critical in maintaining the conducting pathway, any stress relaxation as a result of this form of corrosion will enhance the likelihood of an increase in CR or even open circuit. Whether or not stress corrosion will occur will depend on the metals and anions involved, these being in either gaseous or aqueous form. Engel and Klingele<sup>69</sup> in their "*An Atlas of Metal Damage*" make reference to the results of a study carried out by the NACE Data Survey, of media likely to induce stress corrosion in a variety of metals and alloys. Interestingly, particularly for copper and brass alloys commonly used as connectors in automotive environments, potassium chloride is cited as a harmful electrolyte whereas sodium chloride is not.

## 2.8 Intermetallic Formation

With ageing, pure tin will undergo compositional changes due to interdiffusion reactions with the substrate to produce a variety of intermetallic compounds. The phase diagram for copper/tin is shown in Fig. 2.14. This predicts the formation of two main equilibrium intermetallic phases at the lower temperatures:  $\text{Cu}_3\text{Sn}$  ( $\epsilon$ ) and  $\text{Cu}_6\text{Sn}_5$  ( $\eta$ ). The  $\eta$  phase forms rapidly during the solid (copper) - liquid (tin), tinning process but more slowly during the solid state reaction. This relatively coarse grained phase has been found to form at the copper/tin interface at all temperatures, whereas the ( $\epsilon$ ) phase tends to form at the copper/  $\text{Cu}_6\text{Sn}_5$  interface at elevated temperatures<sup>45</sup>.

There are three types of intermetallic compounds: electrochemical, size-factor and electron. Electrochemical compounds occur where one metal is strongly electropositive and the other strongly electronegative and as a result there is a tendency to form compounds with crystal structures similar to those with classic ionic compound lattices such as sodium chloride. This type of phase is a poor conductor or semiconductor of electricity. Depending on the differences in atomic diameters, atoms may take up interstitial or substitutional positions in the lattice to accommodate efficient packing without distortion. Substitutional compounds form where the atoms involved tend to crystallise in the same type of structure and/or have similar ionic radii. If, however, in special cases where the radius ratio is between 0.41 and 0.59 times that of the basic metal, an interstitial compound will be formed, such as a boride or carbide. The copper/tin intermetallic  $\text{Cu}_6\text{Sn}_5$ , has an atomic radius ratio between 1.2 and 1.3 and has a special hexagonal nickel arsenide structure with four atoms per unit cell<sup>70</sup>.

$\beta$ ,  $\gamma$  and  $\epsilon$  phases found in chemically dissimilar systems with widely different compositions, occur as a result of the relative number of atoms to electrons in the crystal structure, rather than being due to the elemental chemical properties. These compounds, known as electron compounds, form when the ratio of electrons to atoms is of a particular value: 3:2, 21:13, and 7:4. There are three electron compounds in copper tin binary alloys:  $\text{Cu}_3\text{Sn}$  with an electron/atom ratio of 7:4 ( $\epsilon$  - close packed

hexagonal);  $\text{Cu}_5\text{Sn}$  with a ratio 3:2 ( $\beta$  - body centred cubic) and  $\text{Cu}_{31}\text{Sn}_8$  of 21:13 ( $\gamma$  - complex cubic).

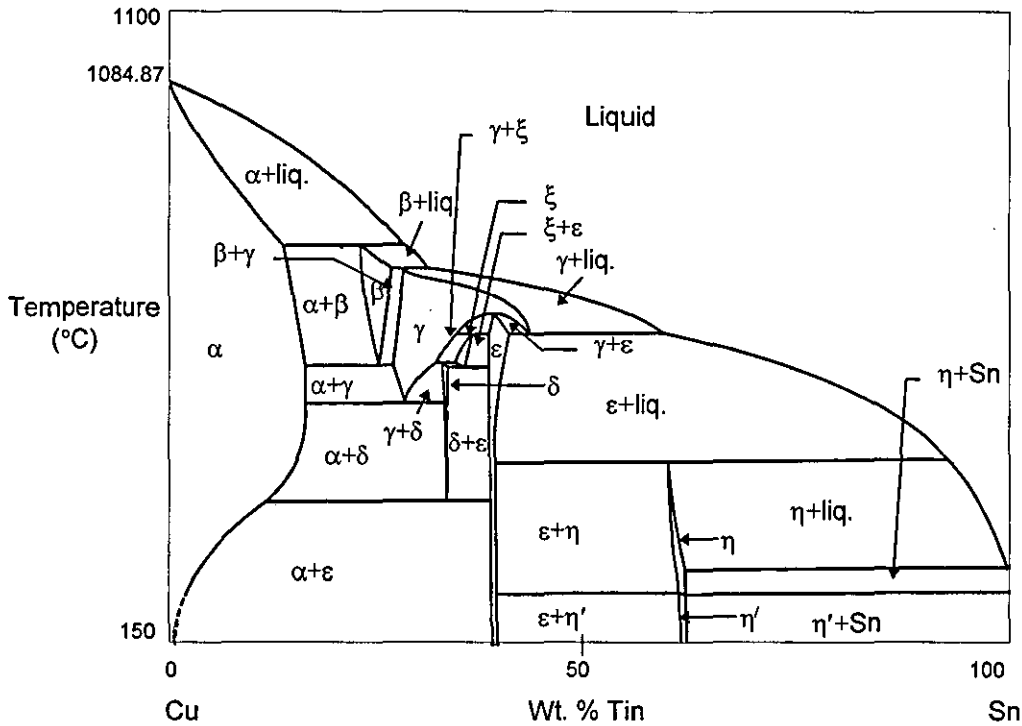


**Fig. 2.14 Phase Diagram for Copper Tin Showing Intermetallic Phases**

### 2.8.1 Kinetics of Cu/Sn Intermetallic Formation

Diffusion rate is not surprisingly strongly material and temperature dependent and can be expressed in terms of the amount of material moving across a unit area of a plane in unit time by Fick's first law. Diffusion in metals of atoms having small atomic radii, such as hydrogen or carbon, is via interstitial channels in the lattice. For larger atoms, however, such as copper, the activation energy required for interstitial movement is very high and diffusion by vacancy transport, i.e. the relative interchange between vacancy lattice sites and the migrating atoms, is the preferred route. Diffusion

occurs more rapidly at grain boundaries and where there are dislocations, producing irregularities in the lattice resulting in the creation of more vacancies. Revay<sup>71</sup> calculated that the intermetallic layer formed during solid state diffusion of copper in tin, is mainly by bulk diffusion from about 120°C and below this temperature it is dominated by grain boundary diffusion.

Smigelskas and Kirkendall<sup>72</sup> demonstrated that as their diffusion coefficients are rarely equal, dissimilar metals diffuse at different rates. As the activation energy ( $Q$ ) needed to move a copper atom among the tin atoms is less than that required to move a copper atom among the copper atoms, the rate of copper diffusion down the concentration gradient is higher in tin than in itself. This would be anticipated because the lower melting point of tin (232°C) versus 1083.4°C for copper, indicates that the tin-tin bonds are weaker than the copper-copper bonds. Similarly the rate of copper diffusion in open-packed lattices will be faster than in close-packed structures. Copper will be expected to diffuse readily through tin to produce the  $\text{Cu}_6\text{Sn}_5$  phase and further diffusion through itself will be relatively rapid due to its open structure. The abundance of copper at the substrate/intermetallic interface will allow the conversion to the  $\text{Cu}_3\text{Sn}$  phase. Further diffusion of copper from the substrate would be at a much reduced rate due to its close-packed structure.

The formation of intermetallics in tin and copper systems has been extensively researched and although this has mainly been restricted to tin/lead solders at near melting temperatures, in studies to determine the effects on wettability and solder joint integrity, it is generally agreed that intermetallic growth is a diffusion limited process, with the increase in thickness being linear with the square root of heat treatment time. From examining microsections of thermally aged samples, Kay and Mackay<sup>73</sup> found that tin coatings on copper and bronze form a duplex intermetallic compound layer of  $\text{Cu}_6\text{Sn}_5$  and  $\text{Cu}_3\text{Sn}$ , the former at the tin/ intermetallic interface and the latter at the copper/intermetallic interface. Using electroplated tin/lead on copper it was shown that when plotting total compound layer thickness against the square root of the heat treatment time, an initial rapid growth occurred over the first 1 - 2  $\mu\text{m}$  , followed by a slower linear growth rate. However, these thickness measurements were determined



from light microscope images and it could be conceivable that over the initial period measurement errors were high.

Braunovic and Aleksandrov<sup>74</sup> examined and analysed polished sections of HDT plated copper by SEM (in BSE mode) and EDS and similarly observed these two distinct layers and confirmed that during ageing, copper diffuses into the pure tin until eventually all of the tin is converted to intermetallic. They determined intermetallic growth rates from micro-sections of 6  $\mu\text{m}$  thick coatings by measuring thickness changes with time. By this method, plots of thickness versus the square root of heat treatment time were linear but showed deviations from the mean of approximately  $\pm 1 \mu\text{m}$ , which indicate the poor reproducibility of the technique. Errors would be expected to be significant, particularly over the initial ageing period where there would already be present intermetallics with a thickness of at least 0.5  $\mu\text{m}$  from the liquid/solid reaction. From Braunovic and Aleksandrov's results it was found that for the temperature range investigated, the growth of the intermetallic phases could be described satisfactorily by a single activation energy,  $Q = 25 \text{ kJmol}^{-1}$ . Although not stated, this is assumed to be for both the  $\eta$  and  $\epsilon$  phases. Mackay and Unsworth<sup>75</sup> had earlier estimated an activation energy of  $80 \text{ kJmol}^{-1}$  for calculating the total intermetallic layer thickness.

A number of other workers have shown that the microstructure of the substrate and the coating can affect intermetallic growth. For example Lindborg *et al*<sup>76</sup> again from the examination of microsections, found a significant difference in intermetallic growth characteristics between dull and bright tin on brass having an intermediate copper layer. Dull tin showed an irregular growth front whilst bright tin was more even, indicating that the coarse microstructure of the former coating provided regions of increased atomic mobility. Haimovich<sup>77</sup> showed that for large grained HALT on copper, when aged at relatively low temperatures, there was a slow growth rate when compared to fine grained electroplated tin. This is consistent with Revey, Owen<sup>78</sup> and with Reed-Hill<sup>79</sup> in that grain boundary and/or dislocation short circuit diffusion is the dominant transport mechanism in a polycrystalline metal at lower temperatures but as temperatures increase there is a switch from grain boundary to bulk diffusion, the transition temperature being lower for metals with larger grains.

Geckle<sup>80</sup> used electron microprobe analysis for quantitative 'surface' analysis of bright and matte tin/lead platings on copper after heat ageing for various times in a reducing atmosphere at 150°C. His interest was principally in the migration of lead towards the plating surface but he also observed that copper concentrations showed a marked increase at or near the outer surface between 356 and 670 hours ageing. Normalising his results shows that after this period of time the copper concentration in the bright tin was three times greater than that of the matte plating. This again supports grain boundary diffusion as the bright tin/lead is composed of small grains. The researcher also performed elemental line scans across a microsection of the same sample and identified the duplex  $\epsilon$  and  $\eta$  intermetallic layers. After ageing, the pure tin showed an almost complete conversion to intermetallic, with slightly less than fifty percent being  $\text{Cu}_3\text{Sn}$ , indicating that full conversion to the copper rich phase would require a considerably longer ageing time.

From the results available in the literature, an attempt has been made to compare the diffusion coefficients at 150°C as reported by different workers (Table 2.2). The results are not all available for this ageing temperature and where necessary have been obtained by interpolation from the published data.

Researcher(s)	Diffusion Coefficient ( $\mu\text{m}^2\text{s}^{-1}$ )	Coating
Braunovic et al <sup>72</sup>	$1.6 \times 10^{-5}$ (total)	HDT
Haimovich <sup>75</sup>	$3.7 \times 10^{-6}$ (total)	HALT
Geckle <sup>78</sup>	$1.5 \times 10^{-6}$ ( $\text{Cu}_6\text{Sn}_5$ ) $1.2 \times 10^{-6}$ ( $\text{Cu}_3\text{Sn}$ )	Bright electro tin/lead
Kay and MacKay <sup>71</sup>	$1.7 \times 10^{-6}$ (total)	Bright or Matte Tin
Dabritz <sup>81</sup>	$1.9 \times 10^{-8}$ ( $\text{Cu}_6\text{Sn}_5$ ) $2.2 \times 10^{-9}$ ( $\text{Cu}_3\text{Sn}$ )	Tin/Lead

**Table 2.2 Survey of Diffusion Rates Measured for Copper in Tin and Tin/Lead**

There are caveats, however, that should be considered. In most cases the microstructure, which has been shown to influence the diffusion rate dramatically, the effect of the substrate alloy and whether or not the intermetallic measured is a single phase or the total combined phases are not known. It is thought that these, together with the errors associated with the microsectioning method and the variability in the intermetallic growth characteristics during diffusion, will contribute strongly to the large variations in the results.

## 2.9 Tribology

Wear can be described as the progressive loss of material from the operating surface of a body occurring as a result of one or more of the following agencies:

- (i) The relative movement of one surface over another.
- (ii) Abrasion by a harder phase either as protuberances in the counterface or as free particles.
- (iii) Erosion of the surface by impact of a solid, liquid or gas.
- (iv) Chemical corrosion of one or both surfaces with accompanying mechanical removal of corrosion products.

The importance of wear as a failure mechanism, responsible each year for the degradation of countless engineering components and assemblies, cannot be overestimated and as a consequence, an abundance of scientific and technological literature has accrued on the subject. For example, Czichos<sup>82</sup> has reported that 55,000 papers had been published over a period of eleven years since 1966 when the Jost Committee carried out an intensive survey into financial savings through improved tribological practice in UK industry.

Although there is some confusion of nomenclature and lack of good definition, it is generally agreed that when wear takes place it is usually due to the action of a combination rather than to one single mechanism. However, depending on the major contributor, the wear regime is usually described by one of the five principle types proposed by Burwell,<sup>83</sup> namely: adhesive, abrasive, corrosive, surface fatigue and 'minor wear types'. In this study, we are concerned principally with small oscillatory relative movement of two contacting surfaces which will mainly involve the first three types.

### **2.9.1 Adhesive Wear**

Adhesive wear takes place when two solid surfaces are in rubbing contact. Although it is commonly referred to as adhesive wear, adhesion is generally only one of several processes both physical and chemical, which may be involved at the interface. As described previously in Section 2.5, surfaces on a microscopic scale appear as an irregular series of crests and troughs, where actual contact is made at comparatively few asperity pairs with often only a small area of each being in mutual contact. As a normal load is applied, the pressures at these contact sites are often extremely large causing the yield stress to be exceeded resulting in plastic deformation of the asperity.

Adhesion at the contact sites will take place if the surfaces are perfectly clean. For example it has been shown that if two metal plates particularly of ductile metals such as copper or gold, are held together under Ultra High Vacuum (UHV), strong adhesion will take place<sup>19</sup>. As already stated, under normal conditions all materials which have been exposed to the atmosphere will be coated with some degree of contaminants, which will prevent adhesion under purely normal loading conditions. However, the application of relative tangential motion at the interface could mechanically disperse the contaminant films lying between the asperity contacts, allowing cold welding to take place. Continued sliding will shear individual microwelds at sites away from the original interface with distances dependant on the mechanical properties of the contacting materials. This results in material transfer from one surface to the other. Further rubbing may cause complete material removal as wear debris. Thus the initial

wear rate for two 'as machined' surfaces may be significant and be achieved for only a small increase in friction. As load and sliding velocity influence the interface temperature,<sup>84</sup> debris particles generated as a result of adhesive wear are hotter than the bulk material and the surrounding gas or liquid making them prone to oxidation.

The degree of wear in terms of wear volume per unit sliding distance ( $Q_s$ ), can be calculated using the Archard wear equation:<sup>85</sup>

$$Q_s = \frac{KP}{P_m} \quad (2.18)$$

Assuming there is no change in wear mechanism say from mild to severe,  $K$  represents the fraction of junctions involved in wear debris generation and is known as the wear coefficient.  $P$  is the applied load and  $P_m$  the yield pressure for the plastically deformed asperity which is close to its indentation hardness ( $H$ ).

For practical purposes the quantity,  $\frac{K}{H}$  is often more useful and is known as the dimensional wear coefficient ( $k$ ) and generally expressed in  $\text{mm}^3 \cdot \text{Nm}^{-1}$  and can be used to compare wear rates for different materials. Lancaster<sup>86</sup> has shown that for a brass pin sliding against steel, there is a crucial role played by oxide formation on the transition between mild and severe wear. The process involves the initial transfer of brass to the steel during a brief period of severe wear. This brass transfer layer is harder than the bulk brass of the pin due to work hardening. Oxide particles are picked up by the pin and this locally hardened surface causes back-transfer of the original layer together with oxides removed from the steel, to form a composite low shear strength layer. Mean local temperature at the contact interface, sliding speed and availability of oxygen will affect oxide formation and thus influence wear rate. The first of these will be dependent on ambient temperature and frictional power dissipation which itself is influenced by sliding velocity and load.

### 2.9.2 Abrasive Wear

The second type of wear involves the presence of a hard, sharp component. This may be in the form of:

- (i) an abrasive which rolls between the two contacts (three-body abrasion or lapping);
- (ii) an abrasive which embeds itself into one or both surfaces (two-body abrasion or grinding);
- (iii) hard phases within one or both of the contact metals, such as intermetallics (two-body abrasion).

The degree of penetration is given by:

$$\frac{P}{H_v} \quad (2.19)$$

where  $P$  is the load on the particle and  $H_v$ , the surface (Vickers) hardness, at a specific normal applied load. Moore<sup>87</sup> proposed that to cause plastic deformation of a surface, the ratio of abrasive hardness  $H_a$  to surface hardness  $H_s$  must be greater than 1.25. This has been observed experimentally in a series of studies reported by Hutchings.<sup>19</sup>

Wear rate is also dependant on particle morphology and size distributions, where sharp, angular particles cause greater wear than rounded ones when only the larger components take part in the abrasive wear process. If the crushing strength of the abrasive component is exceeded, particles fracture causing high-stress abrasive wear. The action of the components produces pits in the surface and generates swarf-like wear debris, which for most metals will oxidise to form more abrasive material. This debris, if not dispersed by the relative movement of the contacts, will assist in the

continuation of the abrasive wear process. For similar abrasive particle size, the wear rates due to three-body abrasion are generally lower than those due to two-body abrasion.

Two-body abrasion involves the material(s) bulk properties where the primary requirements for its occurrence are:

- (i) a large difference in hardness between the two contact surfaces, and;
- (ii) the harder contact material possessing a rougher surface finish.<sup>88</sup>

The small hard particles of grit or dust trapped between rubbing surfaces responsible for three-body abrasion may originate from the environment or from corrosion products. Another source may be from work-hardened debris formed as a result of adhesive wear which may be hard enough to abrade one or the other of the parent surfaces.

### **2.9.3 Fretting Wear and Fretting Corrosion**

Both 'Fretting Wear' and 'Fretting Corrosion' involve mechanical wear and chemical corrosion processes and are influenced by:

- (i) the contact geometry affecting wear debris removal from the contact region;
- (ii) the frequency of oscillation and amplitude of slip of the contacting surfaces;
- (iii) the hardness of the contact materials and their coefficients of friction;
- (iv) the normal load applied;
- (v) the presence of residual stresses near the contacting surfaces;
- (vi) the mutual solubility of dissimilar metal couples;
- (vii) ambient and localised temperatures, particularly in electrical contacts due to localised Joule heating;

- (viii) the chemical reactivity of the mating materials;
- (ix) the presence of corrosive species, particularly oxygen, and;
- (x) the application of lubricants, which can reduce friction and act as a barrier to the air and retard the formation of corrosive products.

In any particular situation, the type of fretting regime depends on which processes dominate. For example, small amplitude high frequency oscillatory wear of steel on steel at room temperature in air would be described as fretting 'wear' when compared with low frequency wear of magnesium on steel at 100°C in the presence of aqueous sodium chloride. Here fretting 'corrosion' would describe more accurately the principle mechanism involved.

Fretting is a combined wear type. Essentially, although the same mechanisms are involved as those during adhesive and abrasive wear, it is different from continuous sliding even at an equivalent velocity, in that where the two surface are held together by high normal loading, wear debris can escape from the contact zone with difficulty. As in adhesive wear, normal loading causes adhesion between asperities which rupture when subjected to vibration or other oscillatory relative motion of small amplitude, such as that produced by differential thermal expansion of the mating materials or even changing magnetic fields.<sup>89,90</sup> The fine wear debris generated, unless protected by a barrier, will oxidise to form hard particles and thus promote abrasive wear. For example, with ferrous metals, the debris oxidises to  $\alpha$  -  $\text{Fe}_2\text{O}_3$ , which is characteristically brown in appearance and is commonly referred to as 'cocoa'.

Oxidised wear debris will for most metals generally occupy a larger volume than that of the parent metal. If the debris is not removed this may result in seizure of components or alternatively it may escape and reduce clamping pressures. More importantly, for electrical contacts the build up of oxide can cause changes in CR by the formation of an insulating layer, which itself may fracture or separate previously



welded or contacting asperities, resulting in open circuits or intermittent or distorted signals.

To summarise, three basic processes are at work during fretting:

- (i) As most metals and alloys will possess a natural oxide layer this will be disrupted during the first half cycle, exposing a highly active surface which rapidly oxidises in the atmosphere. During the second half cycle, this newly-formed film is distributed both within and across the surface.
- (ii) The presence of asperities, either intrinsic due to surface finish or induced by the grinding action of the oxide particles, allows the formation of welds at points of contact. These in turn are fractured by shearing or fatigue at a position away from the original surface producing wear debris having highly active surfaces, which in turn suffer rapid oxidation.
- (iii) Resultant oxide debris from (i) and (ii) above, then acts as an abrasive to generate further wear debris.

The connector designer regards friction as both a beneficial and a deleterious property. If frictional forces are high, oscillatory movement may be restricted to elastic strain of the asperities, but with the result that high insertion forces are needed when making and breaking the connector. For low normal loading, an oxide film can separate the contact surfaces and reduce the coefficient of friction ( $\mu$ ), by acting as a low shear strength material or, because of its low ductility, limiting junction growth. As the load increases there may be a sudden transition to a higher value of  $\mu$  as the film is penetrated and there is metal to metal contact.<sup>19</sup>

Where reactive species are in abundance, wear of the contact surfaces is described as *fretting corrosion* and deterioration at the contact interface by this process occurs principally as a result of chemical reaction. When two metals rub together in a

corrosive environment, either gaseous or liquid, the corrosion products formed on one or both surfaces are often weakly adherent and are continually being removed to expose clean metal, whose nascent surfaces are susceptible to further rapid corrosion. This process will therefore appear to accelerate the corrosion rate of many metals. For example, the rate of growth of an oxide film on steel will be self limiting and decrease exponentially with time, whereas with continual mechanical removal of the oxide, a linear corrosion rate will be observed. Some metals possess protective oxide films or passive reactive layers which are resistant to progressive chemical attack with mildly reactive media. Mechanical interaction of the surface removes these protective layers thus continuously exposing bare metal to the corrosive media. This process will therefore render a metal less corrosion resistant to what is normally a benign media.

The literature contains several reports related to electrical connectors investigating the effects on the fretting process of the intrinsic properties of the contacts such as topography and contact geometry and external influences such as temperature, electrical power and lubrication. Examples of those pertinent to this study are given below.

### *Topography*

A number of models have been constructed to predict wear rates by fretting. Amongst these and specific to electrical connectors, have been those proposed by Bryant<sup>22</sup>. He calculates the ultimate lifetime (T) in cycles-to-failure of a connector system using the following relationship:

$$T = \frac{Z A_n}{\frac{(\gamma-1)}{\gamma} (\bar{h}_o \bar{A}_{\text{exposed}})} \quad (2.20)$$

where (Z) is the average distance between peak height and valley depth, ( $A_n$ ) the nominal contact area, ( $\gamma$ ) the ratio of the volume of corrosion product to that of the reactant metal and ( $A_{\text{exposed}}$ ), the exposed portion of the real contact area. Note that the that “-” notation refers to the average value taken over the number of cycles required

to fill the valleys to overflowing. Here, the parameters ( $Z$  and  $A_n$ ) are dependent upon geometry and load and the set of parameters making up the divisor are determined by material properties and environmental conditions. The thickness of the corrosive layer formed after each cycle is ( $h_o$ ).

Bryant applied the model to copper contacts at room temperature using an estimate of real to apparent contact area for a typical connector of  $10^{-2}$  to 1. An average peak to valley height of between 1 and 10  $\mu\text{m}$  was assumed and from previous work by Holm,<sup>91</sup> a value for  $h_o$  of 0.1 to 10 nm was used. This gave an ultimate lifetime of between  $10^3$  and  $10^6$  cycles which compare well with experimental results obtained by Braunovic.<sup>92,93,94</sup> Notwithstanding that there are a number of major assumptions, not least that the insulating film is assumed to be continuous and of constant thickness, the accuracy of the model is highly dependent on two measurements: Holm's calculations of  $h_o$  and the measurement of the amount of exposed area produced after each cycle by fretting wipe i.e.  $A_{\text{exposed}}$ . The real area of contact can be taken as the upper bound for  $A_{\text{exposed}}$  and modern surface profilometry techniques may be used to obtain a determination of this measurement. However,  $A_{\text{exposed}}$  over  $m$  cycles will in reality be significantly less than  $A_{\text{real}}$ , with the effect that the calculation of ultimate lifetime will be underestimated. To experimentally determine the value of  $A_{\text{exposed}}$  would be difficult to achieve irrespective of the inability to examine the surfaces whilst in contact. For example optical techniques such as confocal microscopy could be applied but may be limited by resolution and the difficulty in differentiating between exposed and unexposed, i.e. oxidised regions of the surface. Although prohibitive in terms of equipment time, as the chamber must be vented after each cycle, in principle, at least, it may be possible to use electron imaging techniques with stereo pairs calculations to provide the resolution required, together with AES mapping to determine oxygen (i.e. oxide) distribution.

From the relationship proposed by Bryant, it is obvious that the number of cycles to failure may be maximised by increasing  $Z$ , the average peak to valley height. In other words for large  $Z$ , there is a greater volume available for oxide containment. Saka *et al*<sup>95</sup> had favourable results when testing a 'checkerboard' surface with rectangular high spots having cavities 50  $\mu\text{m}$  deep. At the same time Holden *et al* demonstrated

that surface microstructure is the dominant factor for low CR, albeit for static contact.<sup>96</sup> Theoretically, if the microstructure and thus the morphology of each contacting surface is modified by forming a multitudinous number of asperities of uniform but significant height, using a material with high hardness low resistivity and ideally a high resistance to oxidation, a consequential improvement in fretting performance would be anticipated. Bramhall<sup>97</sup> has proposed that such a structure would increase fretting life. He found a significant improvement by introducing distressing grooves in the contact surface. Leadbeater<sup>98</sup> *et al* also suggested that rough surfaces have a beneficial effect on reducing fretting failure and Suh<sup>99</sup> reported a way of reducing overall friction by deliberately engineering depressions or hole patterns to trap wear debris. Such surfaces, with the addition of a suitable boundary lubricant residing in the 'valley reservoirs', would reduce friction and therefore lower the wear rate and result in the generation of less wear debris.

### *Temperature*

When testing electroplated matte tin at 10 Hz, Lee *et al*<sup>100</sup> discovered that fretting performance decreased as temperatures were raised up to approximately 70°C but above this level began to show some improvement. He concluded that this was due to softening of the tin at the higher temperatures, which in turn increased the contact area, reduced the effective track length and resulted in the generation of less wear debris. Their results indicate that for the fretting test conditions used (10 Hz), the beneficial effects of the increase in contact area with ambient temperature are more significant than the accompanying higher oxidation rate. It also suggests that when the test coupon is at ambient temperature, local frictional heating of the contact surface does not exceed 70 °C or if it does, heat transfer away from the contact is so rapid that softening does not occur. Archard's model<sup>101</sup> predicts that for sliding steel contacts at least, if one considers both the instantaneous normal and tangential load being carried by a single asperity, then, depending on load and sliding velocity, flash temperature rises could exceed temperatures of 1000K. Consistent with this model, temperatures of this order have, according to Hutchings,<sup>102</sup> been confirmed by thermoelectric and infrared measurements and it is not inconceivable that tin contacts although softer, would behave in a similar manner.

### Electrical Power

In further work,<sup>103</sup> Lee *et al* also investigated the effect of power on the performance of electroplated tin contacts and discovered that fretting corrosion during the first few tens of cycles at 8 Hz, was not affected by electrical loads but as fretting continued, with accompanying oxide build-up, the electrical resistance increased steadily before showing a sustained plateau near the melting voltage of tin. Ireland<sup>104</sup> *et al*, using a higher test frequency of 50 Hz, reported that powered tin/lead plated contacts failed at approximately half the number of cycles that unpowered contacts failed (50,000 cycles). They proposed that fretting performance was reduced due to the thermal effects of a current passing through the a-spots causing the rate of oxidation to increase. Their results would therefore suggest that frictional heating was less significant in promoting oxide formation than Joule heating.

Comparing unpowered with powered contacts, Stennett and Swingler<sup>105</sup> found that with the application of an electrical current, low cycle fretting contact life improved by a factor of four. A current of 1 A was maintained during the test and failure was taken to be the open circuit value of 200 mΩ for the majority of the wear track length. It was proposed that the improvement in performance with electrical power was due to electrical breakdown of the insulating film. The term 'electrical breakdown' is assumed to refer to the phenomenon known as 'fritting'<sup>106</sup> that occurs when the electrical field within a surface film reaches of the order of  $10^6$  Vcm<sup>-1</sup>. For their experiments, they carried out tests at ambient and for the low frequencies and loading used, frictional heating would be expected to be negligible. By applying the Kohlrausch<sup>107</sup> relationship:

$$T_m^2 = T_o^2 + \frac{V^2}{4L} \quad (2.21)$$

where  $T_m$  is the maximum contact spot temperature;  $T_o$  the bulk temperature;  $V$ , the contact voltage drop (up to 200 mV at failure) and  $L$ , the Lorentz constant for the material, the contact peak temperature would exceed the melting point of tin well before failure. Therefore, as an alternative to the fritting hypothesis, it is possible that the localised heating caused by the application of power could be sufficient enough to

soften the tin which would extrude between fractured oxide film to promote the continuous formation of new a-spots as the rider moved across the contacting surface. If Stennett and Swinger are correct in their conclusions, testing with cyclic electrical loading would achieve the same fretting life as continuously powered contacts, as their hypothesis suggests that the wear process is unaffected by the passage of an electric current.

### *Contact Geometry*

It has been claimed that the stability of the CR of fretted surfaces is affected by the contact geometry. Garte<sup>108</sup> using tin alloy plated surfaces, found that wedge contacts were more stable than domed contacts and Lee *et al*<sup>109</sup> similarly concluded that out of three contact types, hemisphere, cone and wedge, the latter with a 60° angle provided the best compromise of good electrical performance with acceptable contact wear for tin plated contacts. This contact shape gave the best performance as it provided the minimum accumulation of oxide in the contacting area.

### *Amplitude of Slip*

In fretting wear and fretting corrosion the quantity of wear debris and ultimately the amount of insulating film that is produced, is dependant upon the amplitude of the slip, that is the relative distance moved by the contacting surfaces. Hoover *et al*<sup>110</sup> showed substantial gains in the number of cycles-to-failure for tin base connector contacts, if the relative contact movement could be restricted to less than 5 µm. Antler<sup>111</sup> reported that the longer the wear scar, the more rapidly the CR degraded. It has also been shown that there is an upper limit to the slip amplitude<sup>112</sup>. Plots of wear rate versus amplitude are sigmoidal and become constant at amplitudes >100µm. Here the wear rate changes to those of unidirectional and reciprocating sliding.

### *Fretting Rate*

Oxide formation involves rate dependant chemical reactions. Thus the lower the frequency, the greater the thickness of the oxide film formed between wipes. From the

literature it appears that the higher wear rate and accompanying particle oxidation obtained with high frequency fretting is less influential on CR than the greater oxide formation with time for low cycle fretting. The early work of Feng and Uhlig<sup>113</sup> on the effects of frequency on wear rates showed an inverse relationship, thus the lower the frequency the higher the wear rate for a given number of cycles. By extrapolating their results to lower frequencies, wear rates show a significant increase below 10 Hz.

Stennett and Swingler<sup>105</sup> using the same materials as in the experiments of Ireland *et al* but testing at the low frequency of 2.38 mHz, found that unpowered fretting performance was poor, being of the order of tens of cycles, compared to the high frequency results obtained by Ireland *et al*. It was concluded that under low frequency conditions, oxide growth and build-up was more significant due to the long wipe intervals. It could also be argued, however, that for the case of high frequency fretting, frictional heating is significant and for low melting point metals such as tin this could result in local softening and the generation of numerous a-spots surrounded by oxide. Thus the rider would effectively be supported on a 'pool' of tin with a discontinuous oxide layer of SnO, or by SnO<sub>2</sub> at higher temperatures.

### *Normal Load*

The real area of contact ( $A_r$ ) is directly proportional to the applied load ( $P$ ). That is:

$$A_r = \frac{P}{P_m} \quad (2.22)$$

where  $P_m$  is the yield pressure, being approximately equal to three times the yield stress in tension. If wear only takes place at the contacting asperities, the degree of fretting wear is directly proportional to the applied load.

Antler<sup>111</sup> has shown that with solder fretted against itself with a contact force of between 0.29 and 2.9N, there is an improvement in fretting performance with load. This has been explained as being due to the enhanced penetration of the fretting corrosion products. However, increasing the load, particularly if local frictional

heating has occurred, would plastically deform the contact material and increase the contact area. Also, rather than describing what occurs at the contact as ‘penetration’, it would be more accurate to characterise the mechanism in terms of the applied load forcing or extruding the metal between fractured regions of the oxide film. Such a mechanism has been observed for aluminium contacts.<sup>114</sup>

### *Lubrication*

From the above we can see that there are several parameters which influence fretting behaviour. A further method of improving fretting performance is to reduce the coefficient of friction and restrict oxygen access to the metal surfaces by using a suitable lubricant.<sup>115, 116</sup> Lubrication regimes are described in terms of the lubricant’s viscosity, the bearing load and the sliding velocity versus friction as predicted by the Stribeck curve (Fig. 2.15) and are generally classified as: hydrodynamic, elastohydrodynamic or boundary.

Under hydrodynamic lubrication conditions conformal sliding surfaces are completely separated by a relatively thick film of fluid. The normal load is supported by viscous forces being generated within the lubricant due to the relative motion of the two surfaces. For hydrodynamic lubrication, the mean lubricant film thicknesses are too great to allow electron tunnelling and therefore these conditions are not applicable to electrical contacts.

Elastohydrodynamic lubrication occurs where contacting surfaces are non-conformal, such as between gear teeth. Here there will be nominally point contact, and high local pressures in the contact zone. In this mode of lubrication, depending on the elastic modulus of the surfaces, the lubricant film for metals would have thicknesses typically of the order of microns or tenths of microns allowing some asperity contact. This region is also known as *mixed* lubrication and could occur between insufficiently loaded mating electrical contacts under high frequency vibration conditions.



Much of our current knowledge of boundary lubrication is based on the classical work of Bowden and Tabor.<sup>117</sup> As contact pressures are increased or slow sliding conditions exist, there will be direct contact between asperities resulting in high wear rates. It was shown that boundary lubrication can protect the surfaces by the adsorption of molecular films consisting of polar end-groups on hydrocarbon chains. The two surfaces are kept apart by the interaction of these hydrophobic hydrocarbon chains but

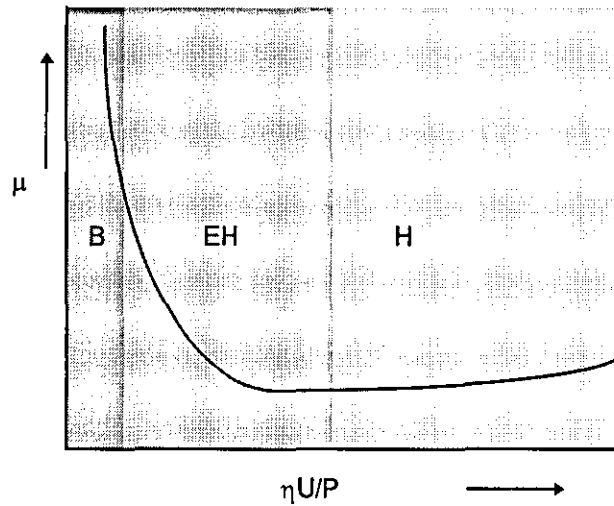


**Fig. 2.15 Stribeck Curve<sup>84</sup>: Boundary (B), Elasto-hydrodynamic (EH), Hydrodynamic (H) (Full Film) Lubrication Showing the Variation of the Coefficient of Friction ( $\mu$ ) with  $\eta U/P$ , ( $\eta$  is Viscosity of Lubricant,  $U$  is Sliding Velocity and  $P$  is Normal Load).**

there are still areas of exposed asperities which allow electrical contact with limited wear. It was proposed that lubricant reservoirs are formed in the microscopic depressions and cavities in the surfaces of the wear couple and when a protective layer on the load carrying asperities is sheared off during sliding wear or fretting, the lubricant is immediately replaced, the rate being dependent on the fluid's surface tension and viscosity, which will decrease as the temperature increases.

Boundary lubricants are generally straight chain alcohols and carboxylic acids whose hydroxyl or acid groups adhere strongly to the metal oxide by chemisorption,<sup>118</sup> so called Langmuir Blodgett films<sup>119,120</sup>. Non polar hydrocarbons (e.g. paraffins) do not adhere strongly but rely on their high viscosity to support loads. A boundary lubricant may have a chain length of only 2-3 nm and only required to be present on the surface one molecule thick to reduce friction.<sup>121</sup> It has been shown that for steel surfaces lubricated with carboxylic acids and alcohols, increasing the hydrocarbon chain-length will dramatically reduce the friction coefficient<sup>122</sup>.

Bowden and Tabor have also suggested that the temperature range over which good lubrication can be maintained can be extended by the use of soaps, particularly with reactive metals. These polar molecules, such as fatty acids and fatty acid esters (triglycerides), adsorb onto metallic surfaces to provide the necessary boundary lubrication, which according to Beltzer *et al*,<sup>123</sup> can be improved where there are strong cohesive interactions between hydrocarbon chains.

Often compounds having boundary lubricant properties are incorporated into base oils as extreme pressure (EP) additives. Early work by Hardy<sup>124</sup> showed how the ability to lubricate was dependent on molecular type and structure and that for constant chain length, fatty acids are superior to alcohols, which in turn are better than alkanes. The physical interaction of the carboxyl group with the surface can be increased by the presence of oxide, with hydroxyl and water involving hydrogen bonding, being a prerequisite for good boundary lubrication. Recent work by Timist<sup>125</sup> using Infrared Reflectance Absorption Spectroscopy together with shear strength measurements, has determined the degree of chemisorption of stearic acid to aluminium on glass and gold on glass.

### *Tribochemistry*

Tribochemistry is the study of chemical reactions which take place at the contact due to the mechanical shear and temperature effects of friction. Temperatures are found to increase linearly with sliding velocity whilst the load determines the real contact area

over which the friction power is dissipated. Comparison with experimental values of wear volume changes ( $\Delta V$ ) leads to the conclusion that friction (resulting in localised heating), changes the growth law of the oxide film from logarithmic to parabolic and causes the oxidation rate to be as large as it would be at 900°K in the absence of friction.<sup>126</sup> It was found that during rubbing of the surfaces, diffusion becomes more rapid than electromigration, particularly as the diffusion process is greatly facilitated by structural defects introduced as a result of plastic deformation such as grain boundaries, dislocations and vacancies. Razavizadah and Eyre<sup>127</sup> have reported the formation of relatively thick oxide in wear tracks in aluminium due to defects introduced as a result of mechanical interaction causing increased reactivity and the formation of diffusion paths in the exposed surfaces. Structural modification of the material, with the creation of highly excited defects is demonstrated by such phenomena as triboluminescence and electron emission. For metallic bodies separated by a lubricant, electrochemical electron emission is thought to be a cause of tribochemical reactions. For the four platinum group metals having importance for contact applications, frictional polymers may form from different adsorbed organic compounds which, due to the catalytic activity of the metals, produce high molecular weight cross-linked solids.<sup>128</sup>

## 2.10 Lubricants for Automotive Connectors

Lubricants both solid and liquid are primarily designed to minimise the frictional forces between moving surfaces, thus reducing wear. In addition, the lubricant can remove the heat of friction and wear particles from the load carrying zone and impede the penetration of foreign matter including reactive gases and liquids such as oxygen and aqueous solutions. Lubricating oils are either produced from natural sources, e.g. mineral oils prepared from crude oils by fractional distillation, or are manufactured synthetically. Several classes of synthetic oils have been developed with properties suited to a wide range of applications. They are generally superior to mineral oils in terms of their viscosity characteristics and low volatilities. A number of solid lubricants such as graphite, waxes, molybdenum disulphide, niobium and tungsten and polymers such as polyethylene have also been used. Lubricants may have a variety of compositions and Table 2.3 lists a number of the more common compounds.

Thickening agents include soaps, bentonites (mineral clays), silica and polymers such as polytetrafluoroethylene (PTFE). Soaps are prepared from carboxylic acids or their glycerides and alkali or alkaline-earth hydroxides, such as lithium, sodium, aluminium, calcium and barium. They form characteristic long, thread-like, polar molecules which interweave and retain the base oil. It is the cations and anions of the soap greases which influence their properties such as thickening ability, water resistance and melting point. Soaps may also be made using mixtures of cations and by co-crystallization of two or more compounds. These are known as complex soaps which show improved performance at high temperatures<sup>129</sup>.

BASE OILS	
Synthetic hydrocarbons	Diesters
Polyol esters	Polyalkylene glycols (PAG)
Polyalkylene glycol ethers	Polyalkylene glycol ethers
Polyphenyl ethers (PPE)	Natural petroleums/mineral oils
Fluoroethers	Polyhexafluoropropylene epoxide (PHFP)
Perfluoropolyethers (PFPE)	Polychlorotrifluoroethylene (PCTF)
Microcrystalline waxes	Esters-Phosphates
Chlorofluorocarbons	

**Table 2.3 Common Base Oils Used in Lubricant Formulations**

Lubricants for separable electrical connectors have been in use since the early 1960's in the USA for aerospace and computer applications and, due to demands for higher reliability, this has been extended to automotive circuitry. Sophisticated high cost oils were introduced for sealing pores and reducing wear in noble metal coatings<sup>130</sup> but for automotive connectors, greases have been generally employed in conjunction with tin and tin/lead platings for corrosion protection. For the vehicle harness and electrical/electronic component designer, the choice of connector material, platings and lubricants have often been on an *ad hoc* basis due to lack of information with respect to their performance in the various automobile environments. Indeed these

environments may be unpredictable or so complex that they cannot always be accurately characterised.

Unless the connector resides in an oil filled environment, such as, for example, within a sealed transformer or generator housing, lubrication can only be reliably achieved by the application of a solid lubricant or a grease. The grease being a material with a semi-solid consistency comprising of a base oil and a thickener which acts as a reservoir. Grease base oils can be both mineral and synthetic and together with the large number of available thickening agents, numerous formulations are available. As well as the base oil and thickeners, greases often include the same additives as used in lubricating oils to, for example, reduce oxidation and provide corrosion protection to metal surfaces.

Lubricants used for electrical connectors demand certain properties in addition to the aforementioned requirement of reducing friction between moving surfaces. For example volatility or evaporation loss should be low to prevent substantial increases in viscosity and it should be chemically compatible with any polymeric insulation. A detailed yet not exhaustive list of properties is given in Table 2.4.

### 2.10.1 Lubricant Reactivity

Electrolytic cells have been used to determine the electrochemical reactivity of lubricants in order to assess the degree of current leakage between insulated multi-pin connectors. Adaptation of the cell to measure the reactivity of greases and relate this to fretting performance, however, is novel and only one paper has, to the author's knowledge, been published. In a study by Wang *et al.*<sup>131</sup>, the reactivity of silicone greases was measured and showed some correlation with fretting performance. The reactivity, as given by the voltammetric current, correlated with the amount of oxide and other corrosion products formed on plated electrodes and thus the electrical contact resistance stability. Wang argued this would imply that low reactivity lubricants are not only more stable but also more effective in prolonging the fretting life of electrical contacts.

Surface oxidation of a lubricated contact can, however, be due to a number of additional causes, including the diffusion of oxygen from the environment through the lubricant to the metal surface and from oxygen dissolved in the grease. Oxygen can also be absorbed from the atmosphere and cause oxidation of the lubricant. The rate of surface oxidation of a metal coated with a lubricant is dependant on a number of variables, e.g:

- (i) the permeability of the lubricant to oxygen;
- (ii) the thickness of the lubricant applied to the surface;
- (iii) the contact true surface area;
- (iv) the environment (humidity, temperature, oxygen partial pressure);
- (v) the percentage and effectiveness of any antioxidant package in the lubricant;
- (vi) the size of the current and voltage leading to localised heating.

It could be argued that, in addition to the effects on metal oxidation at the contact, the current leakage test relates to two further key areas with respect to fretting performance:

- (i) the reactivity of the grease is a measure of its mobile (polar) constituents, the concentration of which varying between lubricants and with time and temperature. Polar molecules have been shown to form boundary layers which affect friction and therefore fretting wear at the contact;
- (ii) the chemical changes of the lubricant, e.g. oxidation with time and temperature.

Oxidation of the base oil can lead to acidic products or residues which will affect the leakage values as well as contributing to oxidation of the metal surface. The latter in turn will have some contribution to the increase in current leakage.

The above can be summarised by the equation:

$$I = A \frac{dP}{dt} + B \frac{dO_l}{dt} + C \frac{dO_s}{dt} + \sum D_i \frac{dX}{dt} \quad (\text{at temperature } (T)) \quad (2.23)$$

where:

$I$  = current leakage

$P$  = polarity of lubricant

$O_l$  = oxidation of lubricant

$O_s$  = oxidation of surface

$X$  = any other contributing factor affecting the current leakage e.g. oil separation from the grease.

$d/dt$  = rate of change of variable with time (not necessarily, linear)

$A, B, C, D$  = constants

PROPERTY	REQUIREMENT
Lubricity	High lubricity to reduce friction and wear
Compatibility	To minimise attack of insulation materials
Low gas and liquid permeability	To protect from corrosive attack by the surrounding atmosphere
Low volatility	To reduce evaporation and a resultant increase in viscosity
Viscosity	Low viscosity/temperature relationship to reduce a viscosity increase at low temperatures and drain-off at high temperatures
Temperature stability	To reduce oxidation, polymerisation, polycondensation, cracking, etc. causing an increase in viscosity
Insulation resistance	To prevent current leakage between conducting pins etc.
Chemically inert	Free from corrosive agents

**Table 2.4 Desired Properties of Lubricants for Electrical Connectors.**

## 2.11 Materials Analysis Techniques

The materials scientist has today an extensive range of techniques at his disposal to study surface and near-surface compositions and morphologies. It is, however, important that the selection is made with a thorough knowledge of the benefits and, more importantly, the limitations of a particular technique. All too often results are quoted in technical reports which have been taken at face value without an understanding of, for example, the condition of the sample being examined or the effects of the analytical parameters used. The major techniques utilised for this study are described below.

### 2.11.1 Scanning Electron Microscopy (SEM)

The first commercial scanning electron microscope became available in 1965 and since then has become the most important technique available for the study of materials and failure analysis. As the resolution of the light microscope is limited by the wavelength of light, in order to resolve objects smaller than this, the shorter wavelengths of electrons are utilised.

Essentially the microscope consists of an electron source, an anode plate, magnetic lenses, a raster coil and various detector systems. The electrons are emitted by thermionic emission from a heated tungsten or lanthanum hexaboride filament, focused by a negatively biased Wehnelt cylinder to a point just above a hole in the anode plate, which is positively biased from as little as a few hundred volts to 40 kV. The diverging beam of accelerated electrons passes through the hole and are focused by a series of magnetic lenses to a very small spot on the sample surface. Finally, a coil rasters the beam over a variable area of the sample and as the beam of electrons impinge on the specimen surface, a number of subsurface phenomena occur; see Fig. 2.16. The signals generated are utilised by various detectors.

The general mode of imaging uses the low energy (<5 eV) inelastically scattered secondary electrons, generated from within the first few tens of nanometers of the



specimen surface. These are attracted towards the positively biased grid of a detector consisting of a scintillator and photomultiplier. The signal generated is fed to a cathode ray tube and is synchronised to that of the electron beam raster, the magnification being the ratio of the area rastered over the CRT to that over the specimen.

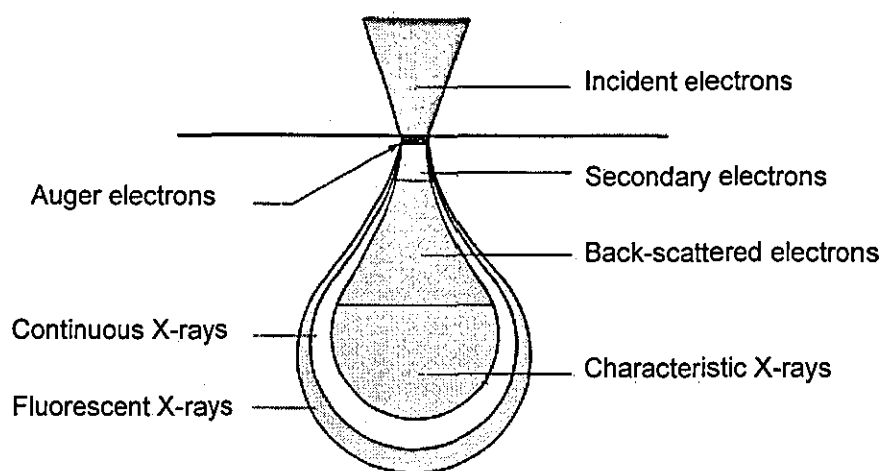


**Fig. 2.16 Relative Depth of Quantum Generation.** (after Goldstein<sup>132</sup>)

Many of the impinging electrons are elastically scattered and therefore possess the same energy as that of the electron beam. The electron mean free path of these primary more energetic electrons is much greater than that of the secondaries and therefore they can provide information from deeper within the specimen. This must be borne in mind when comparing the two images. Detection of these BSE electrons, is by means of a solid state detector located directly above the specimen and back-scattered electron imaging is generally used to provide phase contrast, where grey level indicates differences in average atomic number - white being high  $Z_{av}$  and black low  $Z_{av}$ , as the number of back-scattered electrons produced increases with atomic number. Therefore, in this current study, for example, metallic oxides would appear darker than the parent metal. The depth from which they originate depends both on the primary beam energy, the specimen density and their angle relative to the specimen surface. Hitherto, poor signal to noise has precluded the use of low beam

energies but with present day high efficiency BSE detectors, recent work by Richards *et al*<sup>133</sup>, has shown that the technique can be used to provide stepwise 'sectional' information with incrementing beam energies from as low as 3-4 kV.

Although the above imaging techniques are most widely used in materials studies, the scanning electron microscope is capable of a number of further developments. For example specimen current imaging utilises a signal from the absorbed current (i.e. the difference between that of the incident beam and the sum of the secondary and back-scattered electrons). This technique produces a phase contrast image which is the inverse of that generated by back-scattered electrons. A related application of specimen current imaging to semiconductor materials is 'Electron Beam Induced Current', where a current is generated by the primary beam due to the creation of electron hole pairs in the vicinity of a semiconductor pn junction.

The low energy secondary electrons are very sensitive to specimens or areas of specimens which are electrically insulating resulting in charging effects. This can be utilised in 'Voltage Contrast' imaging in for example, detecting open circuits in complex integrated circuits. Normally charging is a major problem which can be overcome by various methods. Generally, a very thin conducting carbon or metallic film is sputtered or evaporated onto the surface to dissipate the charge to earth. Another technique is to use low beam voltages of between a few hundred and two thousand volts and balancing the charge deposited in the sample by the electron beam against the charge emitted from the specimen as various signals. A new technique available on modern instruments utilises a modified backscattered electron detector and a chamber evacuated to a higher pressure than normal. Here air molecules in the vicinity of the specimen are ionized and dissipate the charge.

Three further techniques of note are 'Magnetic Contrast', similar to voltage contrast, 'Cathodoluminescence', which detects the light emitted as a result of electron interaction with the specimen and 'Electron Channelling Patterns and Contrast', used to provide information on crystallographic structures. For the present study, however,

secondary and back-scattered images are used after first ascertaining the optimum excitation voltage which will enhance the desired topographical features, resolution and atomic number contrast.

### **2.11.2 Energy Dispersive Spectrometry (EDS)**

The scanning electron microscope, fitted with a suitable detector, is capable of determining the elemental composition of a specimen by collecting and analysing the X-rays generated by the specimen/beam interactions. This forms the basis of the most important and widely used associated technique available to the materials scientist and failure analyst. EDS is a microanalytical technique providing both qualitative and quantitative elemental analysis with a spatial resolution of the order of 1  $\mu\text{m}$ . It is based on the detection and measurement of characteristic X-rays emitted from a solid specimen when bombarded by a beam of accelerated electrons within the evacuated chamber of a scanning electron microscope. Many of the incident electrons are decelerated and scattered emitting a continuum of X-ray photons (Bremsstrahlung), forming a background which sets the lower limit of detection, while a smaller proportion ionise the inner shells of the target atoms removing electrons, which are replaced by higher energy electrons from outer shells. An X-ray photon is emitted having an energy equal to the difference in energy between the ejected and substituted electron. This energy is characteristic of the ionised element.

Detection of X-ray photons is achieved by using a lithium drifted silicon detector, which, by the photoelectron effect, converts the absorbed X-ray photon into an electrical signal. By use of an FET pre-amplifier, a main amplifier and a multichannel analyser, a channel or memory location, which is proportional to the energy of the incoming X-ray photon, is incremented. As a result a spectrum is produced of element peaks superimposed on the background continuum. The spectrum has axes of energy, measured in KeV, against X-ray intensity and the area of the peak minus the background is proportional to the concentration of the element within the ionised volume of the specimen. Generally for an excitation electron beam energy of 20KeV,

this reactive volume has a diameter of the order of one micron, which is the limit of spatial resolution.

By generating peak profiles from pure element standards or certified reference materials, calibrations can be set up and apparent concentrations determined, which can be corrected for the effects of matrix atomic number, absorption and fluorescence (ZAF) effects. The detector is maintained at liquid nitrogen temperatures but to shield it from the effects of the microscope vacuum system, a thin beryllium window is employed. This window will absorb low energy ( $<0.750\text{KeV}$ ) photons, limiting the elemental detection down to  $Z = 11$  (sodium). Ultrathin windows are now available, however, which will allow the detection of light elements down to  $Z = 4$  (beryllium).

Useful applications of the SEM/EDS technique are in analysing compositional gradients at boundaries and mapping of heterogeneous specimens to show elemental spatial distribution and concentration. Recently this has been extended to include energy spectrum mapping which superimposes onto a secondary electron image, the various X-ray photon energies calibrated to the colours in an optical spectrum<sup>134</sup>.

### **2.11.3 X-ray Diffraction (XRD)**

A crystalline material is a periodic, geometric arrangement of atoms in space and the fundamental properties of a crystal as a whole can be described in terms of one repeating unit, that is the unit cell. XRD is a method of characterising the unit cell in terms of size, shape, symmetry and the arrangement of atoms, by determining the collection of angles at which diffracted X-ray beams are detected.

The technique of XRD is a practical application of the relationship between  $n$  (order number),  $\lambda$  (wavelength of incident X-rays),  $d$  (the perpendicular spacing between the lattice planes) and  $\theta$  (the angle between lattice plane and detector, where constructive interference occurs). This is expressed by the Bragg equation:

$$n\lambda = 2d\sin\theta \quad (2.24)$$

An incident beam of coherent X-rays is generated in an X-ray tube having a target element dependent on the application but usually of copper, silver or gold. The monochromatic radiation is, via a collimator, incident on the sample surface and is diffracted by the lattice planes in the crystal structure of the sample, which must be of the same order of magnitude as the wavelength of the radiation. By rotating a detector or placing a photographic film in the same plane as the incident beam, the specific angles where radiation is at a maximum, i.e. where constructive interference occurs can be measured.

XRD is used extensively in crystallographic studies including atomic arrangements, symmetry, crystal size and orientation and magnitude of strain. Samples may be in the form of solids, films or powders and for this current study the technique has been employed in phase identification. Over many years unit cell parameters for a large number of known compounds, have been determined by various workers. These have been compiled to form a database containing over 36,000 inorganic compounds.<sup>135</sup>

#### 2.11.4 Fourier Transform Infrared Spectrometry (FTIRS)

FTIRS is a form of infrared spectrometry where data are obtained as an interferogram and, by applying a Fourier Transform, an amplitude versus wavenumber spectrum is obtained. The technique is used mainly in materials characterisation to provide information on molecular structure to determine the functional groups present in a solid, liquid or gaseous molecule. Irradiation with light from the infrared part of the electromagnetic spectrum (0.78 - 1000  $\mu\text{m}$ ), of a specially prepared sample, can result in its transmission, scatter and absorption. Absorption usually excites molecules into higher energy vibrational states and by measuring the light transmission relative to that obtained with no sample in the beam path, the absorption can be determined. The spectrum obtained is of intensity versus energy or frequency, usually expressed as wavenumber ( $\text{cm}^{-1}$ ). Depending on the molecule, there will be a number of possible vibrations, each of which may cause distinct absorption effects in the spectrum. These

manifest themselves as absorption peaks or bands which have frequencies characteristic of the particular bond, as for example the asymmetric stretching vibration of the CO<sub>2</sub> molecule, which absorbs infrared radiation strongly at approximately 2350cm<sup>-1</sup>. As a result of these absorptions, functional groups can be identified and the spectra generated can be identified by comparing with those held in a library of standard spectra<sup>136,137</sup>. Although somewhat dated, an extensive study of grease compositions using infrared spectroscopy was reported by Verdura.<sup>138</sup>

The addition of a microscope to the conventional FTIR spectrometer has dramatically extended its capabilities. With the addition of grazing angle objectives, Attenuated Total Reflection (ATR) and Infrared Reflection Absorption Spectrometry (IRAS) are techniques which have been developed to identify and study small organic particles and thin organic films on reflective substrates<sup>139</sup>. Pertinent to the current study, IRAS has been used for investigating the surface reactivity of stearic acid, (CH<sub>3</sub>(CH<sub>2</sub>)<sub>16</sub>COOH), Langmuir - Blodgett films on metals.<sup>140</sup>

#### 2.11.5 X-ray Photoelectron Spectroscopy (XPS)

A sample is placed in a high vacuum chamber and irradiated with a continuum of soft X-rays from an X-ray tube usually fitted with either an aluminium or magnesium target. These X-rays have sufficient energy ( $h\nu$ ), to cause photo-emission of electrons from the core levels of atoms present in the near surface region of the sample. The emitted electrons are produced within the sample but due to their relatively low kinetic energies (50 to 2000 eV), they have a high probability of undergoing both elastic and inelastic collisions with an atom in the matrix if they travel very far before leaving the surface. The distance travelled without collisions occurring is known as the attenuation length and, depending on the material and the kinetic energy of the electron concerned, values generally vary between 1 and 5nm. Thus only those electrons originating from the surfaces or a few atomic layers below the surface, will contribute to a discrete XPS peak. The effective sampling depth ( $d$ ) can be determined from the following equation :

$$d = n\lambda \cos\theta \quad (2.25)$$

where  $\lambda$  is the attenuation length,  $\theta$  is the angle relative to the surface normal, at which electrons are collected and  $n$  is taken to be 2 or 3. Photoelectrons which do emerge from the surface are collected and passed to an electron energy analyser and detector. The kinetic energy of a photoelectron (KE), is a function of the energy of the incident radiation ( $h\nu$ ), the work function of the spectrometer ( $\phi$ ), and the binding energy of a given core electron (BE), and can be determined using the following equation:

$$KE = h\nu - BE - \phi \quad (2.26)$$

The binding energy of a given core electron is the energy with which the photoelectron was bound to the atom and has a value characteristic of the element concerned. Therefore, by measuring the kinetic energies of the generated photoelectrons, elements present within a few atomic layers of the surface can be identified. XPS spectra can be displayed in terms of binding energy or kinetic energy ( $h\nu$  and  $\phi$  being constants), with peak areas being proportional to the concentration of the element present. The binding energy of a core level electron depends principally on the charge on the nucleus of the atom with smaller effects from outer electrons involved in chemical bonding. These latter effects arise because the valence shell electrons exert a repulsive force on the core electrons that screens these electrons from the nuclear charge, reducing the nuclear attractive force. The addition of valence electrons, to change the oxidation state, increases the screening effect, which reduces the binding energy. These effects result in measurable peak shift characteristic of the particular bond, allowing oxidation states to be identified.

XPS can detect all elements with the exception of hydrogen and helium and, for a general analysis of a surface, it is usual to collect a broad scan spectrum recorded over a wide energy range. This allows the identification of the major elements and is fairly rapid but if peak overlaps are suspected, the spectrum needs to be collected over a

narrow energy range using conditions designed to give maximum energy resolution. Quantitative analysis is usually performed using theoretically-derived sensitivity factors.

### 2.11.6 Auger Electron Spectroscopy (AES)

Auger electrons are produced whenever incident radiation - photons, electrons, ions or neutral atoms - interacts with an atom with an energy exceeding that necessary to remove an inner shell electron (K,L,M...) from the atom. This leaves the atom in an excited and unstable state and de-excitation occurs with the production of an X-ray photon or an Auger electron. The kinetic energy of the Auger electron (E), for an L<sub>1</sub> (or 2s) to K (or 1s) shell transition, given to a first approximation is :

$$E = E_K - E_{L2,3} - E_{L2,3} \quad (2.27)$$

The Auger electrons have energies typically in the range 20 to 2500 eV. The de-excitation process by the production of Auger electrons rather than by X-ray emission, is a common mode for weakly bound orbitals, making it a sensitive technique for low atomic number elements. The exceptions are hydrogen and helium, as the generation of an Auger electron requires the participation of at least three electrons.

Conventionally, primary excitation using a beam of 1 to 30keV electrons is used which is easily focused and gives high spatial resolution and the added benefit of the generation of secondary electrons. These may be collected to produce secondary electron images as for scanning electron microscopy, thus areas of interest can be precisely located prior to analysis. Only those electrons from the near surface region can escape without losing a significant portion of their energy and thus be identified as Auger electrons. The average depth from which such electrons can escape is the same as for XPS.



The Auger spectrum can be modified by changes in the chemical environment in the surface region of the solid, resulting in energy shifts and line shape modifications. These effects can be utilised in identifying chemical states of surface atoms. Quantitative analysis can be performed by using standards to produce relative sensitivity factors and, if combined with ion sputtering, a process which sequentially removes atomic layers, depth profiling can be carried out. This is achieved by bombarding the surface with inert gas ions such as argon with energies of 2 to 5 keV.

Sputtered depths may be reported in terms of sputtering time but in order to convert to spatial dimensions, the etch rate ( $\mu$ ), must be known<sup>141</sup>. This can be determined by the following relationship:

$$\mu = \frac{M S j}{\rho N_a e^-} \quad (\text{nm.min}^{-1}) \quad (2.28)$$

where: M is atomic weight, S is sputtering yield<sup>142</sup>, determined empirically, j is the current density ( $\text{A.cm}^{-2}$ ),  $\rho$  density ( $\text{K.gm}^{-3}$ ),  $N_a$  is Avagadro's number and  $e^-$  is the electron charge.

### 2.11.7 Applications of Surface Analytical Techniques

Surface sensitive analytical techniques provide compositional measurements of the outermost atomic layers of solids and of the interfaces between materials within the solid. The surface almost always has a composition which is different from the bulk material. This may be due to the presence of contaminants such as hydrocarbons and/or products formed as a result of chemical changes which have occurred deliberately due to surface modifications by for example, nitriding of steel or by natural reactions with the environment.

SEM and EDS are relatively inexpensive techniques to determine the morphology of surfaces and their chemical compositions to depths of the order of a micron. Together with XRD for phase identification, they are powerful tools in wear and corrosion

studies. In addition to these, a large number of techniques are available for investigating all aspects of surfaces but the majority of these come under the heading of Surface Science and are not appropriate for “routine” compositional analysis of surfaces encountered in everyday products. The three most widely used techniques are: XPS, (also known as Electron Spectroscopy for Chemical Analysis (ESCA)), AES and Secondary Ion Mass Spectroscopy (SIMS), utilising a primary excitation source of X-rays, electrons and ions respectively. Information on the composition of the topmost atomic layers is of immense benefit in the understanding of many technologically important processes such as oxidation and corrosion, catalysis, adhesion, thermionic emission, crystal growth, wear, etc. Surface analysis can provide this and also be used as a diagnostic technique to determine why a surface does or does not possess the desired optical, electrical, mechanical, chemical or decorative properties.

For this study XPS was selected to provide a relatively rapid identification of the elements present in the initial 5-7 nm of the surface of tin coated coupons before and after field testing. In addition, the technique would be able to provide information on the oxidation state of corrosion products. AES depth profiling is the preferred method for determining the thickness of corrosion products and for diffusion studies. An alternative method for measuring oxide formation is Coulometric Cathodic Reduction which determines the charge necessary to reduce surface oxides.<sup>143</sup>

For diffusion studies the “*CRC Handbook of Chemistry and Physics*”<sup>144</sup> quotes four forms of the radioactive tracer methods as the standard techniques used to determine the activation energy ( $Q$ ) and diffusion frequency factor ( $D_0$ ). These are Autoradiography, Residual Activity, Surface Decrease and Serial Sectioning. Essentially the tracer method involves the initial deposition of a suitable radioactive isotope on one of the specimen surfaces by a standard thin film technique, followed by the diffusion annealing treatment. Thin sections are then removed and the radioactivity measured. The thickness of the section can be determined from the weight, mass density and cross-sectional area. Kaur and Gust<sup>145</sup> quote detection sensitivities of between 0.1 and 1 at%. The technique has the benefit of being able to

determine self diffusion rates but is limited by the availability of suitable stable isotopes and is complicated by the use of involved sample preparation. Ion beam sputter profiling by, AES and SIMS, is not limited in this way but is not without its own drawbacks. For example topographical effects can occur during the etching process due to crystallographic orientation causing preferential sputtering around grain boundaries with similar effects being caused by selective sputtering of a higher yield component in a multi-component material.

From the literature, serial sectioning and measuring the thickness of intermetallic phases from optical and SEM backscattered electron images is the method that has been adopted by workers measuring intermetallic growth kinetics for electrical connector applications. This method is limited by grey level resolution but may be improved using suitable etchants to delineate phases. The technique, however, would not be sensitive enough to measure the degree of grain boundary or 'pipe' diffusion. An improvement on the technique is the use of EDS and WDS element line scanning across the microsection, with lower limits of detection being achieved by the latter due to its superior sensitivity. In both cases, however, the limitation is that of spatial resolution. The excitation volume, having a diameter of approximately  $1\mu\text{m}$ , limits accurate measurements to intermetallic thicknesses of several microns. Thus for both the sectioning and the line scanning approach, diffusion across coating thicknesses of the order of  $1\mu\text{m}$  can only be achieved from extrapolation back to zero of the thickness/ageing time graph of thicker platings.

Depth profiling by AES and SIMS using ion beam sputtering is a preferred method particularly where diffusion through thinner coatings are to be measured. Nakamura and Takahashi<sup>146</sup> when comparing thermal ageing effects on electro-tin and reflowed electro-tin used AES profiling to depths of  $1\mu\text{m}$  through a coating thickness of  $1.3\mu\text{m}$ . However, apart from preferential sputtering errors, the techniques are normally prohibitive due to long sputtering times and the need to perform large numbers of analyses over the sample to give statistically reliable results. No references have been found in the literature where intermetallic growth rates have been measured over such small distances from the tin/copper interface.

## 2.12 Conclusions from the Literature Survey.

The tin plated contact has been chosen by the automotive industry for its low cost and generally good corrosion resistant properties but it is apparent from the survey that, when used in a vehicle electrical connector system, it is vulnerable to a variety of environmental factors, not least being those responsible for inducing fretting corrosion. Whether manifested by high or low frequency micro-motion, the formation of resistive oxide films are the prime cause of contact failure. Although the oxidation of tin has been extensively studied, there appears to be little or no published data on specific long-term field testing of the metal for automotive connector applications.

Fretting corrosion has been shown to be a major reliability issue, which, although difficult to eliminate, may be minimised by the selection of a suitable lubricant. The choice nevertheless generally appears to be made on an *ad hoc* basis with little understanding of the effects on this particular wear regime.

The mechanism of the fretting process has been examined and modelled by a number of workers, but not always with the same conclusions and none to the author's knowledge, with respect to the possible beneficial effects of intermetallics on fretting performance. An interesting finding of the literature survey was that although several researchers had investigated the effects of copper/tin intermetallics on CR, there was limited reference to the role of these phases with respect to their wear characteristics. In addition, from the experimental data published, there appears also to be no consensus of opinion on the growth kinetics of these hard phases. This is probably due to the significant errors which are inherent in the standard sectioning techniques used to characterise them.

The presence and variable spatial distribution of the intermetallic phases in the tin layer, compounded by their increase in volume with time and temperature, complicate any evaluation of wear and corrosion properties. It is apparent, therefore, that the coating cannot be regarded as a monolithic material but rather as a composite having an initial oxide surface layer, an intermediate region of pure tin and underlying hard irregular phases, with physical and chemical properties unlike their parent metals. Any

wear process will result in the exposure of these intermetallics, accompanied by a change in the contact properties and an effect on fretting performance.

From the subject areas examined in the literature survey, the present study will focus on the following aspects which influence contact resistance of the HDT plated separable connector:

- (i) Surface oxidation using XPS to identify the valence state of the tin oxide and thickness determinations from AES depth profiles. From this the relationship between contact resistance and oxide thickness will be determined.
- (iii) Intermetallic formation and growth kinetics and the development of a method of determining solid state diffusion rates in thin ( $>1\mu\text{m}$ ) coatings, using AES depth profiling, XRD phase identification and SEM/EDS analysis.
- (iv) The fretting corrosion process and the influence of intermetallics on wear rate. This will be examined primarily by SEM/EDS.
- (v) The relationship between lubricant formulation, reactivity and fretting performance using IRAS and SEM techniques.

## References

- <sup>1</sup> Carroll, J., "Connectors: Roadside Experiences", Colloquium on "Connectors on Vehicles", IEE Digest No: 1993/228, (1993)
- <sup>2</sup> *ASM Handbook*, Vol. 2, "Properties and Selection: Nonferrous Alloys and Special-Purpose Materials", ASM International, (1990).
- <sup>3</sup> *ASM Handbook*, Vol. 2, (ASM International, Ohio), p. 355, (1990).
- <sup>4</sup> Liljestr nd, L., Sj gren, L., Revay, L.B. and Asthner, B., "Wear Resistance of Electroplated Nickel-Hardened Gold", IEEE Transactions on Components, Hybrids and Manufacturing Technology, Vol. CHMT-8, No. 1, (1985).
- <sup>5</sup> Geckle, R.J. and Mroczkowski, R.S., "Corrosion of Precious Metal Plated Copper Alloys Due to Mixed Flowing Gas Exposure", Thirty Sixth IEEE Holm Conf. On Electrical Contacts, Quebec, (1990).
- <sup>6</sup> Yasuda, K, Umemura, S., and Aoki, T., "Degradation Mechanisms in Tin and Gold Plated Connector Contacts." 32nd IEEE Holm Conference on Electrical Contacts, (1986).
- <sup>7</sup> Sproles, E.S., "The Effect of Frictional Polymers on the Performance of Palladium Connector Contacts," Proc. Electronic Components Conference, pp. 317-323, (1980)
- <sup>8</sup> Jowett, C. E., *Environmental Hazards in Electronics*, (The October Press, Fareham), (1982).
- <sup>9</sup> Nakumura, A., Takahashi, M., "The Reliability of Tin Plated Terminals in Automotive Applications", Sumitomo Wiring Systems Ltd., 1820 Nakanoike, Mikkaichi-cho, Suzuka Mie-ken 513, Japan, (Unpublished).
- <sup>10</sup> Tan, A.C., *Tin and Solder Plating in the Semiconductor Industry*, (Chapman and Hall, London), (1993).
- <sup>11</sup> Karpel, S., "Tin and Tin Alloys for Connector Finishes", *Tin and its Uses*, No: 146, International Tin Research Institute, (1985).
- <sup>12</sup> Blackler, R.W., Warwick, M.E., and Long, J.B., "Preliminary Studies of Tin and Tin Rich Coatings as Electrical Contact Materials", 26th IEEE Holm Conference on Electrical Contacts, Chicago, (1980).
- <sup>13</sup> Pike-Biegunski, M.J., "Electrical Conductance at Tin-Tin Interfaces Under Stationary and In-Motion Conditions", 36th IEEE Holm Conference on Electrical Contacts, Quebec, (1990).
- <sup>14</sup> Mamrick, M.S., "Fretting Corrosion of Tin at Elevated Temperatures", 34th IEEE Holm Conference on Electrical Contacts, San Francisco, (1988).
- <sup>15</sup> Abbott, W.H., and Whitley, J.H., "The Lubrication and Environmental Protection of Alternatives to Gold for Electronic Connectors", 21st IEEE Holm Conference on Electrical Contacts, Chicago, (1975).
- <sup>16</sup> Sugimura, K. and Nagae, A, "Lubricants for Some Plated Contacts", 36th IEEE Holm Conference on Electrical Contacts, Quebec, (1990).
- <sup>17</sup> Young, W.C., *Roark's Formulas for Stress and Strain*, 6th ed., Chap. 13, (McGraw-Hill, New York), (1989).

- 18 Kantner, E.A. and Hobgood, L.D., "Hertz Stress as an Indicator of Connector Reliability", *Connection Technology*, (March 1989).
- 19 Stennett, N.A., Ireland, T.P. and Campbell, D.S., "Normal Force Reduction in Electronic Contacts", 36th IEEE Holm Conference on Electrical Contacts, Montreal, (1990).
- 20 Hutchings, I.M., *Tribology: Friction and Wear of Engineering Materials*, (Edward Arnold, London), (1992).
- 21 Bowden F.P and Tabor, D., *Friction and Lubrication of Solids Part I*, (Oxford University Press); Revised edition (1954).
- 22 Bowden F.P and Tabor, D., *Friction and Lubrication of Solids Part II*, (Oxford University Press), (1964).
- 23 Bryant, M.D., "Resistance Build-up in Electrical Connectors Due to Fretting Corrosion of Rough Surfaces", 39th IEEE Holm Conference on Electrical Contacts, Pittsburgh, (1993).
- 24 Antler M. and Gilbert J., *J. Air Pollution Control Association*, **13**, No. 9, (Sept. 1963)
- 25 Greenwood J.A., "Contact at Rough Surfaces", Proc. of the NATO Advanced Study Institute on Fundamentals of Friction, Braunlage, Harz, Germany, (1991).
- 26 Chapman, A.H., "Tin and Tin Alloy Plating - 63 A Review", ITRI Publication No. 606.
- 27 Pashley, M.D., Pethica, J.B. and Tabor D., *Wear*, **100**, pp.7-31. (1984).
- 28 Adamson, A.W., *Physical Chemistry of Surfaces*, (Interscience Publishers, Inc., New York), (1960).
- 29 Atkins, P.W., *Physical Chemistry*, 3rd Ed., (Oxford University Press, Oxford), (1987).
- 30 *ASM Handbook*, Vol. 2, "Properties and Selection: Nonferrous Alloys and Special-Purpose Materials", (ASM International, Ohio). P. 519, (1990).
- 31 Rollason, E.C., *Metallurgy for Engineers*, (Edward Arnold), (1973).
- 32 Tottle, C.R., *An Encyclopaedia of Metallurgy and Materials*, (McDonald and Evans Ltd., Plymouth), (1984).
- 33 Glossbrenner, E., "The Life and Times of an A-Spot - A Tutorial on Sliding Contacts," Proceedings of the Thirty-Ninth IEEE Holm Conference on Electrical Contacts, Pittsburgh, (1993).
- 34 Holm, R., *Electrical Contacts*, Fourth Edition, (Springer Verlag, Berlin), (1968)
- 35 Lord Rayleigh, Phil. *Trans. Roy. Soc.*, **161**, pp. 77-118, (1871).
- 36 Holm, R., *Wiss., Veroff Siemens - Werken*, **7** (2), pp 217-58, (1929).
- 37 Holm, R., *Electric Contacts*, (Springer Verlag, New York), pp 22-23, (1967).
- 38 Greenwood. J. A., *Brit. J. Appl. Phys.*, **17**, pp 1621-1632, (1966).
- 39 Boyer, L., Noel, S. and Houze, F., "Constriction Resistance of a Multispot Contact: An Improved Analytical Expression", Proceedings of the Thirty-Sixth IEEE Holm Conference on Electrical Contacts, Montreal, (1990).
- 40 Holm, R., *Electrical Contacts*, Fourth Edition, (Springer Verlag, New York), (1967)
- 41 Runde, M., Hodne, E. and Totdal, B., "Experimental Study of the Conducting Spots in Aluminium Contact Interfaces", 35<sup>th</sup> Holm Conference on Electrical Contacts, (1989).

- 
- Levine, E. and Kitchner, J., *IRPS Proc.*, **22**, p. 242 (1984).
- Metals Handbook, Ninth Edition*, Vol. 13, (ASM International, Ohio), p. 20, (1987).
- Cottis, R.A., "Economic Aspects of Corrosion, Corrosion Engineering and Control", University of Manchester Institute of Science and Technology, (1991).
- Shrier, L. L., "*Corrosion*", Vol. 1, (George Newnes, London) (1963).
- Metals Handbook, Ninth Edition*, Vol. 13, ASM International, Metals Park, Ohio, p. 20, (1987).
- Britton, S.C., "Tin Versus Corrosion", International Tin Research Institute Publication No. 510. (1975)
- Lyon, S., "Corrosion of Metals in the Atmosphere, Corrosion Engineering and Control", University of Manchester Institute of Science and Technology, (8th-12th April 1991).
- Warwick M.E. "Atmospheric Corrosion of Tin and Tin alloys" Publication 602, Tin Research Institute, (1980).
- Wagner, C. *Diffusion and High Temperature Oxidation of Metals*, Atom Movements, American Society for Metals, Cleveland.
- Higgins, R.A., *Properties of Engineering Materials*, (Hodder and Stoughton), (1977).
- Pilling N.B., and Bedworth, R.E., *J. Inst. Met.* **29**, 529, (1923).
- Kenworthy, L., *Trans, Faraday Soc.*, Vol 31, p 1331, (1935).
- Britton S.C., "Tin Versus Corrosion", Publication 510, Tin Research Institute, (1975).
- Boggs, W.E., Kachik R.G. and Pellisier, G.E., *J. Electrochem. Soc.* Vol 108 (No.1), (1961).
- Boggs, W.E., Trozza, P.S. and Pellisier, G.E., *J. Electrochem. Soc.* Vol 108 (No.1), p. 13, (1961).
- Boggs, W.E., Kachik, R.G. and Pellisier, G.E., *J. Electrochem. Soc.* Vol 108 (No.1), (1961).
- Boggs, W.E., Kachik, R.G. and Pellisier, G.E., *J. Electrochem. Soc.* Vol 108 (No.2), (1961).
- Boggs, W.E., Kachik, R.G. and Pellisier, G.E., *J. Electrochem. Soc.* Vol 111 (No.6), (1964).
- Warwick, M.E., "Atmospheric Corrosion of Tin and Tin alloys" Publication 602, Tin Research Ins. (1980).
- Gruhl, W., *Metall*, Vol 6, p 177, (1952).
- Ackroyd, M.L. and Mackay, C. A., "Solders, Solderable Finishes, and Reflowed Coatings", Publication 529, International Tin Research Institute, (1977).
- Bilbrey J.H., Wilson D.A., and Spendlove, M.J., US Bur. Mines Rep. Invest., (1955).
- Pike-Bieganski M.J., "Electrical conduction at Tin-Tin Interfaces Under Stationary and In-Motion Conditions", Proceedings of the Thirty-Sixth IEEE Holm Conference on Electrical Contacts, Quebec, (1990).
- Leidheiser, H. Jr., "The Corrosion of Copper, Tin and Their Alloys", (Kreiger, R.E.), (1979).
- Jenkins, R.D., *Proc. Phys. Soc.*, **47**, p 107, (1935).
- Yasuhiro et al, "Degradation Characteristics of Connector Contact Systems with Gold/Tin and Gold/Silver Interfaces" *Electronics and Communications in Japan*, Vol. 67-C, No. 1, (1984).



- 
- 68 Yasuda, K. Umemura, S. and Aoki, "Degradation Mechanisms in Tin and Gold Plated Connector Contacts," Proc. of the 32nd Holm Conf. on Electrical Connectors, (1986).
- 69 Engel, L. and Klingele, H, *An Atlas of Metal Damage*, (Wolfe Publishing, London), (1981).
- 70 Hedges, E.S., *Tin and Its Alloys*, (Edward Arnold, London), (1960).
- 71 Revay, L., "Interdiffusion and Formation of Intermetallic Compounds in Tin-Copper Alloy Surface Coatings", *Surf. Tech.*, pp. 57-63, (1977).
- 72 Smigelskas, A.D. and Kirkendall, E.O., *Trans. AIME*, 171, pp.130, (1947).
- 73 Kay, P.J. and Mackay, C.A., *Trans. Inst. Met. Fin.*, 54, pp. 68-74, (1976).
- 74 Braunovic, M., and Aleksandrov, N., "Intermetallic Compounds at Aluminium-to-Copper and Copper-to-Tin Electrical Interfaces, Thirty-Eighth IEEE Holm Conference on Electrical Contacts, (1992).
- 75 Mackay, C.A. and Unsworth, D.A., *Trans. Inst. Met. Fin.*, 51, pp85-89.
- 76 Lindborg, U., Asthner, B., Lind, L. and Revay, L., "Intermetallic Growth and Contact Resistance of Tin Conatcts after Ageing", *IEEE Trans. PHP*, Vol. PHP-12, pp.33-39, (March 1976).
- 77 Haimovich, J., "Hot Air Levelled Tin: Solderability and Some Related Properties", Proc. of the Thirty Ninth Electronic Components Conference, (1989).
- 78 Owen, E.L., "Properties of Electrodeposits, Their Measurement and Significance" (Sard, R., Leidheisrt, H., Jr., and Ogburn, editors, Princeton: Electrochemical Society Inc.), Ch. 6, pp. 80-101, (1975).
- 79 Reed-Hill, R.E., *Physical Metallurgy Principles*, (D.Van Nostrand Company, Inc), (1972).
- 80 Geckle R.J., "Metallurgical Changes in Tin Lead Platings Due to Heat Ageing", Forty First Electronic Components and Technology Conference, Georgia, (1991).
- 81 Dabritz, S., "Resistance Changes in Microelectronic Contact Zones Caused by Diffusion", 7<sup>th</sup> Mikrosonde Conf., Dresden, (1988).
- 82 Czichos, H., *Tribology*, (Elsevier, Amsterdam), (1977).
- 83 Burwell, J.T., *Wear* 1, pp119-141, (1958).
- 84 Hutchings, I.M., *Tribology - Friction and Wear of Engineering Materials*, p. 92, (Edward Arnold, London), (1992).
- 85 Archard, J.F., *J. Appl. Phys.* 24, pp. 981-988, (1953).
- 86 Lancaster, J. K. *Proc. Roy. Soc.*, 273A, pp. 466-483, (1963).
- 87 Moore, M.A., *Materials in Engineering Applications*, pp. 97-111, (1978).
- 88 Bowden, F.P., Tabor, D., *Friction an Introduction to Tribology*, (Heinemann, London), (1973).
- 89 Antler, M., *Wear* 106, No. 1-3, pp. 5-33, (1985).
- 90 Antler, M., "Fretting Corrosion of Solder-Coated Electrical Contacts," *IEEE Trans. Components, Hybrids and Manufacturing*, Vol. CHMT-7, No. 1, pp. 129-138, (1984).

- 91 Holm, R., *Electric Contacts Handbook*, 3rd Ed., (Springer-Verlag, Berlin,), pp. 102-114, 369-377, (1958.)
- 92 Braunovic, M., *Wear*, **112**, pp. 181-197, (1986).
- 93 Braunovic, M., *Wear*, **125**, pp. 53-68.
- 94 Braunovic, M., "Fretting Corrosion Between Aluminium Wires and Different Contact Materials," Proc. Holm Conf. on Electrical Contacts, IIT, Chicago, pp. 223-232, (1977).
- 95 Saka, N., Liou, M.J. and Suh, N.P., *Wear*, **100**, pp. 77-105, (1984).
- 96 Holden, C.A., Law, H.H. and Crane, G.R., "Effect of Surface Structure on the Contact Resistance Measurements of Electrodeposits", Proceedings of the Thirty-fourth IEEE Holm Conference on Electrical Contacts, San Francisco, (1988).
- 97 Bramhall, R., "Studies in Fretting Fatigue," D. Phil. University of Oxford, (1973).
- 98 Leadbeater, G., Noble, B. and Waterhouse, R. B., "The Fatigue of an Aluminium Alloy Produced by Fretting on a Shot Peened Surface," Proc. 6<sup>th</sup> Inter. Conf. On Fracture, (Pergamon), Vol. 3, pp 2125-2132, (1984).
- 99 Suh, N.P., *Tribophysics*, (Prentice-Hall, New Jersey), pp. 416-442, (1986).
- 100 Lee, A., Mao, A. and Mamrick, M.S., "Fretting Corrosion of Tin at Elevated Temperatures," Proceedings of the Thirty Fourth IEEE Holm Conference on Electrical Contacts, San Francisco, (1988).
- 101 Archard, J.F., *Wear*, **2**, pp438-455, (1959).
- 102 Hutchings, I.M., *Tribology - Friction and Wear of Engineering Materials*, p. 94, (Edward Arnold, London), (1992).
- 103 Lee, A. and Mamrick, M., "Fretting Corrosion of Tin Plated Copper Alloy," Proceedings of the Thirty Second Holm Conf. On Electrical Contacts, (1986).
- 104 Ireland, T.P., Stennett, N.A. and Campbell, D.S., *Trans. Inst. Met. Fin.*, **67**, 127, (1989).
- 105 Stennett N. and Swingle J., "Effect of Power on Low Frequency Fretting Corrosion", Proceedings of the Thirty-Ninth IEEE Holm Conference on Electrical Contacts, Pittsburgh, (1993).
- 106 Charman, D.H., Turner, C. and Turner, H.W., "Users Guide to the Correct Use of Electrical Contacts," ERA Report 90-0405R, (1990).
- 107 Kohlrausch, F., "Über den Stationären Temperaturzustand eines Elektrisch Geheizten Leiters," Ann. Phys., **1**, 1900, p. 132.
- 108 Garte, S.M., "The Effect of Design on Contact Fretting," Proc. Holm Seminar On Electrical Contacts, Illinois Inst. of Tech., Chicago, pp.65-70, (1976).
- 109 Lee, A., Mao, A. and Mamrick, M.S., "Effect of Contact Geometry on Fretting Corrosion of Tin-Plated Copper-Alloy" Proc. 14<sup>th</sup> Int. Conf. On Electrical Contacts, Paris, pp. 225-231, (1988).
- 110 Hoover, J.M. and Peekstok, K., "The Influence of Practical Contact Parameters on Fretting Corrosion of Tin-Base Low-Level Connector Contacts" Proc. 33<sup>rd</sup> Holm Conf. On Electrical Contacts, (1987).

- Antler, M., "Fretting Corrosion of Solder-Coated Electrical Contacts" IEEE Trans. Components, Hybrids, *Manuf. Technol.*, 7, pp.129-138, (1984).
- ASM Handbook, Vol. 18, "Friction Lubrication and Wear Technology", (ASM International), (1992).
- Feng, I.M. and Uhlig, H.H., *J. Appl. Mech.*, 21, pp 395 - 400 (1954).
- Williamson, B. "The Microworld of the Contact Spot" Proc. 27<sup>th</sup> Holm Conf. On Electrical Contacts, (1981).
- Bock, E.M. and Whitley, J.H. "Fretting Corrosion in Electric Contacts" Proc. 20<sup>th</sup> Annual Holm Seminar on Electrical Contacts, pp. 128-138, (1974).
- Souter, J.W. and Staunton, W., *Trans. Inst. Met. Fin.*, 66, Pt. 1, pp. 8-14, (1988).
- Bowden, F. and Tabor, D., *Reibung u. Schmierungsfester*, (Korper, Springer, Berlin), (1959).
- Spikes, H.A, "Additive-Additive and Additive-Surface Interactions in Lubrication", *Sci.*, 2, 1, (1989).
- Langmuir, I., *J. Am., Chem., Soc.*, 39, p. 1848, (1917).
- Blodgett, K.B., *Phys. Rev.*, 55, p.391, (1939).
- Landmuir, I., *Trans. Faraday Soc.* 15, 65. (1970).
- Bowden, F.P. and Tabor, D., *The Friction and Lubrication of Solids*, (Carendon Press), Oxford, (1950).
- Beltzer, M. and Jahanmir, S., "Role of Dispersion Interactions Between Hydrocarbon Chains in Boundary Lubrication" *ASLE Trans.* 30.1, pp. 47-54.
- Hardy, W.B., *Collected Works*, (Cambridge University Press), (1936).
- Timsit, R. S., "Effects of Surface Reactivity on Tribological Properties of a Boundary Lubricant", Proc. of the NATO Advanced Study Institute on Fundamentals of Friction, Braunlage, Harz, Germany, (1991).
- Fischer, T.E., "Chemical Effects in Friction", Proc. of the NATO Advanced Study Institute on Fundamentals of Friction, Braunlage, Harz, Germany, (1991).
- Razavizadah, K. and Eyre, T.S., *Wear*, 79, 325, (1982).
- Hermance, H.W. and Egan, T.F., *Bell Syst. Tech. J.*, 37, 739-777, (1958).
- Klamann, D., *Lubricants and Related Products*, Verlag Chemie GmbH, D-6940 Weinheim, (1984).
- Antler, M. and Feder, M., "Friction and Wear of Electrodeposited Palladium Contacts: Thin Film Lubrication With Fluids and With Gold", 36<sup>th</sup> Electrical Components Conference, (1986).
- Wang, S., Lee, A. and Mamrick, M., "An Electrochemical Technique for Evaluating Electrical Contact Lubricants", 33<sup>rd</sup> Holm Conference, (1987).
- Goldstein, J.L., *et al*, *Scanning Electron Microscopy and X-Ray Microanalysis*, 2<sup>nd</sup> ed., Plenum Press, New York, (1992)
- Richards, R.G., Owen, G.Rh. and Gwynn, I., "Backscattered Electron Imaging Revisited", *Microscopy and Analysis*, (Rolston Gordon Communications, Issue 61), (Sept. 1997).

- 
- 134 "CAMEO". A trademark of Oxford Instruments Ltd.
- 135 Joint Committee on Powder Diffraction Standards, (JCPDS International Centre for  
Diffraction Data, Swarthmore, PA).
- 136 "*Perkin-Elmer Library of Infrared Spectra*", the Perkin-Elmer Corporation, 1985.
- 137 *Oils, Lubricants and Petroleum Products*, the Perkin-Elmer Corporation, 1986.
- 138 Verdura, T.M., "Infrared Spectra of Lubricating Grease Base Oils and Thickeners," NLGI 38<sup>th</sup>  
Annual Meeting, Atlanta, (1970).
- 139 Humecki, H.J., *Practical Guide to Infrared Microspectroscopy*, (Marcel Dekker Inc., New  
York), (1995).
- 140 Timsit, R.S., "Effect of Surface Reactivity on Tribological Properties of a Boundary  
Lubricant", Proc. Of the NATO Advanced Study Institute on Fundamentals of Friction,  
Braunlage, Germany, (1991)
- 141 Briggs, D. and Seah, M.P., *Practical Surface Analysis*, 2ns Ed., vol. 1 - 'Auger and  
Photoelectron Spectroscopy', John Wiley and Sons, Chichester, (1990).
- 142 Seah, M.P., "Pure Element Sputtering Yields Using 500 - 1000 eV Argon Ions", *Thin Solid  
Films*, vol. 81, pp 279-287, (1981).
- 143 Britton, S.C., International Tin Research Publication, No. 510, pp 76-77, (1975).
- 144 "*CRC Handbook of Chemistry and Physics*", (CRC Press Inc. Florida), (1979).
- 145 Kaur, I. and Gust, W., *Handbook of Grain and Interphase Boundary Diffusion Data*, (Ziegler  
Press, Stuttgart), (1989)
- 146 Nakamura, A and Takahashi, M, "The Reliability of Tin Plated Terminals in Automotive  
Application", Sumitomo Wiring Systems Ltd., 1820 Nakanoike, Mikkaichi-cho, Suzuka Mie-  
ken 513, Japan, (Unpublished).

### **3. Experimental**

From the literature survey it was apparent that the resistance to electron flow is influenced by a range of environmental factors acting on and modifying the intrinsic physical and chemical properties of the contact materials. Therefore, before a test programme could be embarked upon it was important that these properties and the environments in which the connector must function in service, must as far as possible be evaluated. Only after this initial characterisation could the experimental investigation focus on the specific topic of this study namely the mechanism of fretting corrosion in both dry and lubricated conditions, induced as a result of low cycle micro-motion.

The work programme took the following form:

- (i) Design and construction of test equipment.
- (ii) Analysis of test materials.
- (iii) Analysis of materials tested in controlled and field environments.
- (iv) Dry and lubricated low frequency fretting tests.

## **3.1 Design and Construction of Test Equipment**

### **3.1.1 Field Test Enclosures**

In addition to standard laboratory tests, such as salt spray and humidity testing, 'real' environments were used which, although not controllable, would provide a practical demonstration of the conditions existing under-bonnet and in the passenger compartments of vehicles. Ideally, continuous monitoring of temperature, vibration and local atmospheric composition, to provide a detailed record of the conditions at the test sites would have been desirable. However, the construction of the necessary test equipment was beyond the scope of this study but from the quantity and the composition of significant airborne contaminant reaction products, the conditions existing in the various sites could be deduced.

In order to limit exposure of the coupons to airborne species only, it was necessary to house them in specially constructed enclosures consisting of an anodised aluminium box containing machined ventilation and drainage holes which supported two polypropylene carriers. These were held in place by leaf springs. The coupons were protected from direct incident spray by stainless steel baffles; Fig. 3.1 and Appendix B.

### **3.1.2 Reactivity Cell**

An in-depth study of the effects, on the degree of oxidation, of the tin surface with different lubricants and the multitude of other variables encountered in the various automotive environments, is beyond the scope of this current work. It is sufficient to note that although metal oxidation has been recognised as being the major factor in reducing the fretting life of lubricated contacts, effort here is focused on obtaining a possible correlation between the measured reactivity of the lubricant, due to the presence of polar constituents and the tribological influence of the latter on fretting performance.

The cell designed for this study consisted of a twelve channel power supply used to

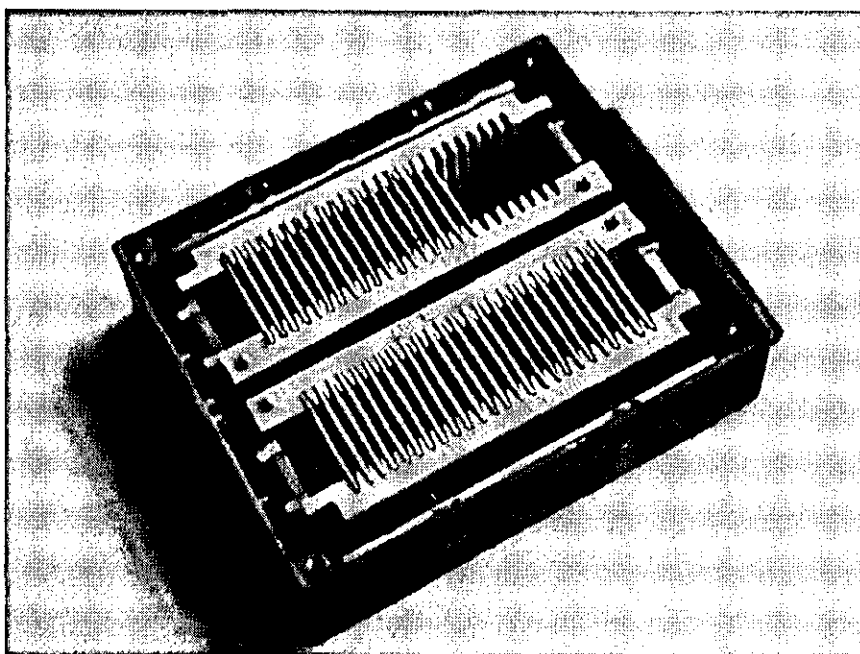


*Fig. 3.1 Test Coupon Enclosure*

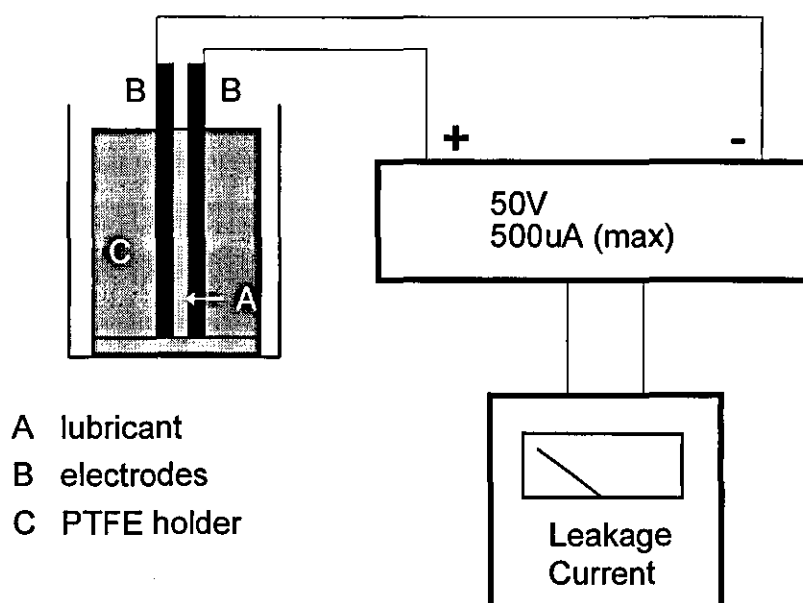


*Fig. 3.2 Schematic of Reactivity Cell.*

apply a potential of 50V across two test coupons immersed in the lubricant. The coupons were held 2mm apart in PTFE holders in a small beaker which was kept at a constant temperature of 125°C for a period of ten days, over which time the current leakage was measured periodically from the voltage drop across a 100K $\Omega$  precision

resistor, see Fig. 3.2. A digital voltmeter (Fluke type 21) was set to 300 mV scale giving a current output in tenths of a micro-amp, i.e. a reading of 12.5 mV was equivalent to a current of 0.125  $\mu$ A. The more current that flowed in the circuit, that is the lower the resistance of the lubricant, the greater the voltage drop across the resistor. The resistor restricted the available current to approximately 0.5 mA per channel at 50V dc, preventing a risk from shock or fire hazard.

### **3.1.3 Contact Resistance Apparatus**

The rig was designed to determine contact resistance changes as a result of the effects on coupons following accelerated tests and exposure to the test environments.

The following factors were considered pertinent to the design requirements:

- (i) The probe contact should be interchangeable and of 3 mm diameter pure gold in contact with a flat sample with a maximum load sufficient to produce local deformation.<sup>1</sup>
- (ii) A minimum of twenty measurements are required per coupon.<sup>2</sup>
- (iii) The z-loading speed and force must be consistent.<sup>3</sup>
- (iv) Extraneous vibrations must be excluded.<sup>4</sup>
- (v) The measurements must be dry circuit, 4 wire.
- (vi) Thermal EMF compensation should be unnecessary (Using the Keithley 580 as the pulsed drive, automatically cancels thermal offsets).
- (viii) Extreme values, for example when the probe hits a site of pore corrosion, should be excluded.<sup>4</sup>

The rig, Figs. 3.3, 3.4 and Appendix B, employed a stepper motor driven X-Y stage to move test coupons under the probe head, which consisted of a 3mm diameter spherical gold tip and two sharp outer electrodes with high contact loadings sufficient to cut through any contaminant films. The probe incorporated a feedback transducer to ensure that a consistent force variable between 0.4N and 1.2N, was applied and the resistance measurements were performed by a Keithley 580 micro-ohm meter and sent down an IEEE 488 bus and stored on computer.



### 3.1.4 Low Frequency Fretting Test Rig

Fretting tests for connector studies have been performed by several workers using high frequencies ( $>10$  Hz), medium frequencies ( $\sim 10$  mHz to 10 Hz) and low frequencies ( $< 10$  mHz) with apparatus employing stepper motors, solenoids and expanding rods.<sup>5,6,7</sup>

For the latter design, a metal bar to which is attached one of the contacts (the rider), is thermally cycled and the resultant thermal expansion provides the desired micro-motion. For this study a simple apparatus utilising an aluminium base (CTE  $23.7$  ppm  $^{\circ}\text{C}^{-1}$ ) and Invar rods with a negligible expansion coefficient. A test coupon was clamped to the base and the whole assembly was thermally cycled in an oven, (Fig. 3.5). A thermocouple was placed inside the aluminium base plate to monitor

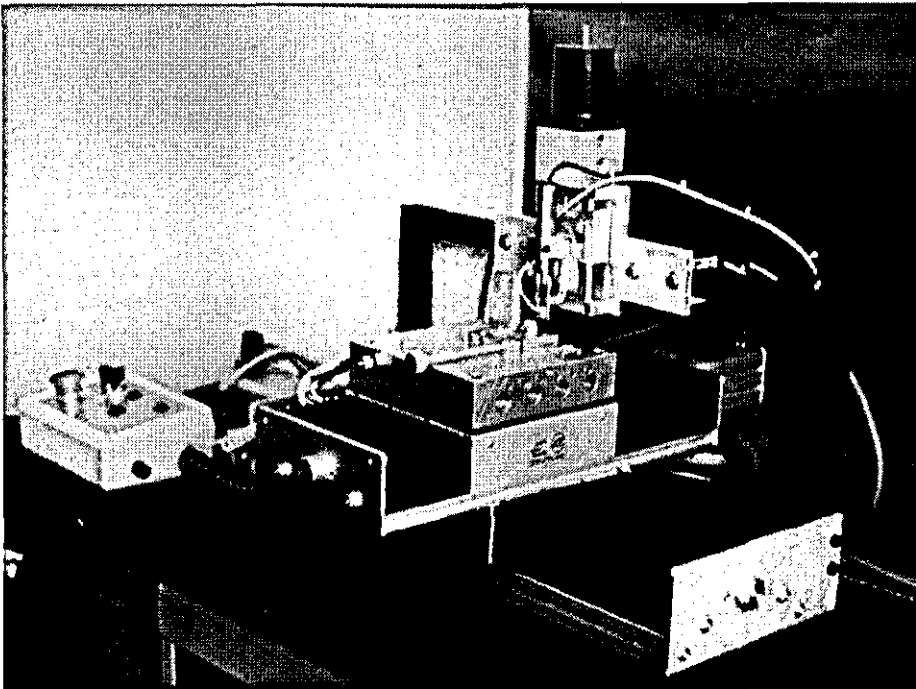


*Fig. 3.3 Contact Resistance Rig*

temperature changes and a load was applied using 100g weights. Using a four wire contact resistance test, 'source' current was supplied through the contacts and the

voltage drop was 'sensed' and monitored by calibrated chart recorders. The open circuit voltage was kept below 20 mV to ensure 'dry circuit' conditions,<sup>8</sup> Fig. 3.6.

Low frequency fretting ( $1.4 \times 10^{-4}$  Hz ) was achieved by thermally cycling between 85°C and 125°C, using a load of 0.98N. The temperature ranges used were typical of those found in an automotive vehicle engine compartment. These conditions resulted in a travelling velocity of approximately  $0.05 \mu\text{ms}^{-1}$  and the formation of a wear scar approximately 300 to 400  $\mu\text{m}$  in length. Such a slip amplitude, i.e.  $>100 \mu\text{m}$  tends towards a wear rate similar to that of reciprocating sliding wear. The wire rider had a cylindrical cross-section giving a 'cylinder on flat' contact geometry.

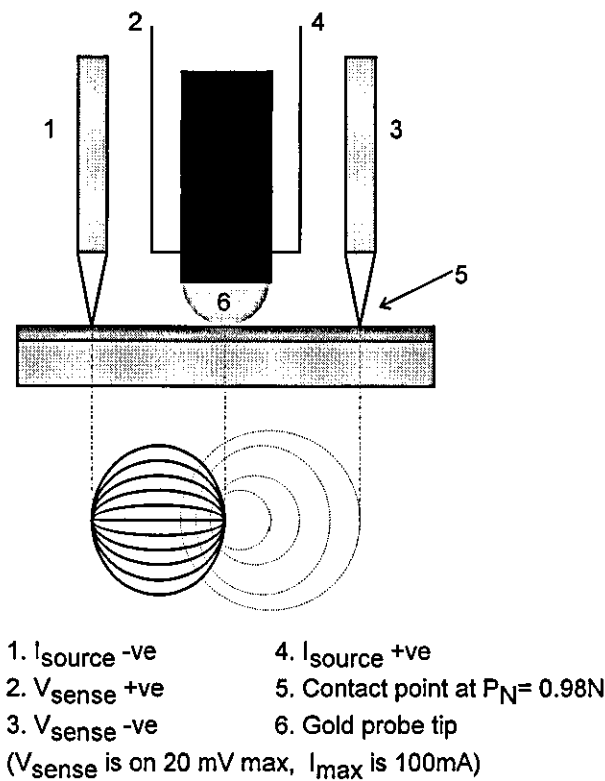


**Fig. 3.4 Schematic of Resistivity Probe Head**

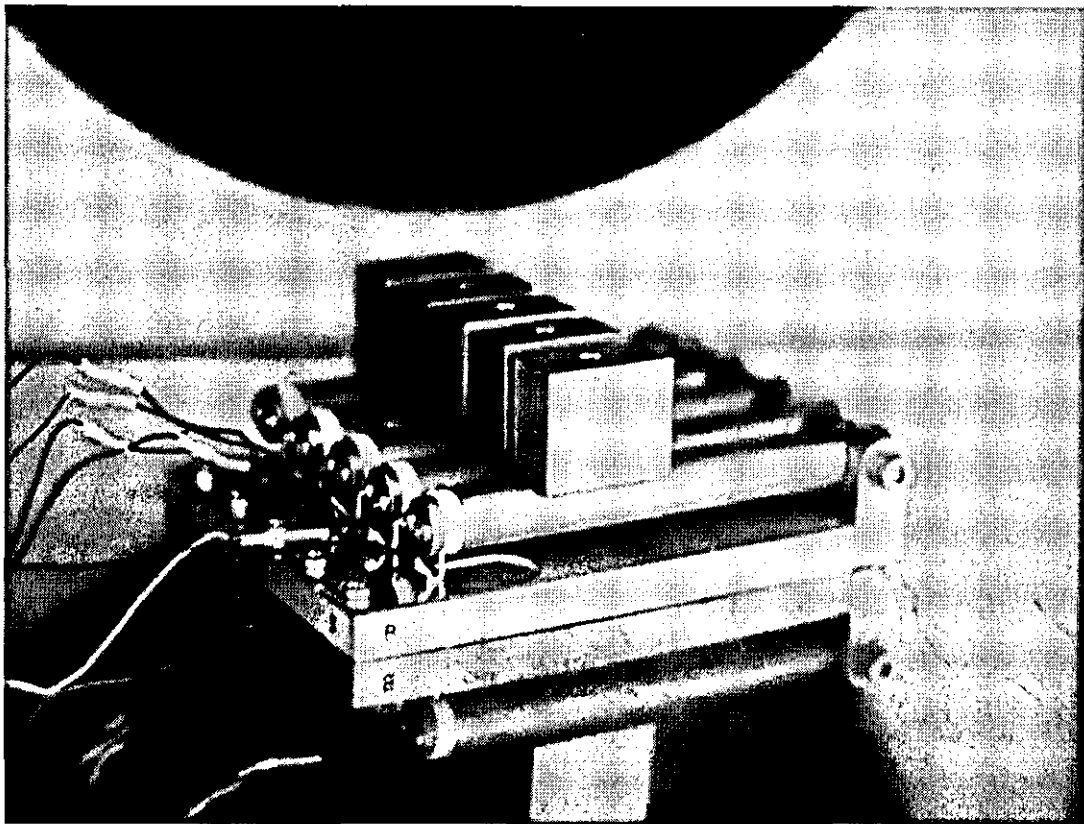


*Fig. 3.5 Fretting Rig*

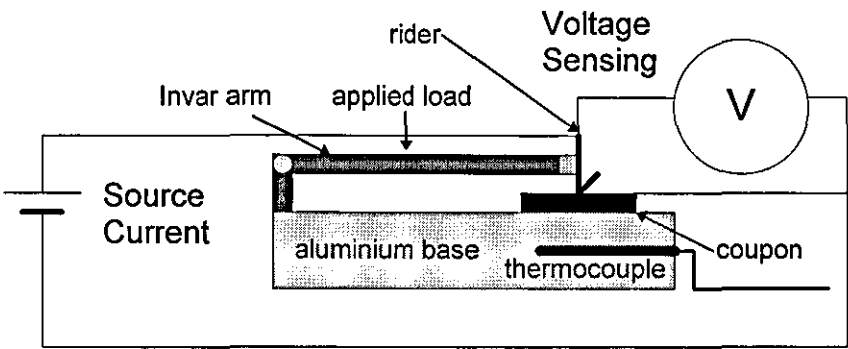


*Fig. 3.6 Schematic of the Low Frequency Fretting Rig*

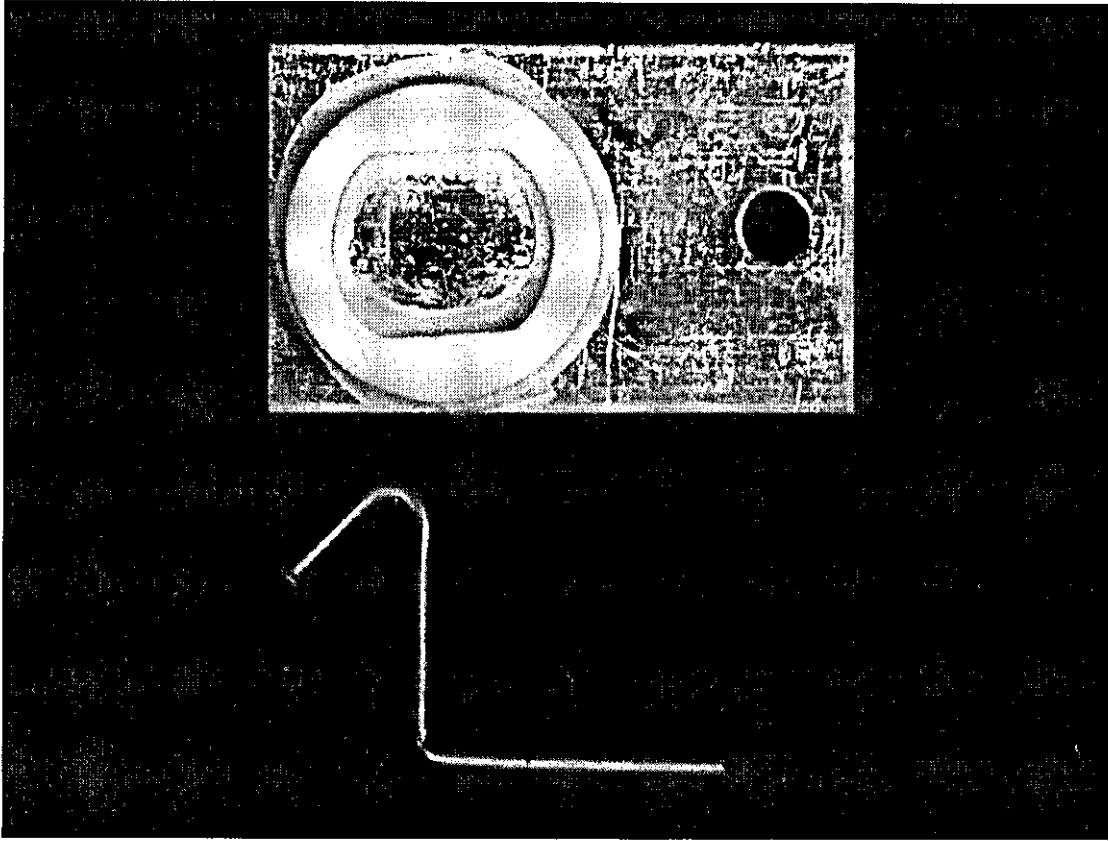


*Fig. 3.7 Coupon with Ceramic Lubricant Retaining Ring and Rider*

## 3.2 Characterisation and Testing

### 3.2.1 Test Coupons

Test coupons were chosen rather than fabricated connectors to enable subsequent surface analysis and contact resistance measurements to be made. They were cut from one continuous strip to maintain a tighter control of the quality of the material and were manufactured using standard processing routes, rather than under controlled laboratory conditions, to deliberately include any processing defects. The substrate alloy composition was confirmed by Inductively Coupled Plasma Spectrometry (ICPS) analysis.

The thickness of metal coatings may be measured by simple micro-sectioning and by XRFs. Results from both methods, however, were found to be susceptible to error due to the presence of intermetallics. As discussed in the *Literature Review*, tin/copper intermetallics are known to form at the tin/substrate interface making an accurate measurement of the absolute value for the tin coating thickness impossible by sectioning. XRF methods were available for determining coating thicknesses where, as in this case, the analyte element is present in the substrate<sup>9</sup> but just as for the micro-sectioning method, this technique was found to be unreliable, as no identifiable interface existed. In addition, the small dimensions of the rider wire made this technique impracticable. Measurements were therefore taken using the calibrated micron marker directly from SEM photomicrographs of ten transverse sections on which were superimposed EDS linescans for copper, the 'interface' being taken as the point where the copper trace was reduced to background, as shown in the schematic; Fig. 3.8. This provided a measure of the pure tin thickness as this dimension would be of greatest benefit in subsequent ageing and fretting tests. EDS analytical conditions are shown in Table 3.1.

Jeol JSM-5800LV SEM with Oxford Analytical Link ISIS System	
Si/Li with ATW Detector	20eV/channel
0° Tilt	1024 channels
0° Azimuthal angle	20Kev range
35° Elevation	20 kV accelerating voltage

*Table 3.1 EDS Analytical Parameters Used (unless otherwise stated in text)*

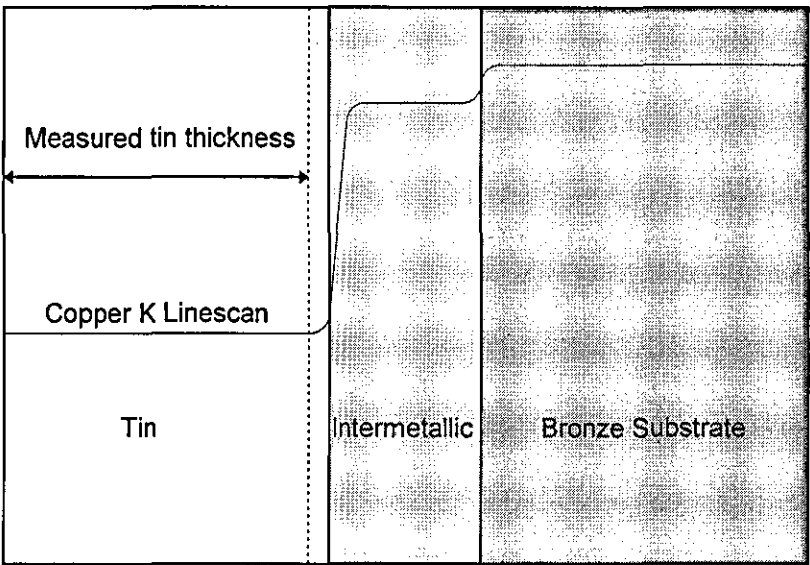


**Fig. 3.8 Schematic of CuK Linescan Across Pure Tin, Intermetallics and Substrate.**

*Surface Analysis*

As an understanding of the surface condition prior to testing was important in order to establish a datum, XPS and AES were used. These techniques were felt to complement the results obtained from SEM/EDS, analysis. XPS is a technique that provides information on the surface composition over a relatively large area, typically 0.4cm<sup>2</sup>, giving the general elemental constituents and oxidation state of the major elements present. The low spatial resolution of XPS was, for the current work, therefore considered to be an asset rather than a limitation and the information provided on the oxidation state(s) of the coating was considered to be beneficial for comparison with the results obtained from samples which had been exposed to hostile environments. The XPS and AES instrumental parameters used for this and subsequent analyses are shown in Tables 3.2 and 3.3 respectively.

*Topography*

A Rank Taylor Talysurf was used to determine the surface topography of the coupons prior to testing. This is a line contact method giving measurements in two dimensions only.

<b>XPS : V G Escalab Mk2</b>	
<b>AlK<math>\alpha</math> radiation</b>	
h $\nu$	1486.6eV
Voltage	15kV
Current	20mA
Power	200W
<b><u>Broad Scans</u></b>	
Scan volts	1250eV
Pass energy	85eV
Aperture	B1
<b><u>High Resolution Scans</u></b>	
Scan volts	125eV
Pass energy	20eV
Aperture	A3

**Table 3.2 XPS Analytical Parameters**

<b><u>Varian Scanning Auger Electron Spectrometer</u></b>	
Background vacuum	$<5 \times 10^{-8}$ torr
<b><u>Electron beam parameters</u></b>	
(a) beam energy	$3 \times 10^3$ eV
(b) beam current	$\sim 0.5 \times 10^{-6}$ A
(c) energy range	20 to 1020 eV
(d) analysis area	$\sim 150 \times 10^{-6}$ m dia.
<b><u>Ion beam parameters</u></b>	
(a) ion species	Ar $^{+}$
(b) ion energy	$3 \times 10^3$ eV
(c) gas pressure	$4 \times 10^{-5}$ torr
(d) ion current density	$< 75 \times 10^{-6}$ A.cm $^{-2}$

**Table 3.3 AES Analytical Parameters**

### *Hardness*

The determination of the hardness of thin platings is difficult to achieve as underlayers will tend to affect any results and the coating thickness was too small for determinations from microsections. An attempt was made, however, using a Leitz microhardness tester with a 15g load normal to the surface.

### *Contact Resistance*

Using the contact resistance rig with a pre-set load of 0.98N, ten determinations across the coupons were made and the median value calculated and reported together with the percentage of open circuit readings ( $>20\Omega$ ).

## **3.2.2 Lubricant Analysis**

### *Lubricant Identification*

The choice of commercially available lubricants, rather than laboratory formulations was to produce data and conclusions which, in addition to furthering the understanding of their effect on in the fretting process, had practical benefits for the connector designer and user. The lubricants selected were commercial grade greases, the formulations of which were unknown and it was therefore necessary to identify the compositions of the base oil and thickeners prior to testing. This was achieved using FTIRS in conjunction with SEM/EDS where necessary, to determine the composition of the thickeners. Specimen samples of each of thirty eight greases were smeared over the surface of a potassium bromide window and analysed in Perkin Elmer FTIR spectrometer. The infrared spectra thus generated were matched where possible against standard spectra held on file.

### *Thermogravimetric Analysis*

Thermogravimetric analysis was carried out to determine the volatility of the greases by measuring weight loss using a Stanton Redcroft TG-750 microbalance at three temperatures, (100°C, 150°C and 200°C). Volatility was considered to be an important property which may have had an influence on the performance of lubricated coupons at the fretting test temperatures used.



### *Reactivity Cell Measurements*

Current leakage measurements for each grease were made over a period of ten days whilst maintaining a temperature of 125° C.

### **3.2.3 Controlled Corrosion and Thermal Testing**

The matching of simulated and accelerated gas test conditions with field environments has been extensively researched, particularly by the Scandinavian countries through the Joint Project on Corrosion of Electronics, initiated in 1983.<sup>10,11,12</sup> From the experience gained in applying corrosive gas stress tests and comparing results with those from the field, recommendations can be specified for the choice of specially designed test variants and degrees of severity. Testing is usually 'single gas', 'mixed gas' or 'gas sequence'. The mixed gas test includes: SO<sub>2</sub>, H<sub>2</sub>S, NO<sub>2</sub>, Cl<sub>2</sub>, NH<sub>3</sub> and O<sub>3</sub> and is closest to the environment encountered in the engine and passenger compartment of a road vehicle. However, such tests were beyond the scope of this study and, due to availability, the following four accelerated corrosion tests were used:

- (i) Salt spray.<sup>13</sup>
- (ii) Humidity.<sup>14</sup>
- (iii) Thioacetamide Test.<sup>15</sup>
- (iv) Thermal ageing in a laboratory atmosphere (non-industrial).

Further field testing was performed by exposing coupons to 'real' in-service conditions. All coupons were rigorously cleaned in acetone by ultrasonic agitation, prior to exposure.

#### *Salt Spray*

The coupons were supported in a vertical position and exposed for 500 hours, in a C & W Corrosion Test System (Model SF/450/DH/H), in accordance with a standard international test procedure, ASTM B117. This corrosion test, utilises a salt fog where the sodium chloride concentration and the pH is carefully controlled. Coupons plated with finishes commonly used for connector contacts, together with a coupon of pure

copper were subjected to the test at the same time in order to compare their performance with the HDT plating. Testing for 500 hours resulted in the total destruction of the plating and it was necessary to repeat the test for lower time periods until measurable contact resistance results ( $<20\text{m}\Omega$ ), were obtained. A final exposure time of 100 hours was used. After testing the samples were removed and dried before being photographed and contact resistance measurements made.

#### *Humidity Testing*

The test was performed to MIL-STD-202M 102B in a humidity cabinet operating at  $85^{\circ}\text{C}/85\text{ RH}$ , for 1000 hours. Comparisons were made both visually and using contact resistance measurements, as above, with coupons having different standard plating compositions.

#### *Gas Testing*

The thioacetamide test, using a self-regulating atmosphere of 305 ppm  $\text{H}_2\text{S}$ , was carried out on test coupons for 240 hours. Again the surface condition and contact resistance measurements were recorded.

#### *Thermal Ageing*

Thermal ageing of the coupons was carried out to study differences in composition between the surface layers formed under different controlled conditions and to study the growth of intermetallics. Coupons were aged for 2000 hrs. at  $100^{\circ}\text{C}$ ,  $125^{\circ}\text{C}$  and  $150^{\circ}\text{C}$  and were subsequently analysed by SEM/EDS, XRD and AES and contact resistances measured. For the intermetallic study the same temperatures were used but in this case the coupons were placed in sealed nitrogen filled containers to prevent surface oxidation.

An in depth study was carried out consisting of the following four experiments to characterise the intermetallics. To determine:

- (i) the composition of tin/copper intermetallics formed during thermal ageing;

- (ii) the diffusion rate of copper in tin from a tin bronze substrate;
- (iii) the morphology and hardness of intermetallics formed during thermal ageing, and;
- (iv) the corrosion resistance of the intermetallic phases.

(i) Composition of Intermetallics

The composition of the intermetallics which had formed during ageing was determined by SEM/EDS using microsections and by AES depth profiling. Identification of crystalline phases formed in the coating was carried out by XRD using the instrumental parameters in Table 3.4.

(ii) Diffusion of Copper in Tin

Microsectioning followed by EDS analysis has been the most common method used for determining diffusion rates of substrate elements into coatings<sup>16</sup>. However, the technique has several limitations not least being the possibility of an unrepresentative section being taken, particularly as in the present case where it is known from SEM

Philips PW1700 XRD Analytical Parameters	
Anode	Copper
Tube Voltage	45kV
Tube Current	30mA
Crystal Monochromator	
Trace (2 $\theta$ )	8 - 85°
Scintillation Counter	

**Table 3.4 XRD Analytical Parameters**

backscattered electron imaging, that the intermetallics are not uniformly distributed across the tin/copper interface. For accurate measurements of intermetallic growth

rate, standard sectioning techniques were therefore unreliable, particularly for the coating thickness available and it was therefore necessary to devise an alternative approach.

From examination of sections, the tin coated coupons used in this study have an average pure tin thickness of between 1 and 2  $\mu\text{m}$  over an underlayer of intermetallics of variable thickness. To determine accurately the time required to fully convert all of the tin to intermetallic, would necessitate the preparation of a large number of microsections. A simpler, more rapid and accurate method requiring no sample preparation, giving the excellent reproducibility of EDS over relatively large areas of the coating, has therefore been proposed. This novel procedure has been termed by the author the "Volume Saturation Method" and utilises the excitation volume or more accurately the emission volume of characteristic X-rays. The X-rays generated within the specimen suffer attenuation on their way to the surface and the maximum depth ( $Z_r$ ), from which X-rays are produced is dependant on the following parameters: density ( $\rho$ ) of the material excited, the maximum spread of X-rays (micro-analysis resolution),<sup>17</sup> the incident electron energy ( $E_o$ ) and the critical excitation energy ( $E_c$ ). Pouchou and Pichoir<sup>18</sup> have defined the following relationship:

$$Z_r = 0.07(E_o^{1.7} - E_c^{1.7}) \left[ \frac{1 + \frac{3}{E_o^{0.5} \left[ \frac{E_o}{(E_c + 0.3)^2} \right]}}{\rho} \right] \quad (3.1)$$

Andersen<sup>19</sup> calculated the maximum depth of X-ray production for  $K\alpha$ ,  $L\alpha_1$  and  $M\alpha_1$  X-ray lines of the chemical elements using various electron excitation potentials for specimens having various densities. His value for  $Z_r$  for copper in tin has been used here and Figure 3.9 is a schematic showing the interaction volume for tin into which copper has begun to diffuse.

Provided the coating thickness exceeds this critical depth for X-ray generation from atoms of the analyte element, it is possible to monitor the diffusion of the substrate element with time until the X-ray emission volume is saturated. By rastering the electron beam over a relatively large area, Fig.3.10, the interaction volume approximates to a cuboid, and by taking a ratio of the intensity of the analyte element with that of the plating element, i.e. for this study, copper and tin respectively, variations in beam current between analyses can be minimised. A ratio technique would also reduce the slight effect on  $Z_r$  of the change in density as diffusion proceeds.

The layer of pure tin had been found by sectioning and EDS to have a thickness of over  $1\mu\text{m}$  and the maximum depth for  $\text{CuK}\alpha$  emission in tin has been calculated by Andersen to be  $\sim 1\mu\text{m}$ . It was, therefore, possible to determine the concentration of copper, in terms of X-ray intensity with respect to time, over this depth.  $\text{CuK}\alpha/\text{SnL}\alpha$  intensity ratios were calculated and plotted against diffusion annealing time and when the sampling volume became fully saturated with copper atoms, i.e. when the tin was fully converted to the  $\text{Cu}_3\text{Sn}$  phase as found by XRD, the intensity/time graph would

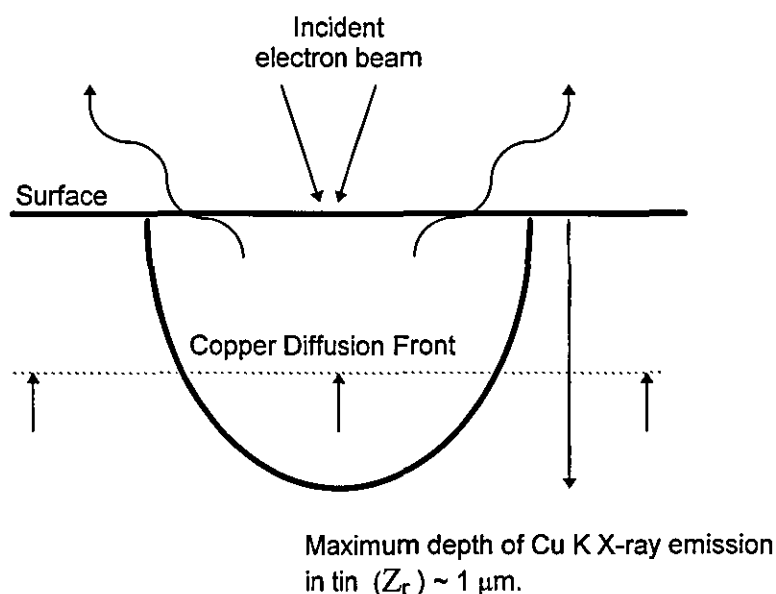


**Fig. 3.9 Schematic Showing Depth of Emission of CuK X-Rays in a Tin Matrix.**

remain constant. Growth rates are normally determined by measuring the thickness of the interdiffusion layers after selected time intervals. Using the Volume Saturation Method, the thickness of the excited volume, is held constant and analyte concentration changes with respect to time are determined as in the schematic, Fig. 3.11, where  $(T_{\text{sat}} - T_s)$  is the period of measured diffusion of copper.

The application of EDS analysis for determining diffusion rates using the electron beam normal to the plating surface has not been found elsewhere in the literature. The technique could, in principle at least, be performed in the chamber of a SEM using a heated stage when dynamic measurements could be obtained. This would also eliminate the need to age the sample in an inert atmosphere. Additional benefits are that no sample preparation is required, large areas may be rapidly scanned by the electron beam to improve precision and the technique is non-destructive allowing the same sample to be aged and measured throughout the test. For this experiment the EDS analysis was performed at intervals over the ageing period using coupons annealed at 100°C, 125°C and 150°C. An SEM magnification of X350 was used for a counting time of 200s. Net intensities for 10 determinations on each coupon of  $\text{CuK}\alpha$  and  $\text{SnL}\alpha$  were ratioed and the mean value used to plot an intensity/time graph for each annealing temperature. The measurements were suspended when the intensity ratio ( $\text{CuK}\alpha/\text{SnL}\alpha$ ) became constant with time.

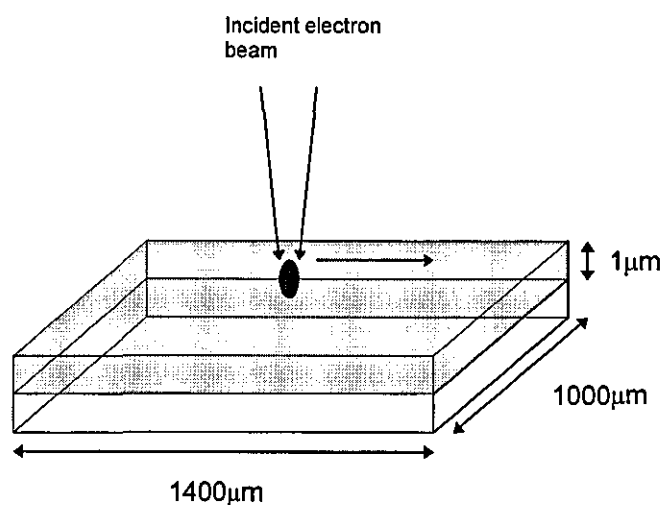


**Fig. 3.10 Volume Excited by Scanned Incident Electron Beam.**

## (iii) Morphology and Hardness

A solution of picric and hydrochloric acids was used to dissolve away unreacted tin to expose the intermetallics. Measurements were made from SEM images and calculations of average grain size using 'PC Image'<sup>20</sup> software. From an area of exposed intermetallics 42 X 270 mm<sup>2</sup>, further topographical measurements were made using a Scantron Proscan 1000. This is a non-contact 3D surface profiling technique utilising a high precision stepper motor table and laser-based displacement probes.

## (iv) Intermetallic Corrosion Testing

An 'as-plated' coupon and one which had been aged for 2000 hours at 150°C, were immersed in a 10% w/vol aqueous solution of sodium chloride for 130 hours. The condition of the surfaces after exposure were recorded by SEM/EDS after washing with de-ionised water.

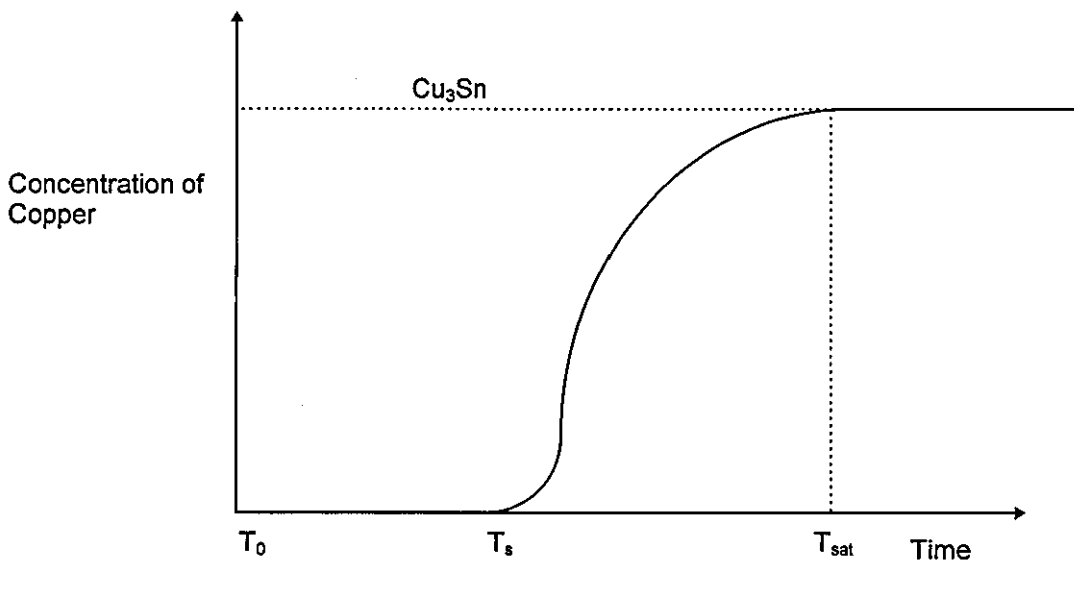


**Fig. 3.11 Schematic of Copper Concentration Changes with Ageing Time.**

### **3.2.4 Field Testing**

The field test coupons were inserted into the specially designed housings and mounted in vehicles which saw service in either rural (Hereford, U.K.) or urban (Rotherham, U.K.), environments and on heavy duty trucks which were known to travel throughout Europe and experience a range of conditions including salt laden atmospheres, Table 3.5. After testing, the samples were examined by SEM/EDS and analysed by XPS. Contact resistance measurements were made on all samples and SEM/EDS together with AES depth profile analysis were performed on a coupon showing a high value.

### **3.2.5 Fretting Tests**

Coupons were tested both in the 'dry' state and lubricated with 1 ml of the previously analysed greases. The coupon and rider were cleaned in isopropanol and for the lubricated samples, the lubricant was retained in the contact region by use of a ceramic ring secured to the coupon using a silicone adhesive, Fig. 3.7. In order to statistically improve the reliability of the test and to obtain a measurement uncertainty, two rigs were used, each utilising five expansion rods with their respective test pieces. The test was terminated when all ten had 'failed', that is when there was evidence of intermittent or permanent high contact resistance on the chart recorder. The value recorded for time to failure was taken when 50% of the contacts had failed ( $t_{50}$ ).



Box No.	Location	Vehicle	Test Duration Weeks/Km( $10^3$ )	Vehicle Environment
1	Passenger compt.	Ford Sierra 2.0i	88/114	Urban
2	Engine bay		88/114	
3	Engine bay	Ford Sierra 2.0i	stopped at 61000 Km (vehicle damaged)	Urban
4	Engine bay	Ford Sierra 2.0i	88/100	Urban
5	Passenger compt.	Vauxhall Cavalier 2.0i	90/120	Rural
6	Engine bay		90/120	
7	Engine bay	Vauxhall Cavalier 2.0i	90/102	Rural
8	Engine bay	Vauxhall Cavalier 2.0i	90/90	Rural
9	Passenger compt.	Volvo F12	93/278	Trans -continental
10	Engine bay			
11	Engine bay	DAF 2800	93/233	Trans -continental
12	Engine bay	Mercedes	93/231	Trans -continental

**Table 3.5 Location and Test Periods of Field Test Samples**

### 3.2.6 IRAS Study of 12-Hydroxystearate

The fretting tests using the formulation of mineral oil/lithium soap gave excellent results and to investigate the cause of this superior performance the bonding mechanism of the stearate to the metal was examined. Timsit<sup>21</sup> has shown, using Infrared Reflection Absorption Spectrometry, with stearic acid films on aluminium substrates, he was able to identify absorption frequency shifts, indicating that the polar group is bonded chemically, i.e. chemisorbed to the native aluminium oxide layer.

For this present study 12-Hydroxystearate on HDT was used. The films were prepared by placing a droplet of a solution of the soap in methanol ( $\text{CH}_3\text{OH}$ ), on the substrates. A HDT plated coupon having a native oxide layer was initially analysed and then again after heating in an oven for a period of one hour at  $125^\circ\text{C}$ , this being the maximum temperature experienced by the lubricants under the fretting test conditions. A HDT coupon, polished to a  $1\mu\text{m}$  finish and supporting the soap, was similarly aged and analysed. For reference, a bulk sample of the stearate, supported on a potassium

bromide window was analysed in transmission. Gold, having no oxide layer, would be expected to have the same IR spectrum as the bulk material but to examine for possible artefacts in the spectra, which may be present due to the technique employed, a second reference sample, consisting of the soap film on a gold substrate was used.

The work was performed using a Perkin Elmer spectrometer using grazing angle optics with radiation incident to the surface at an angle of  $85^\circ$  to the normal. The spectra were generated using 32 scans and a resolution of  $4\text{ cm}^{-1}$ .

---

References

- <sup>1</sup> ASTM Standard B667-80, "Construction and Use of a Probe for Measuring Electrical Contact Resistance".
- <sup>2</sup> Sproles, E. and Drozdowicz, M., "Development of an Automatic Contact Resistance Probe", 14th Electrical Contacts Conference, (1988).
- <sup>3</sup> Horn, J., DDR Patent 215176, Vorrichtung zum Prüfen von Elektrischen Kontakten.
- <sup>4</sup> Bogenschutz, K., *Korrosionsschutz in der Elektronik*, (Leuze Verlag), p13, 62, (1986).
- <sup>5</sup> Antler, M. and Sproles, E.S., "Effect of Fretting on the Contact Resistance of Palladium," 14<sup>th</sup> Annual Conf. On Connectors, Philadelphia, pp 313-329, (1981).
- <sup>6</sup> Antler, M., "Fretting of Electrical Contacts," ASTM Special Tech. Pub. 780, Philadelphia, pp 68-85, (1982).
- <sup>7</sup> Braunovic, M., "Evaluation of Different Types of Contact Aid Compounds for Aluminium - to - Aluminium Connectors and Conductors," IEEE CHMT-8, No. 3, pp 313-320, (1985).
- <sup>8</sup> Whitley, J.H., "Reflections on Contacts and Connector Engineering", IEEE Proc. 33<sup>rd</sup> Holm Conference on Electrical Contacts, pp. 1-7, (1987).
- <sup>9</sup> Bertin, E.P., *Principles and Practice of X-Ray Fluorescence Spectrometric Analysis*, (Plenum Press, New York),
- <sup>10</sup> Henriksen, J.F., Leygraf, C., Zakipour, S., Villien, P. and Wagner, M., "Analysis of Environment and Corrosivity of Thirty Eight Field Test Sites," 13<sup>th</sup> Int. Conf. on Electric Contacts, Lausanne, (1986).
- <sup>11</sup> Leygraf, C., Henriksen, J.F., Hienenon, R., Zachariassen, K., "Classification of Investigated Environments," 11<sup>th</sup> Scandinavian Corrosion Conf., Stavanger, (1989).
- <sup>12</sup> Zakipour, S., Leygraf, C., Henriksen, J.F., Hienenon, R., Zachariassen, K., "Analysis of Corrosion Film Chemistry on Field and Laboratory Exposed Cu-Coupons and Au-Plated Samples," Proc.14<sup>th</sup> Int. Conf. on Electric Contacts, Paris, (1988).
- <sup>13</sup> ASTM B117, *Annual book of ASTM Standards*, (American Society for Testing and Materials, Philadelphia), 1986.
- <sup>14</sup> MIL STD 202M-102B, American Military Standards.
- <sup>15</sup> Gerber, T.P., "An Improved Thioacetamide Corrosion Test", Proc. 13<sup>th</sup> Int. Conf. On Electrical Contacts, Lausanne, 1986.
- <sup>16</sup> Braunovic and Aleksandrov, "Intermetallic Compounds at Aluminium-to-Copper and Copper-to-Tin Electrical Interfaces, Thirty-Eighth IEEE Holm Conf. on Electrical Contacts, (1992).
- <sup>17</sup> Reed, S.J.B., Sixth Int. Conf. On X-ray Optics and Microanalysis, pp. 339 (1972).
- <sup>18</sup> Pouchou, J.L. and Pichoir, F., "Electron Probe X-Ray Microanalysis Applied to Thin Films and Stratified Specimens", *Scanning Microscopy Supplement*, 7, pp. 167-189, (1993).
- <sup>19</sup> Andersen, C.A., *Methods of Biochemical Analysis*, Vol. 15, (Interscience Publishers, Inc., N.Y.), p. 147, (1967).
- <sup>20</sup> 'PC Image' Registered software.

- 
- <sup>21</sup> Timsit, R.S., "Effect of Surface Reactivity on Tribological Properties of a Boundary Lubricant", Proc. Of the NATO Advanced Study Institute on Fundamentals of Friction, Braunlage, Germany, (1991)

## 4. Results and Discussion

### 4.1 Evaluation of Test Materials

#### 4.1.1 Coupon Analysis

Tests were performed on commercial grade hot dipped tin coated connector strip with a width of 16.5mm and a thickness of 0.8mm. The material was supplied by Stolberger Metallwerke GmbH & Co KG, with a specification of its mechanical properties and chemical composition. Tables 4.1 and 4.1a list the nominal mechanical properties and the chemical composition of the bronze strip. The riders were formed into shape from hot dipped tin plated bronze wire.

#### *Coating Thickness*

Table 4.2 shows the measured mean tin thickness on the coupon and the rider as determined using EDS elemental line-scanning.

#### *Surface Topography*

SEM imaging of the surface of the connector strip prior to and after plating revealed rolling marks on the bronze surface, which had a surface roughness ( $R_a$ ) of  $0.19\mu\text{m}$ , when measured by Tallysurf across the rolling direction. After plating the surface roughness of the coupon had *increased* to  $0.21\mu\text{m}$ . This was surprising as the plating process would be expected to tend to smooth out irregularities. However, the 10% increase may be explained by the 'lines' of intermetallics ( $\text{Cu}_6\text{Sn}_5$ ), producing ripples

in the overlaying tin. This can be observed in the secondary electron image taken with a specimen tilt of  $45^\circ$  to enhance topographical features; (Fig. 4.1). When imaged in back-scattered electron mode, the lines of intermetallics close to the surface of the tin are clearly visible; (Fig. 4.2). It was not possible to obtain a quantitative surface profile of the rider wire due to its small dimensions but from SEM imaging, it was assumed to have a surface roughness less than or similar to that of the coupon.

Tensile Strength (N.mm <sup>-2</sup> )	558 (min.)	577 (max.)
0.2% Proof Stress (N.mm <sup>-2</sup> )	533 (min.)	556 (max.)
Elongation (%)	14.6	15.6
Hardness (Hv5) (at R.T.)	184 (min.)	188(max.)

**Table 4.1 Nominal Mechanical Properties of HDT Connector Strip.<sup>1</sup>**

Cu	Sn	P	Zn	Ni	Fe	Pb
94.990 (min)	4.895 (min)	0.071 (max)	0.020 (max)	0.007 (max)	0.007 (max)	0.001 (max)

**Table 4.1a Nominal Chemical Composition of HDT Connector Strip.<sup>1</sup>**

Mean Tin Thickness ( $\mu\text{m}$ )	
Coupon	2.15
Rider	1.27
(95% confidence limit of $\pm 10.5\%$ rel.)	

**Table 4.2 Measured Mean Thickness of Tin Coating**

#### *Hardness Determination*

A mean value of  $102 \text{ Kg.mm}^{-2}$  was obtained but with a 95% confidence limit of only  $\pm 47.9 \text{ Kg.mm}^{-2}$ . The value was probably exaggerated due to the thickness of the tin

layer and the poor repeatability was almost certainly due to the effects of the underlying intermetallics. Engel<sup>2</sup> describes a method for calculating the hardness of composite layers together with error analysis, which has attempted to address this problem. As a consequence, the hardness of a sample of pure tin strip was measured giving a mean value of  $7.8 \text{ Kg.mm}^{-2} \pm 1\%$ . Due to the dimensions of the rider wire, an accurate hardness determination could not be obtained but was assumed to be of the order of that for the coupon.

#### *Determination of Contact Resistance*

Using the contact resistance rig, measurements were made on 10 ultrasonically cleaned samples giving a mean CR of  $2.1 \text{ m}\Omega \pm 4.9\%$  (95% confidence limit).

An accurate contact resistance measurement for the wire was not possible due to its limited surface area for contact with the probe head and therefore for the purpose of this study, the CR of the rider was assumed to be the same as that for the coupon.

#### *Surface Analysis*

Analysis of the coupon and rider by EDS using an excitation voltage of 20kV of selected areas scanned normal to the surface and to a nominal sampling depth of approximately  $1\mu\text{m}$ , detected carbon in addition to tin; (Fig. 4.3). Copper K energy peaks were not present in the spectrum but a small CuL peak was observed. This was thought to be a consequence of the beam energy used. As the primary electron beam diffuses into the tin layer, it incrementally loses energy. Therefore, at the maximum penetration depth only the lower energy L lines are excited. The large CuK and CuL peaks seen in the spectrum obtained from the rider coating were almost certainly due to excitation of the copper substrate. Note the previously measured average tin thickness of  $\sim 1.3\mu\text{m}$  on this material. In order to determine the composition at the surface, an 'as-plated' coupon was analysed by XPS after first ultrasonically cleaning in acetone. Figure 4.4 is the trace obtained together with calculated atomic concentrations normalised to 100%; Table 4.3. Broad scans were performed on all samples with high resolution scanning carried out over regions of interest where peak overlap occurred. Scanning in this mode was able to show a number of features of the spectrum unresolvable by broad scan analysis. For example, 'satellite' peaks could be detected. These are caused by valence electrons which are excited as a result of the

loss of a shielding electron due to photo-ionization of a core level electron. In addition, the  $\text{SnO}_2$  peaks next to the Sn 3d peaks were resolvable and the spectrum showed large Sn oxide 3d peaks with considerably smaller tin peaks adjacent to them. The relative heights of the tin and tin oxide peaks would suggest that either the tin had not full converted to the oxide within the depth analysed or that the oxide layer was thinner than the critical depth, some to 2 to 5 nm.

The XPS results showed that there were high concentrations of carbon and oxygen, being almost certainly due to hydrocarbon and other contamination. Carbon is a ubiquitous element in surface analysis and in this case probably originated from hydrocarbons remaining on the surface after cleaning. Lead and zinc peaks were probably due to the presence of impurities in the coating from previous tinning operations. These tend to migrate and concentrate at the surface of tin layers. The presence of zinc in the tin is unlikely to be due to diffusion from the substrate as has been reported for brass underlayers<sup>3</sup>, as the concentration in the bronze was less than 0.02 wt.%.

An AES depth profile was performed on the 'as plated' coupon; (Fig. 4.5), where in addition to tin, the elements: carbon, chlorine, oxygen and zinc were found in the topmost 10nm, with the two latter elements extending to a depth of 20nm. Apart from some of the oxygen being in combination with carbon as an organic contaminant, it was most likely that the element was present in the form of zinc and tin oxides. If tin oxide, this would be considered to be of a thickness consistent with that which would naturally form from the melt<sup>4</sup>.



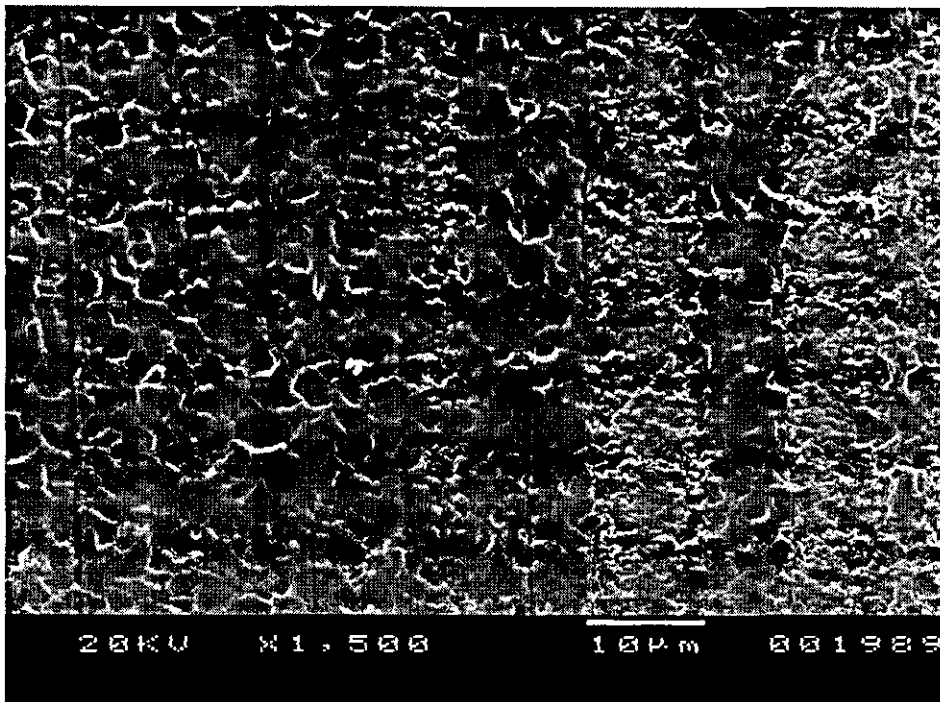


***Fig. 4.1 SEM Secondary Electron Image of Coupon Surface (45° tilt).***

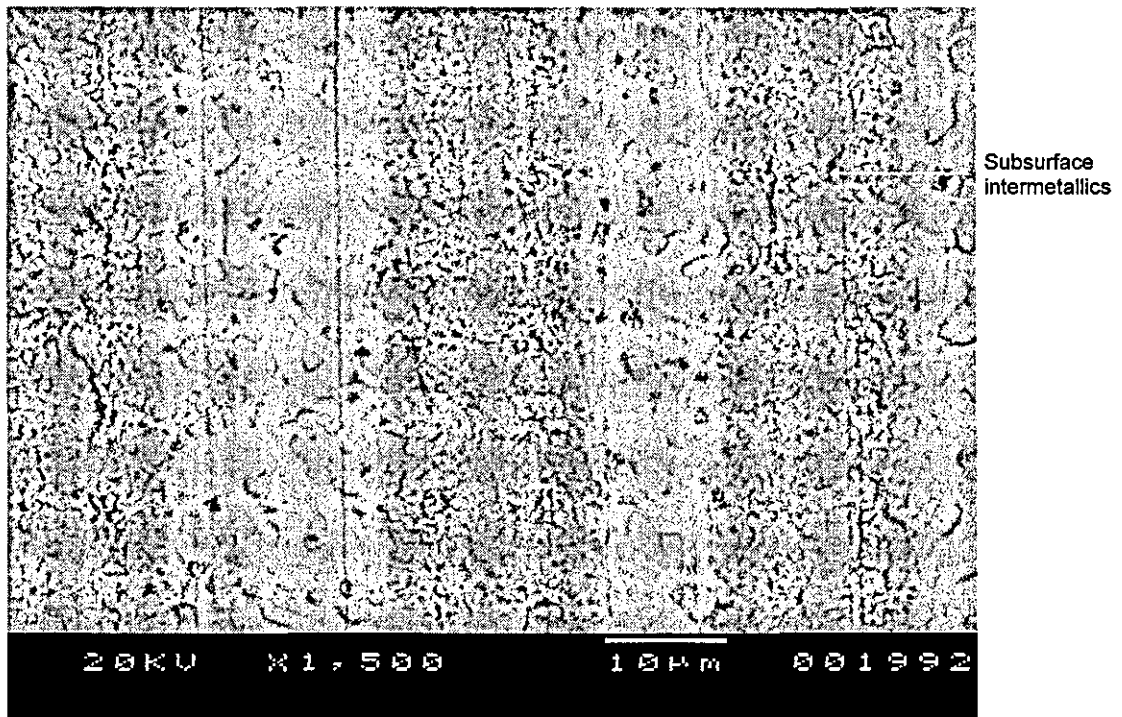


***Fig. 4.2 SEM Back Scattered Electron Image of Coupon Showing Lines of Subsurface Intermetallics.***

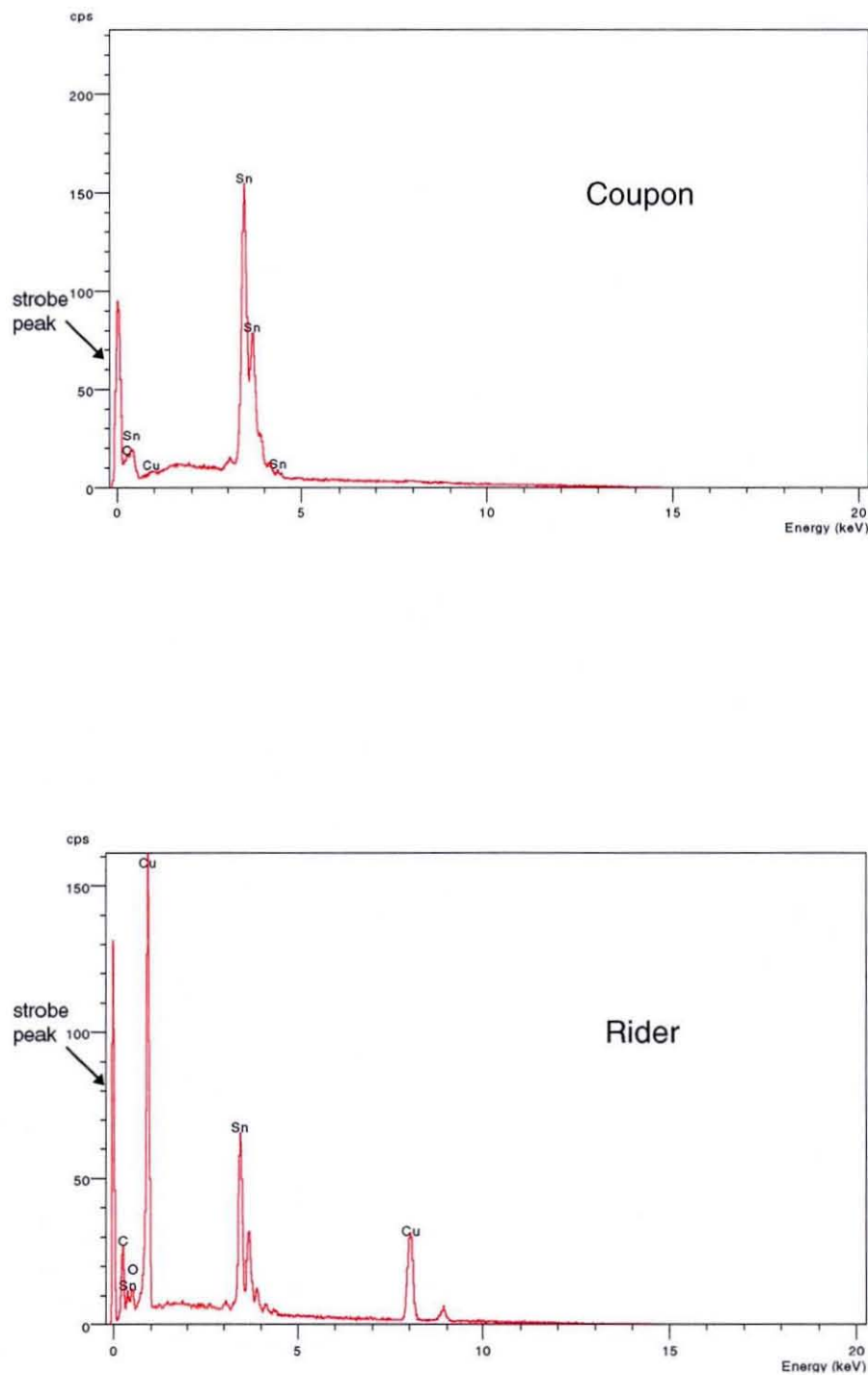


**Fig. 4.3 EDS Spectra of Tin Coating on Coupon and Rider**

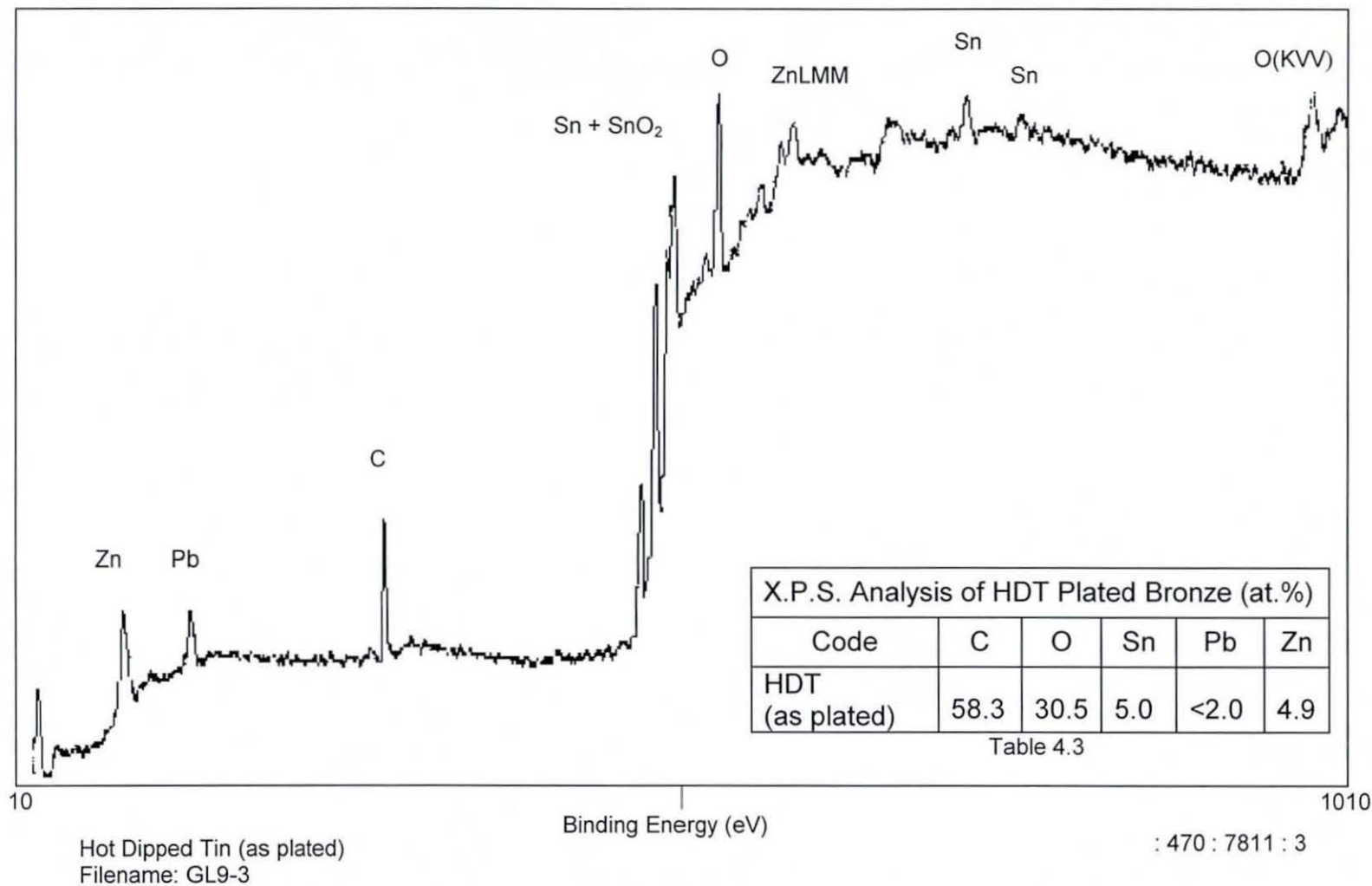


**Fig. 4.4 XPS Trace of the Surface of an 'As Plated' Coupon and Elemental Concentrations (Table 4.3)**

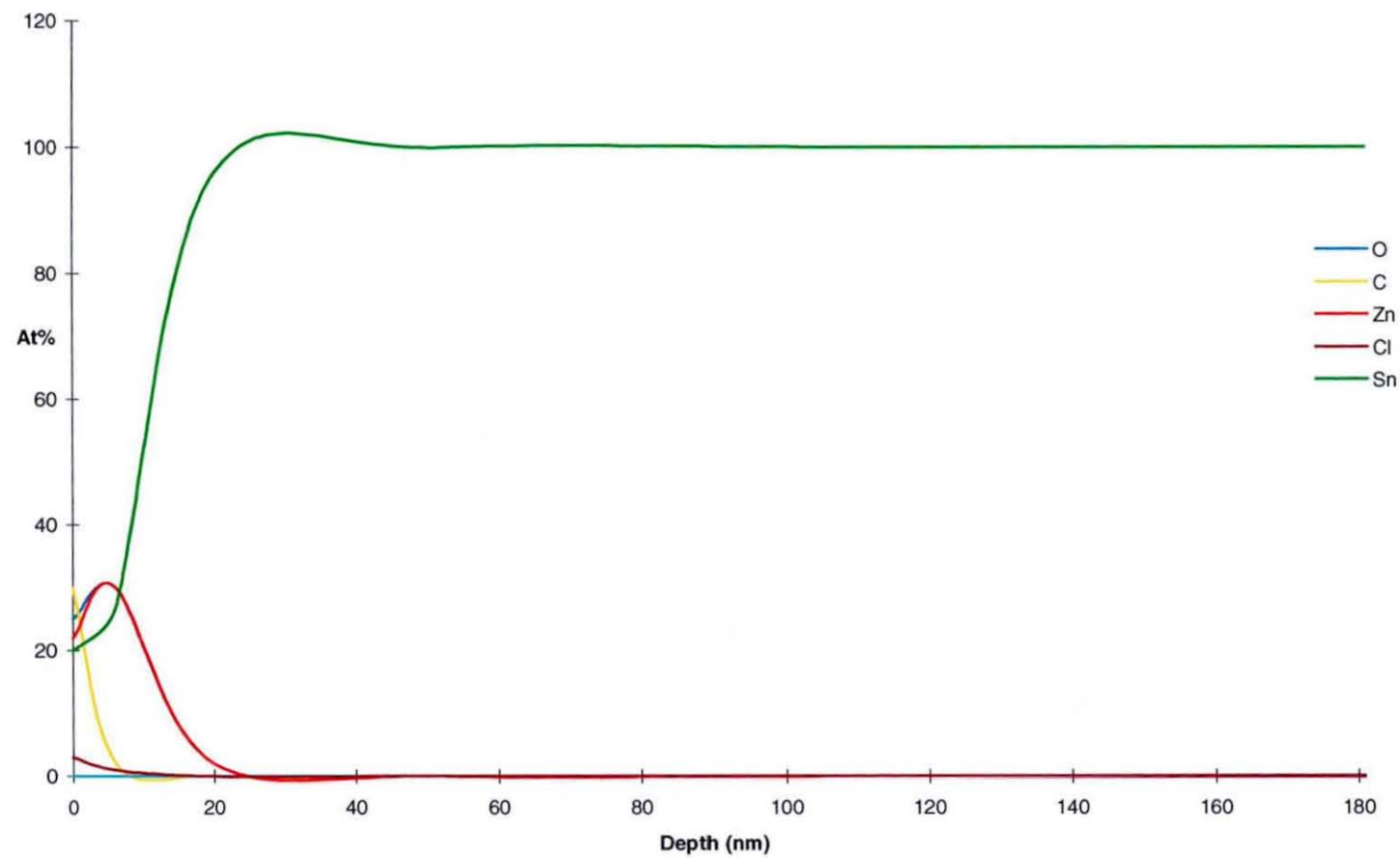


**Fig. 4.5** AES Depth Profile of an 'As Plated' Coupon

### 4.1.2 Lubricant Analysis

#### *Compositional Analysis*

FTIR spectroscopy was found to be a rapid and sensitive technique for identifying the compositions of the lubricants. The greases were found to be formulated from seven base oils and five thickeners. Table 4.4 shows the results of the analyses together with a coding assigned to each and Figures 4.6 to 4.11 are examples of the FTIR spectra for the different base oil/thickener combinations. The oils were identified as: mineral, synthetic hydrocarbon, silicone, PPE, PFAE, PAG and ester based with thickeners of either: bentonite clay, silica, lithium soaps, polymer and lithium and calcium complexes. It is possible that additives used in the grease formulations may result in peak overlap or shift, however, it was apparent that their concentration was not sufficient to prevent identification of the base oils using library spectrum matching. Note that calculations of the proportions of base oil to thickener were not performed.

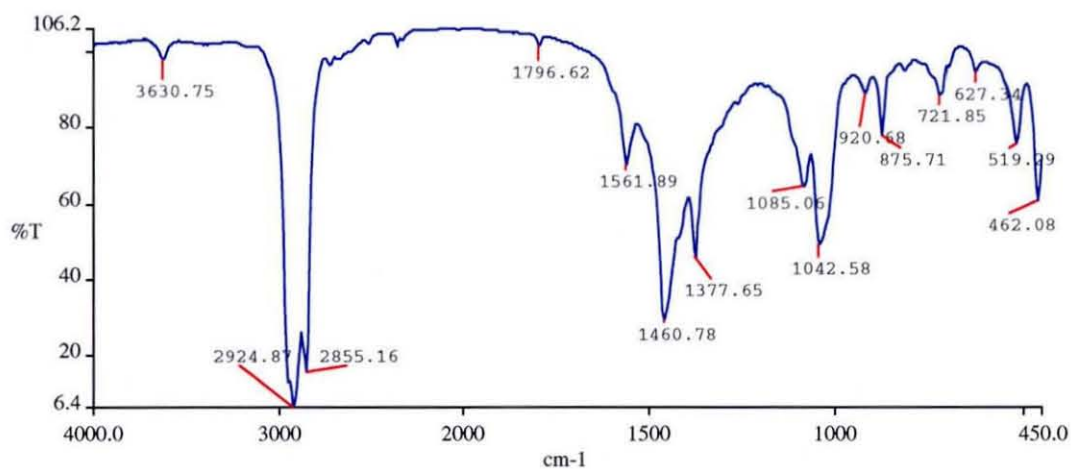
#### *Thermogravimetric Analysis*

The weight loss with temperature for each of the greases is shown in Table 4.5. It can be seen that over the temperature range measured, the grease formulations containing the base lubricants PFAE, silicone and high temperature ester, MP12, were the least volatile, whereas the mineral oils, synthetic hydrocarbon and PAG showed significant weight loss over the 150 - 200 °C range. There appeared to be no correlation between weight loss and the thickener used.

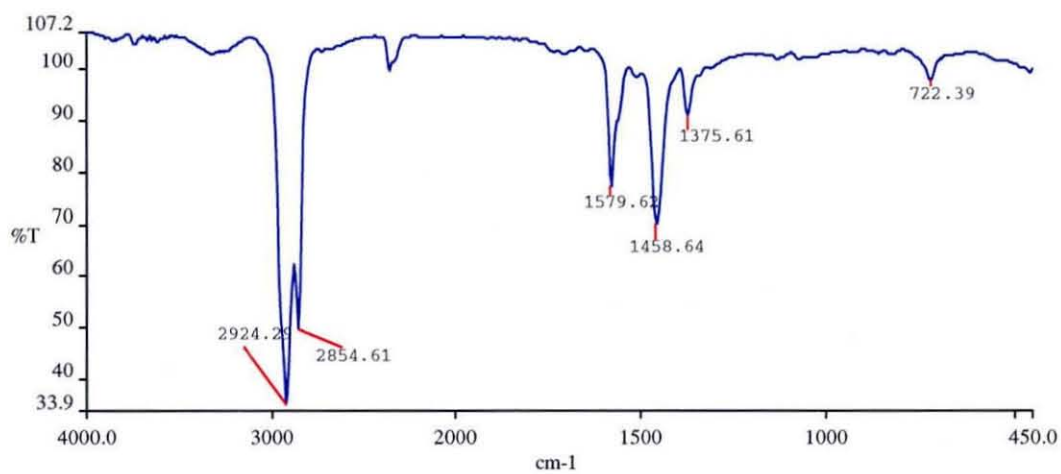
#### *Leakage Current Determinations*

Results of leakage current measurements from the reactivity cell, for each of the test lubricants, are tabulated in Table 4.6. The results show a range of reactivities extending over several orders of magnitude. The formulations showing the highest leakage currents contained either bentonite clays or soap thickeners, whilst the lowest levels were associated with greases containing silica. The lubricants MZ30 and MZ31 containing PAG and lithium soap, however, showed a low reactivity ( $<0.001$ ), which would suggest that the base oil restricted the mobility of the polar molecules. The relatively high reactivity, (4.1  $\mu\text{A}$ ), of the silicone/polymer formulation, (MS50), is

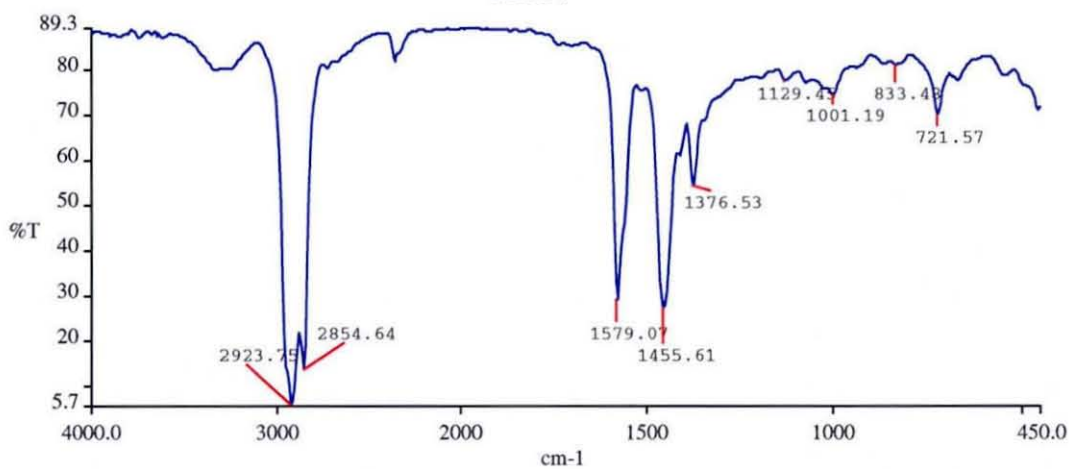
somewhat surprising and would require further analysis to determine if the polymer thickener molecule contained a polar end group.



MC11



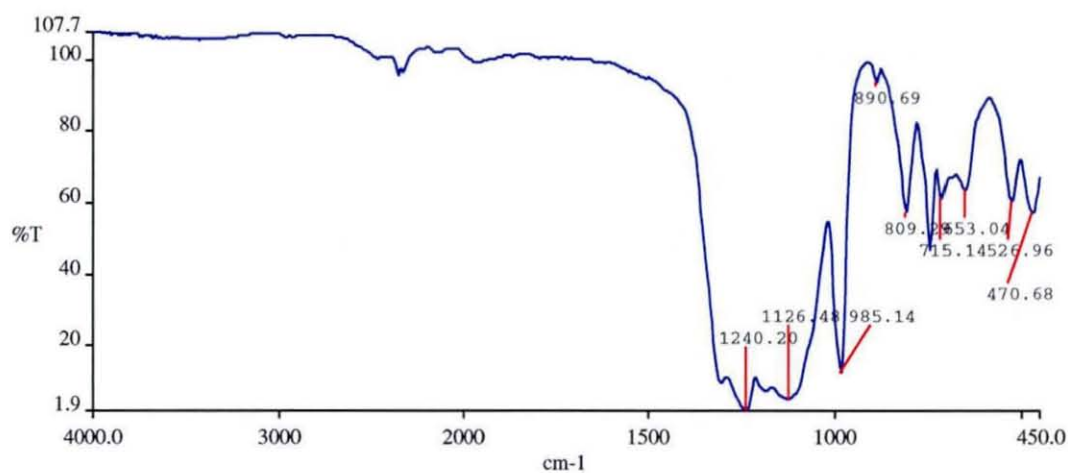
MC37



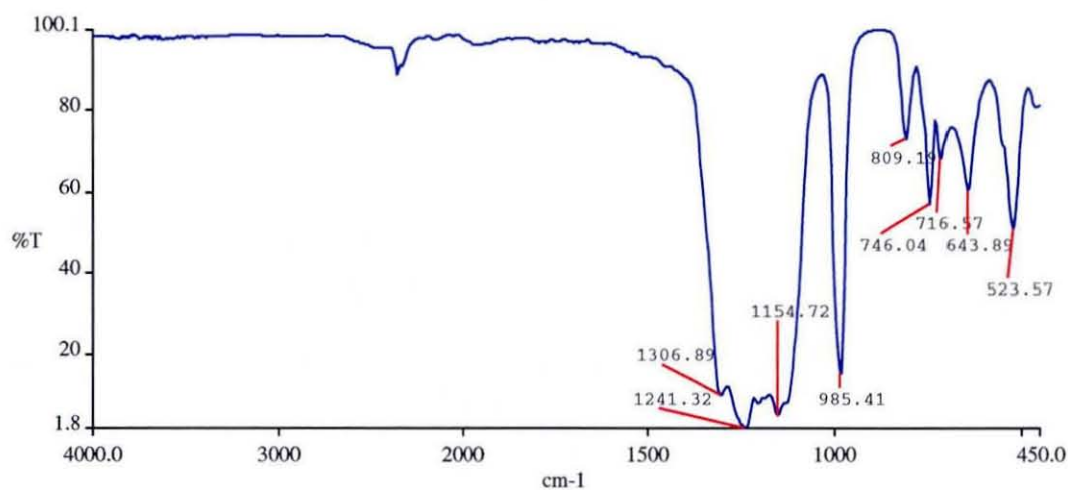
MC41

**Fig. 4.6 FTIR Spectra Obtained from Greases MC11, MC37 and MC41.**

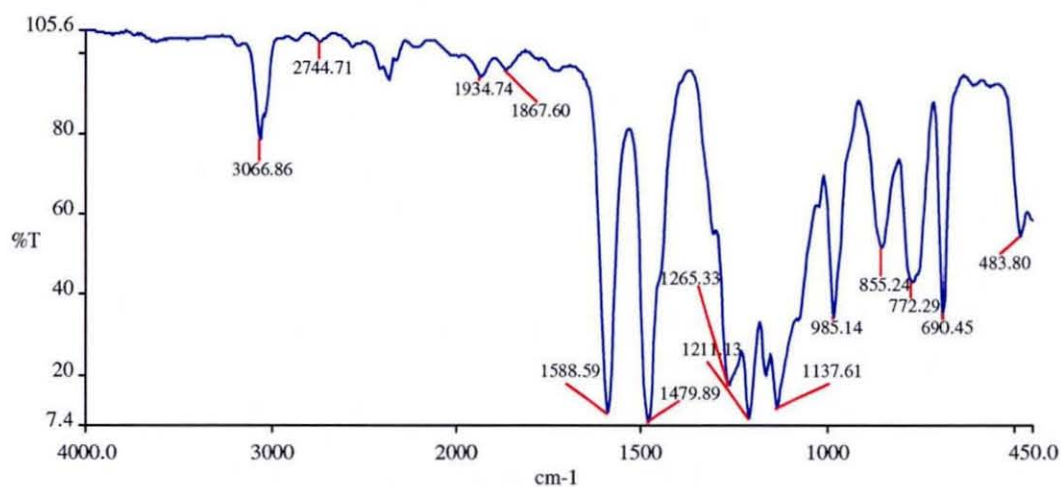




MF24

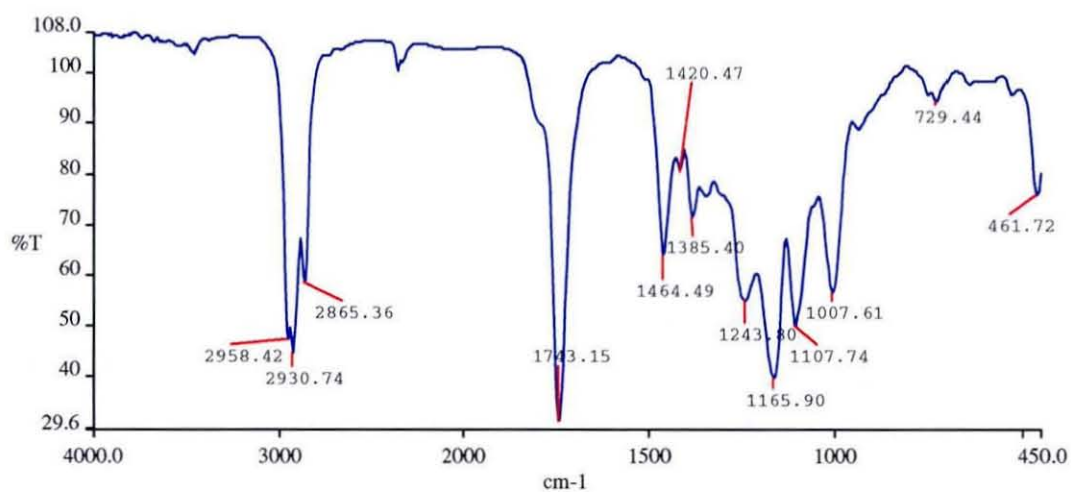


MF52

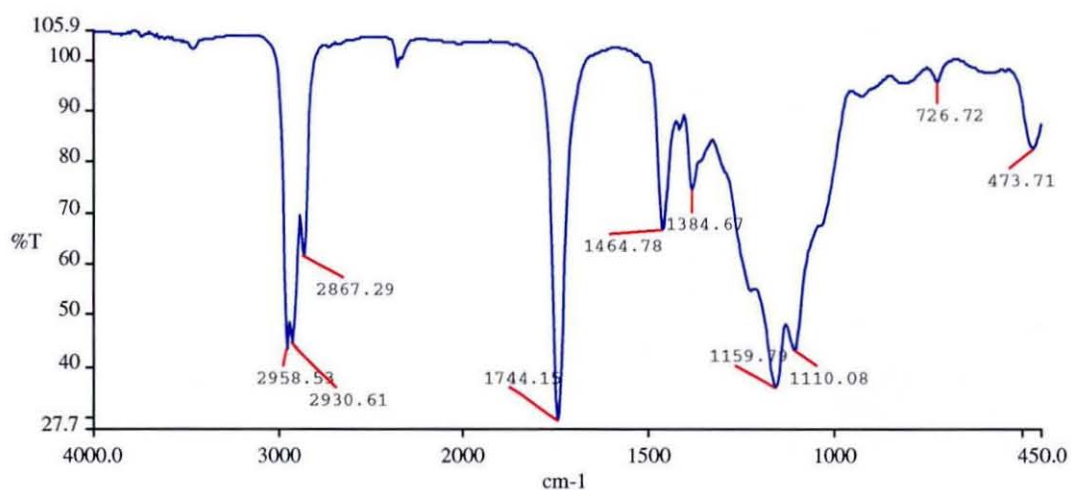


MG21

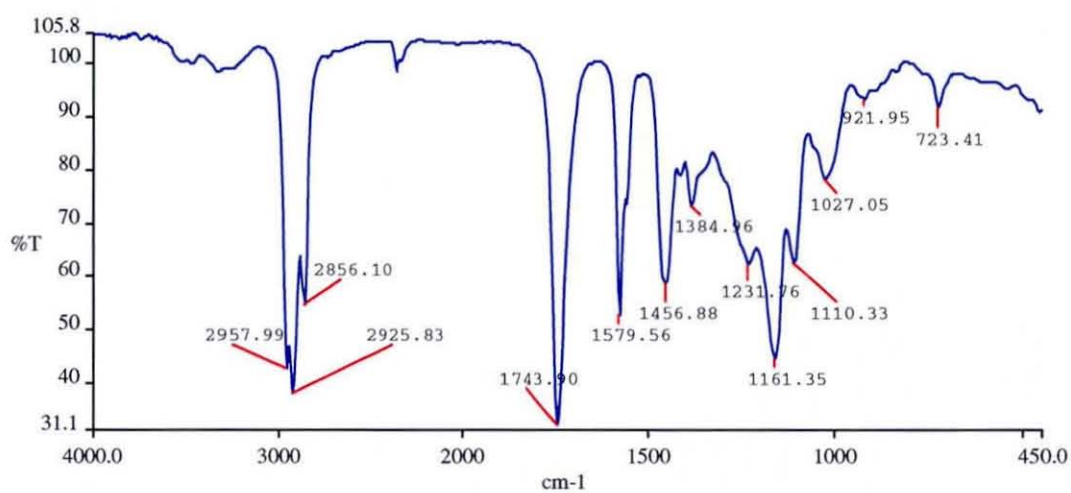
**Fig. 4.7 FTIR Spectra Obtained from Greases MF24, MF52 and MG21.**



MP12



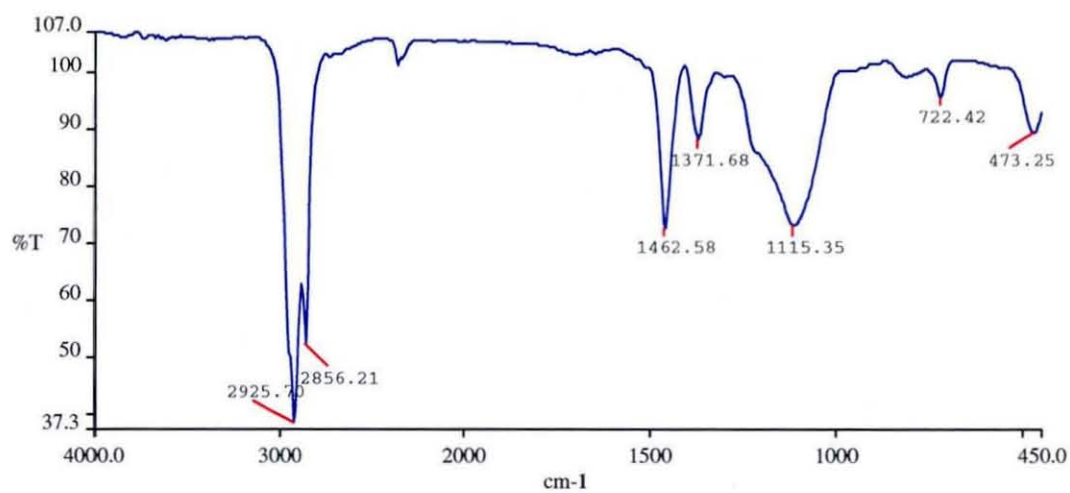
MP22



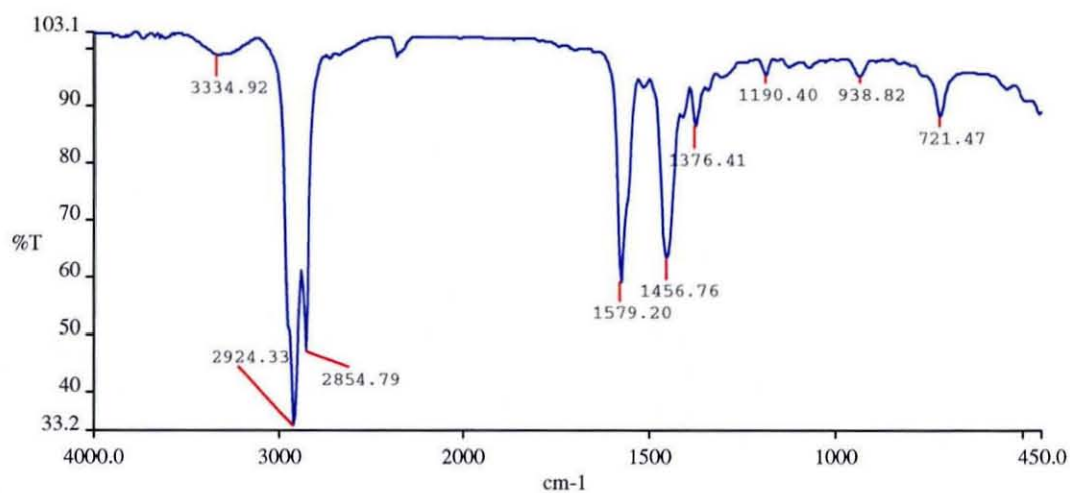
MP40

**Fig. 4.8 FTIR Spectra Obtained from Greases MP12, MP22 and MP40.**

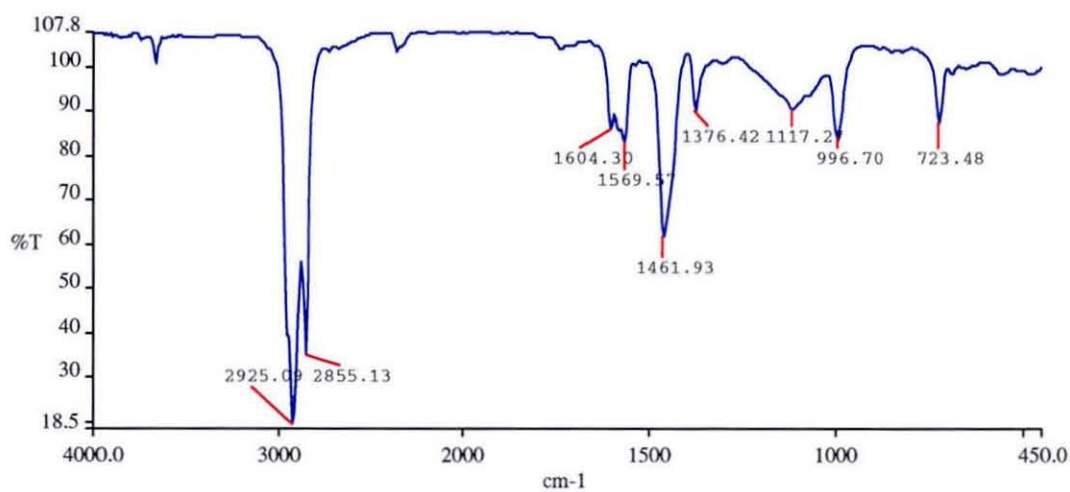




MR27

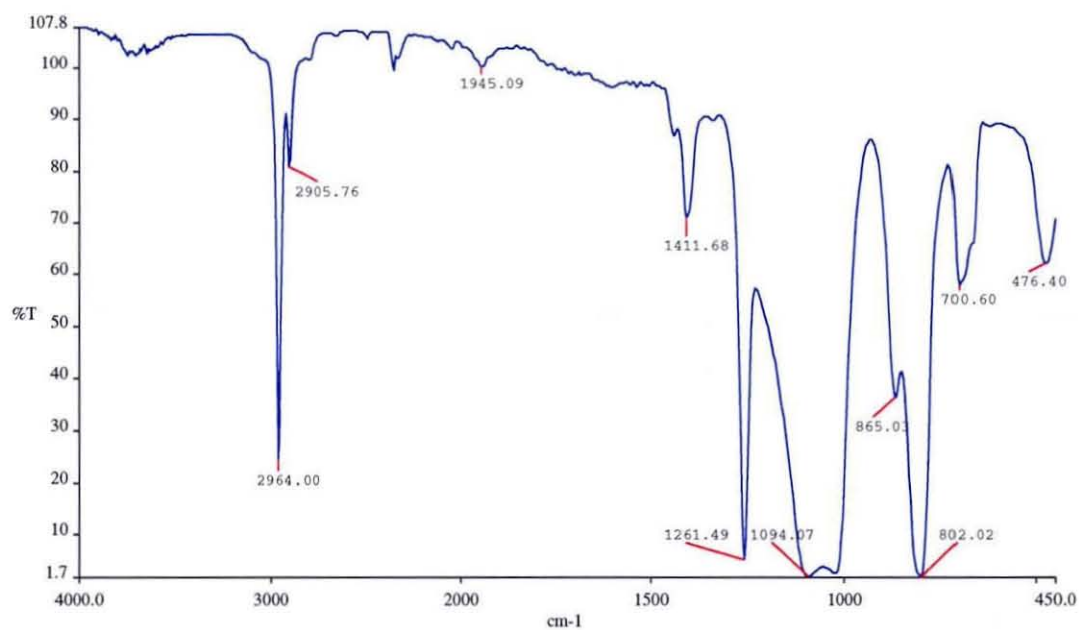


MR32

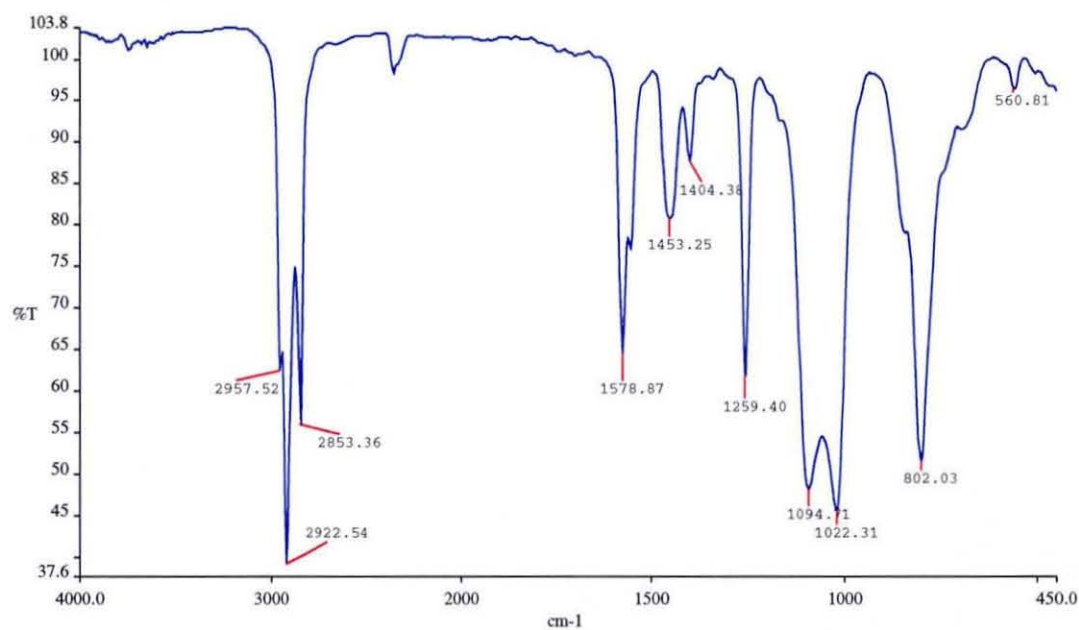


MR49

**Fig. 4.9 FTIR Spectra Obtained from Greases MR27, MR32 and MR49.**

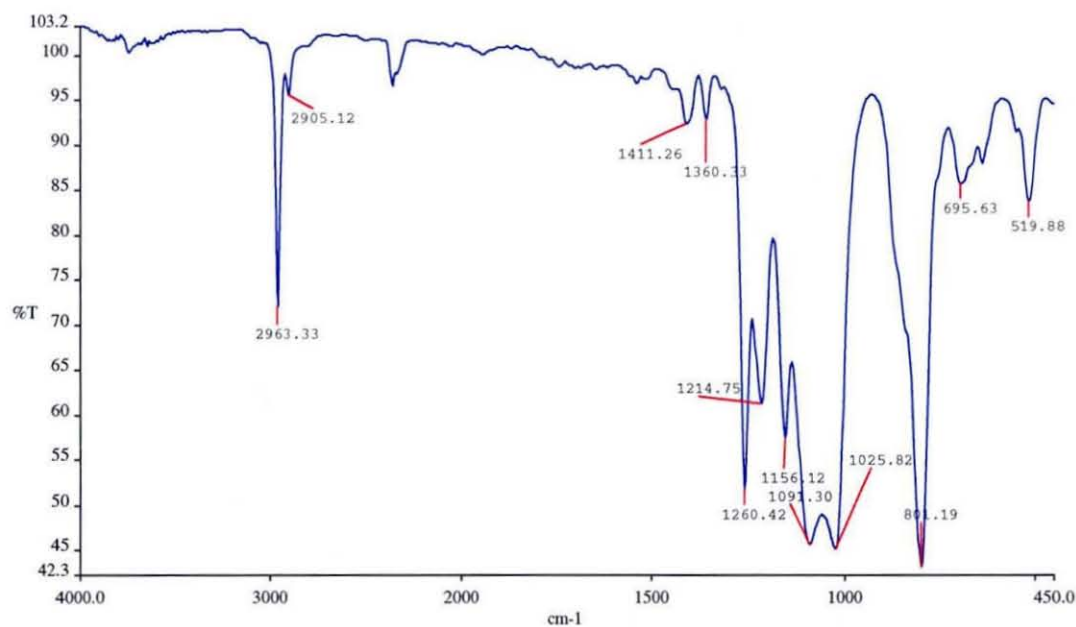


MS20

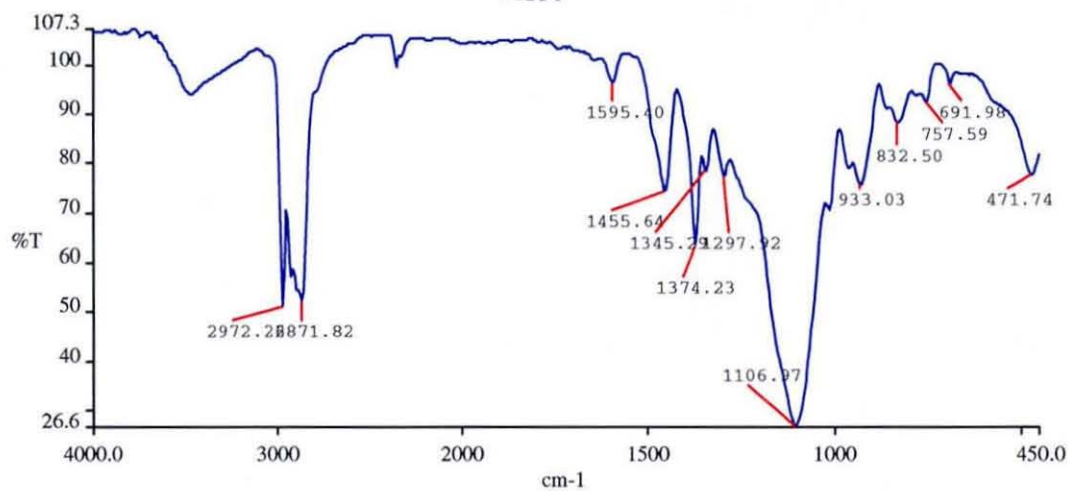


MS30

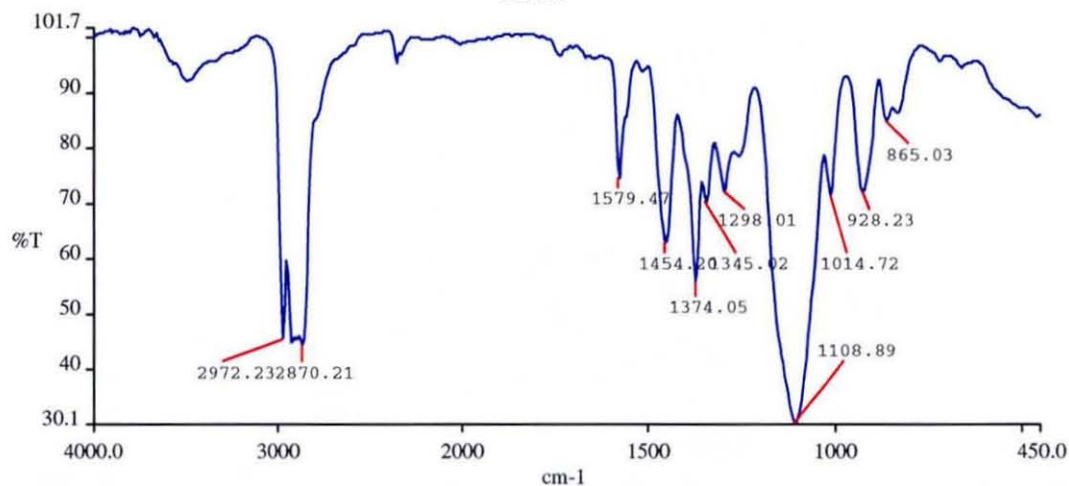
**Fig. 4.10 FTIR Spectra Obtained from Greases MS20 and MS30.**



MS50



MZ21



MZ31

**Fig. 4.11 FTIR Spectra Obtained from Greases MS50, MZ21 and MZ31.**

CODE	Base Oil	Thickening Agent	CODE	Base Oil	Thickening Agent
MC10	Mineral Oil	Bentonite	MP10	High Temp Ester	Bentonite
MC11	Mineral Oil	Bentonite	MP11	High Temp Ester	Bentonite
MC12	Mineral Oil	Bentonite	MP12	High Temp Ester	Bentonite
MC13	Mineral Oil	Bentonite	MP22	High Temp Ester	Silica
MC14	Mineral Oil	Bentonite	MP40	High Temp Ester	Soap Complex
MC25B	Mineral Oil	Silica	MP41	High Temp Ester	Soap Complex
MC30	Mineral Oil	Lithium Soap	MG21	PPE	Silica
MC32	Mineral Oil	Lithium Soap	MF20	PFAE	Silica
MC36	Mineral Oil	Lithium Soap	MF24	PFAE	Silica
MC37	Mineral Oil	Lithium Soap	MF51	PFAE	Polymer
MC41	Mineral Oil	Soap Complex	MF52	PFAE	Polymer
MC42	Mineral Oil	Soap Complex	MS20	Silicone	Silica
MC45	Mineral Oil	Soap Complex	MS30	Silicone	Lithium Soap
MR20	Synthetic Hydrocarbon	Silica	MS31	Silicone	Lithium Soap
MR27	Synthetic Hydrocarbon	Silica	MS50	Silicone	Polymer
MR30	Synthetic Hydrocarbon	Lithium Soap	MZ20	PAG	Silica
MR31	Synthetic Hydrocarbon	Lithium Soap	MZ30	PAG	Lithium Soap
MR32	Synthetic Hydrocarbon	Lithium Soap	MZ31	PAG	Lithium Soap
MR40	Synthetic Hydrocarbon	Soap Complex			
MR49	Synthetic Hydrocarbon	Soap Complex			

**Table 4.4 A Summary of the Composition of Lubricants as Determined by FTIR Spectroscopy.**

CODE	TGA 100°C	TGA 150°C	TGA 200°C	CODE	TGA 100°C	TGA 150°C	TGA 200°C
MC10	98	92	47	MZ30	100	22	17
MC11	98	74	22	MZ31	100	100	91
MC12	100	92	48	MP10	100	95	50
MC13	99	99	90	MP11	100	100	65
MC14	100	98	81	MP12	100	100	100
MC25B	100	94	56	MP22	98	88	39
MC30	99	81	48	MP40	100	98	38
MC32	98	80	40	MP41	100	99	50
MC36	97	85	31	MG21	100	100	89
MC37	100	87	46	MF20	100	100	100
MC41	98	85	45	MF24	100	100	99
MC42	99	78	39	MF51	100	100	100
MC45	100	91	82	MF52	100	100	100
MR20	100	100	60	MS20	100	100	99
MR27	100	91	80	MS30	100	100	76
MR30	96	76	44	MS31	96	97	93
MR31	100	98	55	MS50	100	100	97
MR32	100	99	50				
MR40	100	97	58				
MR49	99	90	67				
MZ20	100	10	10				

**Table 4.5 A Summary of Thermogravimetric Analyses of Test Lubricants (% Wt. Remaining)**

Lubricant	Base Oil	Thickening Agent	Reactivity ( $\mu\text{A}$ )	Lubricant	Base Oil	Thickening Agent	Reactivity ( $\mu\text{A}$ )
MC10	Mineral Oil	Bentonite	6.4	MP10	High Temp Ester	Bentonite	0.4
MC11	Mineral Oil	Bentonite	1.0	MP11	High Temp Ester	Bentonite	0.3
MC12	Mineral Oil	Bentonite	1.78	MP12	High Temp Ester	Bentonite	5.8
MC13	Mineral Oil	Bentonite	3.7	MP22	High Temp Ester	Silica	0.17
MC14	Mineral Oil	Bentonite	0.63	MP40	High Temp Ester	Soap Complex	0.85
MC25B	Mineral Oil	Silica	0.08	MP41	High Temp Ester	Soap Complex	0.5
MC30	Mineral Oil	Lithium Soap	7.1	MZ20	PAG	Silica	0.02
MC32	Mineral Oil	Lithium Soap	0.43	MZ30	PAG	Lithium Soap	<0.001
MC36	Mineral Oil	Lithium Soap	0.54	MZ31	PAG	Lithium Soap	<0.001
MC37	Mineral Oil	Lithium Soap	0.61	MG21	PPE	Silica	<0.001
MC41	Mineral Oil	Soap Complex	0.3	MF20	PFAE	Silica	0.008
MC42	Mineral Oil	Soap Complex	0.15	MF24	PFAE	Silica	<0.001
MC45	Mineral Oil	Soap Complex	0.1	MF51	PFAE	Polymer	0.001
MR20	Synthetic Hydrocarbon	Silica	0.0001	MF52	PFAE	Polymer	0.01
MR27	Synthetic Hydrocarbon	Silica	0.001	MS20	Silicone	Silica	0.003
MR30	Synthetic Hydrocarbon	Lithium Soap	3.5	MS30	Silicone	Lithium Soap	0.833
MR31	Synthetic Hydrocarbon	Lithium Soap	0.005	MS31	Silicone	Lithium Soap	152.0
MR32	Synthetic Hydrocarbon	Lithium Soap	0.111	MS50	Silicone	Polymer	4.1
MR40	Synthetic Hydrocarbon	Soap Complex	0.005				
MR49	Synthetic Hydrocarbon	Soap Complex	148.0				

**Table 4.6 Reactivity of Lubricants (Leakage Current ( $\mu\text{A}$ ))**

## 4.2 Corrosion Testing

### *Salt Spray Tests*

Figure 4.12 records the appearance and Table 4.7 the contact resistance results of the test coupons after exposure for 100 hours in the salt spray cabinet. It can be seen that all of the coupons had experienced corrosive attack, particularly those with noble coatings, the latter probably being due to porosity in the gold. The thin gold over nickel, (AUN1-3), was found to perform worst with a 100% failure rate, whilst the HDT was comparable with the unprotected copper.

### *Humidity Tests*

Figure 4.13 shows the appearance of the coupons after humidity testing, where the results for HDT compared well with the other platings tested. There is little obvious surface tarnishing of the tin which is consistent with the relatively small increase in contact resistance; Table 4.8. From the appearance and generally low CR it would indicate that under the test conditions used, the tin oxide layer formed was relatively thin, that is of the order of  $<20\text{nm}$ . or, if of greater dimensions, fracture of the brittle oxide occurred under loading of the contact probe tip, allowing extrusion of the softer tin to take place, referred to as the “ice-on-mud” effect.

### *Gas Tests*

Figure 4.14 shows the coupons after 240 hrs in an atmosphere of 305 ppm  $\text{H}_2\text{S}$  at room temperature, where visually there appears to be minimal effect on any of the platings. The copper coupons, however, show extensive tarnishing. This is manifested in the contact resistance measurement recorded in Table 4.9.

In summary, it has been shown that, under the specific test conditions used, HDT shows a relatively low CR, supporting its wide selection as a plating for automotive environments. However, the CR determinations were performed under static load and were not influenced by the effects of vibration, with resultant generation of fretting corrosion products.

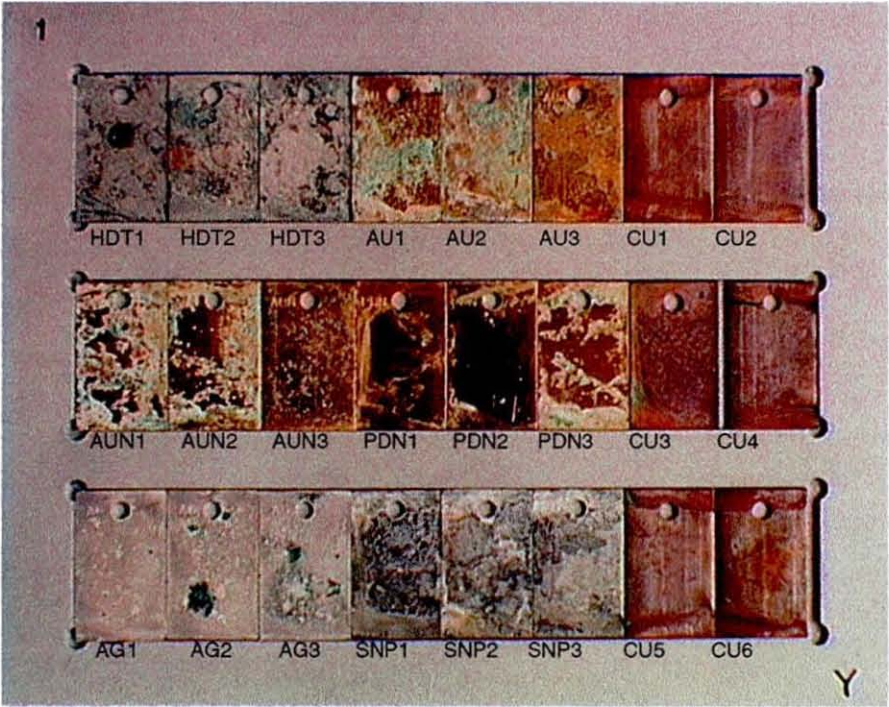


Fig. 4.12 Appearance of Test Coupons after 100 hrs. Salt Spray Testing.

Sample	Initial		After Salt Spray (100 hrs)	
	CR(mΩ)	A%	CR(mΩ)	A%
HDT	2	0	13	0
Tin/Lead (SNP)	1	0	5	0
Gold 0.2μm (AU)	1	0	>20X10 <sup>3</sup>	97
Gold 0.8μm(AUN)	1	0	1690	25
Gold/Pd/Ni (PDN)	1	0	36	0
Silver (AG)	<1	0	4	0
Copper (CU)	<1	0	15	0

(CR = median value of contact resistance, A = percentage of open circuit readings >20Ω)

Table 4.7 Contact Resistance Results on Test Coupons After 100 Hours Salt Spray Testing.



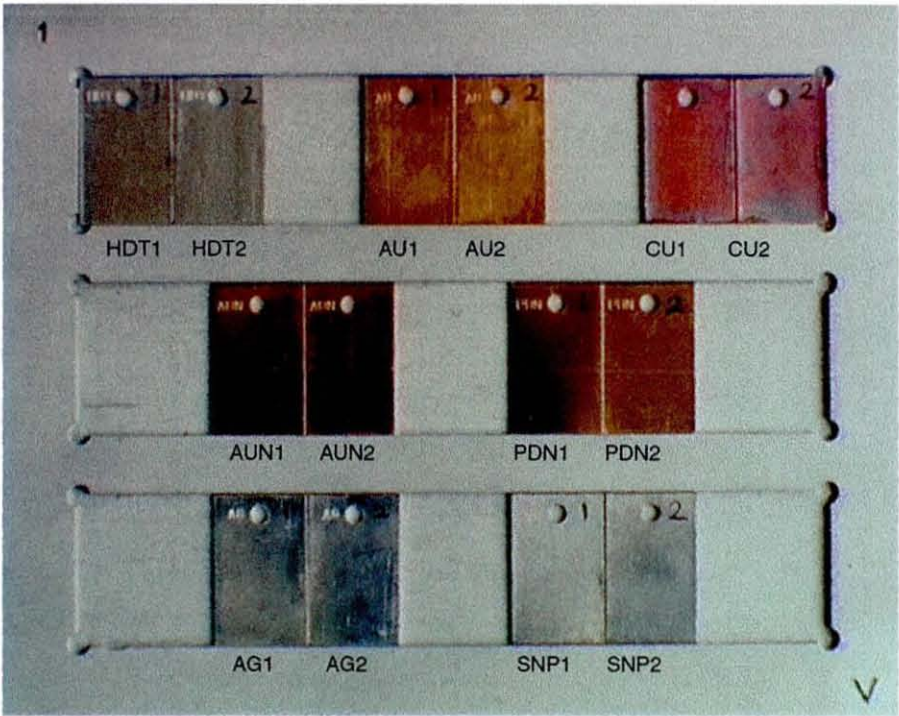


Fig. 4.13 Appearance of Test Coupons after Humidity Testing

Sample	Initial		After Humidity Testing	
	CR(mΩ)	A%	CR(mΩ)	A%
HDT	1	0	3	0
Tin/Lead (SNP)	1	0	2	0
Gold 0.2μm (AU)	1	0	1	0
Gold 0.8μm(AUN)	1	0	2	0
Gold/Pd/Ni (PDN)	1	0	4	0
Silver (AG)	<1	0	1	0
Copper (CU)	<1	0	4	0

(CR = median value of contact resistance, A = percentage of open circuit readings >20Ω)

Table 4.8 Contact Resistance Measurements After Humidity Testing

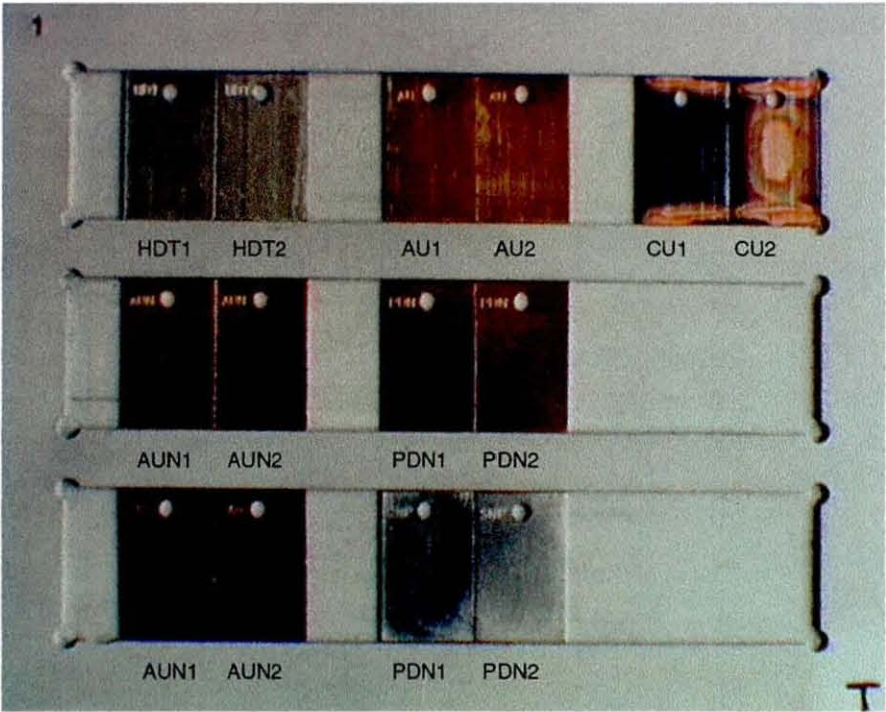


Fig. 4.14 Appearance of Test Coupons After Gas Testing

Sample	Initial		After Thio' Testing	
	CR(mΩ)	A%	CR(mΩ)	A%
HDT	1	0	3	0
Tin/Lead (SNP)	2	0	2	0
Gold 0.2μm (AU)	1	0	1	4
Gold 0.8μm(AUN)	1	0	2	4
Gold/Pd/Ni (PDN)	1	0	4	0
Silver (AG)	<1	0	2	0
Copper (CU)	<1	0	57	0

(CR = median value of contact resistance, A = percentage of open circuit readings >20Ω)

Table 4.9 Contact Resistance Measurements after Gas Testing

### 4.2.1 Field Testing

Coupons exposed to the conditions experienced in passenger and engine compartments in a variety of geographical locations over a period of two years, are shown in Figure 4.15. The coupons sited in the engine bays showed the heaviest oxidation and the CR results, in Table 4.10, correlated well with their visual appearance. For the transcontinental vehicles CR measurements were greater than an order of magnitude over those located in passenger compartments and higher than in the same location on other vehicles.

The exposure period of each of the coupons was similar (88-93 weeks), and, if it can be assumed that their location on each of the vehicles was comparable in terms of their respective operating conditions, it may be concluded from the results that the engine bay experienced the harshest environmental conditions compared to those existing in passenger compartments. The conditions in the engine bays of transcontinental heavy goods vehicles were more severe than those in vehicles operating in urban and rural regions in the UK. However, it could be argued that the higher mileage of the transcontinental vehicles with the consequential longer engine running time would have resulted in longer periods when the coupons sustained high temperatures.

#### *XPS Analysis*

Surface analysis was performed on all samples using XPS, as previously described, Table 4.11. The high levels of carbon and oxygen were almost certainly from carbonaceous deposits. Removal of these using a suitable solvent prior to analysis would, it is thought, have had a major effect on the normalised results, significantly increasing the concentrations of the remaining elements. When comparisons were made with the results from the 'as-plated' sample, there were no significant differences in film composition apart from the presence of small amounts of sulphur and chlorine; see Table 4.3.



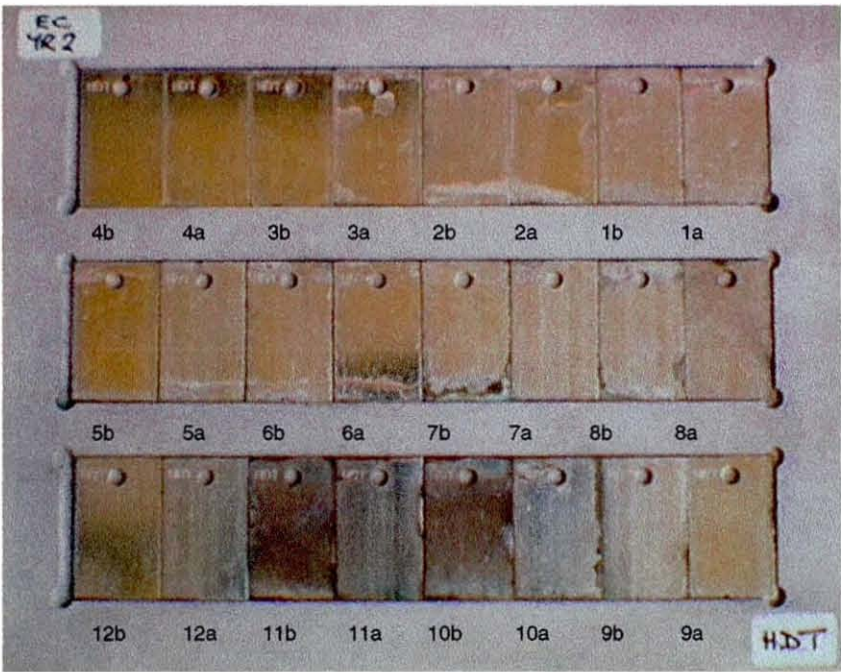


Fig. 4.15 Appearance of Test Coupons after Field Testing.

Location	P	E	E	E	P	E	E	E	P	E	E	E
Vehicle Environ.	U	U	U	U	R	R	R	R	T	T	T	T
Test Coupon	1	2	3	4	5	6	7	8	9	10	11	12
Median CR(mΩ)	2	4	2	6	2	4	12	31	2	52	60	50

(P = passenger compartment, E = engine bay, U = urban, R = rural, T = trans-continental)

Table 4.10 Contact Resistance Results after Field Testing

XPS Analysis of Field Tested Coupons (At.%)							
Sample	C	O	Sn	Pb	Zn	Cl	S
1(P/U)	57	27	7	<2	5	2	2
2(E/U)	64	20	5	<2	3	6	2
3(E/U)	64	23	5	<2	3	3	2
4(E/U)	61	28	5	<2	3	2	<2
5(P/R)	59	28	6	<2	5	<2	<2
6(E/R)	81	15	2	<2	<2	<2	<2
7(E/R)	59	29	5	<2	3	2	<2
8(E/R)	61	26	6	<2	4	2	<2
9(P/T)	56	29	7	<2	6	<2	<2
10(E/T)	59	29	7	<2	3	<2	<2
11(E/T)	61	27	5	<2	3	3	2
12(E/T)	53	33	7	<2	4	<2	3

(P = passenger compartment, E = engine bay, U = urban, R = rural, T = trans-continental)

**Table 4.11 XPS Analysis Results of Field Tested Coupons Reported to Nearest 1%**

#### *SEM/EDS Analysis*

From the contact resistance results, all of the coupons mounted in the engine compartments of the trucks had by inference been exposed to the most severe conditions. It was therefore decided to carry out further analysis of one of the coupons (coupon 12(a)), by SEM, EDS and AES. SEM imaging revealed numerous particulate matter and dried-up deposits. Figure 4.16 is a BSE image showing the distribution of the contaminants. A region was selected and imaged in secondary electron mode at higher magnification using a beam voltage of 3 keV. An X-ray energy spectrum in the form of a polychromatic image was superimposed on this image; Fig. 4.17, and an EDS spectrum generated; Fig. 4.18. It can be seen that carbonaceous matter is distributed widely over the surface with the remaining regions containing traces of magnesium, aluminium, silicon and sulphur. There were significant amounts of zinc and copper which had migrated towards the tin surface. The densely blue areas appear

to be associated with particles showing high relief and are thought to be an artefact caused by shielding effects due to the orientation of the X-ray detector to the sample surface. The particles have absorbed the lower energy X-rays but are transparent to the high energy Bremsstrahlung.

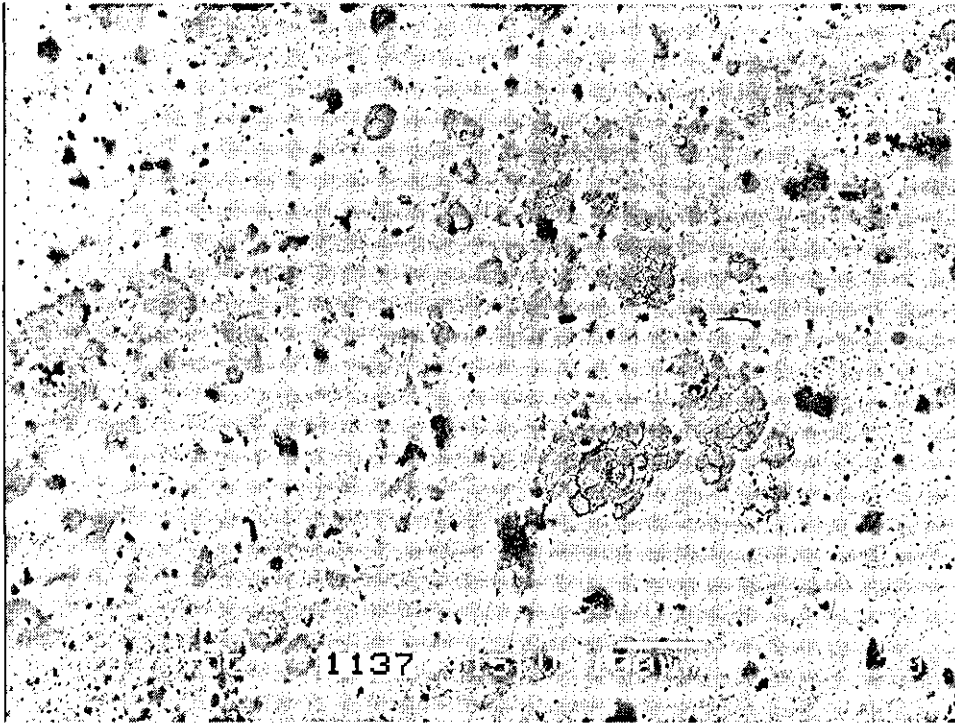


*Fig. 4.16 BSE Image of the Surface of Coupon 12(a)*

#### *AES Analysis*

A depth profile was performed on coupon 12(a) and Figure 4.19 is a trace of elemental composition changes with distance from the coupon surface. Significantly, the depth to which carbon, zinc and chlorine was detected is little changed from the control ‘as-plated’ coupon, Fig. 4.5. However, there is evidence from the trace that a thicker oxide layer had formed and copper had diffused towards the surface indicating a relatively high field test temperature existing for extended time periods in the vehicle engine bay. The low chlorine levels would also suggest that this coupon had not been subjected to high or sustained levels of chloride contamination, being not dissimilar to those found on aged samples in the laboratory atmosphere. However, although in low concentrations in the oxide film, sulphur has shown its presence to a greater degree than in the controlled environment.

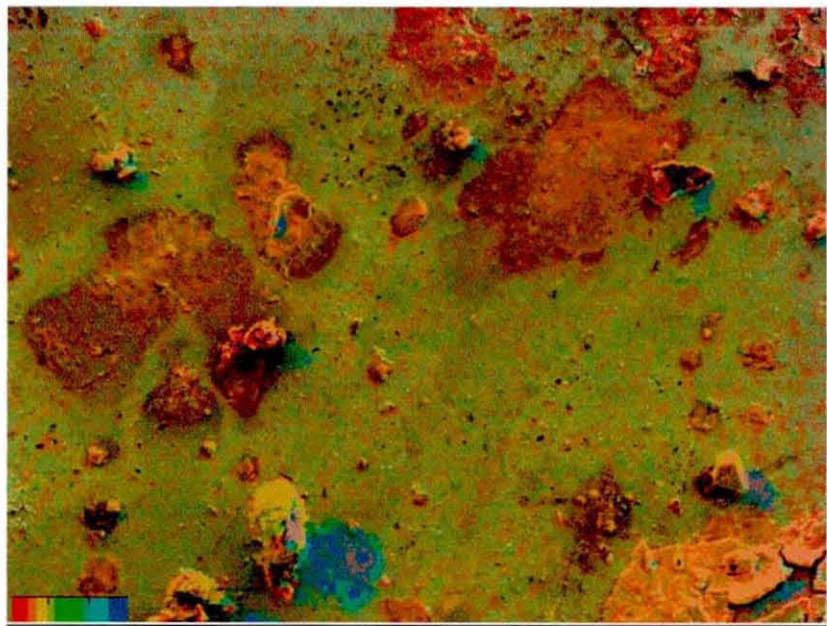


**Fig. 4.17** Surface of Coupon 12(a). X-ray Energy Distribution Superimposed on Secondary Electron Image. (Energy spectrum range 0.15 to 3 keV)

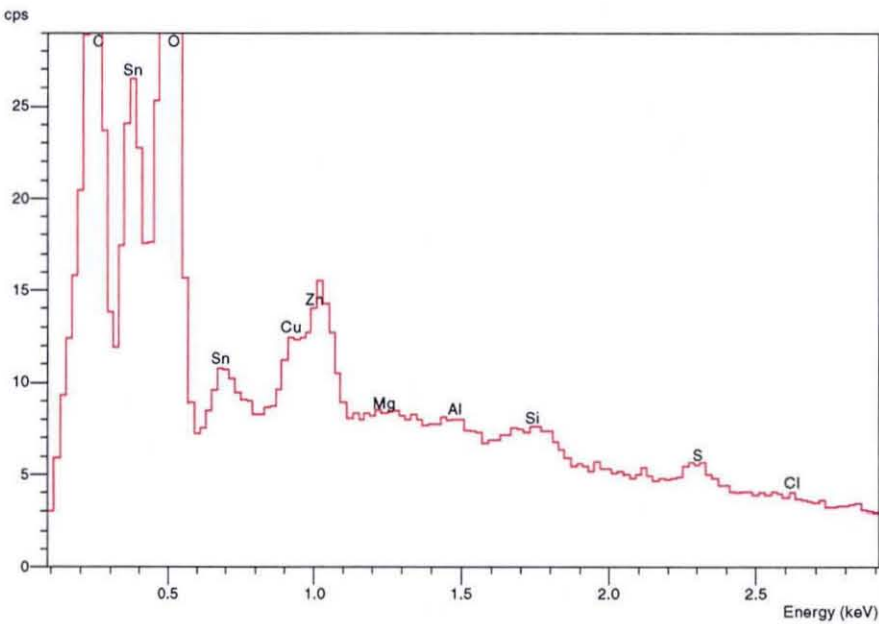


**Fig. 4.18** EDS Spectrum of Region Imaged in Figure 4.17 (3kV excitation voltage)

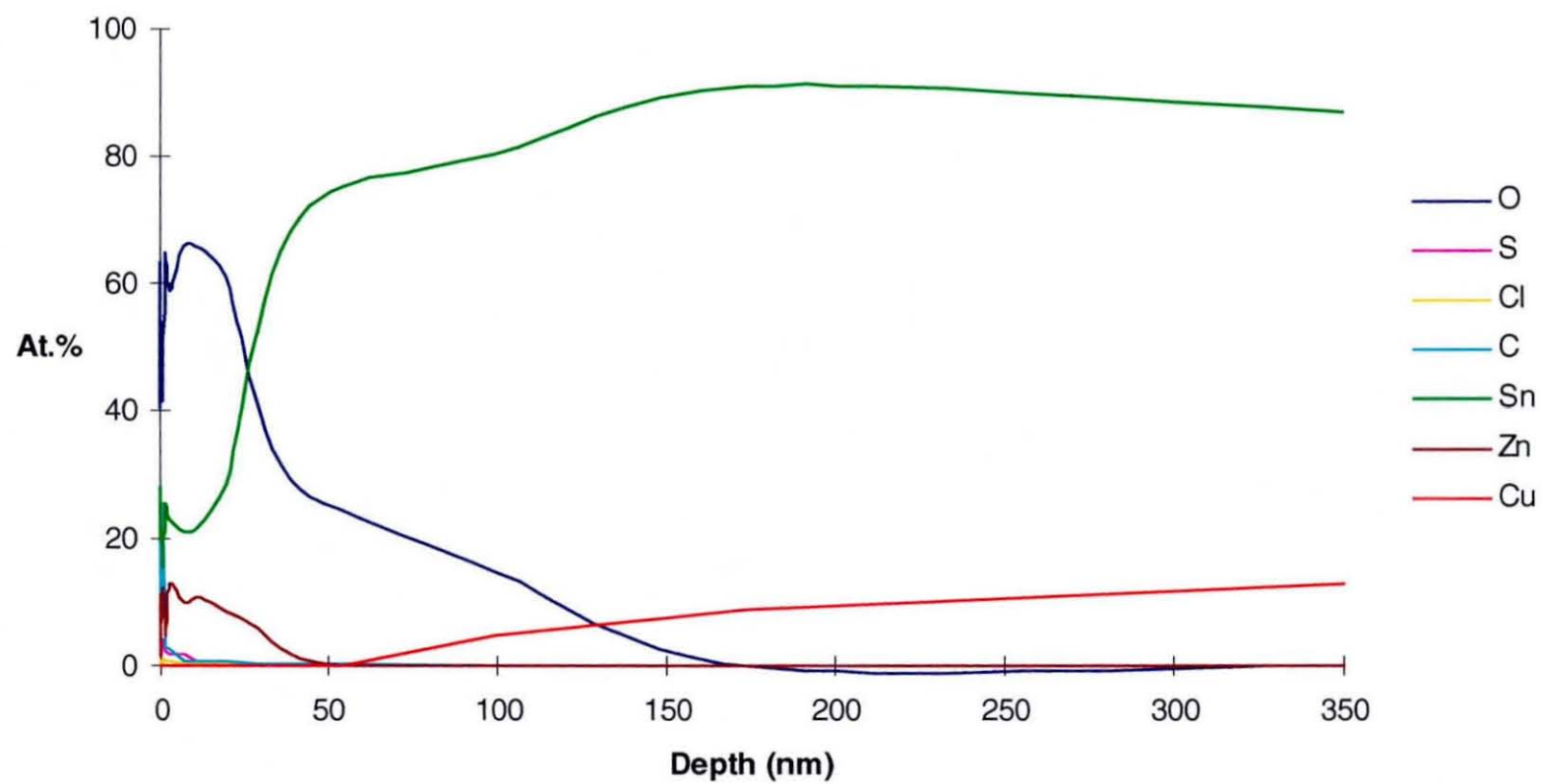


*Fig. 4.19 AES Depth Profile of Coupon 12(a).*



4.3 Analysis of Thermally Aged Coupons

AES profiles through the surface layers of an ‘as plated’ and the coupons aged for 2000 hrs. are shown in Figures 4.20 to 4.23 and contact resistance measurements on the same coupons are displayed in Table 4.12. The profiles indicate an increase in oxide thickness with ageing temperature, which in turn correlates with an increase in contact resistance.

There is also some evidence of an increase in the level of zinc near the surface after heat treatment. High levels of carbon are also apparent but this was probably due to contamination of the surface rather than reaction products or diffusion from within the plating. Traces of the elements chlorine, sulphur and potassium were also present but at insignificant levels.

Ageing Temperature (°C)	Oxide Thickness (nm)	Contact Resistance (mΩ)	Percentage of open circuit readings (>20Ω)
As Plated (with oxide from melt)	20	1	0
100	30	5	0
125	120	34	0
150	160	74	0

Table 4.12 Contact Resistance Measurements After Thermal Ageing

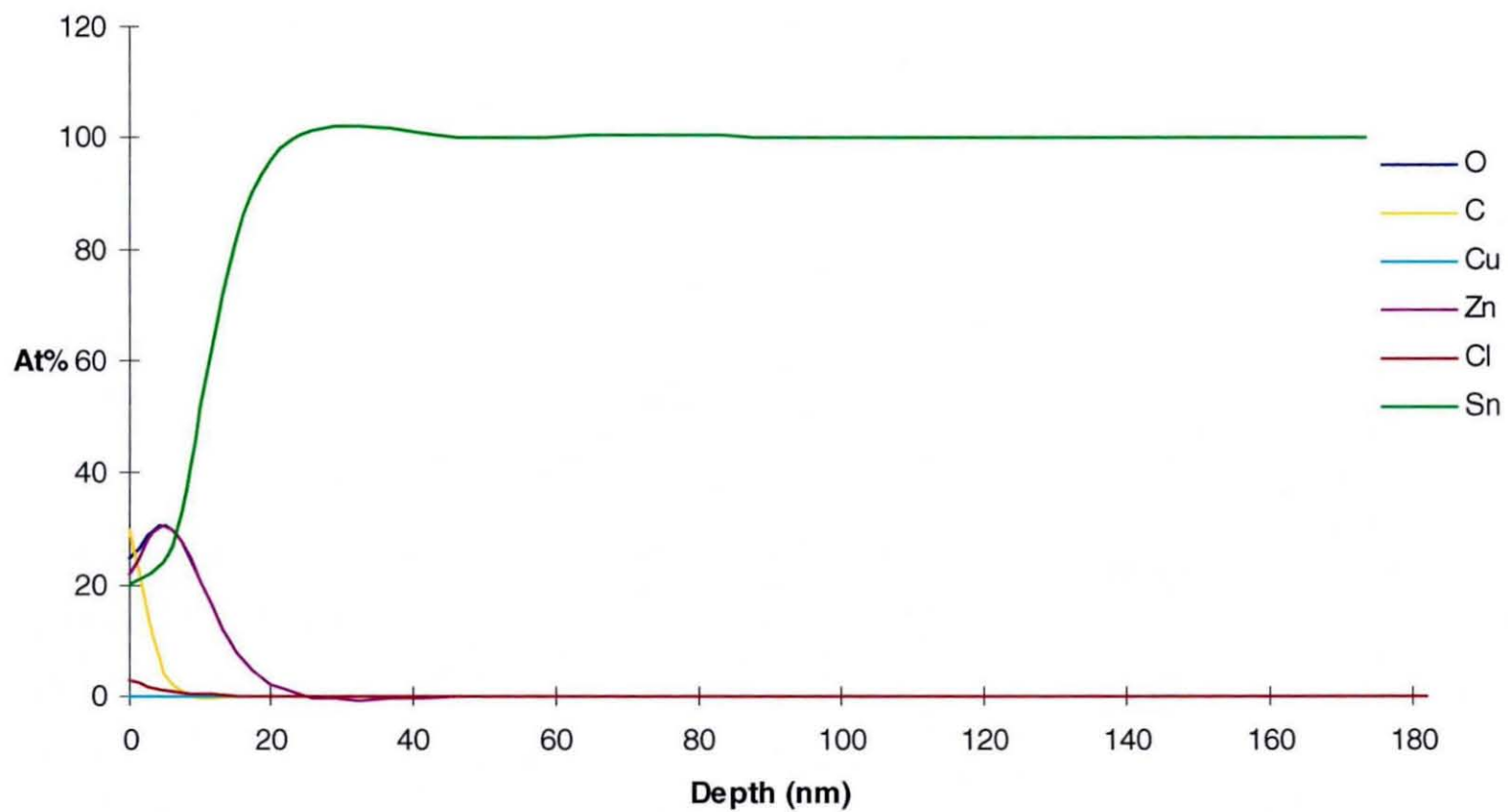


*Fig. 4.20 AES Depth Profile of Coupon ('as plated')*

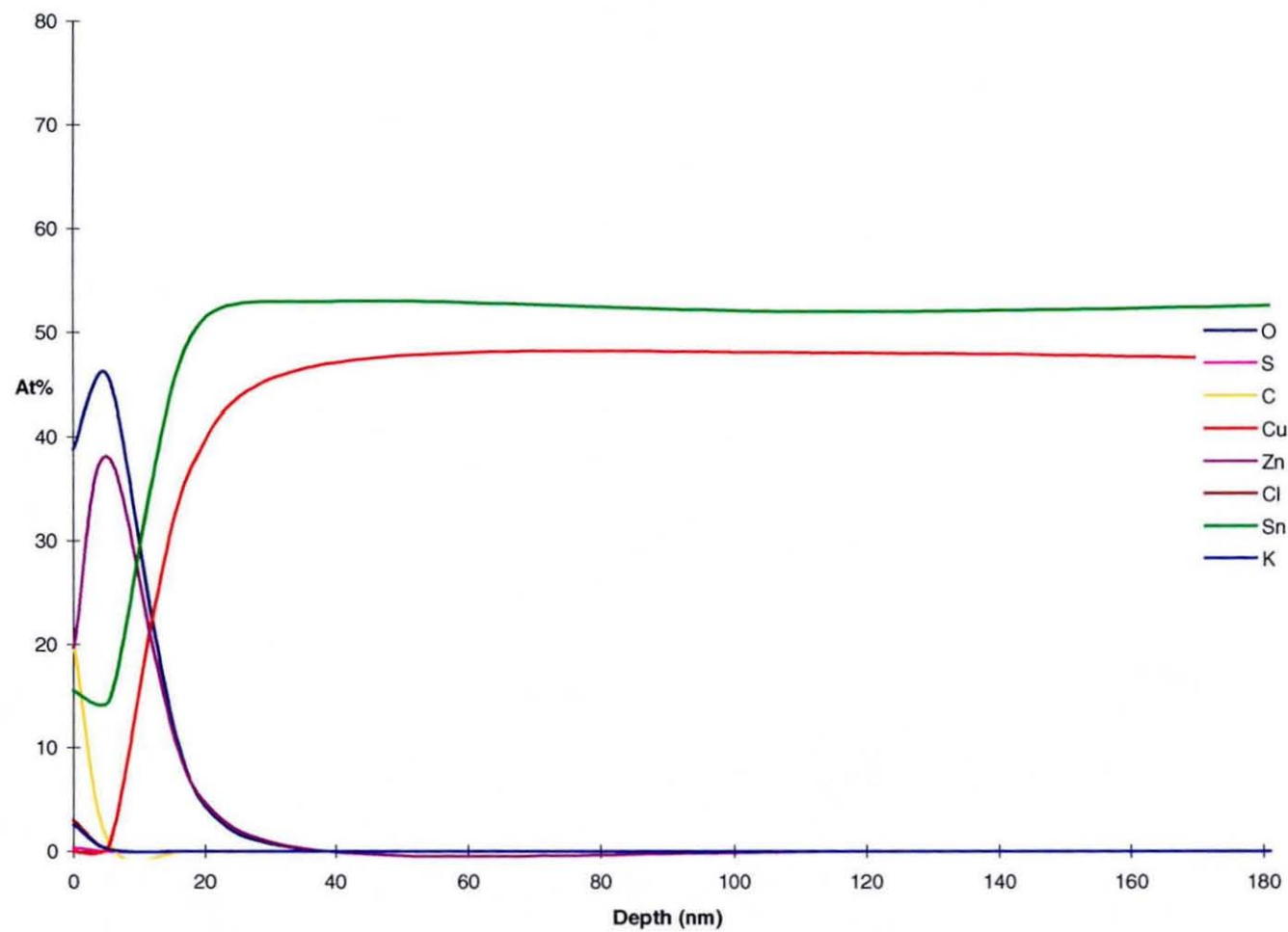


*Fig. 4.21 AES Depth Profile of Coupon Aged for 2000 hrs at 100 °C*

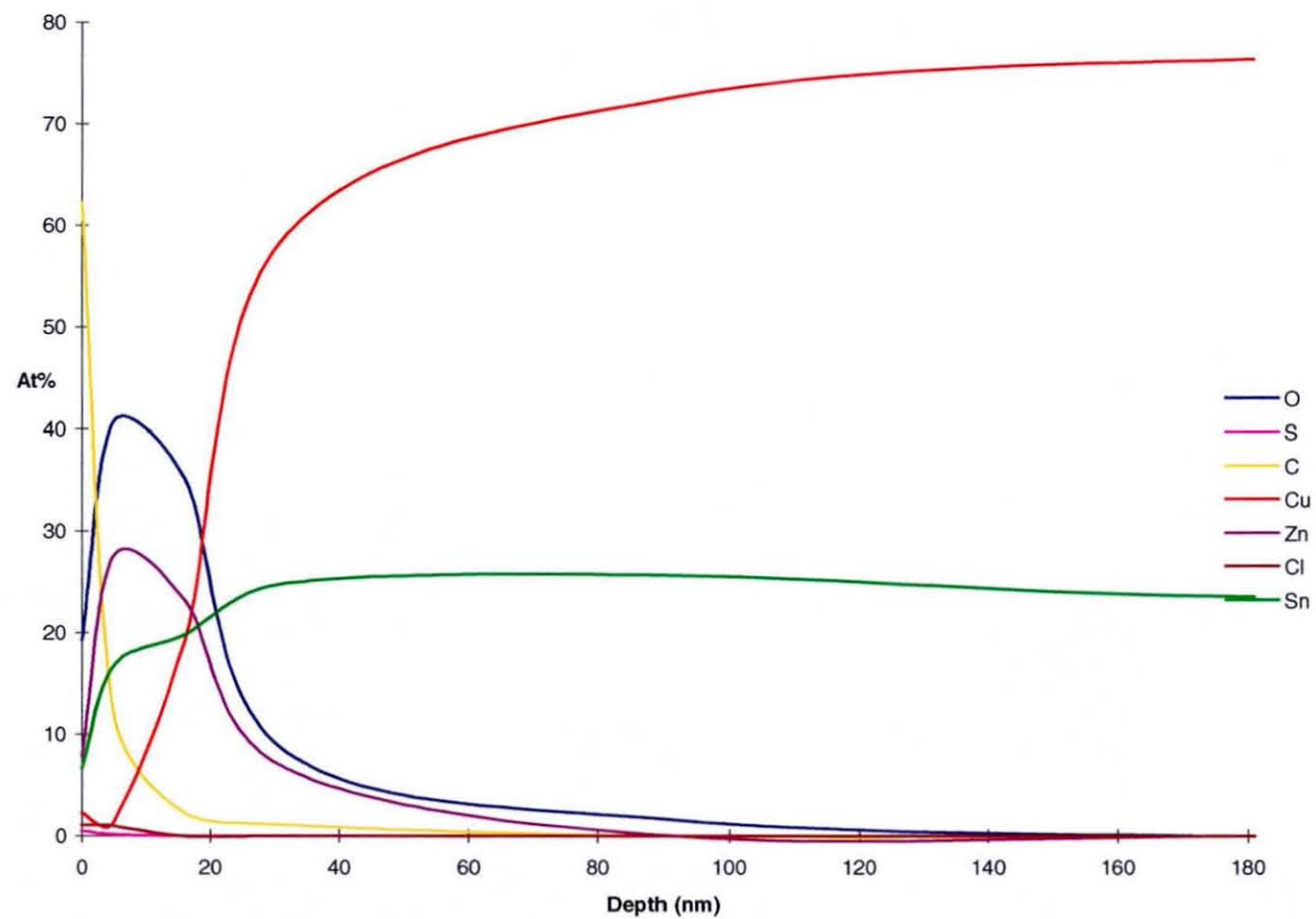


**Fig. 4.22** AES Depth Profile of Coupon Aged for 2000 hrs at 125 °C

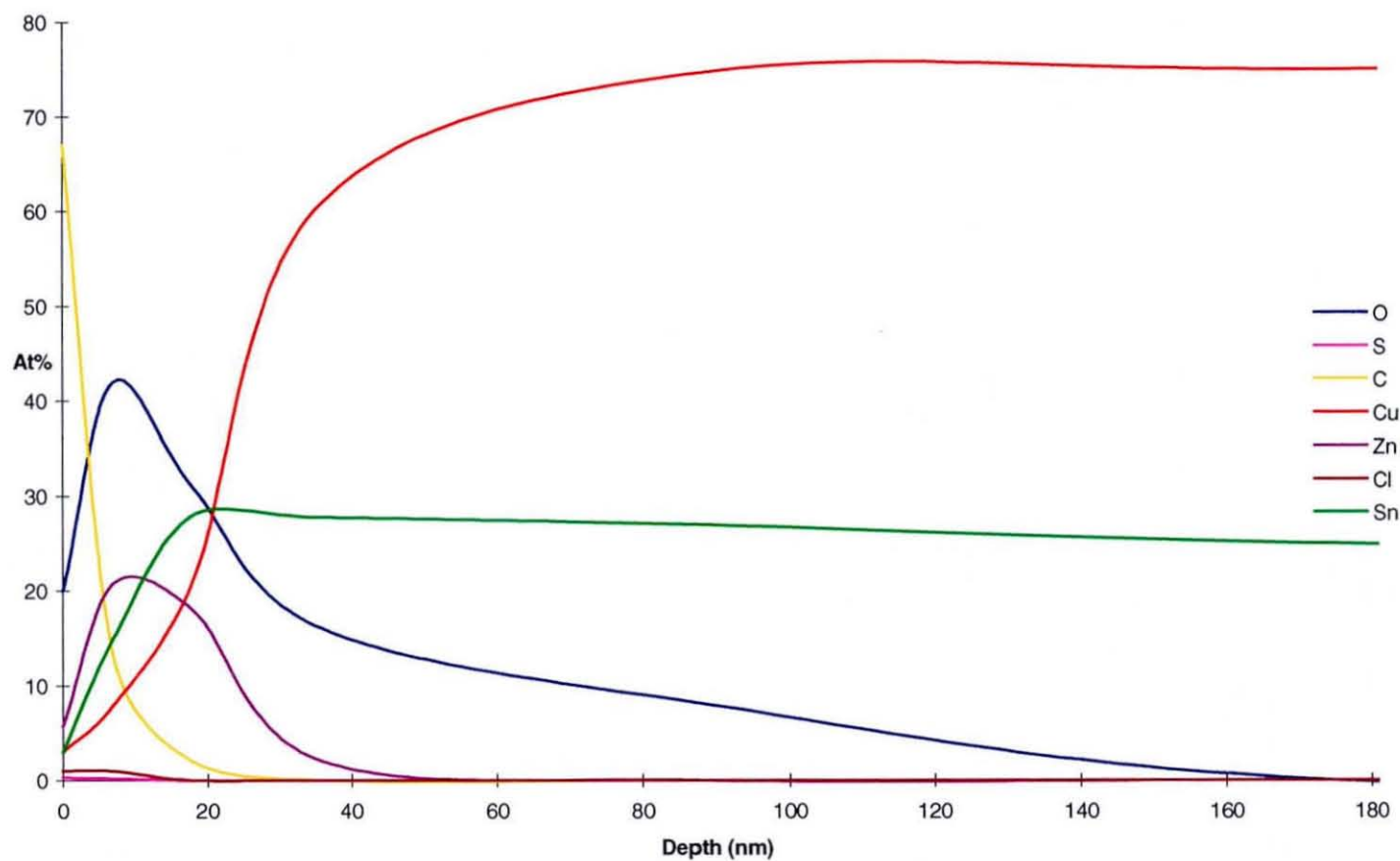


*Fig. 4.23 AES Depth Profile of Coupon Aged for 2000 hrs at 150°C*

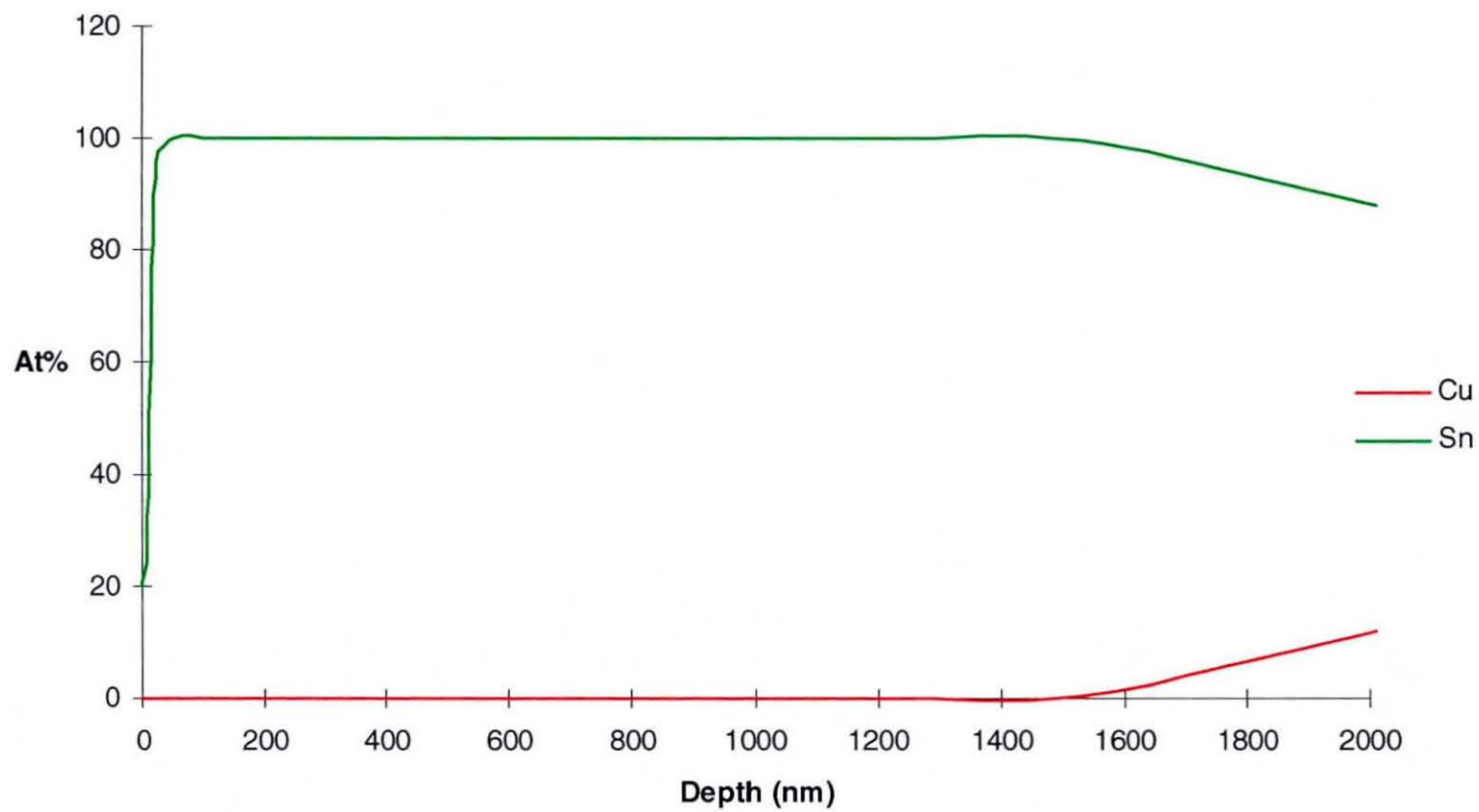


*Fig. 4.26 AES Depth Profile of Coupon ('as plated')*

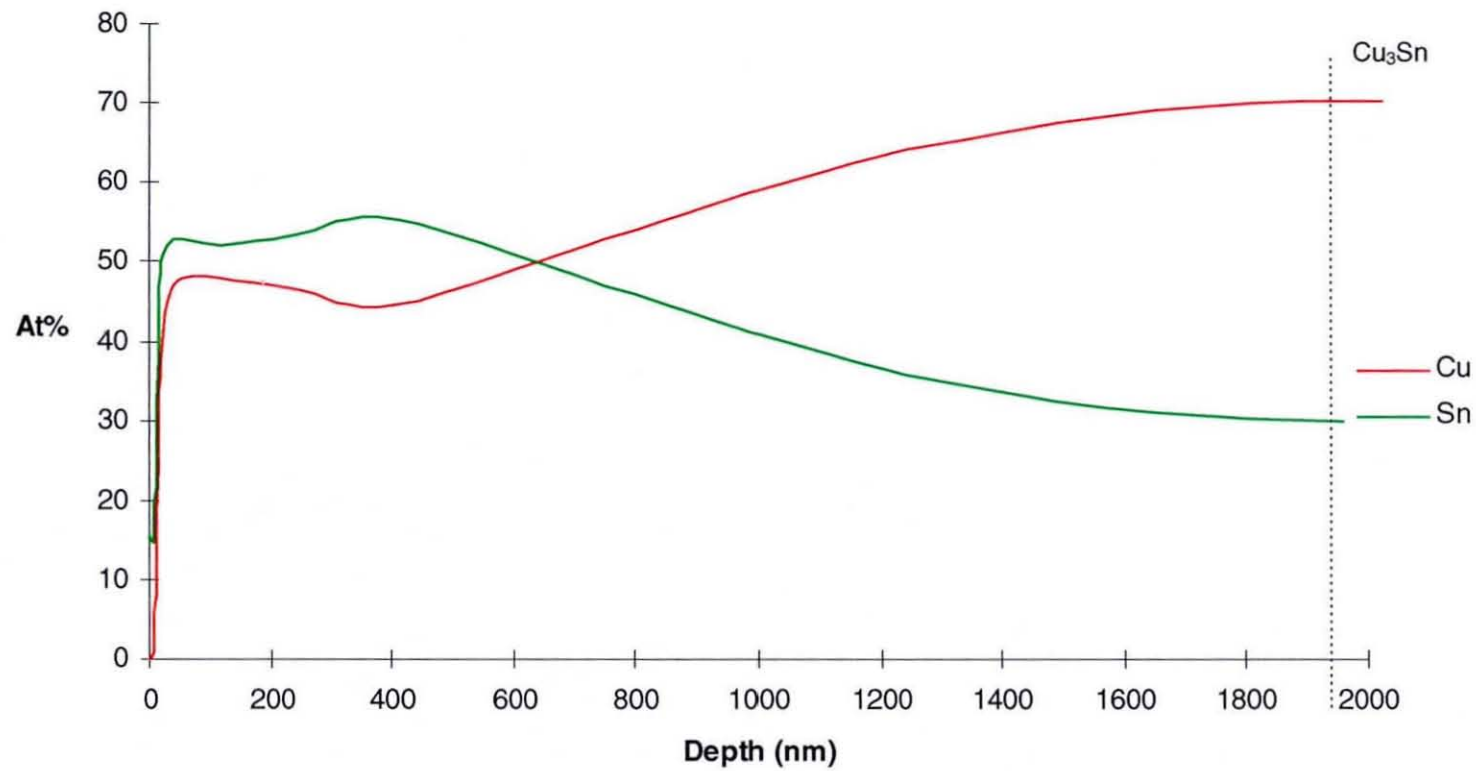


**Fig. 4.27 AES Depth Profile of Coupon Aged for 2000 hrs. at 100°C**  
**Showing Evidence of Possible Bulk and Grain Boundary Diffusion of Copper.**

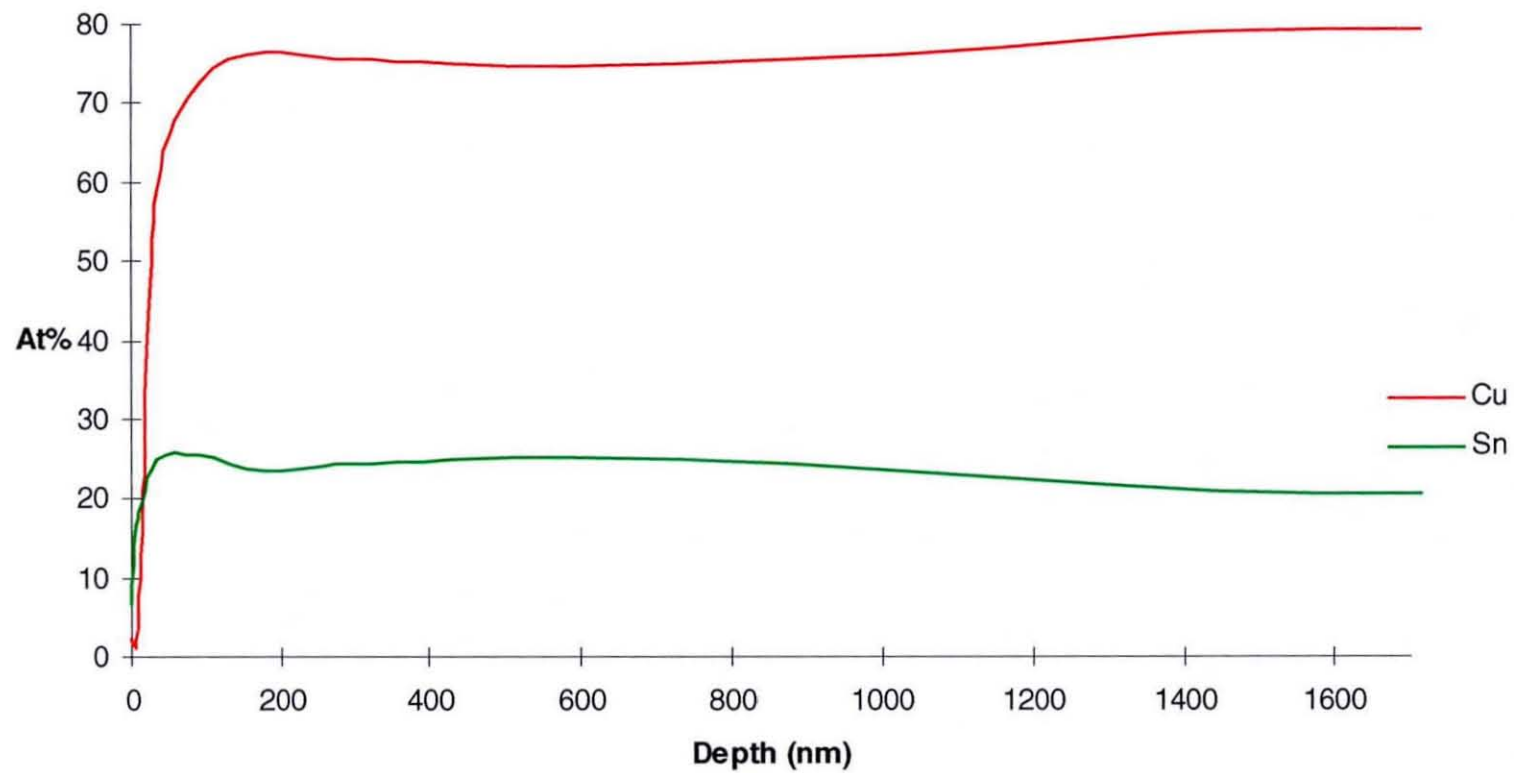


*Fig. 4.28 AES Depth Profile of Coupon Aged for 2000 hrs. at 125 °C*



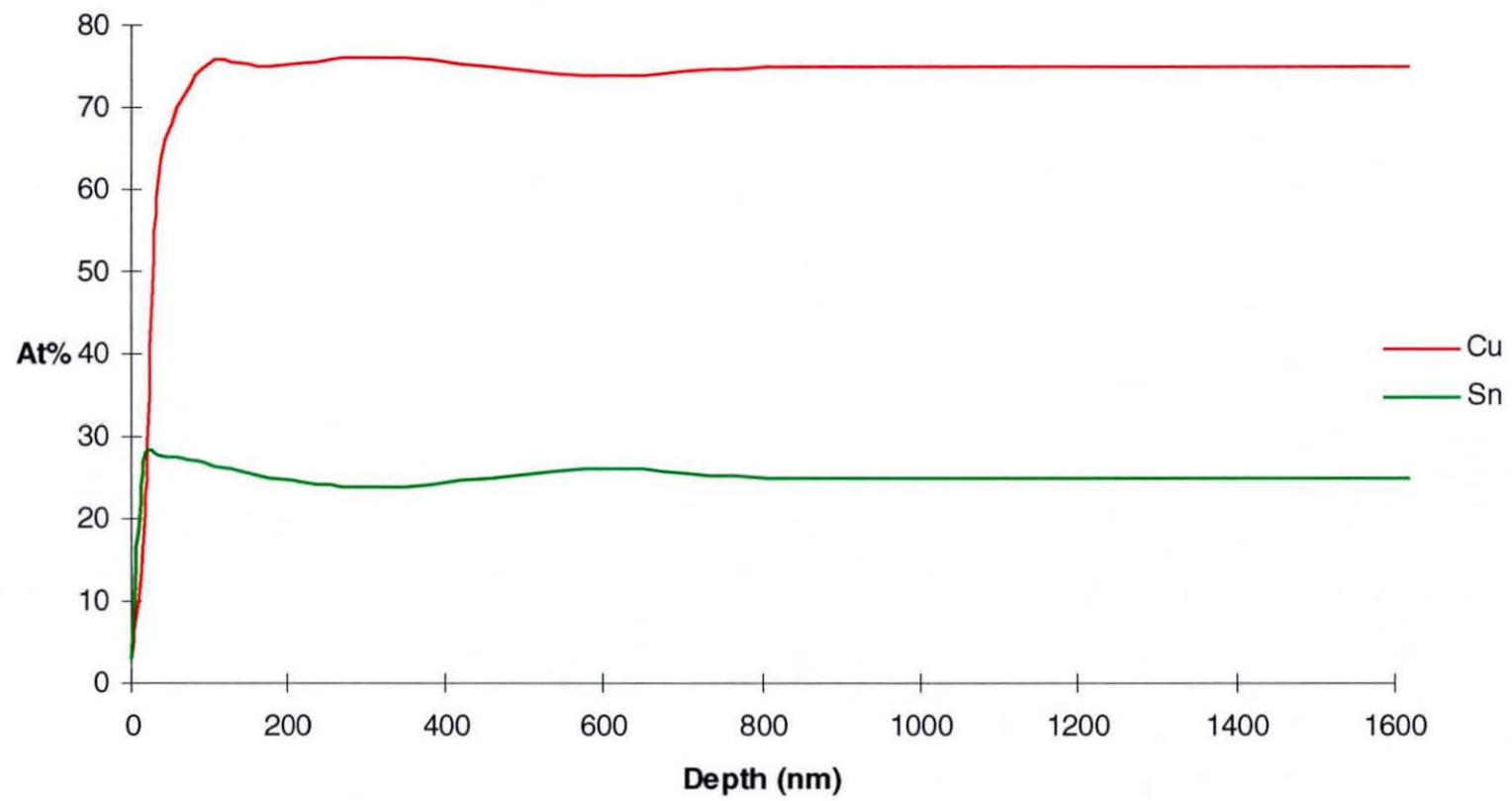


*Fig. 4.29 AES Depth Profile of Coupon Aged for 2000 hrs. at 150°C*

### 4.3.3 XRD Analysis

Figure 4.30 is an XRD trace of the tin coating after ageing at 150°C for 2000 hours, together with peak identification from JCPDS files<sup>5</sup>, which, within the limitations of the technique, confirms the full conversion to  $\text{Cu}_3\text{Sn}$  of the  $\text{Cu}_6\text{Sn}_5$  phase. Examination of the traces from a sample which has been aged at 125°C for the same time period showed an incomplete transformation, Figs. 4.31 and 4.32, with what was thought to be the formation of intermediate phases. This differs from the results obtained by AES depth profiling, Fig. 4.22, but may be explained by the small area analysed by the latter technique compared to XRD. The presence of the two peaks at  $2\theta$  angles of 27.8775° and 73.6000° in both of the samples analysed is interesting, as they were not associated with any known phases which were likely to have been present within the analysed volume. It is possible, however, that they were reflections from a superlattice structure but confirmation of this would be the subject of further work.

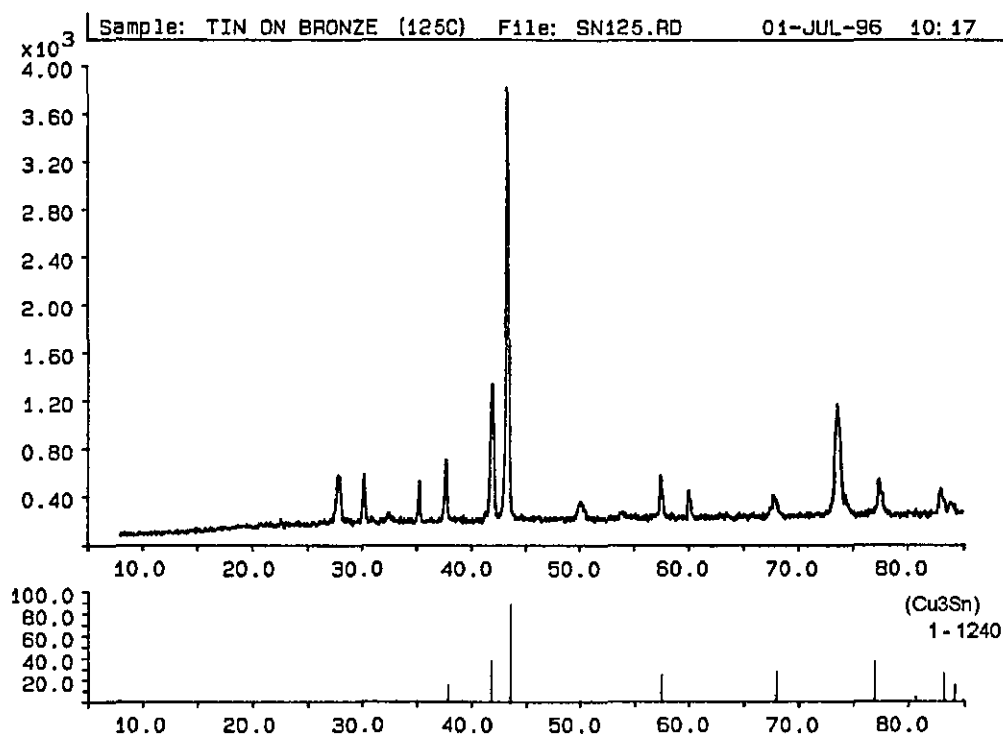


**Fig. 4.30 XRD Trace of Coupon Aged for 2000 hrs. at 150°C (Cu anode 45kV, 30mA)**

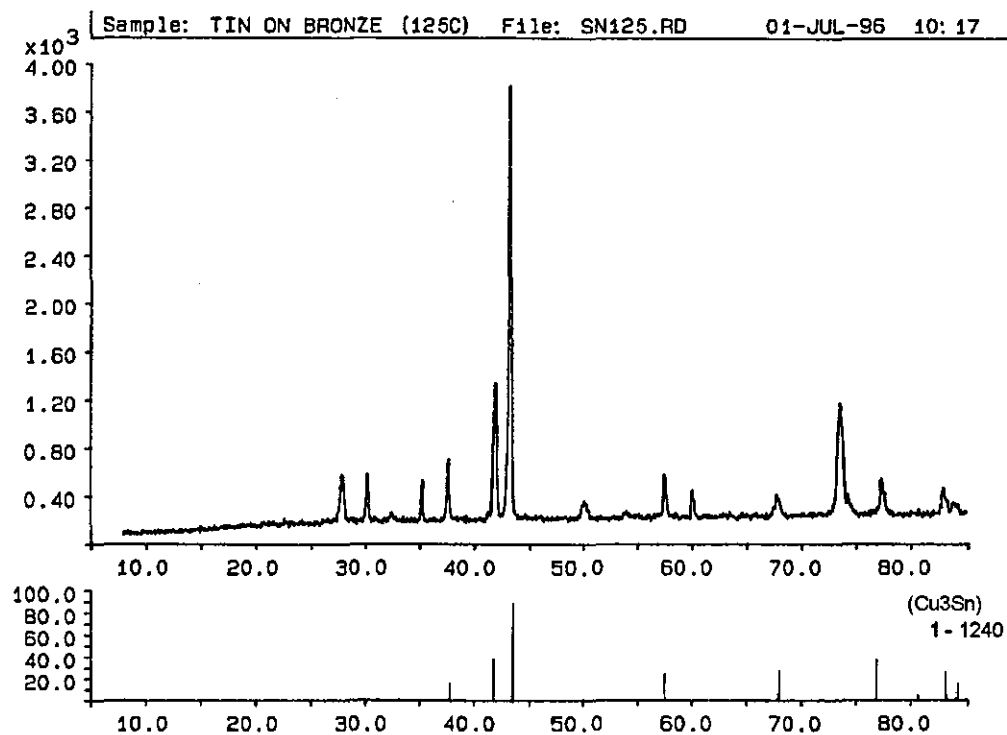


**Fig. 4.31 XRD Trace of Coupon Aged for 2000 hrs. at 125° (Cu anode 45kV, 30mA)**

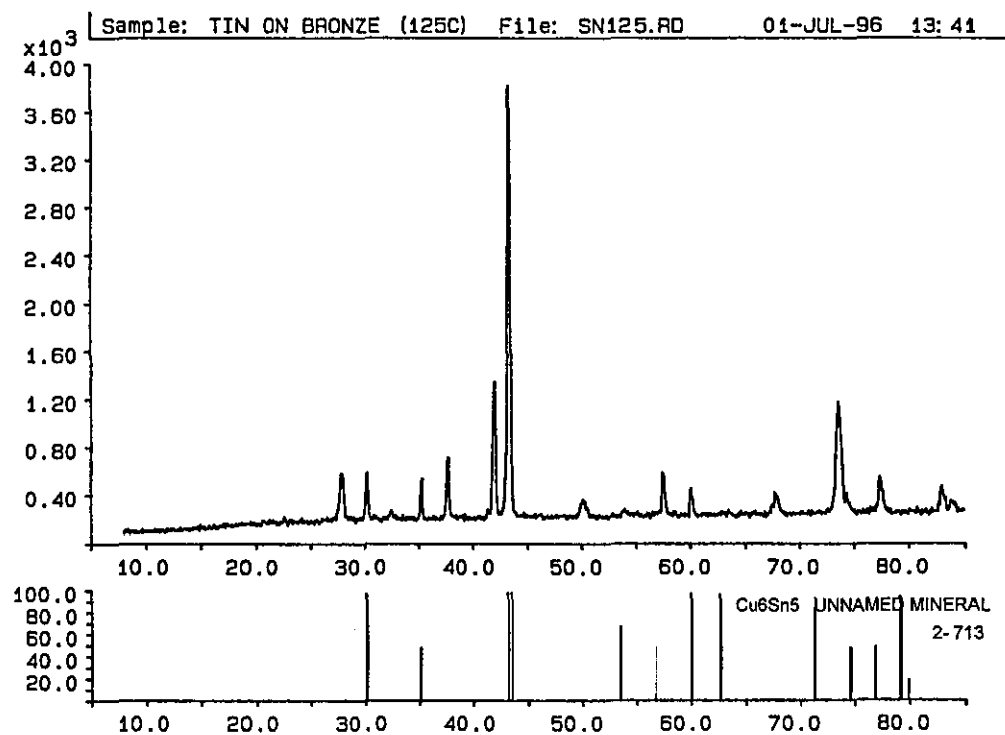


**Fig. 4.32 XRD Trace of Coupon Aged for 2000 hours at 125 °C (Cu anode 45kV, 30mA)**

#### 4.3.4 Copper Diffusion Rate Measurements

From the intensity/time graphs; Fig. 4.33 to 4.35, it can be seen that, within the limitations of the technique, for the coupon aged at 100°C, complete saturation was achieved over the X-ray emission depth after approximately 3000 hrs. ageing. At a temperature of 125°C, saturation occurred at approximately 2250 hrs., whilst at 150°C, transformation to the copper rich phase was complete within 1500 hrs. Using intensities obtained for pure copper and pure tin, the composition for an intensity ratio of 0.34 corresponded to a copper/tin atomic ratio of 3:1, i.e. confirming the conversion to the  $\text{Cu}_3\text{Sn}$  phase as detected by XRD, for the fully saturated tin coating on the coupon aged at 150°C; Fig. 4.30. Over a distance of 1  $\mu\text{m}$  it was calculated that copper diffused to form the  $\text{Cu}_3\text{Sn}$  ( $\epsilon$ ) phase at the rates displayed in Table 4.12 for each annealing temperature.

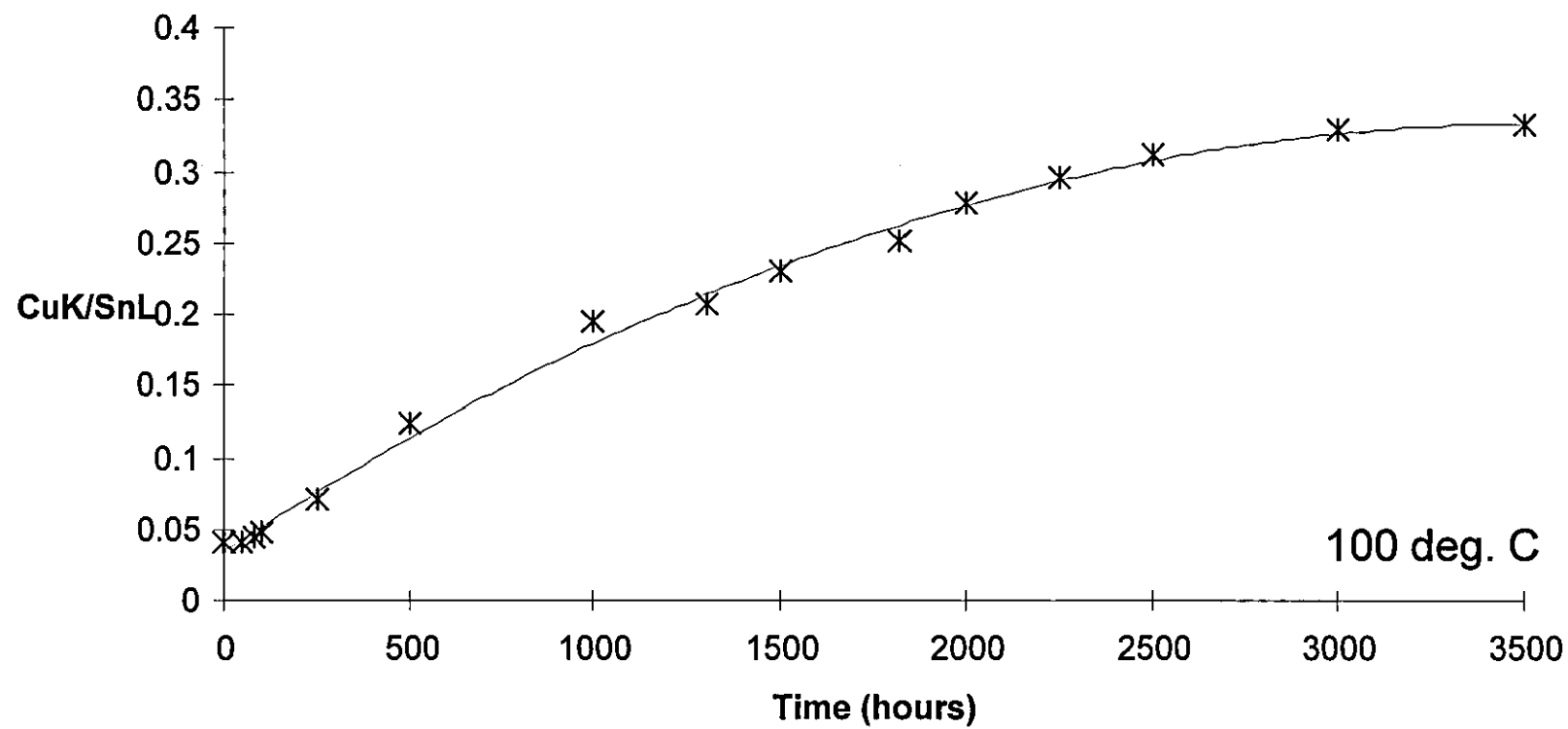


*Fig. 4.33 Diffusion of Copper into Tin Layer at 100°C*

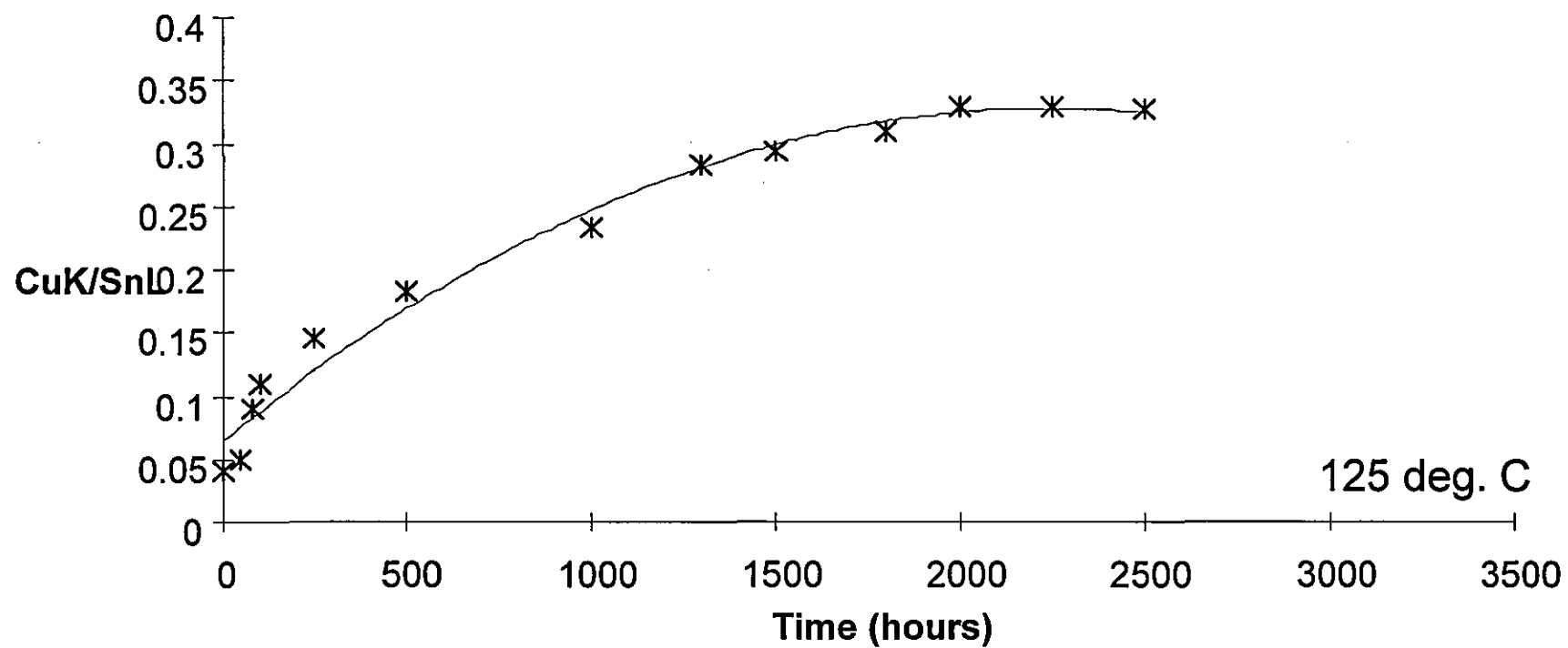


*Fig. 4.34 Diffusion of Copper into Tin Layer at 125°C*

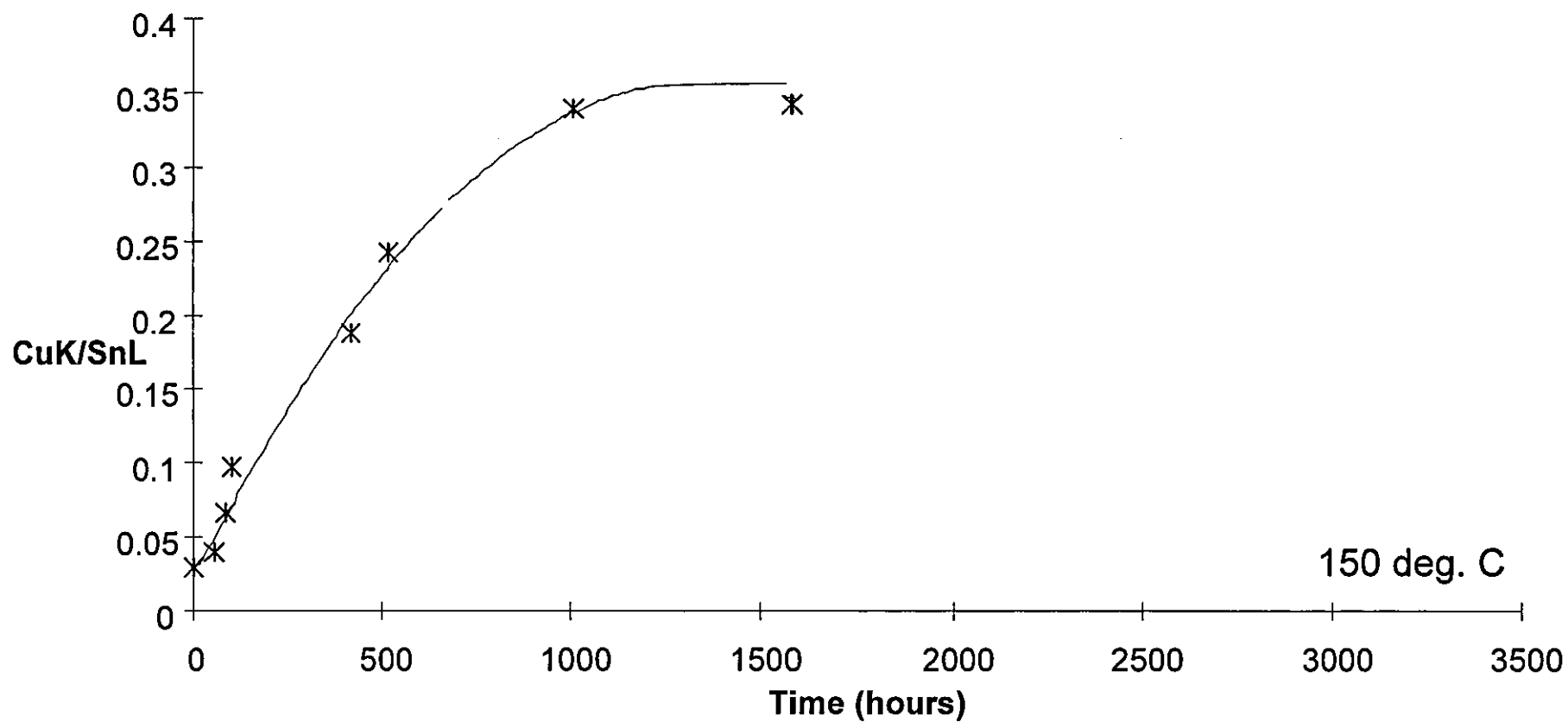


*Fig. 4.35 Diffusion of Copper into Tin Layer at 150°C.*

Annealing Temperature (°C)	Copper Diffusion over 1µm (expressed as µm s <sup>-1</sup> )
100	8.55 X 10 <sup>-8</sup>
125	1.23 X 10 <sup>-7</sup>
150	2.22 X 10 <sup>-7</sup>

Table 4.12 Calculated Diffusion of Copper in Tin to Form the ε Phase over 1µm.

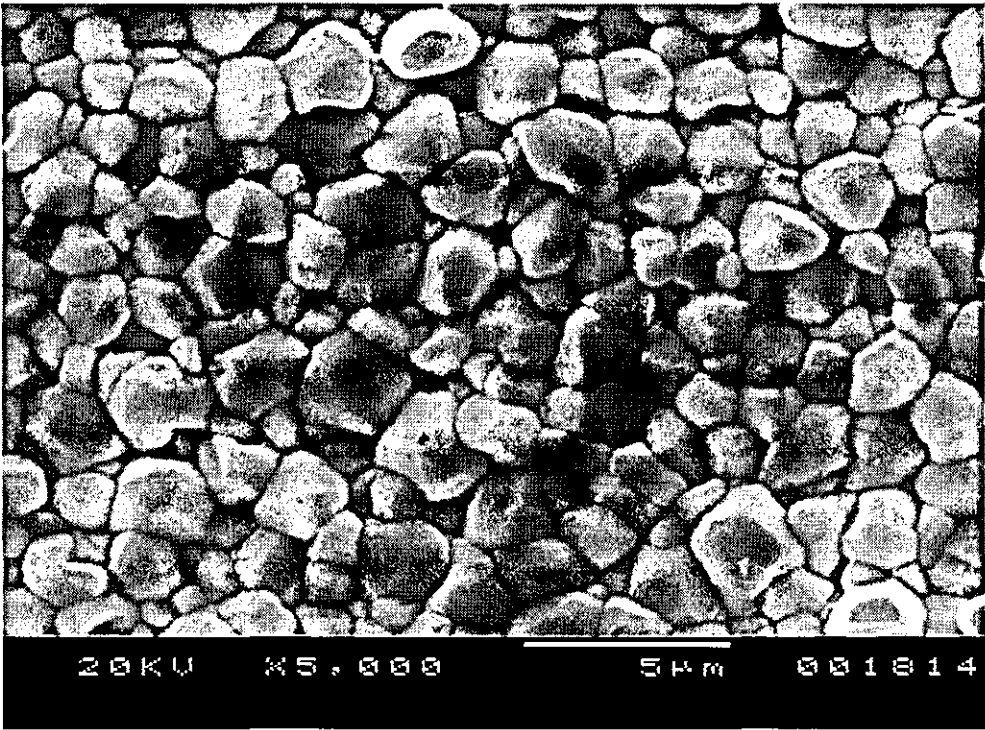


Fig. 4.36 Intermetallics as Formed on Plating from the Melt (Tin Removed by Etching)



### 4.3.5 Intermetallic Morphology

The overlaying tin was etched away in picric/hydrochloric acid to reveal the crystalline structure of the intermetallics. Figure 4.36 is an SEM image showing the intermetallics which are formed from the melt. The grains of the  $\text{Cu}_6\text{Sn}_5$  phase are generally equi-axed ranging in diameter from approximately 1 to  $3\mu\text{m}$ .

Grain Area Determination by Image Analysis ( $\mu\text{m}^2$ ) - SEM Image Fig. 4.36	
Minimum	1.3
Maximum	10.5
Mean	4.5

**Table 4.13 Area Determination of Intermetallic Crystals**

#### *Image Analysis*

The results of an average area analysis using the secondary electron image seen in Fig. 4.36, are shown in Table 4.13. The aspect ratio of the grains suggests that they are generally equiaxial and by taking the average area as  $4.5\mu\text{m}^2$  it could be estimated that the average peak to valley height ( $R_z$ ) was  $\sim 2\mu\text{m}$ .

#### *Surface Profilometry*

Non contact surface profiling was carried out on the as-plated and etched coupon; Fig. 4.37. The resolution of the technique in the XY plane does not allow individual grains to be clearly identified, however, some indication of average peak to valley heights ( $R_z$ ) across the coupon can be obtained. These measurements were taken from a region similar to that shown in Figure 4.36 and are comparable with those obtained from the SEM image. A second scan was performed on a sample which had been aged at  $150^\circ\text{C}$  for 100 hours; Fig. 4.38. The reduction in  $R_z$  although not dramatic over this time period would confirm the grain growth observed from micro-sections.

*Hardness of Intermetallics*

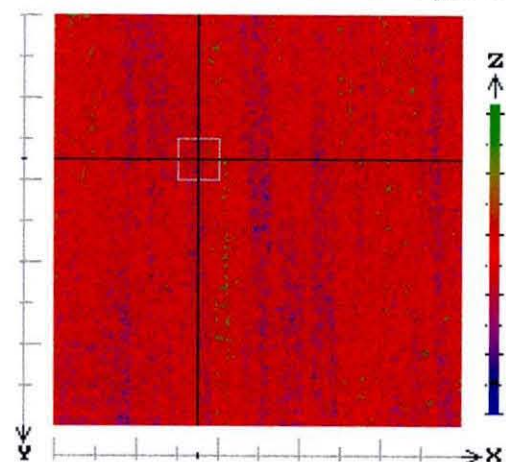
Microhardness determinations of pure tin and the  $\text{Cu}_3\text{Sn}$  phase were  $8 \text{ Kg.mm}^{-2}$  (+/- 1% rel.) and  $390 \text{ Kgmm}^{-2}$  (+/- 2.5% rel.), respectively.

*Corrosion Resistance of Intermetallics*

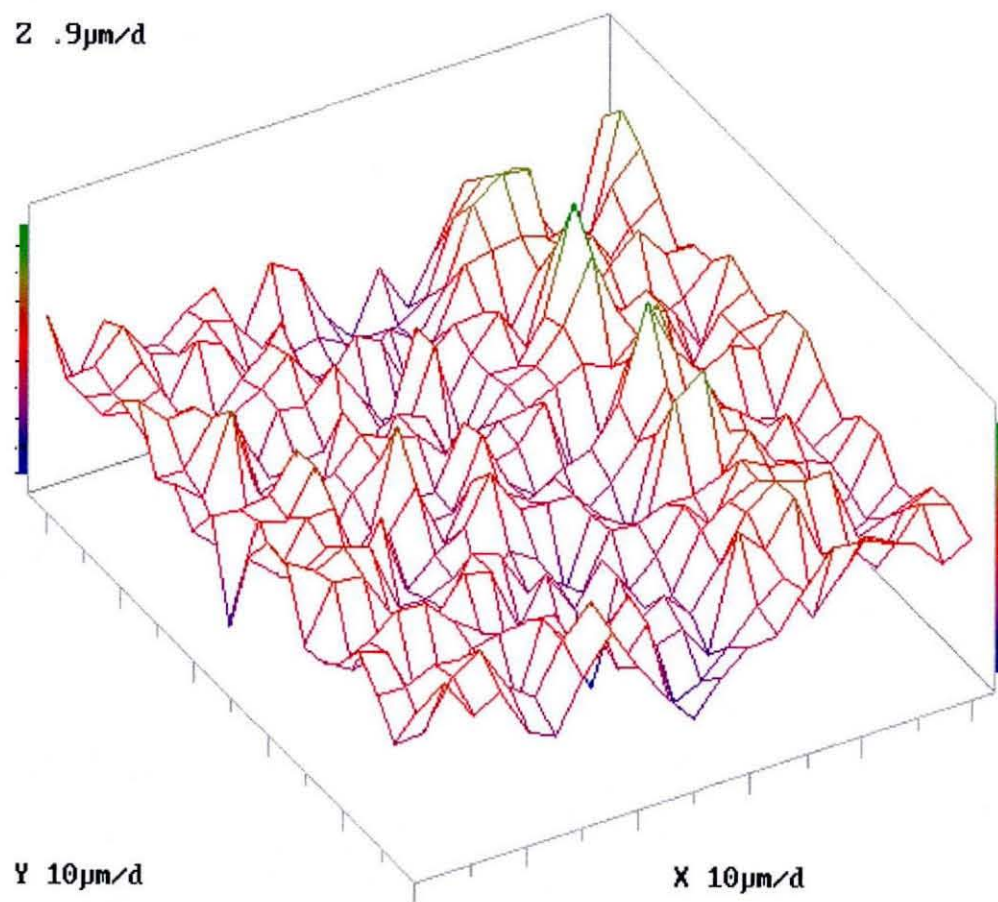
Fister<sup>6</sup> reported that the intermetallic phases were more reactive than pure tin although Britton claimed that they are cathodic to tin. A simple corrosion test was therefore performed by immersion in a 10% aqueous solution of sodium chloride of the as-plated tin strip and a sample which had been fully aged. Figure 4.39 and 4.40 are SEM images of the coupon surfaces showing the appearance of the coatings after immersion for a period of one week, together with the corresponding EDS spectra. It can be seen that there has been significant attack of the tin plate accompanied by oxidation but the  $\text{Cu}_3\text{Sn}$  intermetallic shows little evidence of corrosion, (the surface features in the form of depressions in the surface were as a result of grain growth and existed prior to corrosion testing). There was, however, pitting of the surface of the exposed bronze substrate, indicating that it was anodic to the intermetallic.

It is worthy of note here that although the reactivity cell experiments were designed to evaluate lubricants, subsequent examination of the coupons after testing showed that for highly reactive greases i.e. those which acted as good electrolytes, significant attack of the pure tin at the anode occurred, leaving the intermetallics generally intact; Fig. 4.41.

Y .1mm/d X .1mm/d Z 1 $\mu$ m/d



Z .9 $\mu$ m/d



X-POS 051.350mm Rz 002.97 $\mu$ m



Y-POS 056.050mm Rz 002.03 $\mu$ m



Fig. 4.37 Surface Profile of As plated Coupon (After Removal of Tin to Expose Intermetallics).

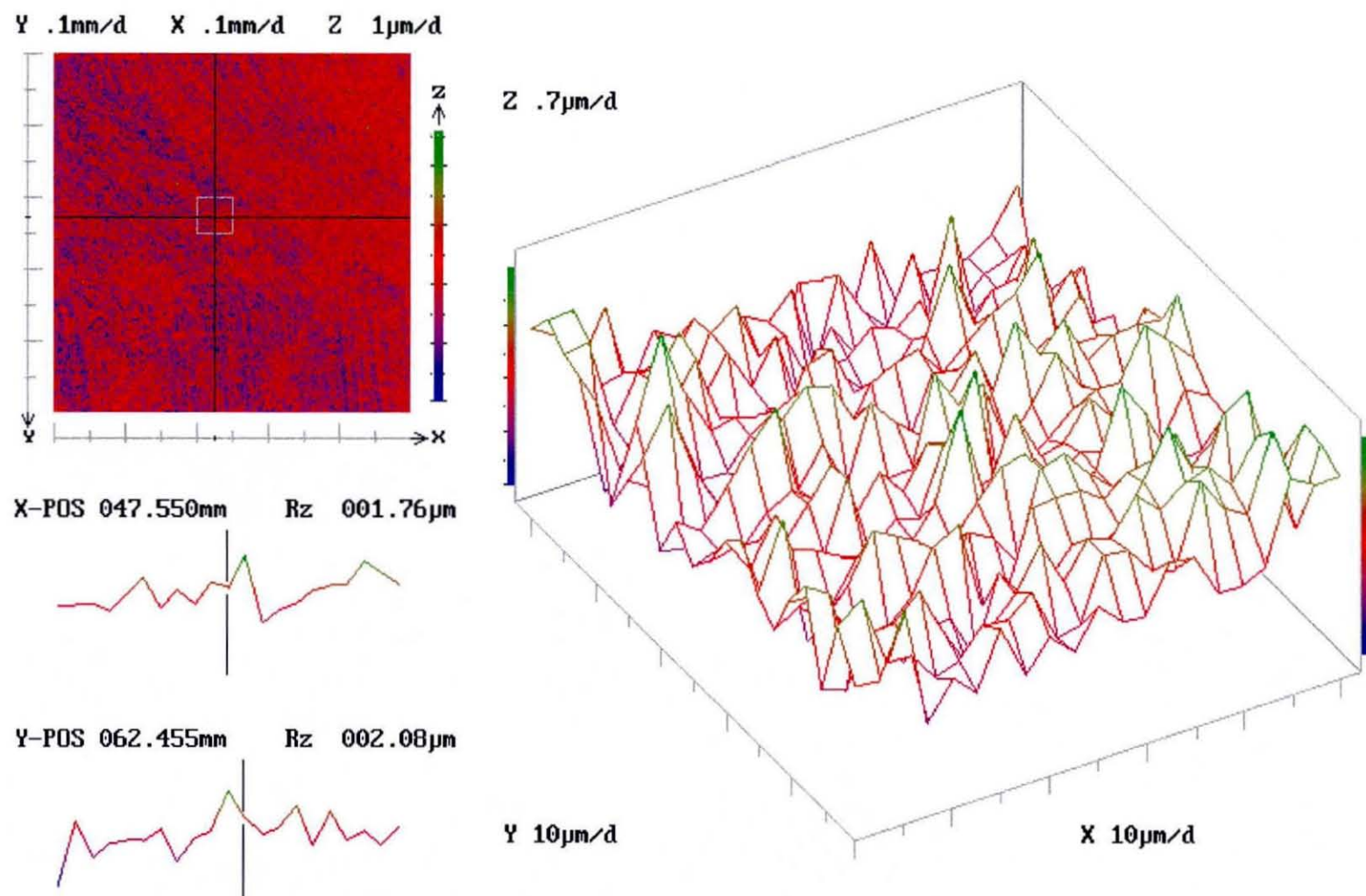
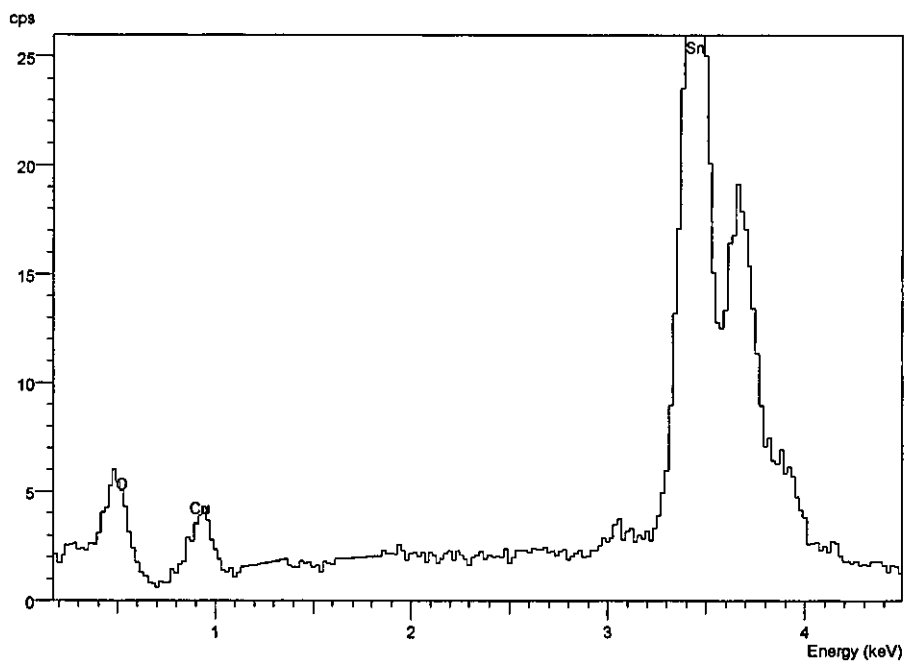
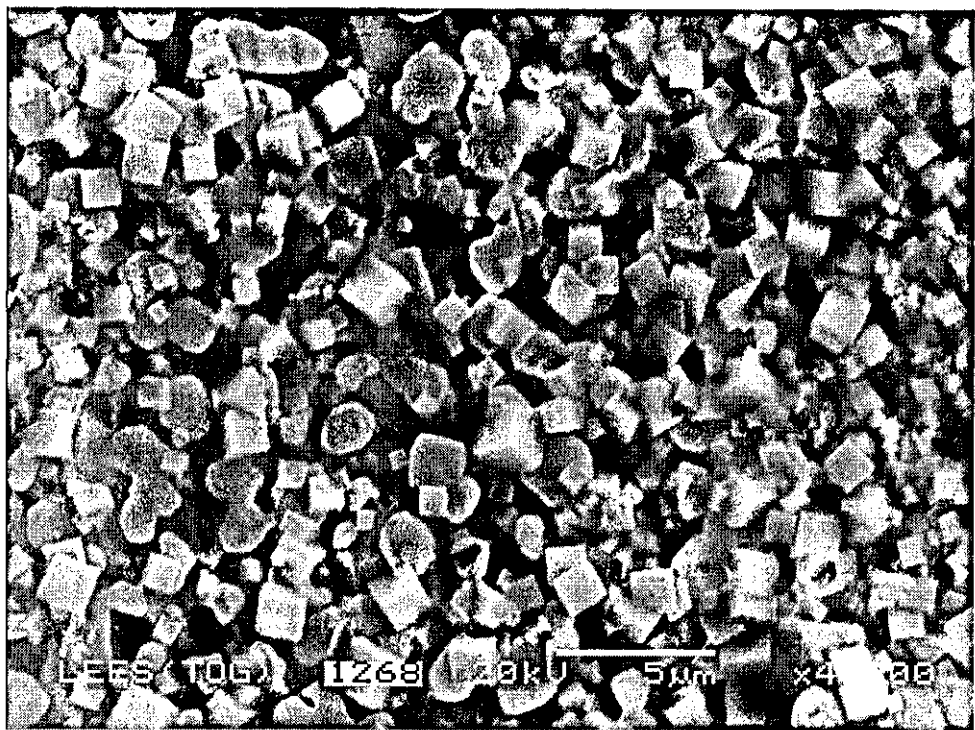
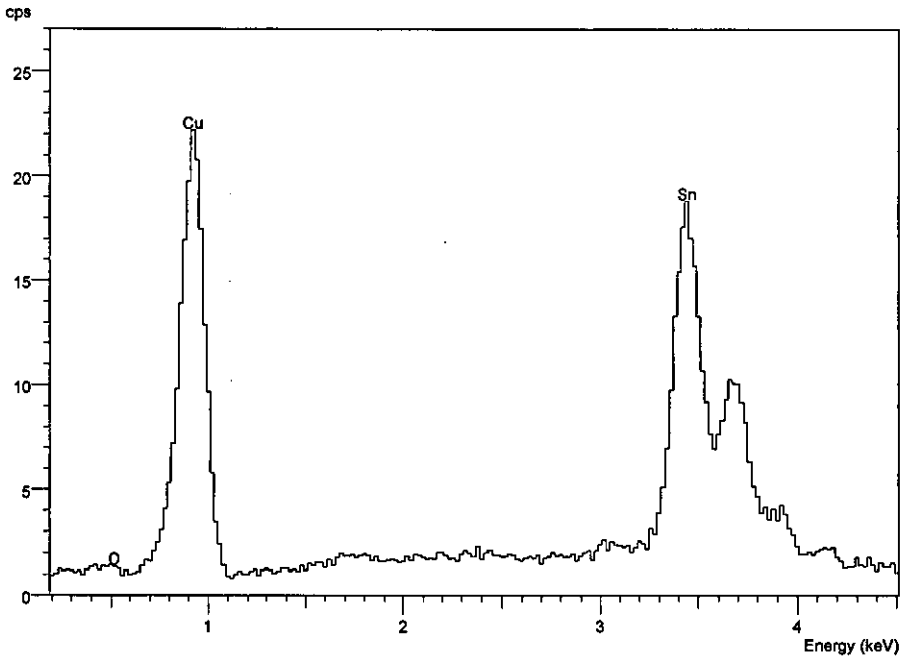
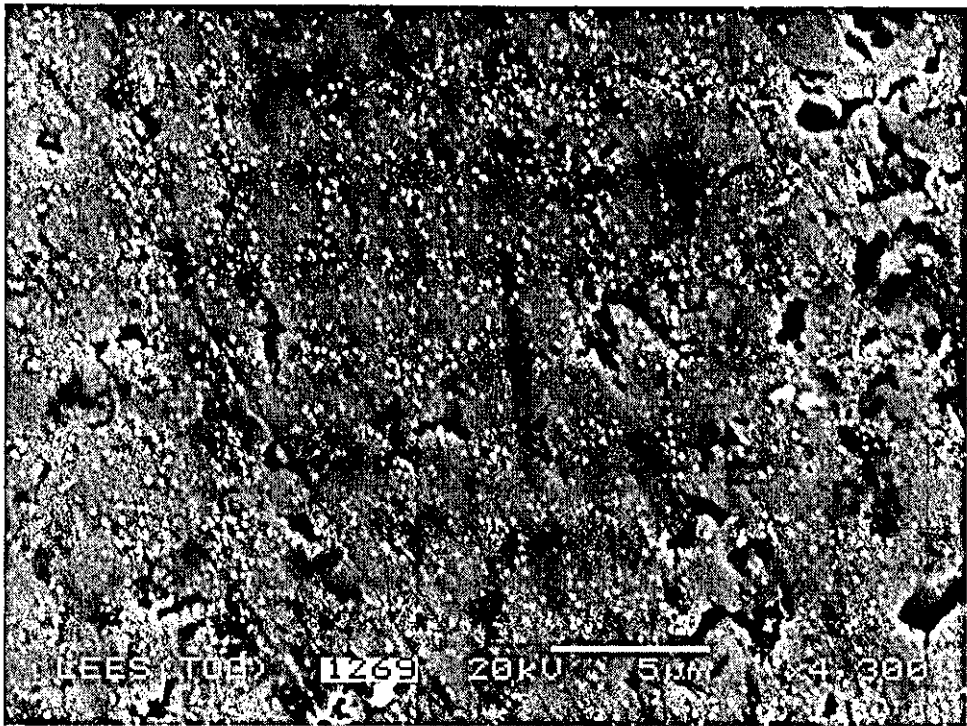


Fig. 4.38 Surface Profile of Coupon Aged for 100 Hrs. at 150°C (After Removal of Tin to Expose Intermetallics).



*Fig. 4.39 Appearance and Composition of Tin Surface After Corrosion Test*



**Fig. 4.40** *Appearance and Composition of Tin/Copper Intermetallics After Corrosion Test.*



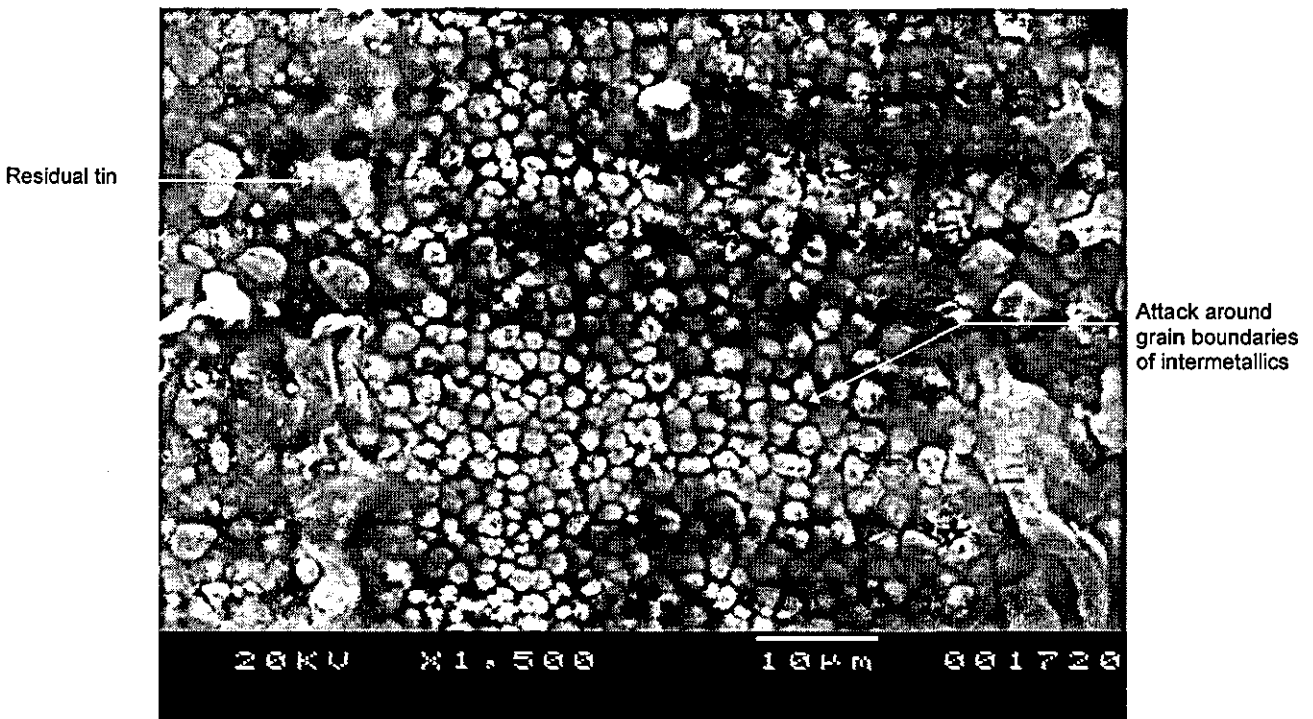


*Fig. 4.41 Anode Surface After Testing With a Reactive Grease*

## 4.4 Fretting Tests

### 4.4.1 Dry Fretting Tests

From a total of ten tests performed on dry (unlubricated) contacts, 50% had failed after 42 hours (21 cycles), with all of the contacts failing within 55 hours. The mean TTF was 48 hours with a standard deviation of  $\pm 6$  hours. This was considered to show a good repeatability given the variable nature of the coating microstructure.

Figure 4.42 shows the appearance of the wear scar of a dry coupon which exhibited open circuit. Softening of the tin at the high temperature end of the cycle has resulted in plastic flow and X-ray mapping for oxygen shows the distribution of oxide across the wear scar transforming the site to a region of high CR. Figure 4.43 is a trace of contact resistance and cycling temperature taken over a period of 40 hours when a contact was undergoing incipient failure. It can be seen that at the 'hot' end of the

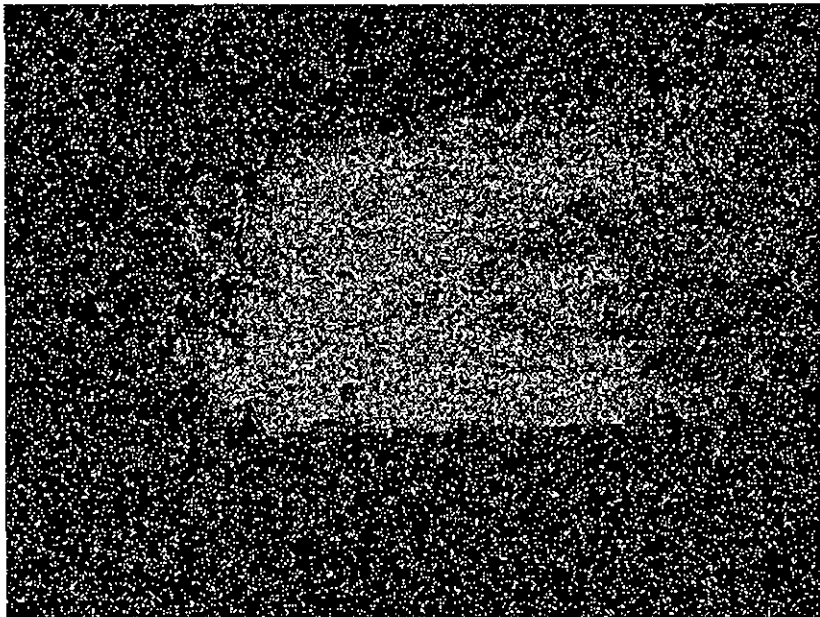
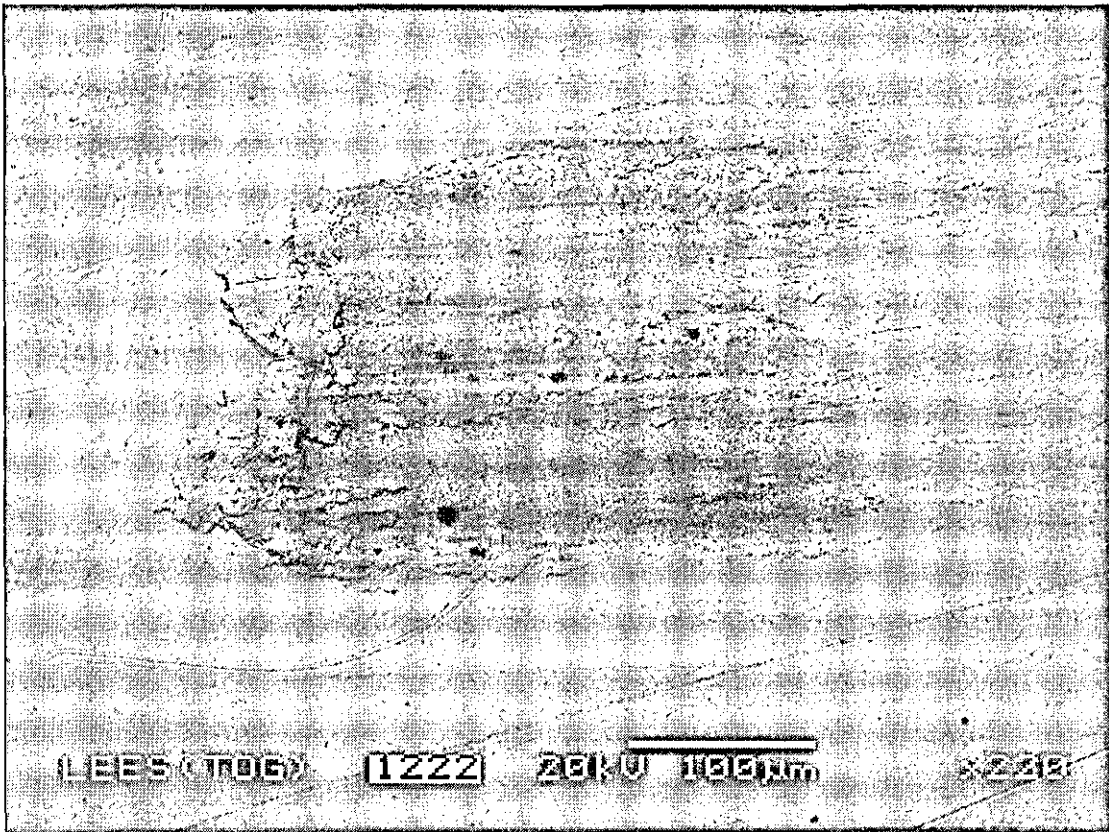
wear scar there is a sustained period of high CR, whilst over the remainder of the cycle there are periods of low CR intermittents. It is also apparent that over this time interval resistive oxide has been transported, deposited and re-deposited to sites along the wear scar.

Several failures showed evidence of grains of intermetallics in the wear scar exposed by the wear process; Fig. 4.44. At low magnification in BSE mode, it could be seen that these corresponded with the lines of subsurface intermetallics observed on the 'as-plated' coupon, Fig. 4.2.

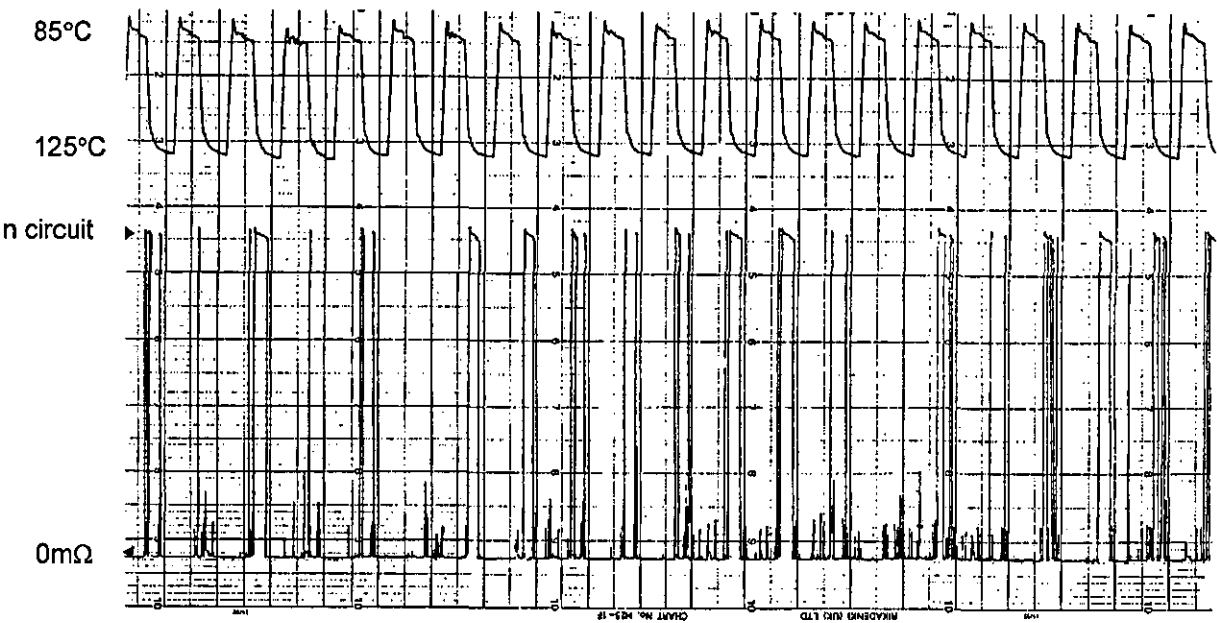
#### **4.4.2 Lubricated Fretting Tests**

Table 4.14 shows the results of the fretting tests of the lubricated contacts with the 'dry' test result for comparison. Figures 4.45 and 4.46 show wear scars from test runs using the mineral oil/lithium soap (MC37) and synthetic hydrocarbon/lithium soap (MR30). These contacts sustained over 1000 hours and 745 hours respectively without failure. There is little oxide formed over the majority of the worn region and the load bearing surface is at this stage of the wear process, the intermetallic. It can be seen from the grey level contrast that much of the overlaying tin has been converted to intermetallic. Figures 4.47 and 4.48 are of lubricated coupons which had low TTF results, MZ30 (187 hrs.) and MF51 (51 hrs.) respectively. Features were similar to the dry contact wear scars with oxide over much of the contact zone.





**Fig. 4.42 Wear Scar After Failure (Unlubricated) with Oxygen X-ray Map (Oxygen Light Regions)**



*Fig. 4.43 Contact Resistance Changes With Temperature Cycling.*

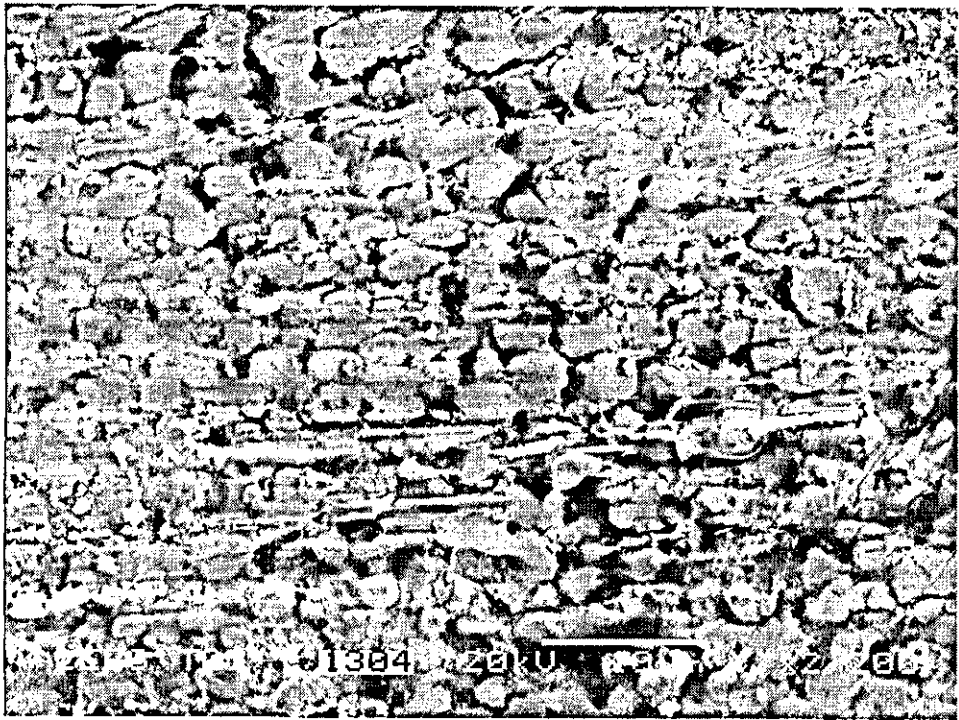


*Fig. 4.44  $\eta$  Phase Intermetallics in Wear Scar Surrounded By Oxide (Dry Fretting)*

Lubricant	Base Oil	Thickening Agent	Fretting Time to Failure (hours)	Lubricant	Base Oil	Thickening Agent	Fretting Time to Failure (hours)
MC10	Mineral Oil	Bentonite	127	MP10	High Temp Ester	Bentonite	133
MC11	Mineral Oil	Bentonite	70	MP11	High Temp Ester	Bentonite	101
MC12	Mineral Oil	Bentonite	89	MP12	High Temp Ester	Bentonite	254
MC13	Mineral Oil	Bentonite	92	MP22	High Temp Ester	Silica	88
MC14	Mineral Oil	Bentonite	68	MP40	High Temp Ester	Soap Complex	174
MC25B	Mineral Oil	Silica	178	MP41	High Temp Ester	Soap Complex	123
MC30	Mineral Oil	Lithium Soap	733	MZ20	PAG	Silica	90
MC32	Mineral Oil	Lithium Soap	587	MZ30	PAG	Lithium Soap	187
MC36	Mineral Oil	Lithium Soap	710	MZ31	PAG	Lithium Soap	186
MC37	Mineral Oil	Lithium Soap	>1000	MG21	PPE	Silica	187
MC41	Mineral Oil	Soap Complex	76	MF20	PFAE	Silica	55
MC42	Mineral Oil	Soap Complex	53	MF24	PFAE	Silica	58
MC45	Mineral Oil	Soap Complex	662	MF51	PFAE	Polymer	51
MR20	Synthetic Hydrocarbon	Silica	57	MF52	PFAE	Polymer	50
MR27	Synthetic Hydrocarbon	Silica	53	MS20	Silicone	Silica	36
MR30	Synthetic Hydrocarbon	Lithium Soap	745	MS30	Silicone	Lithium Soap	53
MR31	Synthetic Hydrocarbon	Lithium Soap	55	MS31	Silicone	Lithium Soap	47
MR32	Synthetic Hydrocarbon	Lithium Soap	84	MS50	Silicone	Polymer	53
MR40	Synthetic Hydrocarbon	Soap Complex	69	DRY TIN			42
MR49	Synthetic Hydrocarbon	Soap Complex	38				

**Table 4.14 Fretting Time To Failure for Lubricated Contacts.**

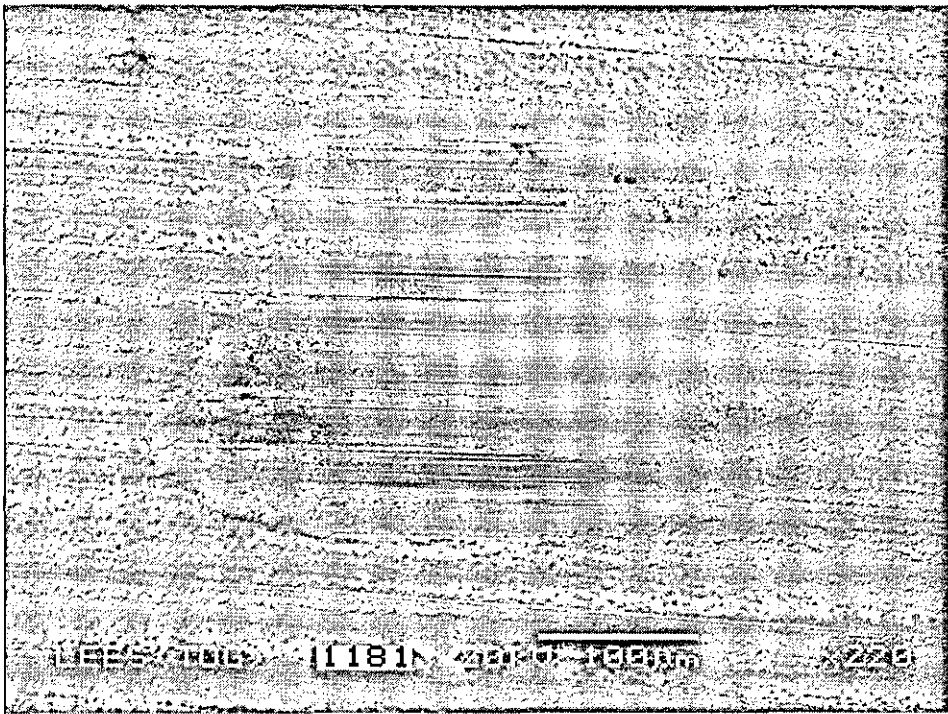


*Fig. 4.45 Wear Scar of Lubricated Coupon (MC37)*

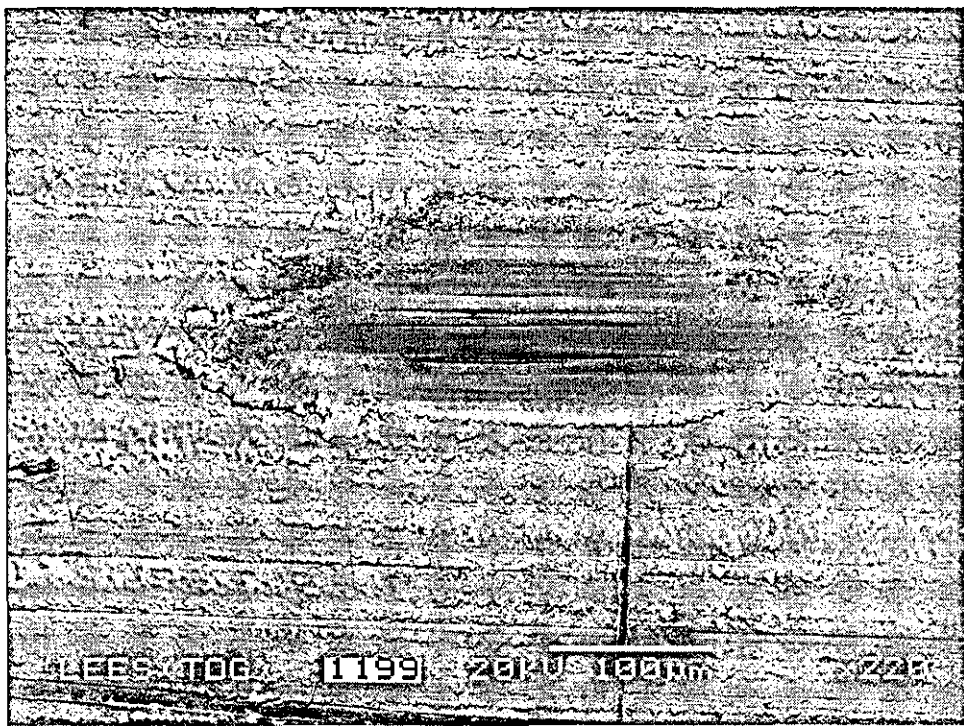


*Fig. 4.46 Wear Scar of Lubricated Coupon (MR30)*

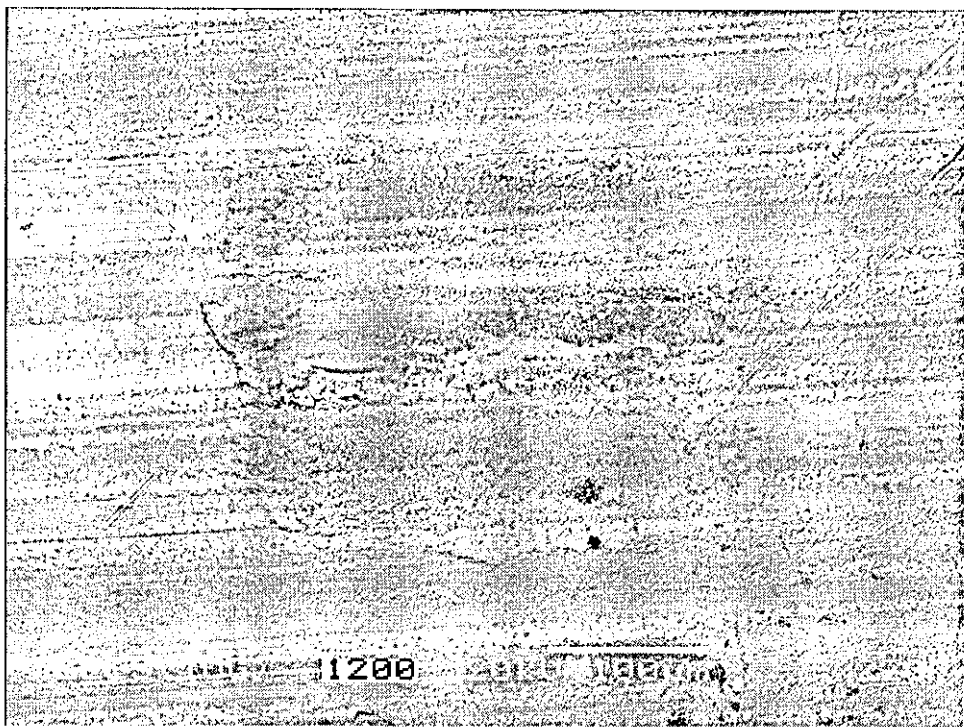


*Fig. 4.47 Wear Scar of Lubricated Coupon (MZ20)*

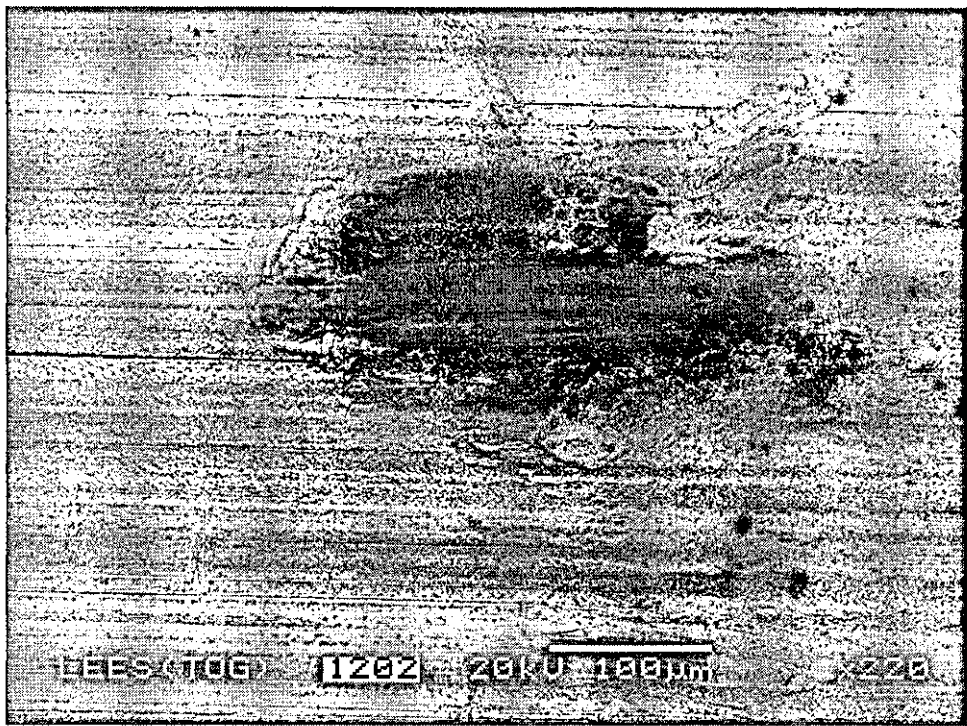


*Fig. 4.48 Wear Scar of Lubricated Coupon (MF51)*

## 4.5 IRAS Analysis of 12-Hydroxystearic Acid Films on Tin

The spectra in Figures 4.50 to 4.53 were obtained from the soap films formed on substrates under various conditions together with a spectrum from the bulk acid. The absorption bands in the  $1800\text{--}3000\text{ cm}^{-1}$  region are known to be due to vibrations of the  $\text{CH}_2$  and  $\text{CH}_3$  groups, where differences in relative intensities are due to molecular orientation effects of the hydrocarbon end of the stearate<sup>7</sup>. The spectra show only small differences, indicating that the molecules show little self-organisation when adsorbed onto the metal surface. The peaks in the  $1500\text{ to }1600\text{ cm}^{-1}$  range, found in all spectra except the bulk stearate, would suggest that there is an absorption frequency shift due to chemical bonding to the substrate. The absorption intensities at these frequencies indicate that there is some degree of chemisorption to the polished tin after 1 hour at  $125^\circ\text{C}$  and to the native oxide layer at room temperature, whilst exposure of the latter to the ageing time/temperature, results in a significant increase in bonding. The chemical bond is probably via the OH group to the oxygen in the oxide layer, rather than the  $\text{C}=\text{O}$ , as illustrated in Figure 4.49.

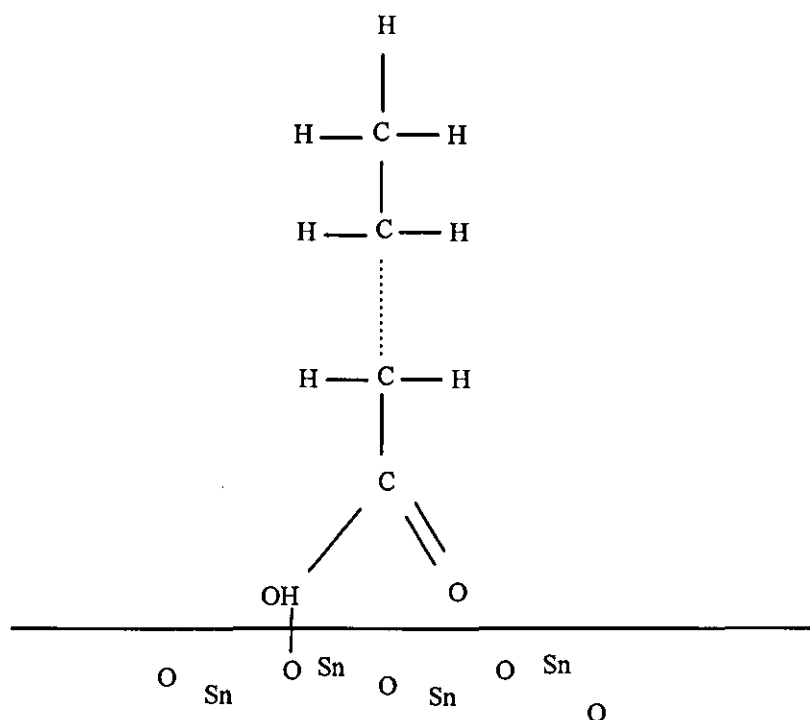


**Fig. 4.49 Chemical Bonding of OH Group to Oxygen in Tin Oxide Layer.**

The degree of wetting can be demonstrated by examination of figures 4.54 and 4.55, which are SEM images of the films taken at low excitation voltage, (2kV), to enhance topographical features. The islands of hydroxystearate on the polished tin indicate a high contact angle, whereas on an oxidised surface there is evidence of greater bonding.



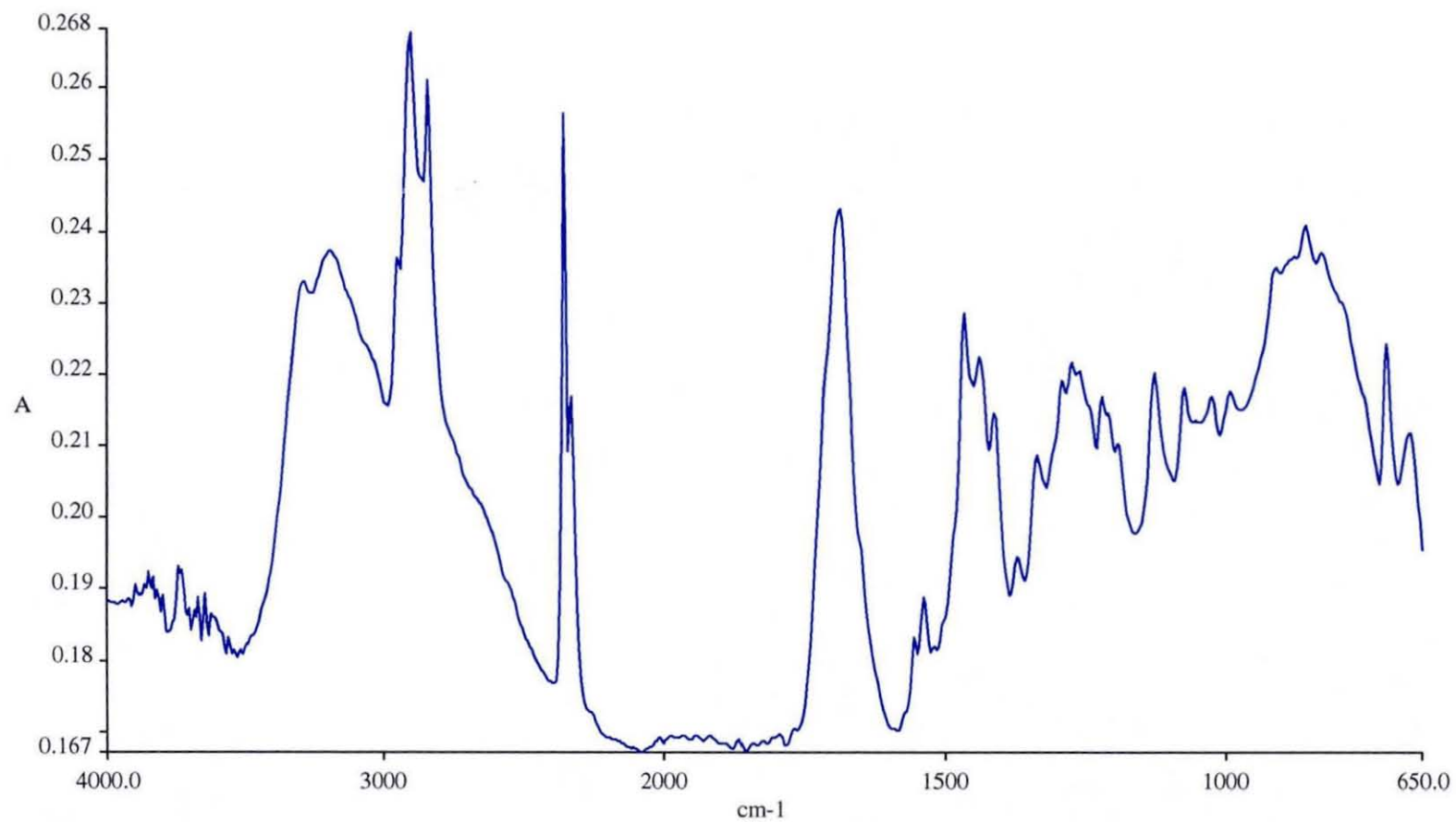


*Fig. 4.50 FTIR Absorption Spectrum of 12 - Hydroxystearic Acid on the Native Oxide Layer of HDT.*



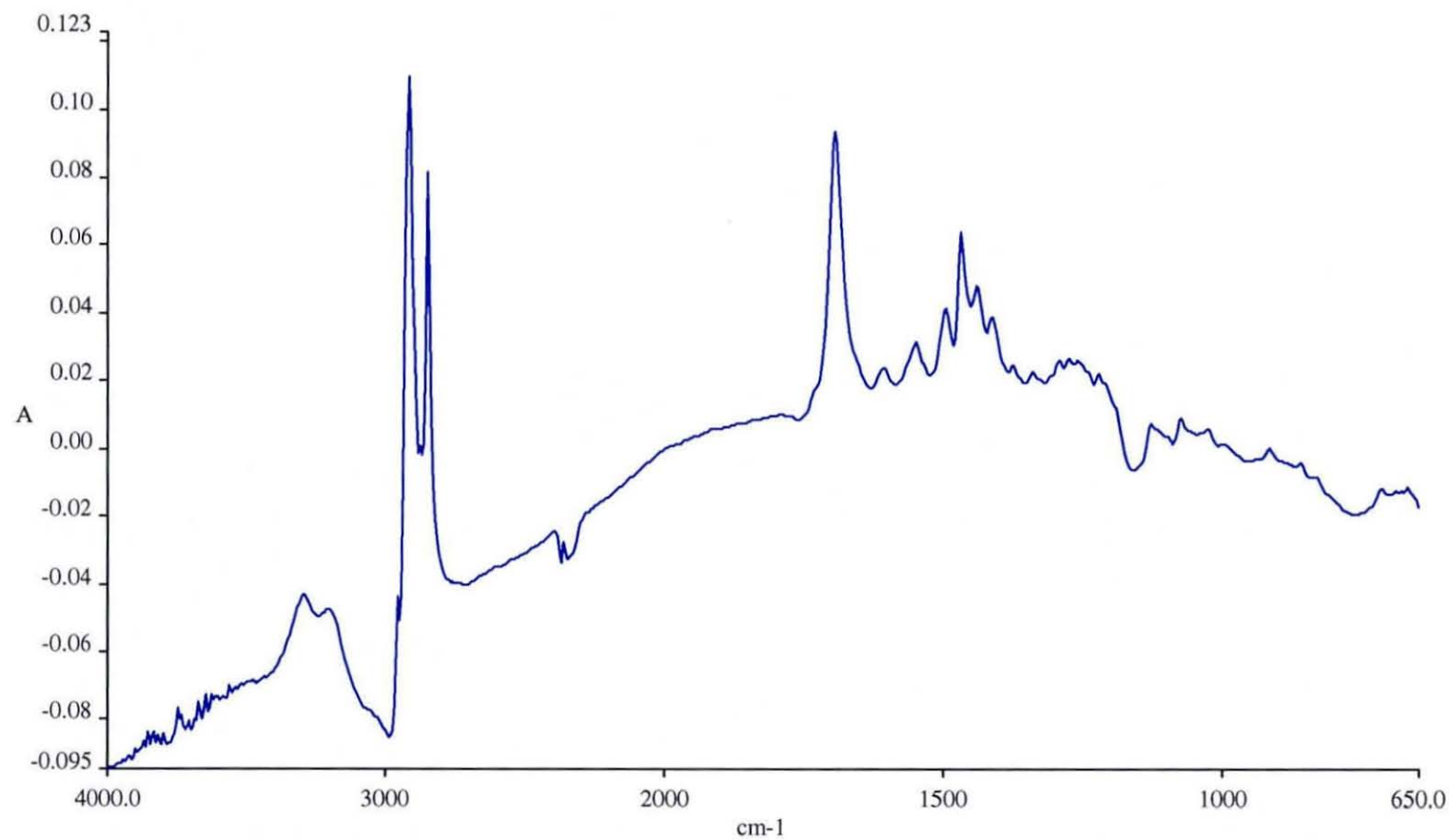


**Fig. 4.51 FTIR Absorption Spectrum of 12 - Hydroxystearic Acid on the Native Tin Oxide layer After Ageing for 1 Hour at 125 °C**

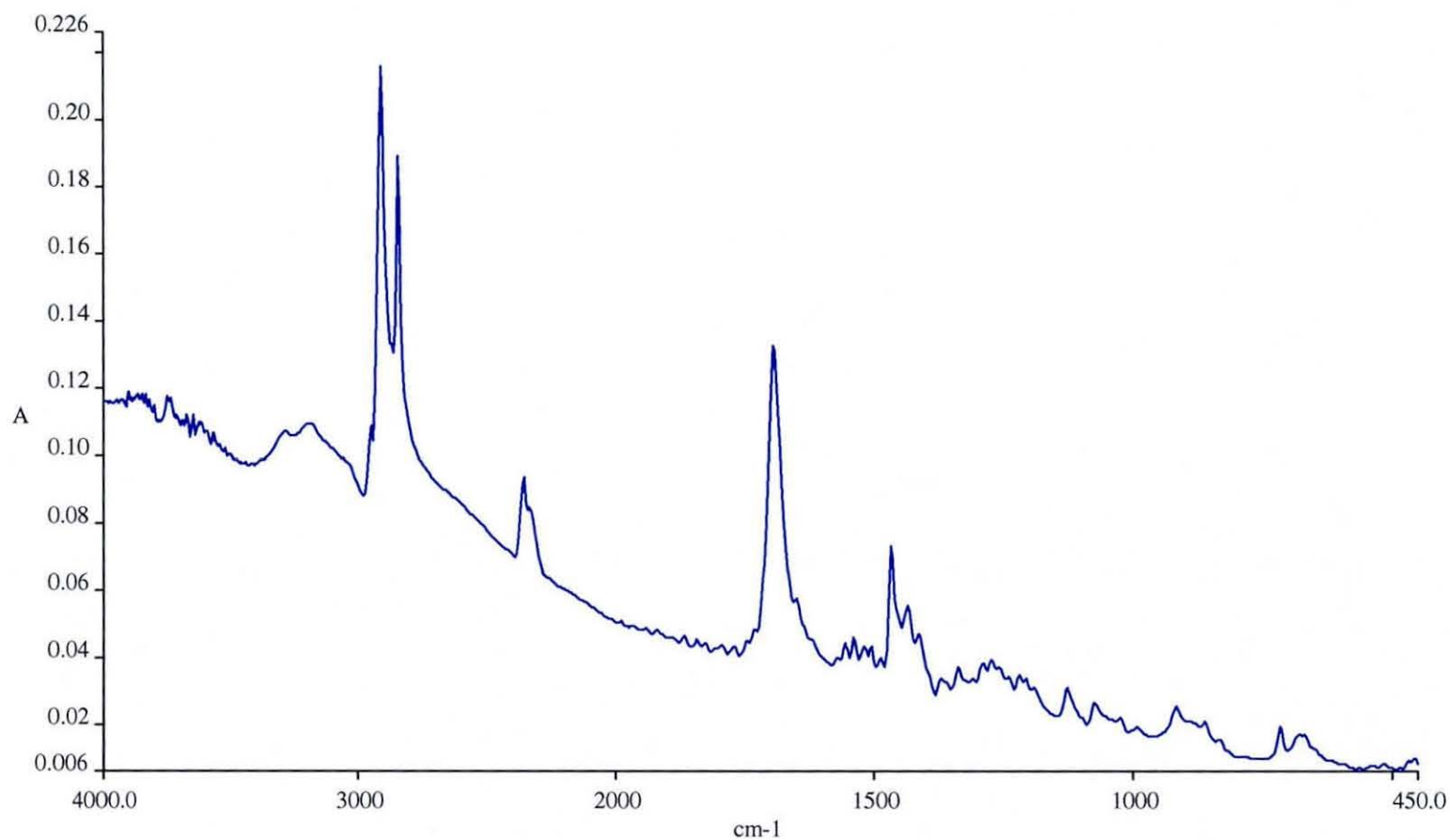


***Fig. 4.52 FTIR Absorption Spectrum of 12 - Hydroxystearic Acid on Polished Tin After Ageing for 1 Hour at 125 °C***

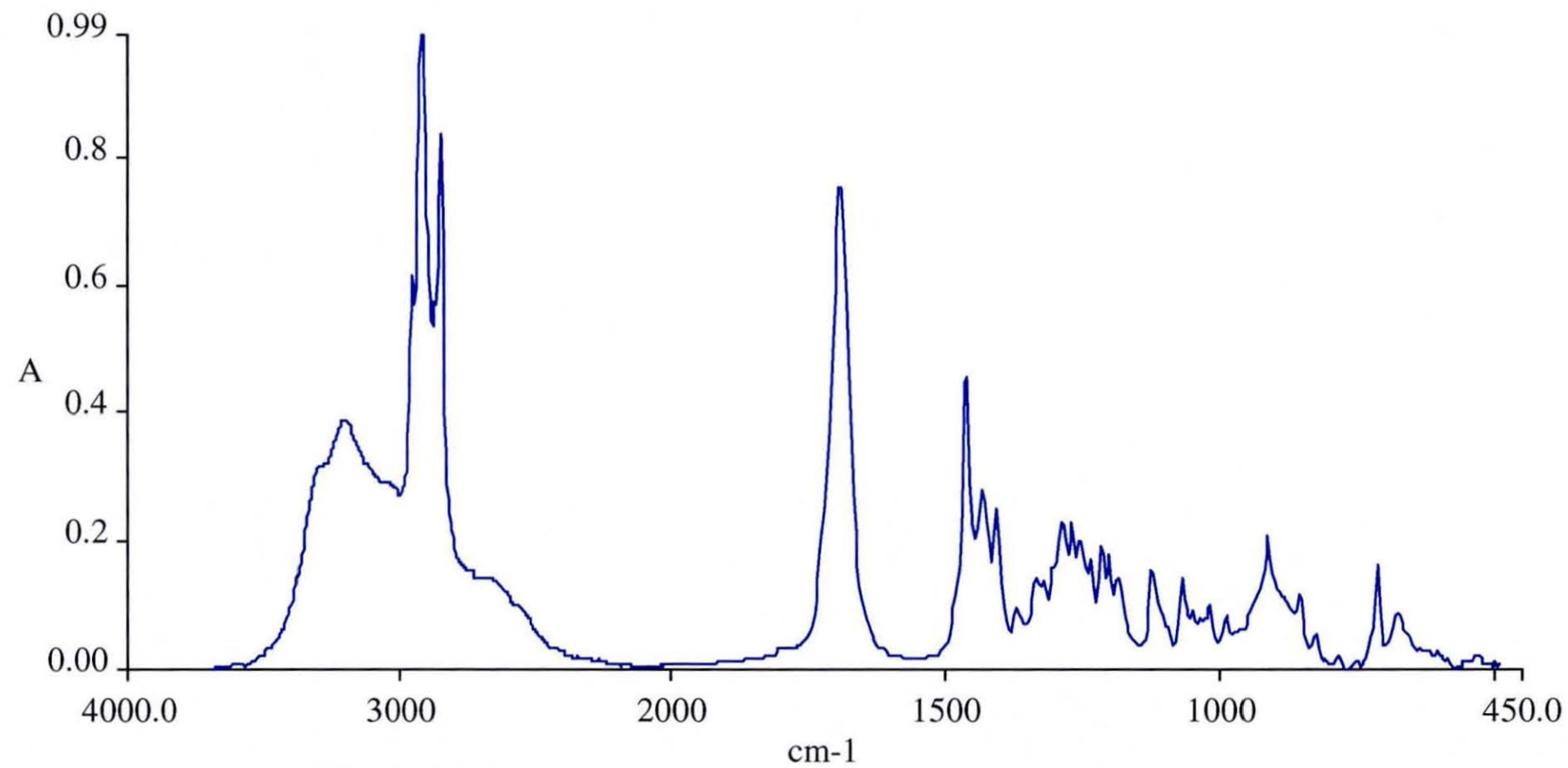


*Fig. 4.53 Bulk 12 - Hydroxystearic Acid*

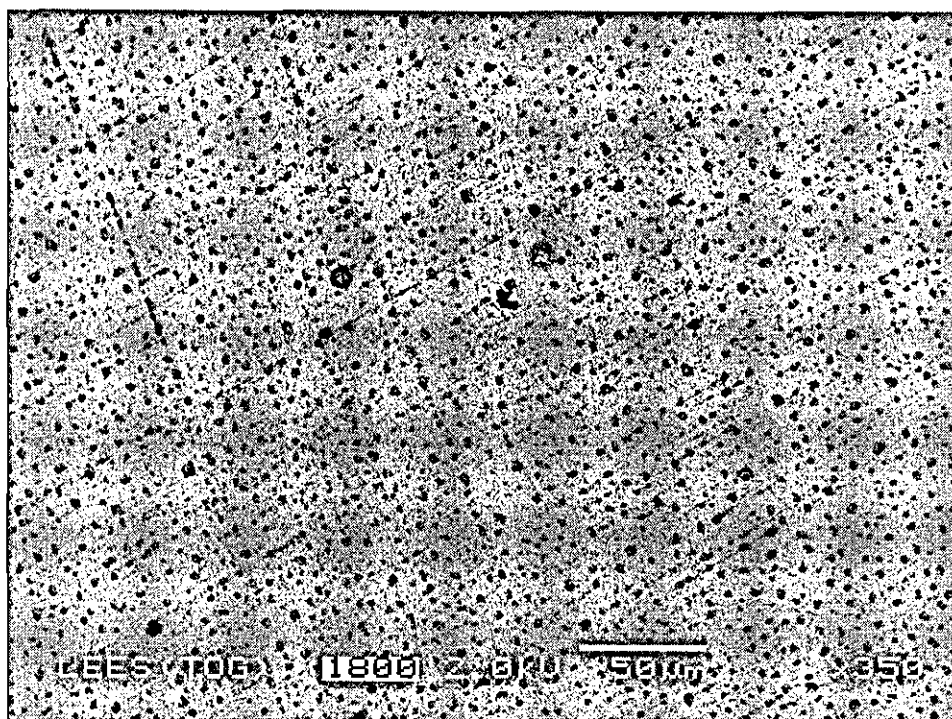


*Fig. 4.54 12 Hydroxystearic Acid on Polished Tin. Aged for 1 Hour at 125°C, Showing Degree of Surface Wetting. (SEM Image at Low kV Excitation).*

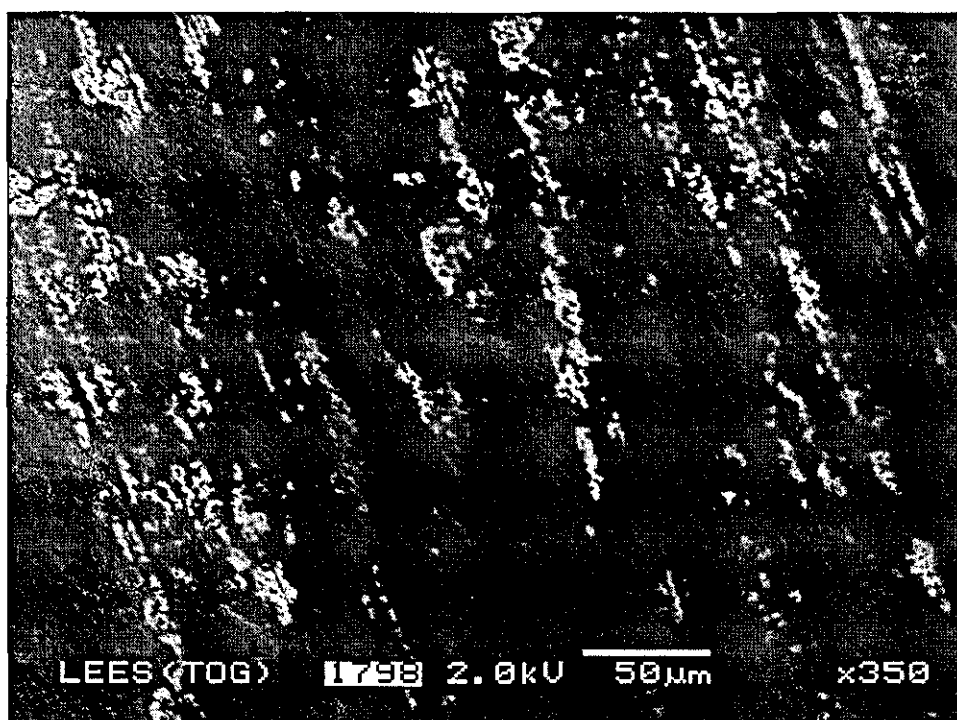


*Fig. 4.55 12 Hydroxystearic Acid on Polished Tin. Aged for 1 Hour at 125°C Showing Degree of Surface Wetting. (SEM Image at Low kV Excitation).*

## 4.6 Discussion

Many studies have approached the fretting corrosion process by using model systems. It is the intention here, however, to advance knowledge of the properties of 'real' as opposed to idealised materials, when subject to this wear regime. Similarly, an investigation into the changes in CR which may occur as a consequence of exposure to actual conditions experienced in service, has been performed. Unfortunately this approach is not without its drawbacks. For example, it could be argued that the variable distribution of tin/copper intermetallics in the tin layer or the presence of an unidentified additive in a lubricant, may dramatically affect fretting corrosion performance and repeatability and, as a consequence, complicate the understanding of the various mechanisms involved. This study is, however, in the author's opinion, intended to be a broadly based investigation into the fretting corrosion phenomenon, where the results will possibly pose more questions than supply answers. It is therefore to be regarded as a precursor to further focused studies.

Firstly the results of the various environmental tests which have been performed on the selected materials are examined. Such tests have modified the contact surface causing oxidation/corrosion with subsequent effects on CR and introduced microstructural changes to the coating during ageing. The discussion then focuses on the contact wear scar, which for separable connectors is invariably the site of failure and describes the wear mechanism involved in its formation. The results of fretting corrosion tests are in turn analysed and any trends relating the lubricants' reactivity properties, to fretting performance are identified and discussed. Finally the discussion ends with a proposal for a novel means of improving contact reliability by using the intermetallics as a wear resistant coating.

### 4.6.1 Degradation of the Contact

The tin layer, formed from the melt, was found to have a significant surface roughness due, in part, to intermetallics which are known to grow at the tin/substrate interface as a result of the particular processing route employed. The total CR of 2.1 m $\Omega$ ,

measured for the as-plated condition, was proportional to the real contact area, which was influenced by the underlying intermetallics and the interfacial film of oxides and hydrocarbons which had formed or had been deposited on the surface. In addition, compositional analysis of the surface layers also detected zinc which was thought to be present as an impurity and had migrated towards the coating surface and oxidised, contributing to the measured, CR. A total film thickness of less than 20nm was measured from the AES depth profile. The thickness of such insulating or semiconductor films would allow charge transfer by electron tunnelling<sup>8</sup>.

Tin oxide was probably present in the bivalent state ( $\text{SnO}$ ), being formed whilst cooling from the melt. Within the sampling depth of XPS, there appeared to be a conversion to the quadrivalent stannous oxide ( $\text{SnO}_2$ ), at the air/oxide interface. From the oxygen concentrations profiles determined by AES, a correlation was found between oxide thickness and CR. This enabled the construction of a CR v thickness plot for use in estimating dimensions for the environmentally tested samples, Figs. 4.56 to 4.58.

It is assumed that conduction through the films is linear, as measured here by the standard method for CR determinations. If a more valid characterisation of the contact is required, it would be necessary to use the equivalent electrical circuit and analyse the current-voltage characteristics (I-V), of the contact point.

From the laboratory corrosion tests it was found that tin was comparable with other common connector coatings, showing relatively small increases in CR as a consequence of exposure to the hydrogen sulphide and water vapour environments. The conditions for the salt spray test, however, were considered to be too severe as an accelerated test. This was particularly evident when comparing the condition of the coupons and their CR measurements of the tested samples, to the relatively low degree of chloride reaction products found on the surface of the field samples and their relatively low CR.

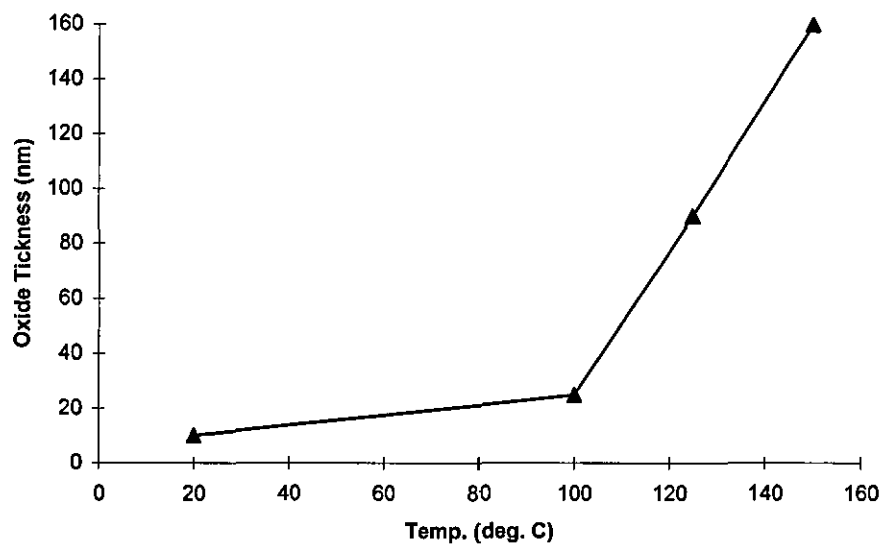


*Fig. 4.56 Oxide Thickness as a Function of Temperature*

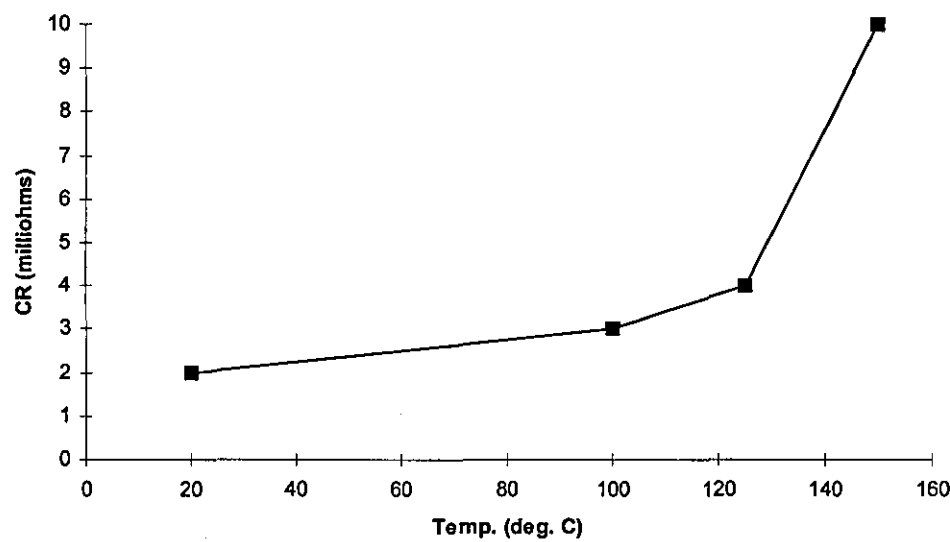


*Fig. 4.57 Contact Resistance as a Function of Temperature*

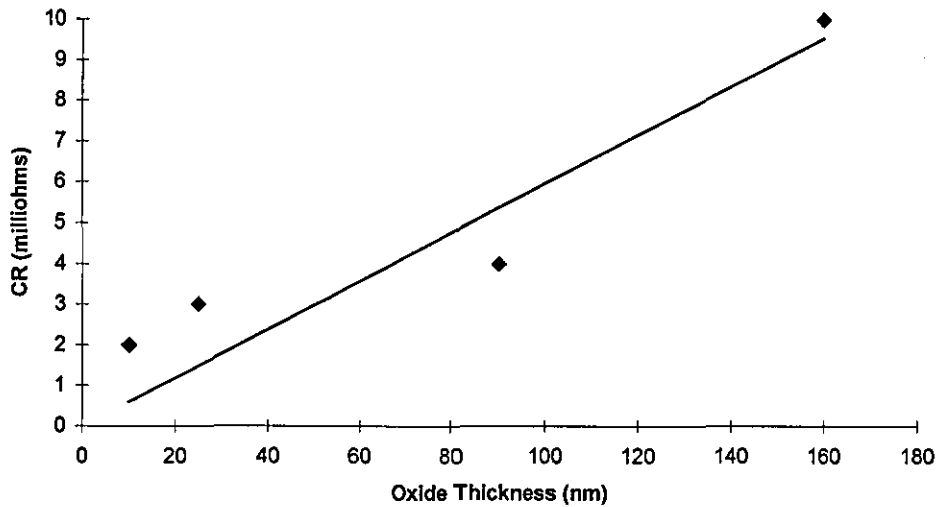


**Fig. 4.58** *Contact Resistance as a Function of Oxide Thickness*

The coupons which had been exposed to field environments for up to approximately  $15 \times 10^3$  hours, showed that the relatively benign atmosphere of all passenger compartments of vehicles operating in the three regions was, as expected, responsible for the low CR, being comparable to the measurements following the 1000 hour humidity test. Generally, the higher temperature conditions existing in the engine bays resulted, for the most part, in correspondingly higher measurements. It is somewhat surprising, however, that two of the three coupons in engine bays of vehicles operating in rural areas, where atmospheric pollution would be expected to be least, showed a higher CR. A possible explanation is that the engine bay design of the particular vehicle is such that higher ambients are achieved and maintained resulting in a thicker oxide growth. The high resistances measured on coupons exposed to the conditions in the engine compartments of the heavy vehicles were similarly thought to be due to the high temperatures experienced during the two year exposure period promoting significant oxide growth.

XPS analysis showed no dramatic surface compositional differences when compared with the as-plated condition, apart from the presence of small amounts of chlorine and sulphur. The low concentrations of these elements restricted the identification of their



valence states but it is likely that they were in the form of chloride and sulphide ions. It is probable that the high carbon levels as seen by SEM, were in the form of organic deposits whose presence reduced the apparent concentration of the other elements on the metal surface when measured by XPS, as the technique is sensitive to only the topmost few nanometres. This restriction on sampling depth made XPS limited in its value as a method for determining surface compositional changes and, as a consequence AES depth profiling proved superior.

The results of the AES analysis on a coupon which exhibited high contact resistance, showed a significant oxide growth over the two year period, reaching a thickness of ~150nm. It was concluded that oxygen was almost certainly present as stannic oxide and was comparable with the growth achieved on the test coupon subjected to 150°C for 2000 hours in the laboratory atmosphere. Carbon was found to have increased over the exposure time but only to a depth of ~25nm, whilst sulphur was restricted to the first few atomic layers. It is therefore less likely that their presence influenced the resistance measurements to any great degree. If it is assumed that the vehicle which housed the field test coupon (12) operated at an average speed of 50 Km.h<sup>-1</sup>, this would result in a total engine running time of at least 4660 hours. Over this period copper diffusion had taken place, with the element being detected to within 100 nm of the tin surface. The low concentration of copper, however, would suggest that the coupon had been exposed to ambients of less than 100°C over the two year period.

It can be concluded that in the vehicle passenger and engine compartments the major influence on static contact resistance was oxide growth, being significant under-bonnet, where temperatures are high but where a high oxide growth rate becomes critical in increasing low cycle fretting corrosion failure.

#### **4.6.2 Intermetallic Formation**

Analysis of the thermally aged coupons by the various techniques was able to confirm that interdiffusion between the copper alloy and the thin tin coating resulted in the  $\epsilon$  phase forming at the substrate/intermetallic interface and the  $\eta$  phase at the

intermetallic/tin interface, with final full conversion of the pure tin to  $\text{Cu}_3\text{Sn}$ . The presence of the unidentifiable phase(s) as determined by XRD in the coupon aged at  $125^\circ\text{C}$ , would, however, require further study. The AES depth profile of the sample aged for 2000 hours at  $100^\circ\text{C}$  is interesting as it may confirm the results of Revay<sup>9</sup>, namely that below  $120^\circ\text{C}$  grain boundary diffusion is the dominant mechanism.

The dimensions of the thin tin coating ( $\sim 2\mu\text{m}$ ) and the non-uniform thickness of the underlying intermetallics presented a major problem to overcome in determining accurately the rate of copper diffusion. Micro-sectioning, the method used by other workers, would almost certainly have resulted in poor repeatability and accuracy. AES depth profiling, although having high sensitivity, analyses over an area of only  $150\mu\text{m}^2$  and would thus have required a significant number of sampling sites to be statistically reliable. The Volume Saturation Method, however, was able to measure the change in copper concentration within the excitation volume, over a number of relatively large areas of the coating. This reduced measurement uncertainties due to variations in tin and intermetallic thicknesses.

The results of diffusion studies reported in the literature by other workers have been obtained from micro-sections using grey level contrast from SEM back-scattered electron images, optical measurements from etched specimens giving phase delineation, or from EDS linescans. With the exception of the latter, these techniques determine the intermetallic growth rate rather than the copper diffusion rate, as they are not sensitive to the small changes in copper concentration resulting from short circuit diffusion via structural defects such as grain boundaries and/or dislocations. Therefore, comparisons with results obtained by other workers should be made with caution, as using the Volume Saturation Method can only determine the growth of the copper-rich phase and tends to result in an apparently slower rate. This is particularly significant for ageing temperatures less than  $120^\circ\text{C}$ , when there is a long period over which copper is detected due to short circuit diffusion, followed by the slow movement of the  $\text{Cu}_6\text{Sn}_5$  and  $\text{Cu}_3\text{Sn}$  intermetallic front.

As discussed in the *Literature Review*, the wide spread of the published results is probably due, in part, to the varied metallurgical history and composition of the platings and also to the poor repeatability which would be expected with the techniques used. The diffusion time to convert a 1  $\mu\text{m}$  thick layer of pure tin to  $\text{Cu}_3\text{Sn}$  at 150°C, as measured here was ~1250 hours, giving a diffusion rate of  $2.22 \times 10^{-7} \mu\text{ms}^{-1}$  which is of the same order as the mean of Dabritz and Geckle's results; see Table 2.2.

From the experimental results generated, Table 4.15, an activation energy ( $Q = 25.2\text{KJmol}^{-1}$ ) and frequency factor, ( $D_0 = 2.75 \times 10^{-15} \text{cm}^2\text{s}^{-1}$ ) have been determined, using the Arrhenius equation:

$$D = D_0 \exp^{(-Q/RT)} \quad (2.5)$$

Temp. (K)	D ( $\text{cm}^2\text{s}^{-1}$ )	1/T ( $\text{K}^{-1}$ )	Log <sub>10</sub> D
373	$8.55 \times 10^{-16}$	$2.68 \times 10^{-3}$	-15.07
398	$1.39 \times 10^{-15}$	$2.51 \times 10^{-3}$	-14.86
423	$2.22 \times 10^{-15}$	$2.36 \times 10^{-3}$	-14.65

**Table 4.15 Results of Diffusion Measurements Obtained from the EDS Volume Saturation Method Used to Determine  $Q$  and  $D_0$ .**

The linear plot, Fig. 4.59, suggests a single activation energy over the temperature range rather than two, as would be expected if there had been a significant sudden change from short circuit to volume diffusion.

The activation energy is the same as that obtained by Braunovic<sup>10</sup> but less than that reported by Tan<sup>11</sup> of  $80\text{KJmol}^{-1}$ . Tan suggests a figure of approximately  $10^{-10} \text{cm}^2\text{s}^{-1}$  for  $D_0$ . Braunovic does not quote a frequency factor but from his results a  $D_0$  of approximately  $10^{-6} \text{cm}^2\text{s}^{-1}$  can be calculated. It must be remembered, however, that he

measured the growth rate of the  $\text{Cu}_6\text{Sn}_5$  phase which is considerably faster than that of the copper rich  $\epsilon$  phase.

When attempting to estimate the measurement uncertainty of the technique, the major sources of error will be from the non-uniformity of the microstructure of the plating and the difficulty in determining accurately the saturation time ( $T_{\text{sat}}$ ). In this study measurements were made for only three annealing temperatures, with a limited range of only  $50^\circ\text{C}$ . As the materials used here were of standard production quality, the homogeneity of the tin was, in this experiment, uncontrollable but for future evaluation of the technique it would be necessary to prepare coatings with uniform thickness and homogeneity. For tin it is difficult to extend the heat treatment temperature range due to the low melting point of tin ( $231.8^\circ\text{C}$ ), particularly when only volume diffusivity alone is required to be determined, as temperatures must be in excess of  $120^\circ\text{C}$ .

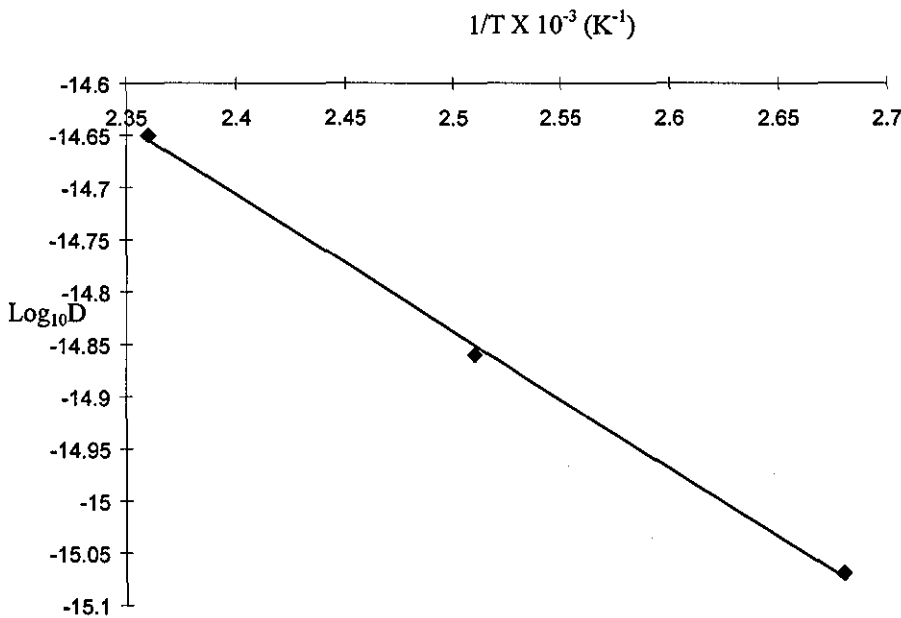
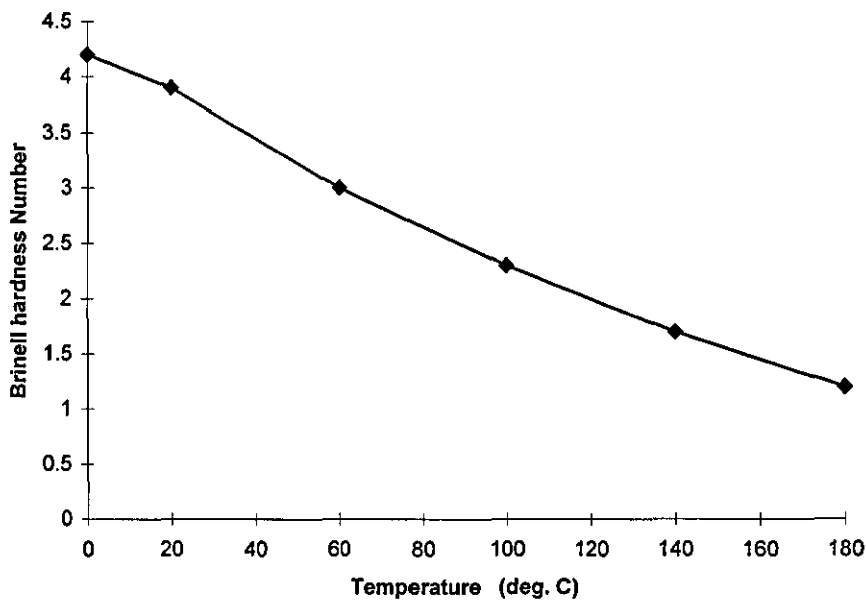


**Fig. 4.59** Experimental Diffusion Data Plotted to Obtain the Activation Energy ( $Q$ ) and Frequency Factor  $D_0$ .

### 4.6.3 Fretting Corrosion

In the *Literature Review* it has been shown that the fretting wear process is influenced by a large number of factors. Many of these variables have, as far as possible, been minimised or eliminated for the fretting tests carried out in this study. They have essentially been reduced to the effects of wear rate, debris generation and oxidation, intermetallic growth and lubrication.

It has been shown that for a typical dry couple, the static contact resistance is minimal, being less than  $2\text{m}\Omega$ . The EDS results show that the natural oxide film, as formed from the melt, is up to  $20\text{nm}$  in thickness and, due to its hard brittle properties, is easily penetrated by the probe or rider at the load used. This is almost certainly due to the relatively soft under-layer of tin producing the aforementioned 'ice-on-mud' effect.



(10Kg/5mm/180s).

**Fig. 4.60 Hardness Change of Pure Tin With Temperature<sup>12</sup>**

As micro-motion commences good electrical continuity is maintained, due to metal-to-metal contact via a-spots as the soft tin extrudes between the fractured oxide. During this stage, wear is severe and occurs by plastic deformation and fracture. With time the wear rate can reduce due to the presence of small oxidised wear particles

which may form a layer causing a reduction in the local stresses. This film is initially thin enough to allow quantum electron tunnelling. Because of the different crystal structure of tin and its oxide, incompatibility stresses at the metal/oxide interface allow the removal of oxide particles by the action of friction. By this stage a wear scar has formed. Continued micro-movement eventually results in electrical 'glitches' caused by high CR at the extremities of the wear scar, particularly at the end where the tin has softened. Here, there accumulates wear debris which has been fully or partially oxidised. If wear continues without failure, the removal of the top layer of tin by the initial wear process described above, exposes the underlying intermetallics, which act as a second contact surface. No evidence has been observed from the contact resistance traces of this transition from the relatively soft tin contact surface to the hard irregular intermetallics. This would suggest that (a), the resistivity of the intermetallics is similar to that of the tin layer, as plated, and that (b) a similar contact area is maintained. It has been reported by Braunovic and Aleksandrov<sup>1</sup> that copper/tin intermetallic compounds have a significantly higher resistivity than tin, although Kay and Mackay claim them to have similar values<sup>13</sup>. The results presented herein are in agreement with those of Kay and Mackay. Examination of other wear scars showed the contact peaks of the intermetallics, which were supporting the load, surrounded by oxidised wear debris, Fig. 4.44. At this stage the wear rate would be expected to reduce. However, by this point in the wear process, the abundance of wear debris at the periphery of the scar would have been sufficient to indicate failure based on the criteria used.

Bryant<sup>14</sup> has described the fretting mechanism as being essentially asperity wear out and a steady build up of an oxide film. However, it has been shown that this process is further complicated by thermal cycling. The reduction in hardness of tin with temperature is shown in Figure 4.60 and the softening of the metal is illustrated in the SEM images of the wear scars, where there is plastic flow of the tin at the hotter (125 °C) end. Here there is a 24% drop in hardness, when compared to the 'cooler' end of the wear scar. Accompanying this build-up of metal, there is an increase in oxidation rate at the elevated temperature. Evidence from the CR trace along the worn region and SEM examination, confirms that at the onset of failure there is a steady increase in contact resistance at the wear scar extremities, with the highest values obtained at the

'hotter' end, with oxidised wear debris being transported and deposited over the central region. Softening of the tin will of course tend to increase the contact area but this appears to have no detectable effect on CR.

For the HDT plated copper contact, the frictional forces operating during fretting may change in magnitude several times during the wear process. After the initial break-down of the oxide layer, that is with soft metal-to-soft metal in contact, adhesion is strong, resulting in high frictional forces. As intermetallics are exposed, frictional forces may then drop as both the real contact area ( $A_r$ ) and the shear stress ( $\tau$ ), are low. Finally, when the intermetallics are touching, the frictional forces remain relatively low due to the large shear stress but small  $A_r$ . From this it is apparent that the major contribution of oxidised wear debris occurs early on in the fretting process, that is from the initial break-up of the native oxide film and during the high friction stage. This process for connector contact degradation due to fretting corrosion is graphically displayed in Fig. 4.61.

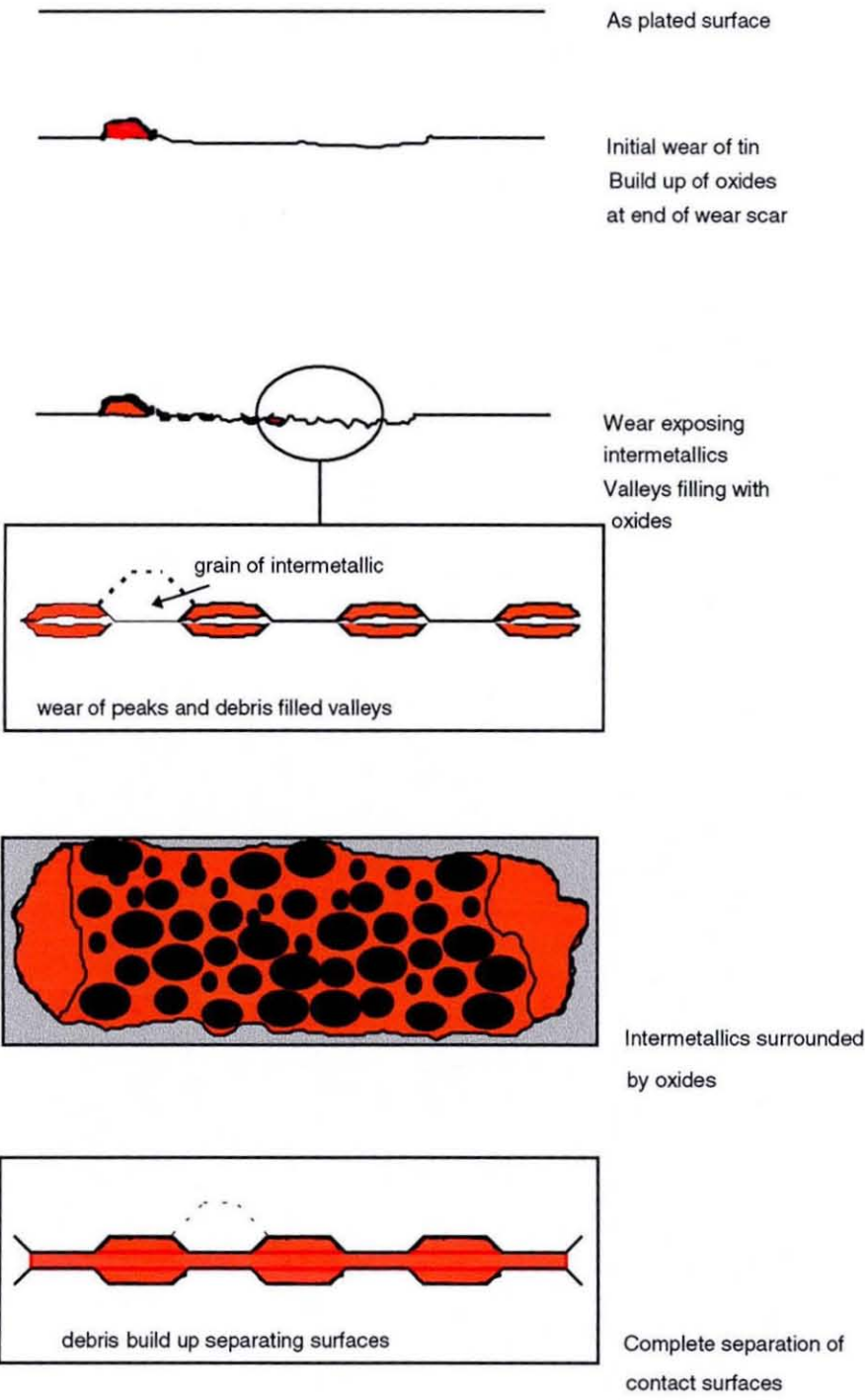


**Fig. 4.61 Schematic of the Fretting Process of Hot Dipped Tin Plated Copper Connectors**



#### 4.6.4 Lubricants for Fretting Regimes

The practice of using lubricants in order to reduce fretting corrosion on tin plated separable connectors has gained wide acceptance<sup>15</sup>. Scientific research into lubricant formulations, which will offer the best performance for the particular operating environment is, however, from the published literature at best, limited. Lubricants are used to reduce friction and provide a seal against the environment but not all perform this role to the same degree. The lubricated fretting tests in this study were therefore intended to establish an initial ranking of several commercial formulations and to hypothesise on and test a possible mechanisms relating composition to superior performance. At the same time a novel technique was evaluated which attempted to relate the reactivity of a grease to TTF. If successful this could be used in lubricant selection without the need for time consuming fretting tests.

Assuming a reactive grease to have a leakage current  $>0.1 \mu\text{A}$ , the reactivity tests, Table 4.6, show that there are two categories of greases - 'Reactive' and Non-Reactive'. Of the former, all bentonite thickened greases gave high leakage current readings. Bentonite is an organoclay composed of platelets onto which are attached long organic chains. The platelets are de-agglomerated by a combination of wetting and shear forces and activated by the use of a solvent such as acetone ( $\text{CH}_3\text{CO}\cdot\text{CH}_3$ ). It is the presence of water and the solvent which was probably responsible for the high reactivity results. Bentonite thickened greases cannot therefore be included in reactivity/fretting evaluation tests until excess water and activator are driven off by subjecting the lubricant to an initial period at high temperature.

Of the remainder of the greases, it was apparent that those thickened with soaps generally showed the highest reactivity due to the highly polar molecular structure of the thickener. The fretting test results, Table 4.16, exhibited some correlation in most cases between reactivity and fretting performance with soap thickened greases achieving the longest TTF. This was not the case for all, however, as the soap filled silicone greases showed both a low reactivity and poor fretting performance. One possible explanation is the strong adsorption of silicones to metal surfaces inhibiting

charge transfer in the reactivity cell and the bonding of the soap molecules to the metal surfaces of the electrodes. Of the six formulations showing a poor correlation, with the exception of MG21, the lubricants: MC41; MC42; MR49; MP22 and MZ20, showed high reactivity with poor fretting performance. Of these MZ20, a polyalkylene glycol, exhibited high volatility from the thermogravimetric analysis but at the same time contained surface active end groups.<sup>16</sup> MP22 similarly showed a significant weight loss, which is surprising for a high temperature ester base oil. High volatility would, however, suggest the formation of electrically insulating lacquers. The lubricants containing the complex soaps, MC41, MC42 and MR49, as expected, showed a high leakage current but their fretting performance was poor and an explanation for their behaviour under the fretting test conditions would be worthy of further investigation. MG21 was a silica filled PPE and although showing a low reactivity, its fretting performance was probably enhanced by the lubricant's high viscosity/temperature relationship.<sup>16</sup>

Figures 4.62 and 4.63 are histograms showing the relationship between fretting performance and lubricant composition. The complex soaps used here had calcium cations attached to the acid chains and, although the fretting performance was variable between samples, it did relate to the reactivity values. It is apparent, however, that those containing the micelle network of a lithium-12-hydroxystearic acid soap gave superior results, particularly with a mineral oil base. The thermogravimetric analysis showed this lubricant to have significant volatility in the temperature range used for the fretting tests and, therefore, it may be concluded that the lithium soap rather than the base oil played the major role in reducing fretting corrosion. Of course it is not known whether acid products formed due to oil degradation or additives were contributory factors. Fretting tests, using the base mineral oil alone and with additives, would assist in further studies in identifying their role.

As found in the literature survey, soaps are known to exhibit strong adhesion to metal surfaces, giving good boundary lubrication and reducing friction and wear. Although it is likely that the molecules require at least a few atomic layers of metal oxide for good bonding, fatty acids have been found to chemisorb on freshly machined surfaces, activated by the Kramer effect<sup>17,18</sup>. At room temperature the soap molecules begin to

attach themselves to the contact surface. As the temperature increases it would be expected that the reactivity increases and the number of polar molecules attaching themselves would similarly multiply, giving greater protection against fretting wear, both by reducing frictional forces and by providing a barrier to oxygen.

To study the chemisorption of soap molecules to both polished and oxidised tin at room and elevated temperature, 12-hydroxystearate films were measured by IRAS. It was found that the technique was able to provide information on the degree of bonding shown by peak broadening and absorption frequency shifts. These shifts indicate that the polar group is bonded chemically to tin oxide ( $\text{SnO}_2$ ). There was also an increase IR absorption when the soap was heated to  $125^\circ\text{C}$ , which would indicate that the acid chemisorbs more strongly at this temperature.

Application of this mechanism to the fretting process, at the temperatures used for this study, would suggest that, initially, the native oxide on the tin surface is coated with hydroxystearate molecules, reducing friction and wear. Inevitably some wear takes place and debris is generated. Subsequent oxidation of the metallic particles occurs as a result of diffusion of oxygen through the lubricant. Their oxidised surfaces provide further sites for chemisorption. It is conceivable that with the local shear forces involved during sliding of the rider over the coupon, shearing of the stearate molecules at the lubricant/substrate interface, would result in their deposition along the wear track to provide lubrication at the freshly exposed metal surface. In addition, at the test temperatures employed, the formation of tin oxide is rapid on this highly active surface, with only a few atomic layers being sufficient to provide bonding sites for the polar group.

The non-reactive greases were generally those not containing the polar soap molecules, where the properties of the base oil would be expected to dominate the wear process at the test temperatures used. For example the polyphenyl ether/silica grease (MG21 reactivity  $<0.1$ ), gave a time to failure of 187 hours. As temperatures increase, the viscosity of the base oil decreases, while at low temperatures when the viscosity is high, it is expected that there will be improved boundary lubrication and a consequent improvement in fretting performance.

From the reactivity/ fretting tests the following conclusions may be drawn:

- (i) The reactivity of the grease is directly proportional to its polar molecular content but Bentonite thickened greases must be heated to above 100°C prior to testing to drive off excess activator and moisture.
- (ii) Base oils (apart from silicones), containing lithium-soaps, generally give the best fretting wear performance at higher temperatures. (The exceptions to this require further investigation).

Examination of the wear scars after fretting tests with lubricants shows several interesting features. Due to the good boundary lubrication properties of the greases containing soap thickeners, there is less adhesive wear of the tin and less build up at the softer end of the wear scar, Fig. 4.46, when compared with the unlubricated test sample, Fig. 4.42. For the lubricated fretting tests which had achieved the highest TTF, (MC37 (>1000 hrs.) and MR30 (745 hrs.)), it is apparent from the BSE image that contact was with the intermetallic layer which had grown during the test period, when aged at a mean temperature of 105°C, Figs. 4.45 and 4.46.

Lubricant	Fretting Time to Failure (hours)	Reactivity ( $\mu\text{A}$ )	Lubricant	Fretting Time to Failure (hours)	Reactivity ( $\mu\text{A}$ )
MC10	127	6.4	MP10	133	0.4
MC11	70	1.0	MP11	101	0.3
MC12	89	1.78	MP12	254	5.8
MC13	92	3.7	MP22	88	0.17
MC14	68	0.63	MP40	174	0.85
MC25B	178	0.08	MP41	123	0.5
MC30	733	7.1	MG21	187	0.02
MC32	587	0.43	MF20	55	<0.001
MC36	710	0.54	MF24	58	<0.001
MC37	>1000	0.61	MF51	51	<0.001
MC41	76	0.3	MF52	50	0.008
MC42	53	0.15	MS20	36	<0.001
MC45	662	0.1	MS30	53	0.001
MR20	57	0.0001	MS31	47	0.01
MR27	53	0.001	MS50	53	0.003
MR30	745	3.5	MZ20	90	0.833
MR31	55	0.005	MZ30	187	152.0
MR32	84	0.111	MZ31	186	4.1
MR40	69	0.005			
MR49	38	148.0			

**Table 4.16 Reactivity and Fretting Performance for Lubricated Tests**

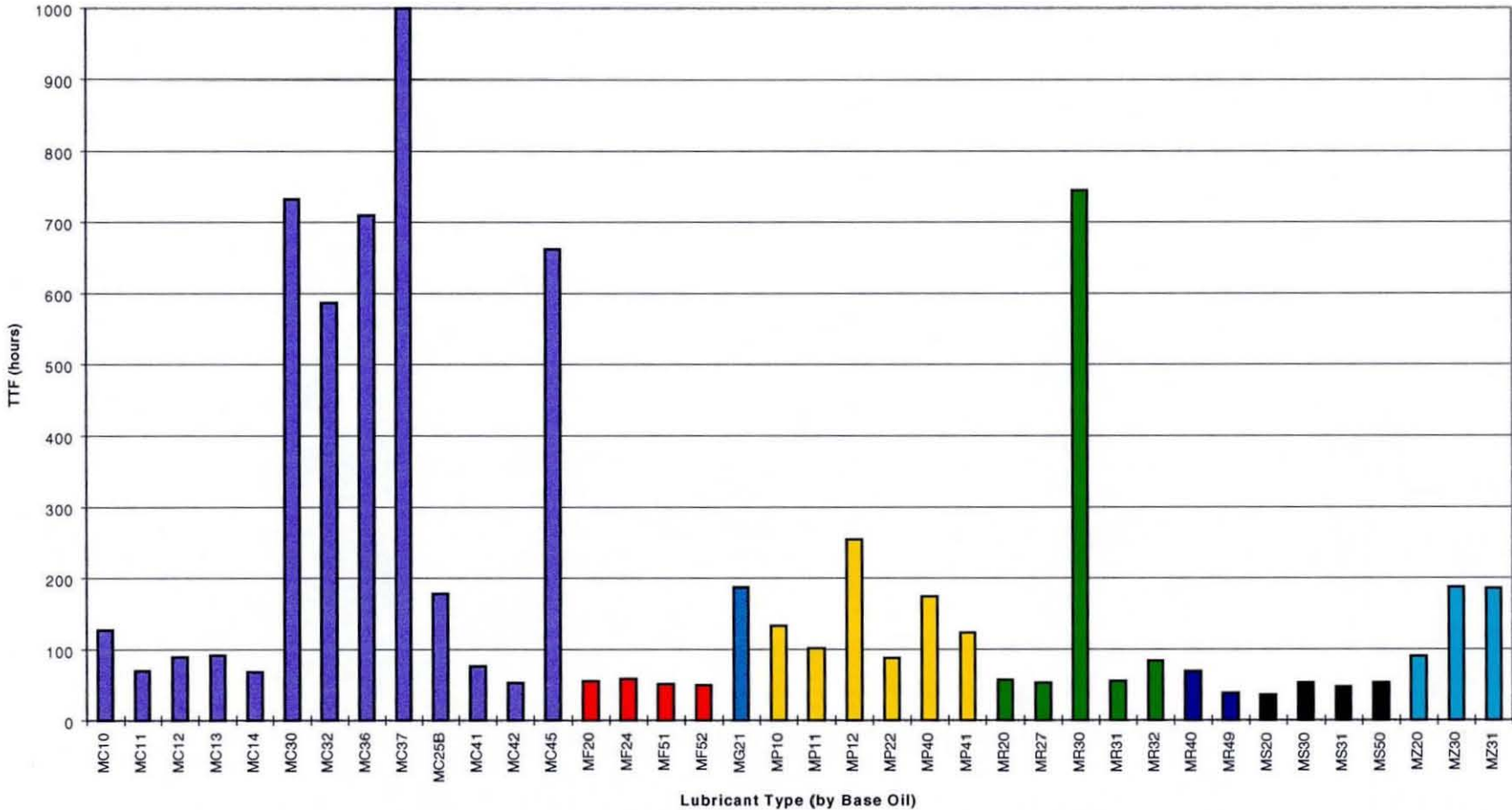


*Fig. 5.6 Relationship Between Lubricant Base Oil and Fretting Performance*

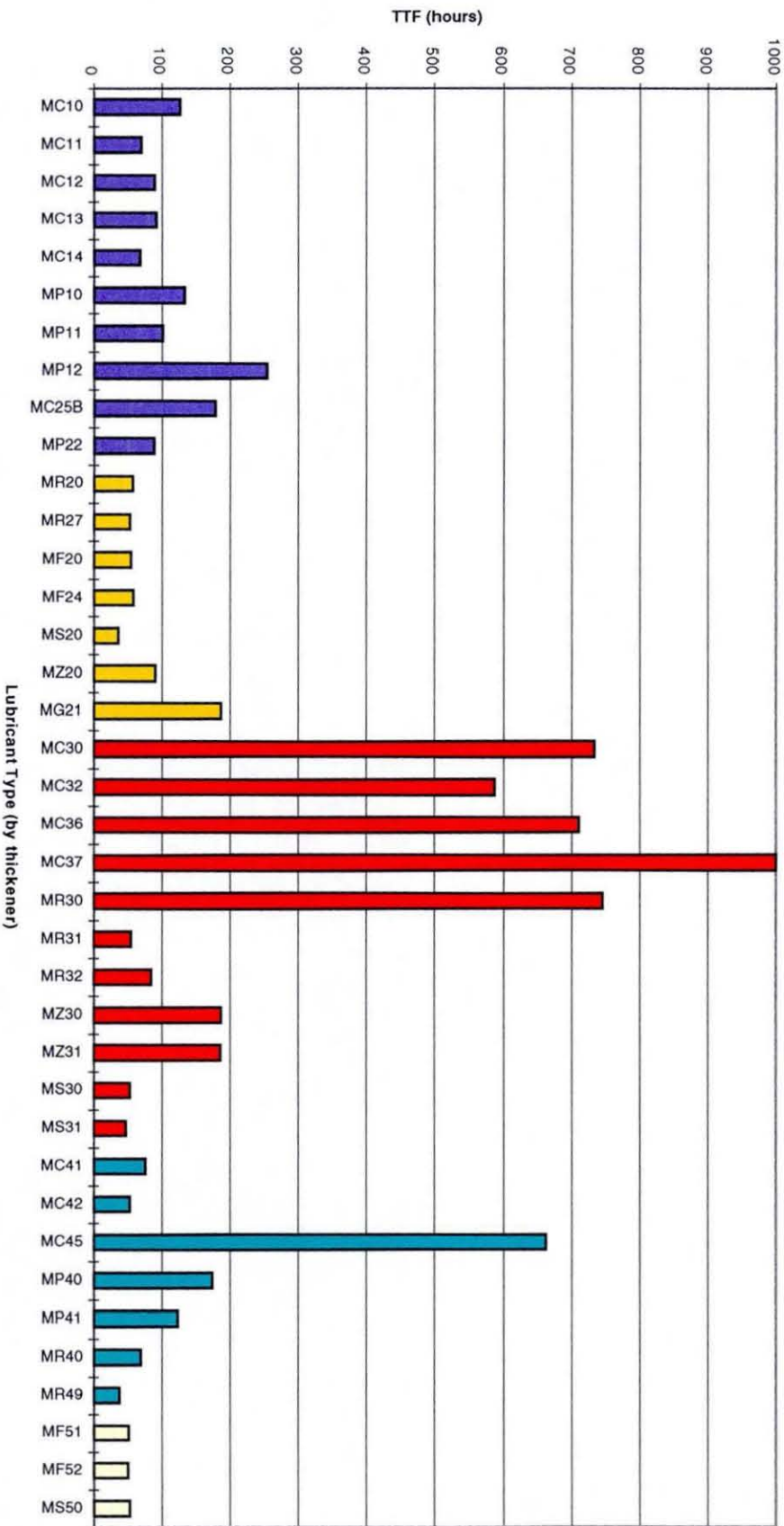


Fig. 5.7 Relationship Between Lubricant Thickener and Fretting Performance

#### 4.6.5 Intermetallics as Contacts

It can be concluded from the above that failure of tin plated separable connectors as a result of fretting corrosion is due to the generation of resistive wear debris. If therefore the source of these corrosion products could be removed or reduced, the likelihood of early failure would be minimised. It has been shown that the correct choice of lubricant to act as a barrier to oxygen and reduce friction can assist in achieving these ends. As an alternative, however, it is proposed here that through heat treatment or ideally during the plating stage, a conversion of the tin coating to fully form the intermetallic can potentially achieve the same results.

It has been shown that the  $\text{Cu}_3\text{Sn}$  phase is cathodic to tin and has a hardness of  $390 \text{ kgmm}^{-2}$  compared to  $8 \text{ Kg.mm}^{-2}$  for pure tin. The hardness of the  $\text{Cu}_6\text{Sn}_5$  was not able to be determined due to its small dimensions but would be expected to be significantly greater than tin. A hardness of  $180 \text{ Kg.mm}^{-2}$  has been reported by other workers<sup>1</sup>. Both intermetallics, however, would provide a hard and low friction contact surface. Such contacts subjected to micro-motion would consequently show a lower propensity to wear particle generation and thus reduce the major source of resistive oxide. The wear test performed on the intermetallic layer has shown experimentally that this is indeed the case, giving a fretting performance in excess of 1000 hours (500 cycles), with minimal wear of the copper rich phase, Fig. 4.64. Alternatively the morphology of the  $\text{Cu}_6\text{Sn}_5$  intermetallic grains, being composed of regular peaks and valleys can be utilised and act as sites for the collection of any wear debris that is generated to extend fretting life as suggested by Bryant's model, see Section. 2.9.3. In addition such a surface may be used as natural reservoirs for suitable lubricants.



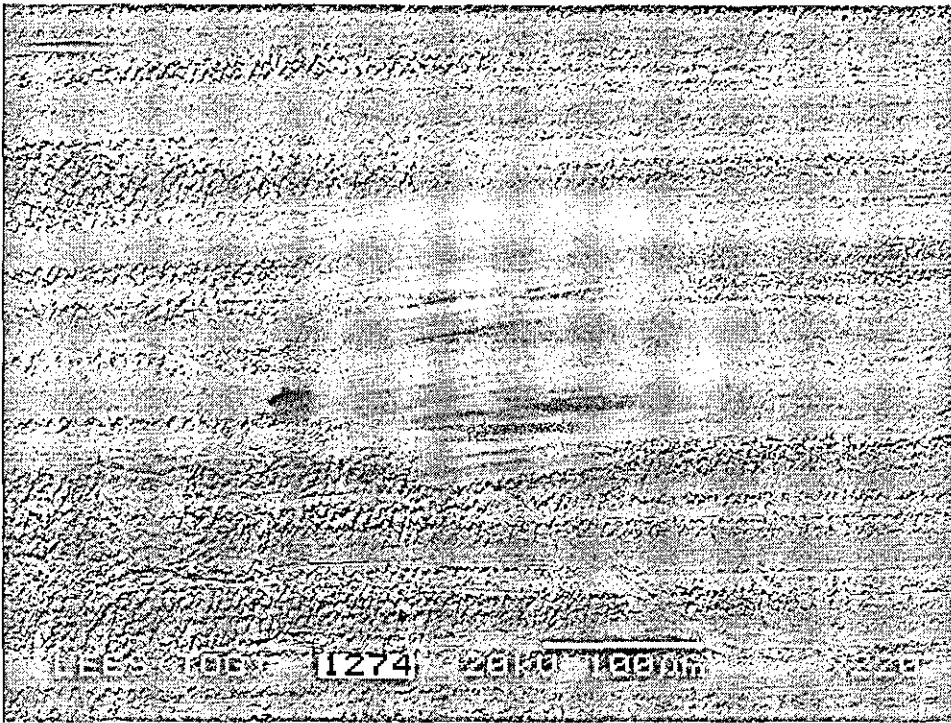


***Fig. 4.64 Wear Scar on Intermetallic Coating***

## References

- <sup>1</sup> Stolberger Metallwerke GMBH & CO KG, 5190 Stolberg, Inspection certificate B 029038 of 04/02/1991
- <sup>2</sup> Engel, P., "Vickers Microhardness Evaluation of Multilayer Platings for Electrical Contacts". 37th Holm Conference, (1991).
- <sup>3</sup> Ackroyd, M.L. and Mackay, C. A., "Solders, Solderable Finishes, and Reflowed Coatings", Publication 529, International Tin Research Institute, (1977).
- <sup>4</sup> Leidheiser, H. Jr., "The Corrosion of Copper, Tin and Their Alloys", (Kreiger, R.E.), (1979).
- <sup>5</sup> Joint Committee on Powder Diffraction Standards, (JCPDS International Centre for Diffraction Data, Swarthmore, PA).
- <sup>6</sup> Fister J.C., 'Solderability Performance of Tin Coated Copper Alloy Strip for Connector Components', Forty First Electronic Components and Technology Conference', Georgia, (1991).
- <sup>7</sup> Chollet, P.A., Messier, J. and Rosilio, C., *J. Chem. Phys.*, **64**, 402, (1976).
- <sup>8</sup> Tamai, T., "Electrical Conduction Mechanisms of Electric Contacts Covered with Contaminant Films", *Surface Contamination*, vol. 2, (edited by K.L. Mittal, Plenum Press, New York and London), (1979).
- <sup>9</sup> Revay, L., "Interdiffusion and Formation of Intermetallic Compounds in Tin-Copper Alloy Surface Coatings", *Surf. Tech.*, pp. 57-63, (1977).
- <sup>10</sup> Braunovic, M and Aleksandrov, N., "Intermetallic Compounds at Aluminium-to-Copper and Copper-to-Tin Electrical Interfaces, Thirty-Eighth IEEE Holm Conference on Electrical Contacts, (1992).
- <sup>11</sup> Tan, A.C., *Tin and Solder Plating in the Semiconductor Industry*, (Chapman and Hall, London), (1993).
- <sup>12</sup> Hedges, E.S., *Tin And Its Alloys*, (Edward Arnold, London), (1960).
- <sup>13</sup> Kay, P.J. and Mackay, *Trans. Inst. Met. Fin.* **54** (1976), 68-74.
- <sup>14</sup> Bryant, M.D., "Resistance Build-up in Electrical Connectors Due to Fretting Corrosion of Rough Surfaces", 39th IEEE Holm Conference on Electrical Contacts, Pittsburgh, (1993).
- <sup>15</sup> Whitley, J., "The Tin Commandments", *Connection Technology*, pp. 27-28, (April 1989)
- <sup>16</sup> Klamann, D., *Lubricants and Related Products*, (Verlag Chemie, Weinheim), (1984)
- <sup>17</sup> Shaw, M.C., "The Metal Cutting Process as a means of Studying the Properties of Extreme Pressure Lubricants", Symposium on Fundamentals of Lubrication, Ann. N.Y. Acad. Sci., **53**, art. 4, pp. 962-978, (1951).
- <sup>18</sup> Smith, H.A. and McGill, R.M., *J. Phys. Chem.* **61**, no. 8, pp. 1025-1036, (1957).

## **5. Conclusions**

This study has attempted to broaden the knowledge and understanding of the various mechanisms in operation in the fretting corrosion process of hot dipped tin plated bronze connectors. The materials used have been deliberately chosen to be the same as those with which the connector manufacturer selects for production. It is possible that this approach may, in some cases, introduce additional variables further complicating an already complex problem but by doing so it has compelled the researcher to procure an in-depth understanding of the physical and chemical properties of these materials. For one of those variables at least, it has necessitated the development of a new analytical procedure, (Volume Saturation Method). The experimental process was designed to provide an initial materials characterisation of the plating followed by materials testing, with emphasis on the wear process in both dry and lubricated conditions.

From the research carried out to date, the following conclusions may be drawn:

- (i) The hot dipped tin coating should not be regarded as a monolithic material, being composed of hard and soft phases non-uniformly distributed. This is particularly pertinent to its corrosion and wear properties.
- (ii) The native oxide layer is thin enough to allow charge transfer between stationary mating contacts under dry circuit conditions. In underbonnet environments oxide growth can be excessive due to the high temperatures experienced. It is oxide formation rather than corrosion products from other

species in the vehicle environments where tests were performed, which contributes greatest to the presence of electrically resistive films.

- (iii) Tin, although a good general anticorrosive coating has poor wear properties, particularly under fretting conditions in high temperature, e.g. engine bay environments. Such conditions result in the generation of oxidised resistive wear debris.
- (iv) Fretting performance at temperatures between 85°C and 125°C can be dramatically improved by the use of a lubricant having a mineral oil base and a lithium hydroxystearate thickener system.
- (v) The reactivity of a grease shows some correlation between its composition and its fretting performance, with highly reactive greases having a high polar content giving good fretting resistant properties.
- (vi) IRAS has been shown to provide information on the chemical bonding of 12 - hydroxystearate films to tin.
- (vii) The intermetallic phases are hard and have both good wear and corrosion resistant properties. Under high temperature low cycle fretting conditions, a layer of the copper rich ( $\epsilon$ ) phase was found to out perform the tin coating by a factor >20 in terms of cycles to failure. Similarly, the ( $\eta$ ) intermetallic phase would also be expected to be superior to tin with the additional benefit of possessing a surface texture beneficial to wear debris entrapment.
- (viii) The Volume Saturation Method has been shown to be the only practical technique (apart from possibly AES depth profiling), which could be used to study the diffusion rate of copper in tin for the samples used in this study. The method is limited, however, to determining solid state diffusion of a single phase but is an extremely rapid technique and has superior reproducibility over other methods.

Scientific research attempts to find answers to particular problems, however, in doing so whole new sets of questions are created, as discussed in the following *Recommendations* section.

## **6. Recommendations**

The conclusions drawn from this study have shown that there are at least three areas of further research which should be pursued:

The intermetallic layer has been shown to have good wear properties and at the same time act as a cathodic coating on copper. It has always been assumed within the electronics manufacturing industry, that intermetallics are deleterious to good electrical contact due to their brittle properties. However, this has always been in relation to the tin/lead soldered joint which can be exposed to mechanical and thermal shear or tensile stresses in service. In this application the intermetallics are subjected to normal compressive stresses only and like a ceramic material would be expected to withstand high compressive forces without fracture. Further measurements of the mechanical properties of the intermetallics are therefore desirable. In addition there is some debate in the literature regarding the electrical resistivity of the phases and it is recommended that further work be carried out to determine bulk resistivity by perhaps using laboratory manufactured intermetallic. Such material could be produced from solid state diffusion of the powdered parent metals blended in the correct atomic proportions, in a reducing atmosphere. The existence of bulk intermetallic could also be exploited in identifying the extra peaks observed in the XRD spectra.

A second area of further research is in lubricant properties. It was found in this study that the lithium soap thickened mineral oils performed best under the relatively high temperature conditions used compared to the low reactive greases. It was hypothesised that this was due to polar molecules attaching themselves to the metal surface and demonstrated that greater numbers were involved as the temperature increased,

producing good boundary layer conditions. The non-reactive greases relied on viscosity and surface tension to keep contacts apart, and reduce with temperature. It is therefore recommended that fretting tests be performed, using both a high and low temperature range to confirm the hypothesis.

Finally the activation energy and diffusion constant calculated using the Volume Saturation Method would be expected to be improved upon by using a thicker tin coating prepared under laboratory conditions together with an electroplated tin coupon to compare diffusion rates.

## APPENDIX A

### A1 Reliability, Failure Modes and Mechanisms

#### A1.1 The Automotive Environments

It is essential to obtain full environmental information before a connector design can be specified with any assurance that the requisite reliability and performance will be achieved. Automotive electrical connectors are subjected to conditions which may be relatively benign such as those found in the interior of a family saloon or severe such as exists under-bonnet. With the advent of engine management and 'brake-by-wire' systems employing a large number of sensing elements, it is now becoming an increasing requirement for connectors to withstand the hostile conditions found in exhaust gases, engine housings and on brake actuators.

Reliability is a function of the prevailing environment and although the operating or 'in-service' conditions will generally be the major influencing factors, the performance and reliability of connectors may in addition be affected by for example, storage conditions and the subsequent assembly procedures adopted by the vehicle and systems manufacturer. It is therefore the complete *life profile* of the connector assembly, which should be known in order to be able to predict in-service reliability and to determine the cause of failure of components both in the field and during testing. Proper classification of environmental parameters and careful interpretation of test results effect substantial gains, provide assurance of maximum information, and allow an efficient estimate of operational reliability. Unfortunately, the connector designer often has little or no control over the manufacturing standard of the other mating half of a connector system. Electrical and electronic components, with which the separable connector may be in contact, could for example be fabricated by more than one manufacturer, each having different design specifications and standards of quality and cleanliness.



The connector system will normally be subjected to the effects of the conditions which prevail in at least five environments of its life profile, that is during: manufacturing, storage, assembly, servicing and operation. Generally, for all but the 'operational' activities, it is possible to introduce some degree of control and reproducibility but once in service, this cannot be achieved without knowledge of the operating conditions and the results of failure investigations.

### *Manufacturing*

Throughout the connector industry quality systems are being introduced not only to reduce the risk of material variations, damage and contamination but also to include procedures for corrective action in order to maintain consistency. The incidence of atmospheric corrosion occurring in the manufacturing environment is generally mitigated by modern workplace conditions. However, due to poor component design or inefficient washing and drying processes, water entrapment of corrosive plating bath residues may occur. In the electroplating process, a connector may be exposed to a number of different concentrated chemicals such as acids, alkalis, de-flashing chemicals (amines, amides or chlorinated solvents), and halides,<sup>1</sup> which may become active due to moisture later in the life profile.

### *Storage*

Although the requirement to store components for long periods of time during assembly is decreasing as a result of 'Just-in-Time' manufacturing processes, the connector may still experience degradation where contamination and high ambient temperatures and humidity conditions exist, both in the short term during transportation or in the long term in uncontrolled storage conditions. The external atmosphere is not the only source of corrosive species. Out-gassing of: phenol; formaldehyde; ammonia; formic and acetic acids from aggressive packaging materials have been reported resulting in corrosion of a variety of electrical and electronic components<sup>2</sup>.

### *Assembly*

In the vehicle manufacturing environment, automation of assembly processes has for many automotive components, reduced the likelihood of mechanical damage during vehicle assembly but electrical connectors are for the most part, reliant on manual insertion with the increased probability of misalignment and resultant plastic deformation or fracture.

### *Servicing*

With improved reliability, however, vehicle servicing intervals have increased lessening necessity to remove components for inspection or examination. During its 'operational' phase, however, the connector system may be disturbed or subjected to cleaning fluids or inappropriate lubricants, promoting possible mechanical damage and corrosion.

### *Operational*

Automotive separable connectors are required to function reliably in temperate, tropical, desert and arctic climates, in rural, urban and coastal regional conditions and in the environments that exist on and within the vehicle itself. Although, in general, temperate regions by definition do not suffer extremes of temperature, humidity and precipitation, surfaces may become and remain wet for substantial periods of time due to rain and snow exposure and dew condensation, where the latter has been calculated to persist for 25 to 50% of total exposure time<sup>3</sup>.

In the tropics there are high temperatures combined with high humidity. In such circumstances metals will rapidly corrode and electrolytic action between dissimilar metals will be accelerated. Current leakage may occur as a result of moisture adsorbed onto insulating surfaces and polymeric insulators themselves may swell due to water absorption. It has been reported that the metabolic processes associated with fungal growth may etch the surfaces of materials or form low resistance pathways.<sup>2</sup> In desert regions the atmosphere has a very low moisture content together with high ambient

temperatures with wide variations between day and night. Such conditions may result in the degradation and warping of connector insulating polymers and the breakdown of metal/polymer joints due to thermal expansion mismatch. Thermal cycling, although of low frequency can be of relatively high amplitude under these conditions promoting fretting of tin plated electrical connector systems.

Although low temperatures generally reduce corrosion rates, particular problems occur with tin plated connectors. Tin is known to revert to the  $\alpha$  phase at temperatures below 13.2° C. This phase, known as 'tin pest' or 'grey tin', has a density of 5.77 gcm<sup>-3</sup> compared to 7.29 gcm<sup>-3</sup> for white tin. With such a volume change, severe disruption of the plating can occur, although it has been found that the presence of impurities in the tin will retard or even prevent the formation of the  $\alpha$  phase<sup>4</sup>. In addition tin whisker growth can occur which can cause short circuiting of adjacent contacts.<sup>2</sup>

Airborne contaminants, which have been identified as significant to military connector systems<sup>5</sup> include both organic and inorganic species, with those of primary importance being classified as follows:

- (i) Reactive chlorides (HCl, Cl<sub>2</sub>, ClO<sub>2</sub>, halogenated organics)
- (ii) Reactive sulphides (H<sub>2</sub>S, S<sub>8</sub>, mercaptans)
- (iii) Sulphur dioxide
- (iv) Oxides of nitrogen

In the same reference, work by other researchers<sup>6,7</sup> is reported. It was found during a study of world-wide indoor pollutant distributions, that in almost 100% of the sites examined, the levels of reactive chlorides (Cl<sub>2</sub>), reactive sulphides (H<sub>2</sub>S) and sulphur dioxide (SO<sub>2</sub>), reached levels approaching 100 µgm<sup>-3</sup>.

Within world climates there will be variations in regional conditions. Mattson,<sup>8</sup> reports mean corrosion rates for iron, zinc, aluminium and copper in four types of

atmosphere: rural, urban, industrial and marine, (Table A1). Note that these figures are for 'steady state' corrosion rates and attack will be greatest during the first few years of exposure as corrosion products themselves generally tend to act as a barrier to further attack. Comparison with an earlier study,<sup>9</sup> (Table A2), shows that the mean corrosion rate of tin is comparable to that of copper in similar sample locations.

Industrial and marine environments not surprisingly show the highest rates of corrosion. This is due to differences in the degree of atmospheric pollutants from industrial processes such as oxides of sulphur and nitrogen (NO<sub>x</sub>), hydrogen chloride and sulphide, carbonic acid and particulates<sup>10</sup> and to airborne sea salt in coastal regions.<sup>11</sup> The chloride concentrations in urban areas may be substantially increased due to the practice by local authorities of using road salt as an antifreeze<sup>12</sup>.

Type of Atmosphere	Mean Corrosion Rate ( $\mu\text{m y}^{-1}$ )		
Location	Iron	Zinc	Copper
Rural	5-10	0.2-3	0.1-0.5
Urban	20-70	2-10	0.5-1.5
Industrial	25-175	5-15	1-2
Marine	25-105	2-35	1-2

**Table A.1 Corrosion Rates of Metals in Four Locations**

Together with any of the previously mentioned climatic and regional conditions, the conditions existing in the local micro-climates within a vehicle will impose the greatest thermal, chemical, electrical and mechanical stresses. Within the engine compartment, for example, the connector assembly may be affected by a range of contaminants. These include: salt mists, solvents, cleaning agents and outgassing products from polymers<sup>13</sup>. For example polyvinyl chloride wire insulation at

temperatures in excess of 100°C can evolve hydrogen chloride causing dezincification of brass connectors<sup>14</sup>.

Sample Location	Mean Corrosion Rate* ( $\mu\text{m yr}^{-1}$ )	
	over 10yrs.	over 20yrs.
Heavy Industrial	-	1.7
Marine Heavy Industrial	-	1.3
Marine (New Jersey)	1.9	-
Marine (Florida)	2.3	-
Marine (California)	-	2.9
Semi-arid	-	0.44
Rural	0.49	-
* Converted from wt. loss (density of tin 7.29 gcm <sup>-3</sup> )		

**Table A.2 Corrosion Rate of Tin in Various Geographical Locations.**

Not only are reaction rates increased by the high temperatures experienced within the engine compartment but also the connector system is subject to thermal cycling which in extreme conditions may range from -40° C up to 150° C. In addition, the high vibration-related stresses imposed on the system result in fretting of the mating contacts with the generation of highly resistive oxidised wear debris. All connectors used for automotive applications will be subjected to vibration to varying degrees. The vibration spectrum will be extremely complex and impossible to predict with any degree of certainty as amplitudes and frequencies will vary depending on location and operation of the vehicle.

The interior of the vehicle is usually considered to possess a relatively benign environment. However, within enclosed electronic housings, reactive polymer out-gassing products may be concentrated and high temperatures achieved due to prolonged heating by direct sunlight. Thermal cycling and the condensation of moisture on unprotected components may still occur as well as vibration induced stressing. The use of electronic sensors and electrically operated actuators within the engine itself is becoming more common. For example, the electronic unit injectors used on modern diesel engines necessitates the use of connector assemblies that are continually bathed in engine lubricant at temperatures approaching 150° C as well as being subjected to high vibration. Oxidation of the lubricant and the subsequent generation of acidic reaction products as well as combustion gases provide a challenge to the connector designer.

## A1.2 Reliability

The reliability of any component will depend on its 'fitness for purpose', that is the design rules must be such that it must survive without failure in normal operation for an acceptable period of time. The separable connector, although a passive component, may, during its life profile, be subjected to a variety of mechanical, thermal and chemical stresses, any of which may promote failure. Although connector failures in service are numerous, the determination of the particular mechanisms responsible at the exact point of failure are often difficult to ascertain precisely, as it is rare that the investigator is presented with both contact halves in situ. Reliability for many components will generally follow a 'bathtub' curve, where there will be an initial high failure rate followed by a long period of low incidences of failure before the onset of wear out and/or degradation due to environmental factors. For the electrical connector, however, initial failures would be expected to be low with only isolated failures resulting from mishandling on assembly or poor storage conditions, see Fig., A.1. In-service environmental factors would be expected to be the main causes of failure.

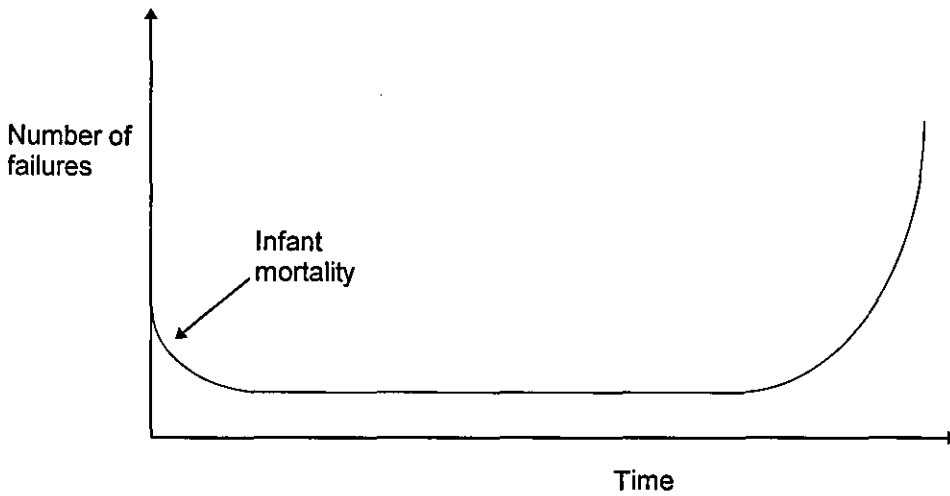


***Fig. A.1 Bath Tub Reliability Curve for Automotive Electrical Connectors***

### A1.3 Failure Modes and Mechanisms

All failures have a mode, mechanism and cause. The failure mode for any separable connector will almost always be high CR, resulting in temporary or permanent decrease or loss of current in a circuit. High CR may be effected by a reduction in contact pressure or by the separation of the contacting surfaces by an insulating or poorly conducting barrier. The failure mechanisms will be many and varied and it is the task of the failure analyst to ascertain which are responsible, in order to determine possible causes. There are numerous processes and materials properties which act directly or indirectly on the contact interface to effect high CR. (Fig. A.2). These can generally be grouped into four categories:

- (i) Mechanical and thermal stress
- (ii) Corrosion
- (iii) Wear
- (iv) Miscellaneous

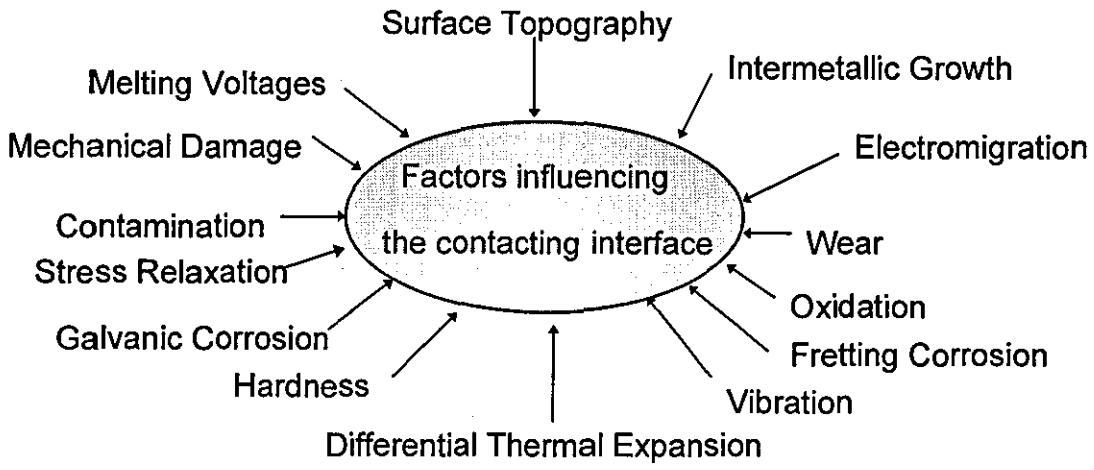
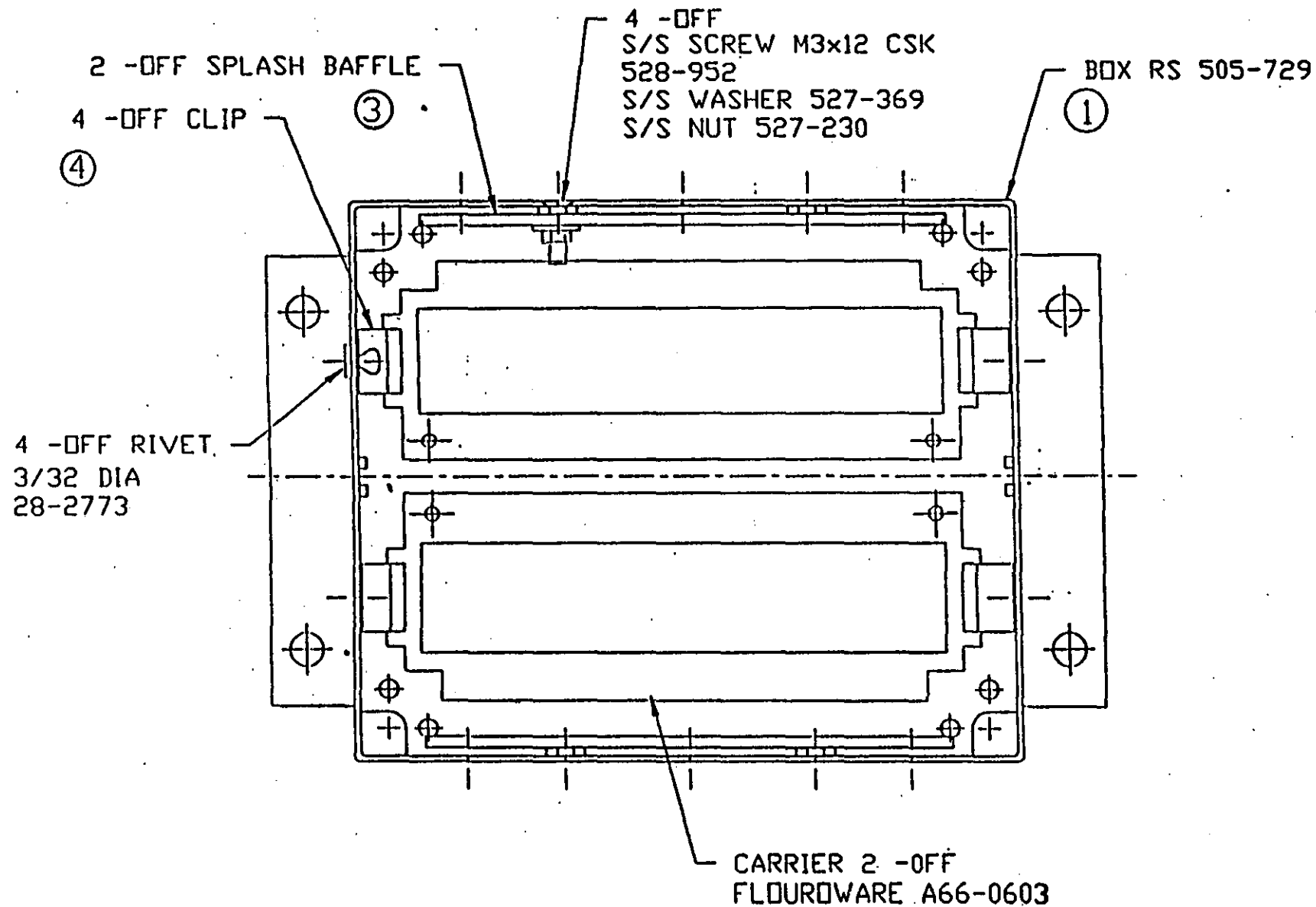


***Fig. A.2 Principle Factors Causing High Contact Resistance***



## References

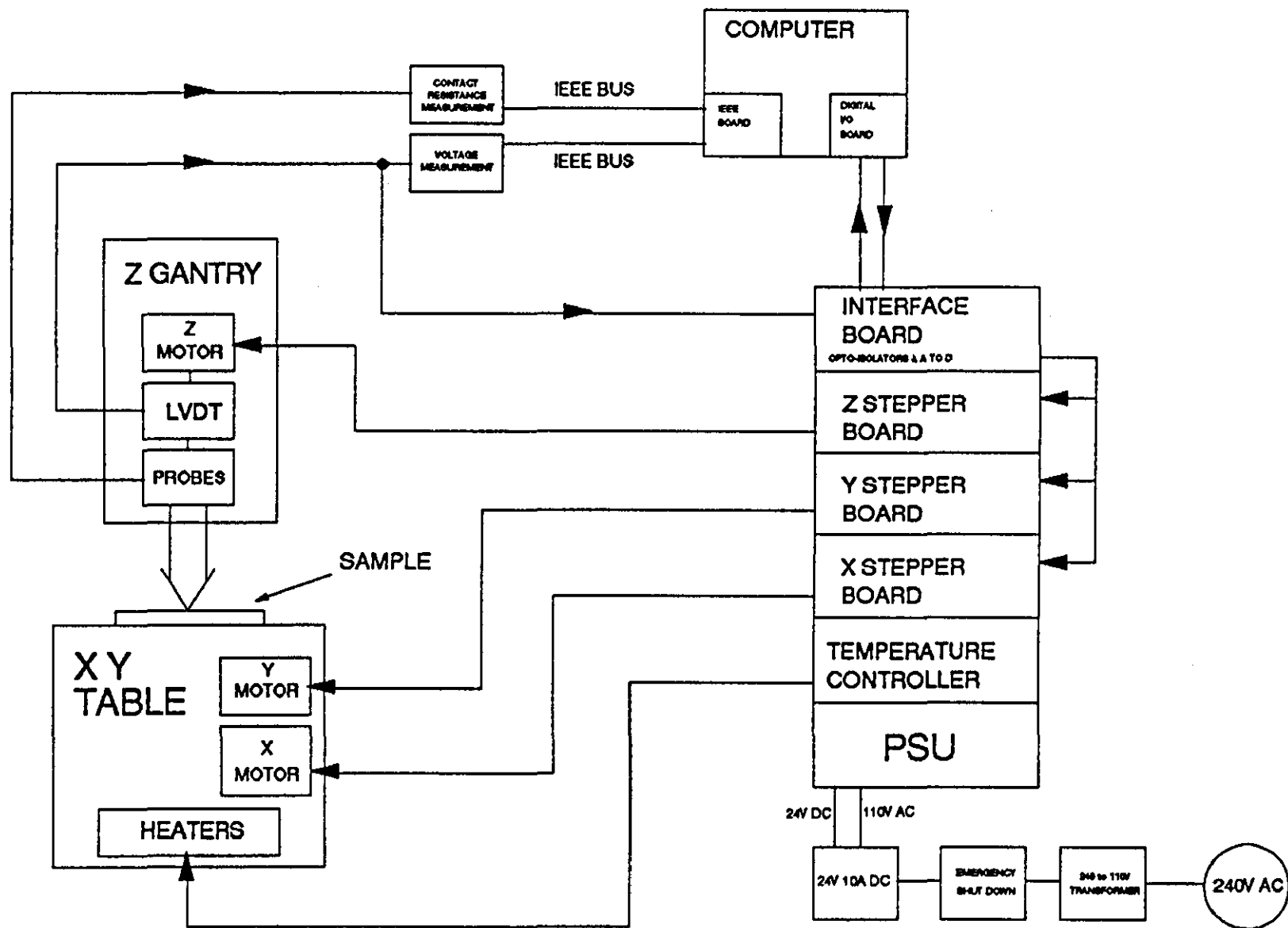
- <sup>1</sup> Tan, A.C., *Solder Plating in the Semiconductor Industry*, (Chapman and Hall, London), pp. 173, (1993).
- <sup>2</sup> Jowett, C.E., *Environmental Hazards in Electronics*, (October Press, Fareham), (1982).
- <sup>3</sup> Sereda P. J. et al, "Measurement of the Time-of-Wetness by Moisture, Sensors, Atmospheric Corrosion of Metals", STP 767, Dean, S. W. Jr. and Rhea, E. C. Eds., American Society for Testing and Materials, Philadelphia, pp. 267-285, (1982).
- <sup>4</sup> Britton, "Tin Versus Corrosion", Publication 510, (Tin Research Institute, England), pp. 8, (1975).
- <sup>5</sup> Davis, G.O., Abbott, W. H., and Koch, G.H., "Corrosion of Electrical Connectors", MCIC Report (MCIC-86-C1), (May 1986)
- <sup>6</sup> Abbot, W.H., "Field Versus Laboratory Experience in the Evolution of Electronic Components and Materials", *Materials Performance*, 24, pp 46, 1985.
- <sup>7</sup> Rice, D.W. and Peterson, P., *J. Electrochemical Soc.*, 128, pp1619, (1981).
- <sup>8</sup> Mattson E., *Materials Performance*, Vol. 21, No. 7, pp. 9 (1982),
- <sup>9</sup> Hiers, G. O., and Minarcick, E., "Symposium on Atmospheric Corrosion of Non-Ferrous Materials", STP 175, *American Society for Testing and Materials*, p. 135, (1956).
- <sup>10</sup> Guttman, H, "Atmospheric and Weather Factors in Corrosion Testing", *Atmospheric Corrosion*, (Wiley, New York), pp. 51-67, (1982).
- <sup>11</sup> Lee T. S., and Money, K. L., "Difficulties in Developing Tests to Simulate Corrosion in Marine Environments", *Materials Performance*, pp. 28-33, (Aug. 1984).
- <sup>12</sup> Slater J. E., "Corrosion of Metals in Association with Concrete, STP 818", American Society for Testing and Metals, Philadelphia, pp.1-5, (1983,).
- <sup>13</sup> Sharma, S.P. et al "Reaction of Contact Materials with Vapours Emanating from Connector Products", *IEEE Transactions on Components, Hybrids and Manufacturing Technology*. Vol. CHMT-6, No.4, (Dec. 1983).
- <sup>14</sup> Locker, G.J. "High Contact Resistance Failures of Automotive Micro Relays", Lucas Advanced Engineering Centre Report, (1994). (Unpublished).



APPENDIX B

Appendix

JOB No. 4215: CORROSION FIELD TEST BOXES



CONTACT RESISTANCE PROBE SCHEMATIC

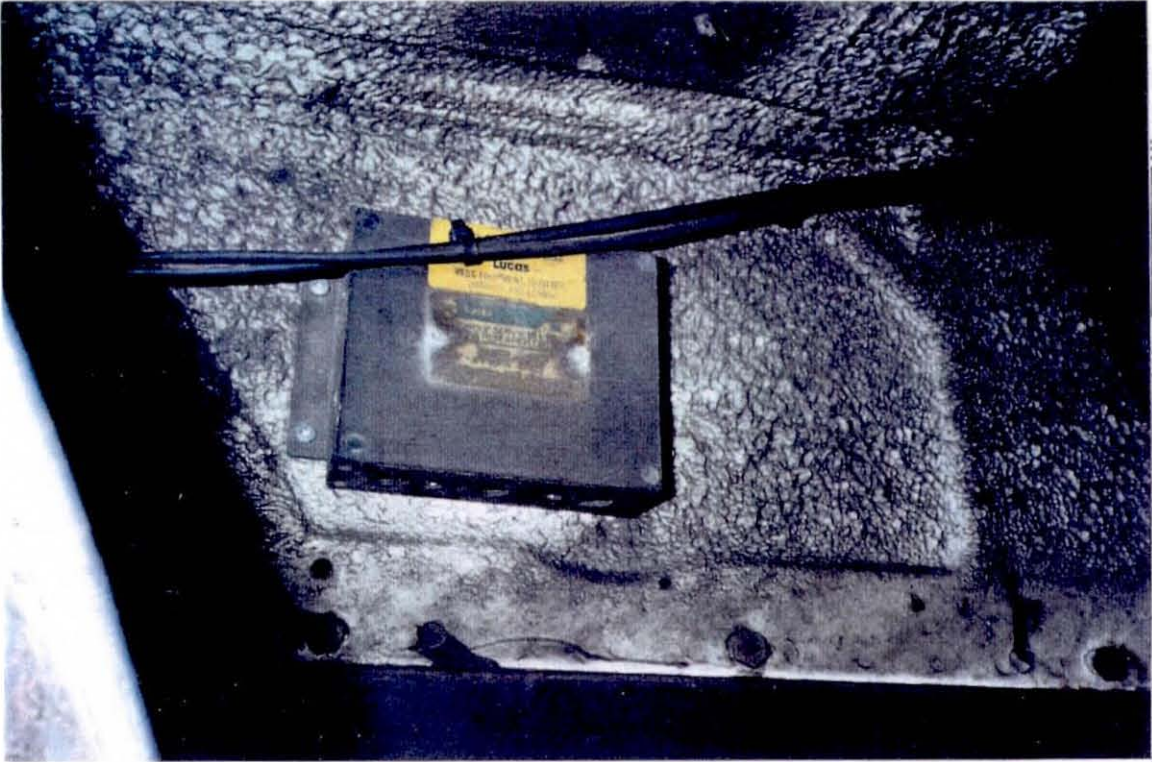


CAVALIER ENGINE BAY MOUNTING

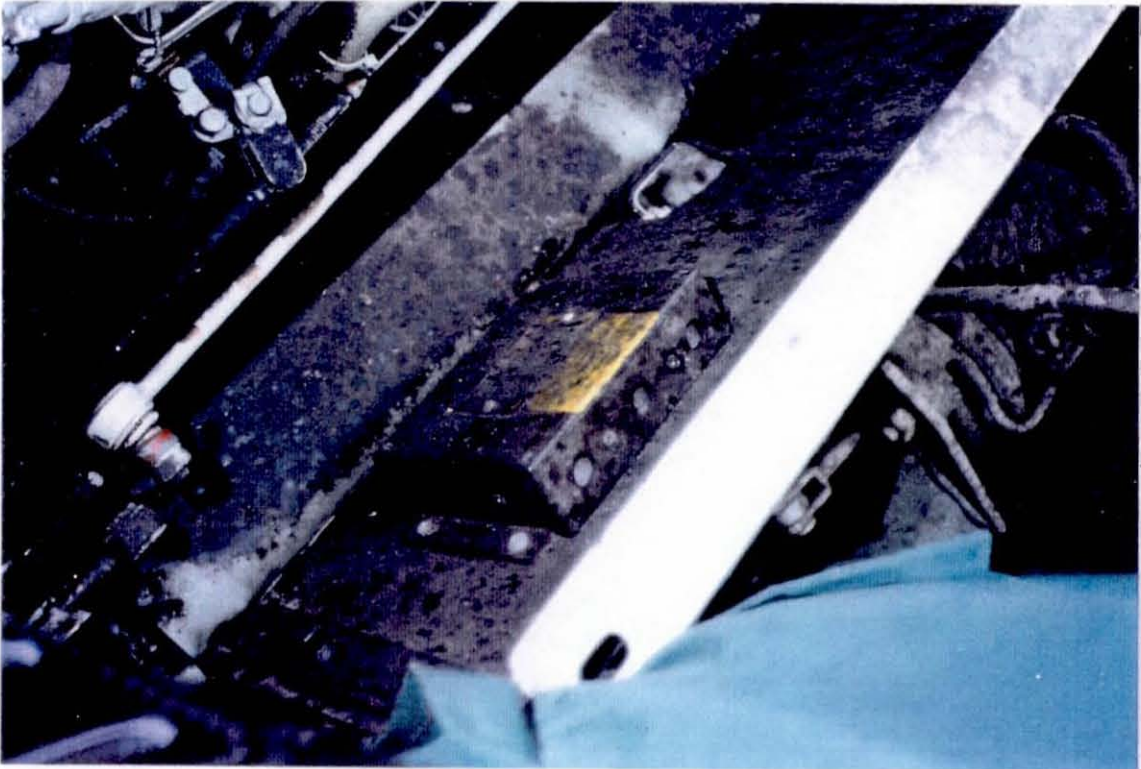


SIERRA ENGINE BAY MOUNTING





MERCEDES ENGINE BAY MOUNTING



DAF 2800 ENGINE BAY MOUNTING

